NtrBC selectively regulates adaptation and intercellular interactions of *Pseudomonas aeruginosa*

by

Morgan A. Alford

B.Sc. (Hons.), The University of British Columbia, 2018

A THESIS SUBMITTED IN PARTIAL FULFILLMENT OF

THE REQUIREMENTS FOR THE DEGREE OF

DOCTOR OF PHILOSOPHY

in

THE FACULTY OF GRADUATE AND POSTDOCTORAL STUDIES

(Microbiology & Immunology)

THE UNIVERSITY OF BRITISH COLUMBIA

(Vancouver)

April 2022

The following individuals certify that they have read, and recommend to the Faculty of Graduate and Postdoctoral Studies for acceptance, the dissertation entitled:

NtrBC selectively regulates adaptation and intercellular interactions of *Pseudomonas aeruginosa*

submitted by Morgan A. Alford in partial fulfillment of the requirements for

the degree of Doctor of Philosophy

in Microbiology & Immunology

Examining Committee:

Dr. Robert E.W. Hancock
Supervisor

Dr. Elitza Tocheva
Supervisory Committee Member

Dr. Natalie Strynadka
University Examiner

Dr. Rosemary Redfield
University Examiner

Additional Supervisory Committee Members:

Dr. Cara Haney
Supervisory Committee Member

Dr. Michael Murphy
Supervisory Committee Member

Abstract

Pseudomonas aeruginosa is an opportunistic pathogen that causes nosocomial and chronic infections contributing to morbidity and mortality in skin wound and cystic fibrosis patients, respectively. One of the reasons for its success as a pathogen is its ability to adapt to a broad range of circumstances. Here, the regulatory two-component system NtrBC is shown to be involved in adaptive and pathogenic states of *P. aeruginosa*. Characterization of adaptive lifestyles *in vitro* confirmed that the double Δ*ntrBC* mutant demonstrated a nearly complete inhibition of swarming motility, a modest decrease and alteration of surfing motility and >40% reduction in biofilm formation; except for swarming, single mutants generally had more subtle or no changes. The *P. aeruginosa* Δ*ntrBC* mutant also had a major increase (~10-fold) in susceptibility to ciprofloxacin. Transcriptional profiles of deletion mutants were defined using RNA-Seq and unveiled dysregulated expression of hundreds of genes implicated in *P. aeruginosa* virulence during chronic lung infections, as well as carbon and nitrogen metabolism.

The role of NtrBC in host-pathogen and interspecies interactions was also examined. *P. aeruginosa* mutants exhibited distinct host interactions, including modestly increased cytotoxicity toward human bronchial epithelial cells, reduced virulence factor production and 10-fold increased uptake by macrophages in vitro. In a high-density skin infection model, mutants were reduced in their ability to invade or cause damage to tissue and were more susceptible to ciprofloxacin in vivo. To compare the infectivity of strains across tissues, and pre-clinically screen antimicrobial or immunomodulatory therapies for the treatment of sinusitis, a murine model of upper respiratory tract infection was developed. In contrast to the wild-type levels of colonization observed in the abscess model, *P. aeruginosa* mutants colonized the respiratory tract less well than wild-type. In contrast to wild-type, Δ*ntrC* and Δ*ntrBC* mutants outcompeted *Staphylococcus aureus*, a commonly co-isolated species in skin wounds and cystic fibrosis patients, during planktonic and biofilm growth. These results indicate that NtrBC is a global regulatory system involved in both adaptive and pathological processes relevant to the success of *P. aeruginosa* in infection.

Lay Summary

Bacteria are microscopic, unicellular organisms that can impact on the health of humans in positive or negative ways, depending on the bacterial species and the context in which it is acquired. *Pseudomonas aeruginosa* is one species of bacteria that is usually only harmful to people with predisposing conditions. For example, cystic fibrosis patients may acquire *P. aeruginosa*, which causes rapid lung function decline. *P. aeruginosa* infection is very difficult to eradicate due to the numerous antibiotic resistance mechanisms it employs. Adaptive resistance is characterized by a transient state of decreased susceptibility to antibiotic therapy that cannot be genetically traced and is reversibly triggered by certain factors that are present in the host environment. Here, I show that a regulatory system, called NtrBC, has a major role in adaptive states of *P. aeruginosa*, suggesting that NtrBC could be targeted by future antimicrobial therapies to prevent adaptive resistance during infection.

Preface

This project was conceived from preliminary data collected from a library screening performed by Dr. Amy T.Y. Yeung, who discovered that transposon insertion in *ntrB* abolished swarming motility of *Pseudomonas aeruginosa* during her graduate studies under the supervision of Dr. Robert E.W. Hancock. Building on preliminary data, I helped conceive this thesis project, developed experimental protocols where necessary and interpreted the data in collaboration with Dr. Hancock. I was responsible for project management, performed most of the experiments and analyzed all the data presented herein (unless otherwise noted below). Thus, this thesis is an original intellectual product.

Parts of Chapter 1 were previously published in the following articles:

1. Alford MA, Pletzer D, Hancock REW. 2019. Dismantling the bacterial virulence program. Microb. Biotechnol. 12: 409-413.
2. Hancock REW, Alford MA, Haney EF. 2021. Antibiofilm activity of host defence peptides: complexity provides opportunities. Nat. Rev. Microbiol. 19:786-797.

   I was involved in drafting both above reviews with Drs. Daniel Pletzer and Evan F. Haney, and Dr. Robert E.W. Hancock extensively revised the manuscripts.

Additionally, parts of Chapter 1 have been incorporated into the following article:

3. Morera FLS, Dostert M, Alford MA, Hancock REW. 2022. *Pseudomonas aeruginosa*: strategies for immune evasion. Manuscript in preparation.

Work described in Chapter 2 was published in the following article:

4. Alford MA, Baghela A, Yeung ATY, Pletzer D, Hancock REW. 2020. NtrBC regulates invasiveness and virulence of *Pseudomonas aeruginosa* during high-density infection. Front. Microbiol. 11: 773.

   I performed all experiments as well as data analysis (unless otherwise noted) and drafted the manuscript. Dr. Arjun Baghela analyzed RNA-Seq data and generated figures for the publication. Dr. Amy T.Y. Yeung performed the library screen that provided foundational knowledge for the project. Drs. Daniel Pletzer and Robert E.W. Hancock provided mentorship and assisted with troubleshooting of experiments, in addition to manuscript revision.

Work described in Chapter 3 was published in the following article:

5. Alford MA, Choi KYG, Kalsi P, Trimble MJ, Masoudi H, Pletzer D, Hancock REW. 2021. Murine model of sinusitis for screening host defense peptides. Front. Infect. Cell. Microb. 11: 621081.

   I established the protocol for shorter-term sinus infections, probed reactive oxidative species production in situ and analyzed most of the data (unless otherwise noted) in addition to drafting the manuscript. Dr. Grace K.Y. Choi established the protocol for longer-term sinus infections and collected/analyzed data from longer-term infections. Pavneet Kalsi assisted with characterization of the LESB65 clinical isolate of *Pseudomonas aeruginosa*. Dr. Hamid Masoudi assisted with histopathology. Drs. Michael J. Trimble, Daniel Pletzer and Robert E.W. Hancock provided mentorship and were involved in troubleshooting assays. All authors were involved in editing the manuscript.

Work described in Chapter 4 was published in the following article:

6. Alford MA, Baquir B, An A, Choi KYG, Hancock REW. 2021. NtrBC selectively regulates host-pathogen interactions, virulence and ciprofloxacin susceptibility of *Pseudomonas aeruginosa*. Front. Infect. Cell. Microb. 11: 694789.

   I was responsible for all experiments as well as data analysis. Beverlie Baquir, Andy An and Dr. Grace K.Y. Choi assisted with cell culture assays. Drs. Grace K.Y. Choi and Robert E.W. Hancock provided mentorship and assisted with troubleshooting assays. All authors were involved in editing the manuscript.

Work described in Chapter 5 was assisted by Simranpreet Mann who performed competition assays with complemented strains of LESB58.

Work described in Chapter 6 was made possible by Drs. Thienh Mah and Clayton Hall who provided the isogenic *P. aeruginosa* PA14 Δ*rpoN* mutant strain for phenotypic screening. Christina Wiesmann created the *P. aeruginosa* LESB58 Δ*rpoN* mutant strain for pathoadaptive screening in vivo. Dr. Arjun Baghela analyzed RNA-Seq data and generated Figures for my thesis.

The use of all bacterial strains presented in this thesis was approved by UBC Risk Management Services under the UBC Biosafety Permit Numbers B14-0207 and B14-0208. Animal experiments were performed in accordance with the Canadian Council on Animal Care (CCAC) guidelines and were approved by the University of British Columbia Animal Care Committee (certificates A17-0253 and A19-0064).

Table of Contents

List of Tables

List of Figures

List of Symbols

α = alpha
~ = approximately
β = beta
°C = degrees Celsius
Δ = delta
e.g. = Latin: *exempli gratia* (for example)
Fmoc = 9-flurenylmethoxy carbonyl
h = hour
κ = kappa
k = kilo
M = mega
μ = micro
m = milli
min = minute
Ω = ohm
± = plus or minus
P = probability
s = second
σ = sigma
tn = transposon
vs. = versus

List of Abbreviations

$\Delta\Delta C_t$ = comparative cycle threshold method
ABC = ATP-binding cassette
ALA = 5-aminolevulinic acid
AMP = antimicrobial peptide
ANOVA = analysis of variance
BM2 = basal medium 2
bp = basepair
C12-HSL = N-(3-oxododecanoyl)-L-homoserine lactone
C4-HSL = N-butanoyl-L-homoserine lactone
CAA = casamino acids
CCAC = Canadian Council on Animal Care
CF = cystic fibrosis
CFU = colony forming units
CIHR = Canadian Institutes for Health Research
CLSI = Clinical and Laboratory Standards Institute
CTAB = cetyl trimethylammonium bromide
CV = crystal violet
DE = differentially expressed
DM = dorsal meatus
DMEM = Dulbecco's Modified Eagle Medium
DNA = deoxyribonucleic acid
dYT = double yeast tryptone
ELISA = enzyme-linked immunosorbent assay
ES = ethmoid sinuses
ETC = electron transport chain
FBS = fetal bovine serum
FC = fold-change
FIMO = Find Individual Motif Occurrences
gDNA = genomic DNA
GEO = Gene Expression Omnibus
GO = Gene Ontology
H&E = hematoxylin & eosin
hBD = human β-defensin
HBE = human bronchial epithelial
HDP = host-defense peptide
HHQ = 4-hydroxy-2-heptylquinolone
HPLC = high-performance liquid chromatography
IHF = integration host factor
IL = interleukin
IQS = 2-(2-hydroxyphenyl)-thiazole-4-carbaldehyde
IVIS = in vivo imaging system
KC = keratinocyte-derived chemokines
KEGG = Kyoto Encyclopedia of Genes and Genomes
LB = lysogeny broth
LDH = lactate dehydrogenase
LES = Liverpool Epidemic Strain
LOD = limit of detection

LPS = lipopolysaccharide
MCP = methyl-accepting chemotaxis protein
MDR = multi-drug resistant
MEM = Minimal Essential Medium
MHB = Mueller-Hinton broth
MIC = minimal inhibitory concentration
MIP = macrophage inflammatory protein
MOI = multiplicity of infection
mRNA = messenger RNA
MRSA = methicillin resistant *Staphylococcus aureus*
MS = maxillary sinuses
MSCFM = modified synthetic cystic fibrosis medium
MyD = myeloid differentiation factor
NAD^+ = nicotinamide adenine nucleotide
NCBI = National Center for Biotechnology Information
ND = not detected
NMIN = NanoMedicines Innovation Network
NPM = nasopharyngeal meatus
NSERC = Natural Sciences and Engineering Research Council of Canada
OB = olfactory bulb
pBBR = pBBR1MCS-5
PBS = phosphate buffered saline
PCR = polymerase chain reaction
PDB ID = Protein Data Bank Identifier
PI3K = phosphatidylinositol-3-kinase
PMA = phorbol-12-myristate-13-acetate
PQS = 2-heptyl-3,4-dihydroxyquinolone
QS = quorum sensing
RNA = ribonucleic acid
RNAP = RNA polymerase
RND = resistance-nodulation cell division
ROS = reactive oxidative species
RT-qPCR = real-time quantitative PCR
SD = standard deviation
SEM = standard error of the mean
SSTI = skin and soft tissue infection
T1SS = type I secretion system
T2SS = type II secretion system
T3SS = type III secretion system
T5SS = type V secretion system
T6SS = type VI secretion system
TCA = tricarboxylic acid
TMB = tetramethylbenzidine
TNF = tumor necrosis factor
UBC = University of British Columbia
WT = wild-type

Acknowledgements

The work performed during my graduate studies was supported by funding from the Natural Sciences and Engineering Research Council of Canada (NSERC), Cystic Fibrosis (CF) Canada, the Canadian Institutes for Health Research (CIHR), the Killam Trusts Foundation, the NanoMedicines Innovation Network (NMIN) and the University of British Columbia (UBC). The content of this thesis is the responsibility of the author and does not represent the views of the funding agencies. I offer my enduring gratitude to the faculty, staff, and my fellow students at UBC, who have inspired me to continue my work in Microbiology. I am particularly grateful to my supervisor, Dr. Robert E.W. Hancock, who provided outstanding guidance and encouragement throughout the course of my studies. He holds a Canada Research Chair in Health and Genomics and is also a UBC Killam Professor.

I owe many thanks to my supervisory committee, lab mates and many collaborators who provided ample mentorship and professional support along the way. The scientific brilliance of each of you inspires me to work persistently and think critically about my data. The countless hours of conversation at the bench, in the lunchroom and elsewhere have been paramount to my enjoyment of research and will be remembered fondly for years to come. Kindness matters as much as talent these days, and I am fortunate to have worked with scholars equipped with both. I owe special thanks to my mentor, Dr. Janet Kluftinger, as well as my mother and four brothers who have modeled resilience and have taught me numerous lessons about perseverance in addition to self advocacy. Last, I am eternally grateful to my companion, Ilia, for his provision of nutrition in the form of peanut butter, for his curiosity about the microscopic world and for stimulating intelligent conversations that helped me think about my work from new perspectives. Life is much sweeter when shared with you.

Dedication

I dedicate this thesis to the female luminaries that paved the way for women in science.

“Let us choose for ourselves our path in life, and let us try to strew that path with flowers.”

– Émilie du Châtelet, 1779

Chapter 1: Introduction

Pseudomonas aeruginosa is a metabolically versatile opportunistic pathogen, to which deficient immune functioning can predispose an individual to infection (1). Due to its metabolic versatility, *P. aeruginosa* is capable of inhabiting diverse biotic or abiotic environments and is generally described as ubiquitous in nature. However, a recent environmental study and meta-analysis revealed that the prevalence of *P. aeruginosa* in pristine environments was relatively low, and that the environmental occurrence of *P. aeruginosa* was associated with intense human contact (1,2). *P. aeruginosa* is capable of infecting various niches of the human body, including the skin, blood, respiratory tract, and urinary tract (1). It is one of the most prevalent causes of chronic, recurrent nosocomial (hospital-acquired) infections of skin wounds (3) as well as acute and chronic infections of the respiratory tract of adults, especially those with cystic fibrosis (CF) (4). In the context of CF, airway infections by *P. aeruginosa* increase the patient's risk of pulmonary exacerbation and lung function decline, thus impacting on treatment of patients. Unfortunately, *P. aeruginosa* is increasingly difficult to manage in the clinic due to its numerous mechanisms of intrinsic, acquired, and adaptive resistance (5,6). Thus, *P. aeruginosa* has been designated by the World Health Organization (WHO) as a pathogen of critical priority for which new antimicrobials are urgently needed (7). Furthermore, nosocomial infections caused by multi-drug resistant (MDR) *P. aeruginosa* represent a huge economic burden, since inpatient treatment is extended when MDR infections occur, and expensive 'last-resort' antibiotics may need to be administered (8,9). Indeed, nosocomial infections caused by MDR *P. aeruginosa* costed the American healthcare system roughly $450 million in 2019 alone (9). Clearly, better understanding of *P. aeruginosa* mechanisms of (adaptive) resistance, and development of therapies that prevent them, is needed.

1.1 Adaptive lifestyles of *P. aeruginosa*

P. aeruginosa and other pathogens display phenotypes that are associated with transient resistance to antibiotics, whereby gene expression is altered due to the growth state or environmental conditions; these are referred to as adaptive lifestyles. Adaptive lifestyles of *P. aeruginosa* include the complex surface colonization phenotypes swarming (10) and surfing (11) motility, as well as biofilm formation (12), each of which influence the expression of approximately one fifth of all genes in *P. aeruginosa*. These surface adherence or motility phenotypes play important roles in virulence (10-12) and adaptation to changing or dynamic environments. Indeed, these phenotypes can be triggered by factors such as fluctuating pH, temperature and oxygen supply, the presence of

stressors, or low availability of nutrients (13), all of which are characteristic of the host environment. Further, in addition to their association with transient resistance to antibiotics (10-14), these adaptations contribute to pathogenesis in vivo (15-17).

1.1.1 *P. aeruginosa* as a model organism of motility

P. aeruginosa is generally considered a model organism for bacterial locomotive processes, collectively termed motility, since it exhibits a wide range of motile phenotypes including swimming, twitching, swarming, surfing, gliding, and darting (18,19). This likely reflects the metabolic diversity and broad environmental distribution of this organism. Relatively little is known about gliding or darting motilities, though they are sometimes considered a passive form of motility powered by bacterial division on the surface of a medium (20). Swimming is one of the better described forms of motility across bacterial species. In *Pseudomonas* spp., it is a unicellular (planktonic) form of motility that relies on the counterclockwise rotation of a single, polar flagellum, which reverses rotation for reorientation of the bacterium until it moves toward a more favourable environment (21). The frequency of directional switching is regulated by a sensory-response process, termed chemotaxis, which enables bacterial movement up a gradient of nutrients that support growth or down a gradient of stressors (22). Twitching motility, on the other hand, is a surface-associated form of locomotion involving the projection, attachment, and retraction of type IV pili that drags the bacterium across a solid medium (19). Swarming motility depends on bacterial flagella and/or type IV pili, as well as a range of regulatory systems including the stringent stress response, one- and two-component system signaling, cyclic di-GMP signaling, and intercellular quorum sensing (QS) signaling (23). Whereas swimming and twitching motility are primarily considered a means of locomotion, swarming and surfing motility are complex lifestyle adaptations influencing the expression of ~20% of all genes in *P. aeruginosa* (10). Indeed, swarming is associated with several adaptive changes including altered virulence factor production, metabolism, and antibiotic susceptibility.

1.1.2 Swarming motility

During swarming, the appendages of *P. aeruginosa* help cells to align along their long axes for multicellular movement and migration of the swarm front occurs after surpassing a critical cellular density needed to initiate this so-called ‘social behaviour’ (23). Many other rod-shaped bacteria undergo swarming motility, including the Gram-positive *Bacillus* spp. and Gram-negative *Vibrio* or *Salmonella* spp. among others (24). Swarming by *P. aeruginosa* relies on the production of rhamnolipids to reduce the surface tension of semi-viscous surfaces (0.5-0.7% agar; thought to be

equivalent to the viscosity of mucous surfaces) and has strict nutritional requirements compared to other species of bacteria (25). For example, *P. aeruginosa* swarming is inhibited by ammonium, and depends on the presence of amino acids or other relatively weak nitrogen sources (25). Otherwise, *P. aeruginosa* requires a strong carbon source, such as succinate or glucose, as well as iron and magnesium supplementation for swarming to occur.

Nutrient availability can impact on the morphology of swarming *P. aeruginosa* colonies, indicative of an association between swarming and physiological processes such as metabolism or stress adaptation, thus requiring standardization of defined nutrient conditions for examining swarming in the laboratory (24). Furthermore, different laboratory reference strains of *P. aeruginosa* have distinct corona-like (PAO1) or dendritic (PA14) swarm morphologies. It should be noted that there is limited consensus in the field regarding the physical characteristics of swarming *P. aeruginosa*. Although many have shown that swarming is dependent on both flagella and type IV pili (23,26), others have documented instances of swarming in the absence of type IV pili (27-29). Though the basis for this is unclear, it is possible that type IV pili are involved in surface sensing (23) or intercellular rafting and branching (30). Additionally, there are variable degrees of cellular elongation and flagellation observed within swarming colonies. However, neither cell elongation nor hyper-flagellation are required for swarming to occur.

Swarming is a complex adaptation influencing the expression of 1,581 genes (compared to planktonic, flagellum-dependent swimming motility), as identified by RNA-Seq, including 104 transcriptional regulators and many genes involved in resistance (collectively termed the resistome), leading to adaptive MDR of *P. aeruginosa* (14,26). Furthermore, swarming is dependent on more than 233 different genes, including more than 25 regulators (26). Mutation of 41 differentially expressed (DE) resistome genes confirmed their role in swarming-mediated adaptive resistance to at least one antibiotic (14). These resistance determinants encoded genes spanning biological functions such as membrane energization (electron transport chain (ETC) activity), lipopolysaccharide (LPS) biosynthesis, nitrogen/carbon transport or metabolism and genes involved in susceptibility to β-lactam and fluoroquinolone antibiotics (14). More specifically, resistance to tobramycin was increased when genes involved in nitrogen metabolism were mutated, including *nirG*, involved in reducing nitrite to gaseous nitrogen, as well as *hutR*, *nosR* and *nirQ*, which are regulators of histidine utilization (31), nitrification and denitrification (32,33), respectively. Taken together, these data indicated that swarming mediated MDR in *P. aeruginosa* is multi-determinant and intertwined with physiological processes such as assimilation

of nitrogen.

Although the ecology of swarming motility is not fully understood (24), it was demonstrated that swarming motility contributed to dissemination from localized *P. aeruginosa* infections in vivo (16). When a mutant defective for swarming, but not swimming, twitching or other adaptive phenotypes, was inoculated subcutaneously in mice, fewer bacteria were recovered from organs distal to the site of infection (16). Furthermore, the therapeutic peptide 1018, which inhibits swarming motility in vitro (16,34), inhibited dissemination of *P. aeruginosa* in vivo (16). These data demonstrate an association between swarming motility and invasiveness, at least during early stages of infection.

1.1.3 Surfing motility

Surfing motility is a more recently discovered form of surface motility that physically differs from swarming in that it has a distinct colony morphology, is independent of pili and rhamnolipid production, can occur on surfaces with a broader range of viscosities, and is dependent on the presence of exogenous lubricants such as mucin (11,35,36). Mucins are polymeric glycoproteins that are the main structural component of mucus that is produced by mucosal and submucosal glands in the upper respiratory tract and elsewhere (37). Surfing can occur in the presence of other lubricants such as Tween-20 but cannot be completely recapitulated in the absence of mucin (35). Surfing motility is significantly more rapid (approximately 2.5-fold faster) than swimming motility, though the rate of colony expansion depends on the concentration of mucin added (35,36). Surfing colonies in *P. aeruginosa* have a thick, white outer edge and a strongly pigmented blue/green centre. Cells at the edge of surfing colonies are longer, lack flagella and are more randomly oriented than their central counterparts (35). Light microscopy revealed that cells at the surfing edge were more concentrated, not strongly aligned and relatively immotile, whereas central cells were actively moving (38). Taken with the observation that cells accumulated at the surfing edge over time, it was proposed that cells from the centre of the colony propel themselves to the edge by "surfing" over their immotile counterparts (38).

Surfing and swarming colonies can further be distinguished by their different gene expression profiles (10,11,36) since only ~10% of DE genes overlapped across conditions. Surfing cells exhibited dysregulation of more than 1,400 genes (compared to swimming motility) (36), 65 of which were resistome genes. Mutation of 36 DE resistome genes confirmed their role in broad-spectrum MDR of surfing cells (36). These included genes involved in ETC activity (*ccmF*, *ccoO1*,

cycH, *etfA*, *nuoB*, *nuoF*, *nuoG,* PA4429), amino acid transport and metabolism (*ddaH, braB*) and energy production (*atpB*). Three of these genes (*ccoO1*, *atpB*, PA4429) were previously shown to be involved in swarming mediated resistance to front-line antibiotics such as tobramycin (14). Taken together, these data suggest that physiological processes such as central metabolism confer swarming and surfing mediated adaptive resistance on *P. aeruginosa*.

Surfing also resulted in dysregulation of virulence factors (36) which, by definition, cause severe harm to host tissues (39) indicating a possible role for surfing in pathogenesis in vivo. Surfing associated virulence may be particularly relevant in the context of CF, in which patients produce copious amounts of mucin-containing mucus (4) from mucosal tissues in the airways. Further, surfing motility depends on the stringent stress response of *P. aeruginosa* (17), which can be triggered by the stressful environment of the CF respiratory tract characterized by increased levels of oxidative species, chronic immune activation and competition from other bacterial species that colonize the diseased airways (40).

1.1.4 Biofilm formation

An increasingly appreciated factor in the growing antimicrobial resistance crisis is the ability of bacteria to circumvent the effects of antibiotics by growing within a biofilm (12,41,42). Biofilms are a distinct growth state in which communities of microorganisms, encased in a protective extracellular matrix (comprised by extracellular DNA, proteins, and polysaccharides), associate with a variety of environmental surfaces, including those in humans (43). The biofilm life cycle consists of four distinct phases: deposition and attachment of planktonic bacterial cells on a surface; irreversible surface attachment and matrix production; biofilm proliferation and maturation; and bacterial cell detachment and dispersal (44). These processes are highly regulated and characterized by considerable changes in metabolism, transcription, and protein expression within the cells. Flagella- and type IV pili-dependent motilities contribute to biofilm formation by promoting adherence, aggregation, and formation of the mushroom-like cap structure characteristic of *Pseudomonas* biofilms (27,45). Bacterial cells within a biofilm are up to 1,000-fold more resistant to antibiotics and disinfectants when compared to their planktonic counterparts (46) creating enormous challenges for surface sterilization and biofilm-associated infection prevention or management. This is particularly problematic in clinical settings, where at least 65% of all infections are caused by biofilm forming bacteria (47,48).

Biofilm cells are equipped by their unique transcriptional program and physiology to survive in

harsh environmental conditions, leading to resistance to several stressors (49) including antibiotic challenge. Numerous studies have reported on the transcriptional profile of *P. aeruginosa* during biofilm formation, several of which have been previously summarized (50,51) and indicate dysregulated expression of at least 850 genes across conditions. Distinct transcriptional profiles of stationary phase and biofilm-forming cells provide further evidence that biofilms are not just a community of surface attached, stationary phase cells (51-53), but rather an adaptive lifestyle characterized by dysregulation of genes involved in transcriptional regulation, metabolism, virulence, motility, and resistance (51). Only 13 of the transcriptional regulators that are DE during biofilm formation are commonly dysregulated in swarming and surfing motilities. These include *nirQ* and *nosR*, which are important for regulation of denitrification and nitrous oxide metabolism, respectively (32,33). This data supports the hypothesis that surface colonization phenotypes of *P. aeruginosa* are distinct, but possibly metabolically related, adaptive mechanisms.

At present it is unclear if canonical mechanisms of resistance to antibiotics extend to bacteria growing within a biofilm in host-like conditions. However, biofilm-specific mechanisms of antibiotic resistance have been interrogated (41,54,55). Studies have focused on the impacts of upregulated production of extracellular matrix components, including the polysaccharides adhesin and alginate (56), which are hypothesized to interfere with antibiotic penetration of the biofilm due to binding by charged antibiotics such as tobramycin (57). However, a recent study revealed that most antibiotics diffuse into the extracellular matrix of biofilms following saturation of binding sites, indicating that inhibited penetration may not be the major source of biofilm-associated antimicrobial resistance in the clinic (58). Other mechanisms of resistance are associated to the slow growth or metabolic quiescence (59) of biofilm-associated cells and activation of specific stress responses (39,60), which are triggered by exposure to antibiotics or other host-associated factors in vivo (39,41,60).

1.2 Adaptation and intercellular interactions

Adaptation is a complex physiological process that impacts on the virulence and immune recognition of *P. aeruginosa* in the hostile environment of e.g., CF airways (61,62). Temporal regulation of the arsenal of effectors that impact on host-pathogen interactions is still poorly understood and should be improved for conceiving therapies effective against *P. aeruginosa* in adaptive states. However, we know that adaptation to growth on epithelial cells leads to massive dysregulation of the PhoPQ regulon that influences susceptibility to polycationic antibiotics (polymyxins, aminoglycosides, cationic antimicrobial peptides) and virulence (46). Thus, PhoPQ

has been studied as a target for therapies that could potentiate the activity of antibiotics during the early stages of infection. More generally, virulence factor production processes have been interrogated to unveil potential targets for emerging anti-infective therapies.

1.2.1 Secretion systems

P. aeruginosa has an extensive repertoire of virulence factors that are triggered in response to different stressors during acute and/or chronic infection (63), enabling colonization of different tissues. Virulence factors of *P. aeruginosa* are loosely defined as molecules that damage host tissue (64) including extracellular (secreted) proteins (66,67) as well as surface bound bacterial appendages such as the flagellum or type IV pili (65). Indeed, at least five secretion systems are documented to facilitate extracellular release of virulence factors during *P. aeruginosa* infection. The type I secretion system (T1SS) facilitates production of alkaline proteases and heme acquisition factor; the type II secretion system (T2SS) secretes toxins as well as lipases and proteases; the type III secretion system (T3SS) injects toxins directly into host (eukaryotic) cells; the type V secretion system (T5SS) secretes lipases and proteases; and the type VI secretion system (T6SS) secretes hemolysin coregulated protein (Hcp) and toxins important for interspecies competition (66-68).

1.2.2 Siderophores

P. aeruginosa must sequester nutrients from the host milieu, particularly iron which is in low supply in the body, to enable growth and survival within e.g., CF airways (69); this is aided by the production of siderophores such as pyoverdine. Pyoverdine is a water-soluble, iron-chelating molecule that captures iron from serum and tissues where it is bound to transferrin and lactoferrin, and iron availability can regulate the production of e.g., secreted bacterial toxins. Ferripyoverdine, the iron-bound form of the siderophore, binds to an outer membrane receptor (FpvA), and if present in low abundance can trigger the alternative sigma factor PvdS to activate the expression of exotoxin A and certain proteases (70) to liberate more iron from the human body. Pyochelin is another iron-chelating siderophore with a lower affinity for ferric iron than pyoverdine (71), although both are needed for full expression of virulence.

1.2.3 Virulence can be regulated by quorum sensing systems

QS systems, primarily involved in cell-density dependent signaling, are systems that can regulate bacterial virulence (39,72), although their mechanisms of regulation are complex. Indeed, *P. aeruginosa* encodes four diffusible QS molecules (73), including N-(3-oxododecanoyl)-L-

homoserine lactone (C12-HSL encoded by *lasI*) and N-butanoyl-L-homoserine lactone (C4-HSL encoded by *rhlI*), as well as the quinolone molecule 4-hydroxy-2-heptylquinoline (HHQ), enzymatically (*pqsH*) converted to 2-heptyl-3,4-dihydroxyquinoline (PQS). Relatively little is known about the fourth *P. aeruginosa* QS autoinducer, 2-(2-hydroxyphenyl)-thiazole-4-carbaldehyde (IQS). Regardless, QS autoinducers are constitutively expressed at a modest level and once accumulated in the medium above a threshold concentration (requiring a quorum of bacteria), can be taken up and activate the expression of their respective regulator. The QS systems of *P. aeruginosa* also regulate the expression of each other in a hierarchical manner, with C12-HSL induced LasR being the master regulator at the top of the hierarchy (73). Some QS regulated virulence factors, such as the redox-active phenazine pyocyanin, are toxic towards bacterial competitors, such as *Staphylococcus* spp., during polymicrobial infection (74) and interfere with innate immune processes (75). Therefore, inhibition of QS signaling could cause *P. aeruginosa* to exhibit more of a commensal phenotype by preventing host-directed virulence and inhibiting interspecies interactions.

1.2.4 Virulence and immunogenicity are associated

Some virulence factors elicit immune responses toward *P. aeruginosa* (76), especially during innate immune processes. In contrast, bacterial virulence factors including elastases and proteases, as well as QS molecules, can dampen adaptive (cellular) responses to infection, conferring immune evasiveness on *P. aeruginosa* (76). Here, I will only focus on the association between bacterial virulence factors and innate immunity.

Phagocytosis, or cellular engulfment of bacteria, plays a major role in the innate immune response to acute *P. aeruginosa* infection (76). Flagellin, the monomeric subunit of flagella, can stimulate phagocytosis of *P. aeruginosa* by alveolar macrophages downstream of Toll-like receptor (TLR)-5 and interleukin (IL)-1β signaling (77). Flagellin-mediated stimulation of epithelial TLR-5 can lead to induction of other rapid antibacterial processes (78) by a mechanism dependent on the TLR adaptor molecule myeloid differentiation factor (MyD)88. Flagellar motility, but not recognition of flagellin per se, can also stimulate phagocytosis following activation of the phosphatidylinositol-3-kinase (PI3K)/Akt pathway (79). Bacteria that are not cleared by phagocytosis may alternatively be killed by neutrophil extracellular traps (NETs) containing the granular components of neutrophils (76). Although the detailed mechanism of NET induction is not completely clear, we do know that flagellar motility can stimulate NET production independent of flagellin recognition (80). These data may explain, at least in part, why flagellar motility is selected against among *P.*

aeruginosa clinical isolates (81) obtained from late-stage CF infections. Nonetheless, antibodies against flagellin as well as elastases and LPS, a well-documented activator of the TLR-4 signaling cascade, have been isolated from the sputum of CF patients.

While type IV pili are important for adhesion to mucosal surfaces (82), the early stages of biofilm formation (15), and phagocytosis by activated macrophages (83), neither positive nor negative selection of twitching motility is well documented in situ, whereas mucoid phenotypes are selected for (84). Mucoidy is characterized by overproduction of alginate, an exopolysaccharide that might also serve as a biofilm extracellular matrix component. Alginate itself might contribute to lung congestion but is not always considered a virulence factor. However, innate immune responses to biofilm infections caused by *P. aeruginosa* are major contributors to the morbidity and mortality of CF patients (84). Endobronchial biofilms may be surrounded by a high number of neutrophils, activated by alginate, LPS or other immune complexes formed in response to *P. aeruginosa* infection, and lead to the liberation of reactive oxidative species (ROS) that deplete molecular oxygen from the local environment as well as damage respiratory tissue. Interestingly, similar impacts of biofilm formation (or biofilm-associated virulence) on innate immune processes have been observed in the context of chronic wound infections (84,85).

1.3 Therapies targeting bacterial adaptation

Therapies that target biofilm formation and motilities, including the adaptive lifestyles swarming and surfing, have great potential to treat infections that do not respond to traditional antibiotics, and may be championed for the prevention of resistance emergence and the eradication of infectious diseases in the pharmaceutical, agricultural, and horticultural industries where traditional antimicrobial agents have failed (86,87).

1.3.1 Host defense peptides as emerging therapies

Host defense peptides (HDPs) are gene-encoded polypeptide sequences that are integral components of immune defenses in all organisms. They vary in length, typically between 12 and 50 amino acids, and they are characterized by a net positive charge (usually +2 to +9) as well as a high proportion of hydrophobic residues (88). However, despite these general features (Fig. 1-1) there is tremendous sequence and structural diversity between HDPs across species.

The structure of an HDP is determined by its primary sequence as well as the local environment in which the peptide resides, either in solution or in the presence of a biological membrane (89).

Conformations range from structured linear peptides to α-helical and/or β-sheet-containing structures, and often peptides display a high degree of structural plasticity, being able to interconvert between unstructured and structured conformations (Fig. 1-1). Many HDPs exhibit broad-spectrum antibacterial effects that can be suppressed under physiological conditions (90) and the susceptibility of bacterial species depends on the peptide of interest. Traditionally, the term antimicrobial peptide (AMP) has been used to describe this class of biomolecules as the direct antibacterial effects of HDPs were traditionally the most widely studied. However, as many HDPs are known to exert a broad array of biological functions, including immunomodulatory activities that have been proposed to be their major function, as well as antibiofilm, antifungal, antiviral, and anticancer activities (91), the term HDP has been adopted to better reflect their diverse and complex nature.

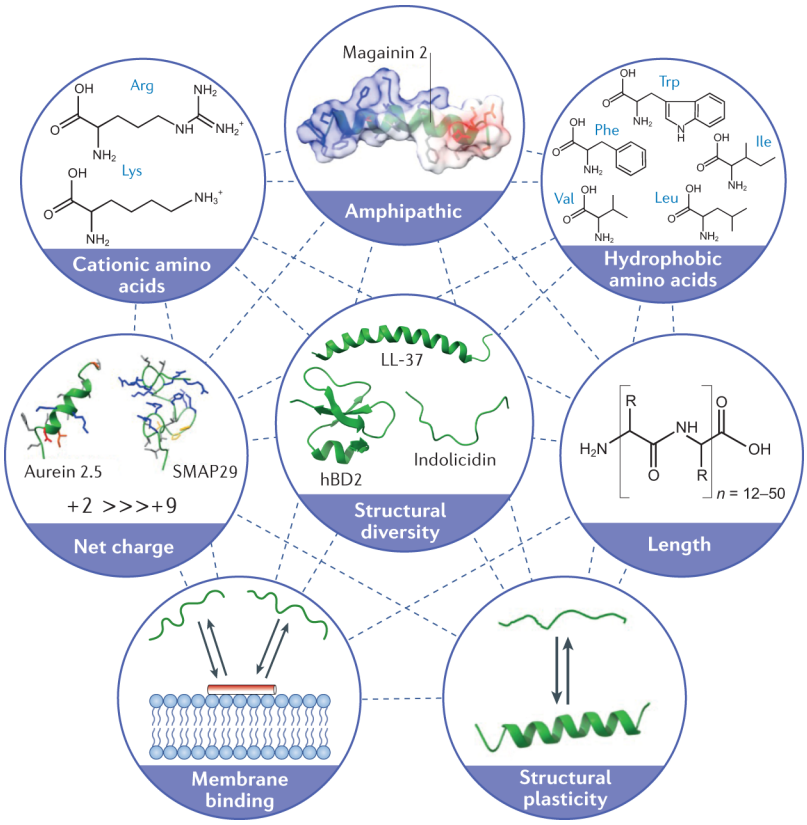

Figure 1-1. General features of host defense peptides (HDPs). Natural HDPs are typically 12-50 residues in length and contain a high proportion of cationic (Arg and Lys) and hydrophobic (Leu, Ile, Val, Phe, Tyr and Trp) amino acids. These properties confer a net positive charge at neutral pH and enables them to adopt amphipathic conformations such as the α-helical structure of magainin (Protein Data Bank identifier (PDB ID) 2MAG). HDPs typically range in charge from + 2, such as in aurein 2.5 (PDB ID 6GS9), to + 9 such as in sheep SMAP29 (PDB ID 1FRY). Many peptides exhibit structural plasticity and adopt a variety of secondary structures, often upon interacting with biological membranes or under physiological conditions. Representative structures of structurally diverse natural HDPs shown are LL-37 (PDB ID 2K6O), human β-defensin 2 (hBD2; PDB ID 1FD4) and indolicidin (PDB ID 1G89). All these interrelated peptide properties

combine to varying degrees in natural and synthetic HDPs to define the breadth of biological functions that a given peptide can exert. HDPs are represented as amphipathic cylinders, with charged surfaces in red and hydrophobic surfaces in grey, in some instances.

Most early AMP studies were focused on evaluating and optimizing peptides for their direct antimicrobial activity against planktonic cells. However, it is well established that the direct antibacterial effects of AMPs are strongly influenced by media composition, and many natural peptides lose their direct antibacterial effects under physiological conditions (for example, high salt content, divalent cations, polyanions) (92). Coupled with issues such as poor absorption, biodistribution, metabolism and excretion properties (93), this may explain in part why synthetic peptide derivatives with potent antibacterial effects in vitro have failed to demonstrate sufficient efficacy in late-stage clinical trials (90). Alternatively, focusing on optimizing synthetic HDPs for the functions that are the most biologically relevant in vivo, particularly immunomodulatory (91) and biofilm-directed functions, may yield greater chances for clinical success.

1.3.2 Mechanisms of emerging host defense peptides

Natural HDPs, such as LL-37 (92,93), indolicidin (93), human β-defensin (hBD)2 (94), and hBD3 (95) have all been shown to exert antibiofilm effects at concentrations lower than those required to kill planktonic cells under the same conditions in vitro, which suggests that the antibiofilm and antibacterial effects of HDPs are independent. Notably, whereas members of the *Burkholderia cepacia* complex are highly resistant to the direct antimicrobial effects of AMPs (96), synthetic peptides can exert potent antibiofilm effects on *Burkholderia* spp. biofilms in vitro (97,98), further reinforcing the concept of antibiofilm peptides as a separate subclass of HDPs. Furthermore, several synthetic peptides have been identified that exert antibiofilm effects at sub-MIC concentrations (99), which highlights the potential for designing peptides with enhanced potency to target biofilm-associated infections. In contrast to the binary antibacterial effects of AMPs (either growth or no growth), the antibiofilm effects of HDPs are more varied. These include preventing initial bacterial cell attachment, suppressing biofilm maturation, eradicating preformed biofilms and/or dispersing the cells within the biofilm (Fig. 1-2).

1.3.3 Anti-biofilm therapies in the clinic

Given their high potency and selectivity for biofilm formation, antibiofilm peptides are considered highly promising candidates for the treatment of skin and soft-tissue infections (SSTIs) (100), in which bacteria display a propensity for the biofilm mode of growth (101,102). In fact, many AMPs that have advanced to clinical trials have been considered in the context of SSTIs (103). Bacterial

SSTIs can include mild superficial injuries that rarely require antibiotic intervention, chronic infections that resist antibiotics and are usually treated surgically, and those that develop into systemic infection and can cause life-threatening sepsis. Skin infections caused by the biofilm-forming species *Staphylococcus aureus* and *P. aeruginosa* can become invasive and elicit immune and inflammatory responses that worsen disease progression and are thus considered high-priority pathogens that require the development of new therapeutics (100-102).

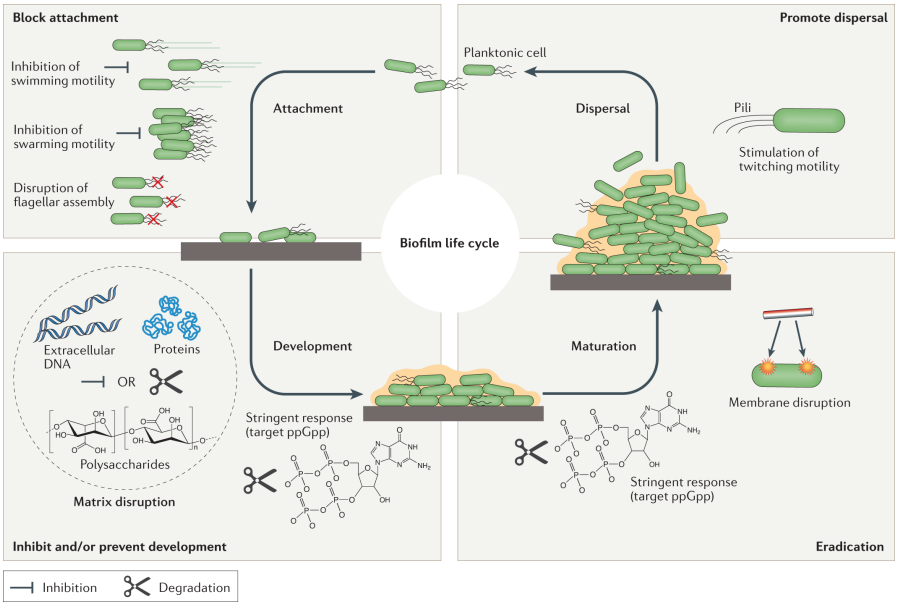

Figure 1-2. Emerging therapies may target adaptive lifestyles. Therapies may block initial attachment to a surface by inhibiting swimming or swarming motility or interfering with flagellar assembly. Alternatively, antibiofilm peptides may inhibit biofilm development by degrading or preventing the production of important biofilm matrix components. Other antibiofilm peptides act on developing or established biofilms by disrupting cell membranes of bacteria within the biofilm or translocating into the cell where they target guanosine tetraphosphate (ppGpp) for degradation, disrupting the stringent-stress response required for biofilm formation. Other peptides promote the dispersal of biofilm cells (by stimulating twitching motility), which would make the bacteria susceptible to the effects of antibiotics or to the antibacterial effects of host defense peptides (HDPs).

Although the use of AMPs for this purpose has been explored, no candidate therapies have successfully completed clinical trials (103), perhaps due to a lack of evaluation or optimization for direct antibiofilm activity. In addition to the lack of optimization for antibiofilm activity, several impediments have limited the activity of peptides in vivo, including their susceptibility to proteolysis, tendency to aggregate, unknown toxicities, and loss of activity due to host cell, tissue and protein binding. These issues can be addressed by developing proteolytically stable peptidomimetics (104) that retain the antibiofilm effects of L-form peptides or using formulation strategies to prevent peptide degradation in vivo (105). Formulations with hyperbranched

polyglycerols or other excipients that can be injected subcutaneously are particularly desirable as the most threatening SSTIs are too deep to treat easily with topical antimicrobial therapies. Further, although AMPs have a relatively larger size and charge when compared to other small molecules (106), they do have some ability to penetrate various tissues when injected intraperitoneally (107). Nevertheless, SAAP-148, a synthetic peptide derivative of LL-37, showed superior antibiofilm activity when formulated in a hypromellose gel (compared to unformulated peptide) and applied topically to a human skin wound model ex vivo (108).

Antibiofilm peptides seem to have some effectiveness in treating infections of the lower respiratory tract (109,110) caused by aggressive MDR biofilm-forming Gram-negative bacteria, including *P. aeruginosa* (111). These studies showed peptide-mediated inhibition or eradication of biofilms in vitro, of virulence in vivo or a combination of the two. A synthetic HDP called WLBU2 exhibited direct antibiofilm activity against *P. aeruginosa* in host-like cell-culture conditions (112) and a mouse model of respiratory tract infection (109,110). Thus, WLBU2 could represent a lead peptide for the prevention or treatment of biofilm-associated airway infections.

Biofilms are equally problematic in diseases of the bladder, oral cavity, ears, nose, and throat and in infections associated with implanted medical devices (113). Fortunately, antibiofilm peptides exhibit promise to address these types of infections as well. For instance, a synthetic LL-37 derivative, P60.4Ac, previously showed the ability to kill 85-90% of biofilm-associated methicillin resistant *S. aureus* (MRSA) cells in ex vivo models of skin and airway infection (114). In a recently completed phase IIa clinical trial, P60.4Ac was assessed as a new treatment for chronic suppurative otitis media or infection of the middle ear (115). Ototopical drops containing peptide or placebo were administered to adults for two weeks, followed by a 10-week period of self-reporting and sampling of mucus for bacterial enumeration. The peptide therapy proved 47% effective, compared to 6% in the placebo group, and no peptide-related adverse events were observed over the course of the study. The excellent safety profile and encouraging efficacy results from this trial were mentioned as justification to move forward with further clinical development of this peptide therapy. With respect to implanted devices, several antibiofilm peptides have been explored to prevent bacterial colonization and biofilm initiation, often through the covalent attachment to the surface of implants or by incorporation into coatings that allow for slow and sustained release of the peptide over time (116).

1.3.4 Disease models for studying efficacy of emerging therapies

Biofilm models have been used to screen the activity of peptides for several years and range in sophistication from simple to complex. Closed in vitro models include some of the most popular methods for determining the biofilm-directed activity of peptides such as the microtiter plate assay (117) and the closely related Calgary biofilm device assay (118). Dynamic models are analogous to continuous culture systems and enable structured biofilm formation over several days. A flow cell method was recently applied to develop specific peptide probes for diagnosing biofilm infections in the clinic (119). The ability to diagnose biofilm infections non-invasively in real-time could revolutionize the diagnosis and management of infectious diseases.

Microcosm methods are the most sophisticated of tissue culture models and aim to closely reflect the physiological environment through the formation of polymicrobial biofilms or by adding materials to which cells adhere (120). Bacterial plaque that occurs in the oral cavity can be modelled by forming biofilms with isolates from human saliva on hydroxyapatite discs or within dentin canals. Studies (reviewed in ref 120) showed that peptides could exert considerable antibiofilm activity in as little as 1-3 min.

Animal models of biofilm infections are important in monitoring mechanisms of bacterial virulence and host responses in a concerted, reproducible fashion (121). Small mammals are preferred as they are genetically tractable and technically simple to handle, whereas larger animals provide anatomy and immune systems that are more reflective of humans. In a murine model of otitis media, scanning electron microscopy was applied to show *P. aeruginosa* biofilm formation in the middle ear after three weeks (122). Furthermore, bacteria exhibited recalcitrance and wounds became purulent at late stages of infection, representing a scenario where conventional antibiotics have failed. This model could be amended for screening de novo peptides, like another wound purulent model used to validate hits generated by screening peptides versus erythrocytes in vitro (123). A recently developed cutaneous abscess model is amenable to studying progressive or chronic infections, depending on the bacterial strain injected (124). More specifically, the more virulent *P. aeruginosa* PA14 laboratory reference strain is highly motile and disseminates from the localized infection site, but the less motile clinical isolate LESB58 does not and is therefore more suitable for forming chronic infections (maintained up to 10 days post-infection). This model can be amended for the study of other Gram-negative and Gram-positive pathogens including the highly antibiotic resistant *ESKAPE* bacterial species. Studies in this model have revealed synergy between HDPs and antibiotics for treatment of chronic infections (125), further indicating the

distinct mechanisms of action for emerging therapies such as antibiofilm or immunomodulatory peptides and conventional antibiotics.

1.4 Adaptive lifestyles of *P. aeruginosa* and transcriptional regulation

Efficient induction of adaptive lifestyles is dependent on rapid signal transduction and transcriptional regulation of effectors needed for the display of the phenotype of interest. Fine-tuning of the transcriptional response to changing environmental conditions increases *P. aeruginosa* phenotypic plasticity and population fitness, facilitating colonization in harsh environments (126).

1.4.1 Two-component system signaling

Two-component systems encoding a sensor kinase and response regulator are one type of regulatory element that have been extensively studied in *P. aeruginosa* (127). Canonical sensor kinases are stimulated by signaling molecules that bind their periplasmic signaling domain. Upon stimulation, sensor kinases undergo a conformational change, then auto-phosphorylate at a conserved histidine residue. This is propagated to their cognate response regulator, which becomes phosphorylated at a conserved aspartate residue and activated (or sometimes repressed) for downstream transcriptional regulation of genes. Two-component systems play a major role in global regulation of *P. aeruginosa*, which encodes 64 sensor kinases and 72 response regulators in its genome (128), many of which are already known to be involved in adaptation and virulence.

Bacterial enhancer binding proteins (bEBPs) are a specialized class of response regulators that are required for transcription initiation of genes from RpoN (σ^{54})-dependent promoters (129). RNA-polymerase (RNAP) holoenzyme containing the σ^{54} alternative sigma factor, unlike that containing a σ^{70}-type alternative sigma factor, cannot initiate transcription without ATP hydrolysis due to energetically unfavorable open-complex formation. Thus, bEBPs are response regulators with ATPase activity that usually bind to an enhancer motif 50-200 basepairs (bp) upstream of the promoter for interaction with promoter bound σ^{54}-containing RNAP holoenzyme, facilitated by DNA bending.

1.4.2 NtrBC is a two-component system encoding a non-canonical enhancer

NtrBC has served as a model of non-canonical two-component system signaling (130) and bEBP function (129). Prior studies revealed that low intracellular glutamine induces GlnD-mediated uridylylation of GlnK (a PII-like protein), which binds to an intracellular signaling domain of NtrB

and triggers autophosphorylation as well as phosphorylation of the C-terminal domain of the bEBP NtrC. Interestingly, NtrC can autophosphorylate independently of NtrB in the presence of select metabolites (131). Phosphorylated NtrC activates the transcription of genes from σ^{54}-dependent promoters through ATP hydrolysis, enabling open-complex formation by the RNAP holoenzyme. NtrC may induce transcription through its interaction with promoter-bound RpoN from solution, or through DNA binding to the enhancer element upstream of the promoter, which may stimulate DNA bending by the integration host factor (IHF) protein (132) and subsequent interaction with promoter-bound RpoN. Although an extracytoplasmic signal for NtrB initiation of the NtrBC signaling cascade has been proposed (133), a function for the periplasmic ligand binding domain of NtrB has yet to be characterized.

1.4.3 NtrBC regulates nitrogen metabolism

Nitrogen is one of the essential elements of life important for synthesis of most macromolecules including nucleic acids, proteins, and cell wall components. Indeed, nitrogen constitutes 14% of the dry mass of bacterial cells on average (134), although the elemental composition of bacteria varies widely as many factors influence energy flow through cells, including the abundance of nitrogen in the growth medium. *P. aeruginosa* can assimilate a variety of nitrogen sources into macromolecules, although ammonium/ammonia supports the fastest growth and is therefore considered its preferential nitrogen source, as also true for *Escherichia coli* (135) and other enterobacteria. Environmental availability of nitrogen is positively correlated to intracellular glutamine concentration, low levels of which result in activation of NtrBC two-component signaling and expression of ~100 genes involved in nitrogen scavenging and assimilation of ammonium or alternative nitrogen sources, including amino acids and (under low oxygen conditions) nitrate (136). Thus, prior studies have focused on the role on NtrBC as a regulator of nitrogen metabolism and coping with nitrogen-limitation (136,137).

Ammonium is taken up across the inner membrane of bacteria through a transporter encoded by *amtB* and is assimilated to glutamine by *glnA* and then glutamate by *gltD* (135). The expression of each of these genes is enhanced by NtrBC signaling during times of N-limitation to scavenge ammonium that may remain in the environment (131) in all Gram-negative species. Nitrate assimilation is thought to be the predominant form of nitrogen metabolism exhibited by *P. aeruginosa* growing in biofilms in the CF lung environment, where oxygen availability is low, and nitrate is abundant (137). Nitrate can be transformed into ammonium through dissimilatory nitrate reduction, involving the products of the *nar* or *nap* operons for conversion of intracellular or

periplasmic nitrate to nitrite, respectively, and *nirBD* for conversion of nitrite to ammonium. Nitrate can also be transformed into nitrite and then ammonium through assimilatory nitrate reduction, involving products of the *nas* operon and *nirA*. Three operons are involved in nitrate reduction to gaseous nitrogen through denitrification: the *nar* operon encodes the reductase that converts nitrate into nitrite, the *nir* and *nor* operons encode the enzymes that detoxify nitrite to nitric oxide and nitrous oxide, and the *nos* operon converts nitrous oxide to inert nitrogen gas (137). These forms of nitrogen can then be shuttled into amino acid metabolic pathways, representing a link between nitrogen and carbon metabolism as many amino acids are catabolized to provide sources of carbon (138). Timely expression of each operon in these metabolic pathways is coordinated by regulators including *nasR* and *nalA*, both of which depend on NtrC for transcription in *P. aeruginosa* and other species including *Klebsiella pneumoniae* and *E. coli*.

1.4.4 NtrBC could link nitrogen metabolism to adaptation

Some enteric pathogens like *E. coli* encode an additional regulatory nitrogen assimilation control (Nac) protein, which is expressed from an NtrC/σ^{54}-dependent promoter (139). In turn, Nac can promote transcription of genes from promoters that depend on σ^{70}-type alternative transcription factors (136,139) including RpoS. This alternative sigma factor is considered a general regulator of adaptation to various stressors (140,141) in Gram-negative pathogens, including *P. aeruginosa*. Therefore, in some species, there is a link between N-stress and general stress responsiveness (Fig. 1-3), which is critical for adaptation to the host environment (including the display of adaptive phenotypes e.g., biofilm formation) and is associated with antimicrobial resistance (141).

When nutrients are not limiting during exponential growth, *P. aeruginosa* expression of *rpoS* remains low. RpoS levels are increased several-fold during stationary phase, when nitrogen and carbon may be depleted from the growth medium, and *rpoS* is known to be regulated by *P. aeruginosa* QS systems including *lasRI* and *rhlRI* (142), which also regulate the expression of virulence factors (see subsection 1.2.3). Relative to *E. coli*, RpoS seems to play a minor role in adaptation by *Pseudomonas* spp. to carbon starvation (143,144), which is co-regulated by RpoS and RpoN. This suggests that NtrC could impact on *P. aeruginosa* stress responsiveness induced by deprivation of nutrients other than nitrogen, despite the lack of a gene homologous to *nac* in the chromosome of this species. NtrC also directly enhances *E. coli* transcription of the (p)ppGpp synthetase, RelA, from an RpoN-dependent promoter during N-limitation (136). Accumulation of (p)ppGpp is largely responsible for triggering the stringent stress response (145) that, in conjunction with RpoS, maintains bacteria during the stationary phase. This is partly accomplished

by binding certain sigma factors and interfering with their transcriptional activity (146), inhibiting the transcription of genes involved in translation (e.g *rpsA*, *rmpH*, *rrsC*), nucleotide metabolism (e.g., *apt*) and (p)ppGpp degradation (e.g., *spoT*), while promoting the transcription of genes involved in nutrient scavenging and adaptation. Whether NtrC directly enhances transcription of RelA and impacts on stringent stress responsiveness in *P. aeruginosa* remains to be determined.

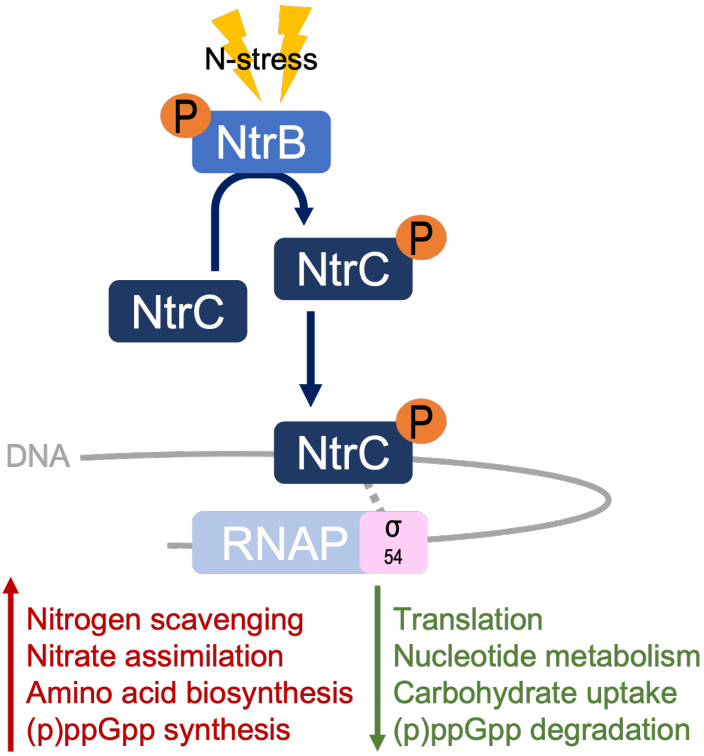

Figure 1-3. NtrC enhances transcription of genes from RpoN (σ^{54})-dependent promoters. N-stress leads to NtrB autophosphorylation and phosphorylation of NtrC. NtrC then binds DNA upstream of σ^{54}-dependent promoters and interacts with σ^{54}-RNAP holoenzyme following DNA bending facilitated by chaperone proteins (not shown). ATPase activity of NtrC enables open complex formation by RNAP holoenzyme and transcription initiation of genes involved in nitrogen scavenging, nitrate assimilation, amino acid biosynthesis and synthesis of the alarmone (p)ppGpp. This is associated with inhibition of translation, nucleotide metabolism, carbohydrate uptake and (p)ppGpp degradation.

Despite what we know about the role of NtrBC in nitrogen metabolism and other physiological processes of *P. aeruginosa*, few studies have examined its direct role in resistance, virulence, and pathogenesis, as has been investigated with *E. coli*. However, computational analyses of RNA-Seq and Tn-Seq data predicted that NtrC is required for full virulence of *P. aeruginosa* in acute and chronic wound infections (147). As well, preliminary experiments revealed that a mutant with a transposon inserted into the *ntrB* coding sequence was defective for surface colonization phenotypes including biofilm formation and swarming motility (38). Thus, NtrBC could represent

a novel target for the development of new antimicrobials that inhibit surface colonization phenotypes, virulence factor production and/or pathogenesis during *P. aeruginosa* infections of the upper respiratory tract of CF patients or skin wounds.

1.5 Hypothesis and Objectives

My dissertation project focused on the previously unstudied role of NtrBC in pathological processes of *P. aeruginosa*, in which adaptation and virulence are implicated. I hypothesized that deletion of *ntrB*, *ntrC* and *ntrBC* from the chromosome of a *P. aeruginosa* laboratory reference strain (PA14) or clinical isolate (LESB58) would cause defects in swarming, surfing, and biofilm formation, in addition to impacting on intercellular interactions between bacterial species and/or the host.

1.5.1 Objectives

1. Study the role of NtrBC in adaptive phenotypes in vitro.

   Approach: mutant strains were created using well-established protocols and confirmed by sequencing. Mutant strains were assessed for swarming, surfing, and biofilm phenotypes, as well as screened for antimicrobial susceptibility. Transcriptional profiles of mutants were characterized using RNA-Seq.

2. Study the impact of NtrBC on host-pathogen and interspecies interactions in vitro.

   Approach: host-directed cytotoxicity of strains toward human bronchial epithelial cells, as well as uptake by macrophages and neutrophils, was measured. Virulence factor production by strains was also assessed. Anti-Staphylococcal activity of strains was measured. Monomicrobial and polymicrobial biofilm formation on human skin equivalents was studied.

3. Design a model of upper respiratory tract infection.

   Approach: use luminescently-tagged reporter strains of bacteria (clinical isolates) to monitor infection progression non-invasively. Use fluorescent probes to monitor inflammatory responses to infection in situ. Collect samples for determination of bacterial load and production of immune factors such as cytokines.

4. Study tissue specific NtrBC regulation of invasiveness and virulence in vivo.

   Approach: inoculate mutants into the respiratory tract or skin of mice and monitor clinical welfare of the animals for up to three days. Compare bacterial load and tissue damage across

conditions for determining relative importance of NtrBC. Test susceptibility of mutants to antibiotics in vivo. Form monomicrobial and polymicrobial infections to determine the role of NtrBC in interspecies competition in vivo.

Chapter 2: NtrBC regulates invasiveness and virulence of *P. aeruginosa* during high-density infection

2.1 Introduction

Nitrogen is an essential element of life that is critical for the synthesis of proteins and nucleic acids constituting 3% of the human body by mass (148) and 14% of bacterial cells on average. Pools of inorganic and organic nitrogen are found in the soil, water, and atmosphere (149). Despite their abundance, environmental forms of nitrogen are largely inaccessible to plants and animals and must be transformed for biological use. Transformation of nitrogen into its several oxidation states (e.g., nitrate, nitrite, nitrous oxide, nitrogen gas, etc.) is dependent on microbial, especially bacterial, activity and can occur through nitrification, denitrification, or nitrogen fixation among other processes (150). *P. aeruginosa* thrives in a wide range of environments, within and outside the host, and is an important symbiont that provides oxidized nitrogen to plants through physical association in the rhizosphere (151).

P. aeruginosa is known for its ability to adapt to many environmental circumstances, which is reflected by numerous regulatory networks essential for sensing and responding appropriately to stimuli (152). The rapid response to environmental changes is often mediated by signaling through two-component systems, which are often encoded as a sensor kinase and cognate response regulator under the control of a single promoter, and these systems can be activated by the binding of a particular stimulant to the sensor kinase (127,128).

NtrBC is a two-component system that is structurally conserved but functionally distinct across bacterial classes (153,154). Nonetheless, it has been described as responsive to intracellular glutamine levels and is important for general nitrogen regulation and nitrate assimilation. Molecular characterization of NtrBC activity in *P. aeruginosa* is limited and most studies of primary nitrogen metabolism have been performed in distinct species such as *E. coli* (132,133,135). Upon stimulation, the sensor kinase NtrB autophosphorylates and a phosphate group is transferred to its cognate response regulator NtrC for activation (133). NtrC mediates the expression of genes implicated in numerous other physiological processes, by enabling open complex formation by the RNAP-holoenzyme including the alternative sigma factor RpoN/σ^{54}, best recognized for its transcriptional regulation of genes involved in bacterial stress responses (130).

In contrast to its potentially beneficial role in the rhizosphere, *P. aeruginosa* is listed among the

most threatening opportunistic human pathogens for which new antibiotics are urgently needed (35). It is a major cause of nosocomial (hospital-derived) infections, causing 10-15% of all nosocomial infections worldwide (155), particularly of the lung. It is well known for causing chronic, eventually fatal, lung infections in patients with the monogenetic disorder CF, as well as being associated with chronic obstructive pulmonary disease and localized infections. In each of these instances, *P. aeruginosa* may undergo formation of biofilms, which is an adaptive growth state that is associated with antibiotic resistance, immune evasion and metabolic traits distinct from those of late stationary phase cells (156). *P. aeruginosa* may form biofilms or exhibit other adaptive surface colonization phenotypes in these contexts to cope with environmental stressors (6,10-12). A virulent laboratory strain (e.g., PA14) is used to model surface motilities such as swarming in vitro, since it displays these phenotypes readily, whereas a less motile CF clinical isolate (e.g., LESB58) is used to model longer-term infections in vivo (17,124) since it causes less mortality due to dissemination.

Motile strains of *P. aeruginosa* benefit by migrating toward certain optimal nutrient sources and migrating away from unfavourable growth circumstances, enabling them to colonize new environments including host tissues distal to the site of infection (19). Motility also enables migration to locations where more persistent lifestyles can be adopted by forming surface-associated biofilms (11). Adaptive surface-associated motility, in the form of swarming and surfing in *P. aeruginosa*, is thought to enable the spread of bacteria on surfaces of the body, such as in the lungs. Consistent with these roles, adaptive motility is intrinsically associated with bacterial metabolism and often coupled with the expression of virulence factors (16,23,24). Phenotypic screening of transposon mutants revealed that NtrC contributes to swarming motility (26).

Here, I examined the role of NtrBC pathogenesis in vivo using a murine abscess model of high-density infection and showed its involvement in invasiveness (using strain PA14) and virulence (using strain LESB58) of *P. aeruginosa*. Accordingly, NtrBC deletion from the chromosome of *P. aeruginosa* PA14 completely inhibited or significantly reduced swarming motility and biofilm formation, respectively. These data were explained by the dysregulated expression of hundreds of genes in deletion mutants that, taken with the phenotypic data, suggests a global role for NtrBC as a regulator of adaptive resistance and virulence that has not been appreciated heretofore.

2.2 Materials and Methods

2.2.1 Bacterial strains and growth conditions

Bacterial strains and plasmids used in this Chapter are described in Table 2-1.

Table 2-1. Bacterial strains and plasmids used in Chapter 2.

Strain or plasmid	Relevant characteristics	Ref.
Escherichia coli		
XL-1 Blue	*recA1 endA1 gyrA96 thi*-1 *hsdR17* (rK- mK+) *supE44 relA1 lac* [*F'proAB laclq ZΔM15Tn10*(Tc^r)]	Stratagene
ST-18	*pro thi hsdR*$^+$ Tp^r Sm^r; chromosome::RP4-2 Tc::Mu-Km::Tn7/λ*pir ΔhemA*	157
Pseudomonas aeruginosa		
PA14	WT *P. aeruginosa* UCBPP-PA14	158
PA14 Δ*ntrB*	PA14 *ntrB* chromosomal deletion	This thesis
PA14 Δ*ntrC*	PA14 *ntrC* chromosomal deletion	This thesis
PA14 Δ*ntrBC*	PA14 *ntrBC* chromosomal deletion	This thesis
LESB58	WT *P. aeruginosa* Liverpool Epidemic Strain (LES)B58	159
LESB58 Δ*ntrB*	LESB58 *ntrB* chromosomal deletion	This thesis
LESB58 Δ*ntrC*	LESB58 *ntrC* chromosomal deletion	This thesis
LESB58 Δ*ntrBC*	LESB58 *ntrBC* chromosomal deletion	This thesis
Plasmids		
pEX18Gm	Gene replacement vector, suicide plasmid carrying *sacB*, Gm^r	160
pEX18Gm.Δ*ntrB*	Cloned 0.94 kbp fusion fragment flanking *ntrB,* Gm^r	This thesis
pEX18Gm.Δ*ntrC*	Cloned 1.01 kbp fusion fragment flanking *ntrC,* Gm^r	This thesis
pEX18Gm.Δ*ntrBC*	Cloned 2.48 kbp fusion fragment flanking *ntrBC,* Gm^r	This thesis
pBBR1MCS-5	Broad host-range cloning vector, Gm^r	161
pBBR.*ntrB*	Cloned 1.08 kbp *ntrB* gene, Gm^r	This thesis
pBBR.*ntrC*	Cloned 1.44 kbp *ntrC* gene, Gm^r	This thesis
pBBR.*ntrBC*	Cloned 2.51 kbp *ntrBC* gene, Gm^r	This thesis

Overnight cultures were routinely grown in Luria-Bertani (LB) broth. Overnight and sub-cultures were incubated for no longer than 18 h at 37°C with shaking at 250 rpm. Modified forms of basal medium (BM2), consisting of salts (62 mM potassium phosphate buffer (pH = 7.0), 2 mM $MgSO_4$, 10 μM $FeSO_4$), 0.4% glucose and a nitrogen source (0.1% casamino acids (CAA), 14 mM $NaNO_3$, 14 mM $NaNO_2$, or 7 mm $(NH_4)_2SO_4$) were used for assays unless noted otherwise.

E. coli strains were routinely cultured in double yeast tryptone (dYT) at 37°C while shaking (250 rpm). *E. coli* XL-1 Blue was used as the cloning host and ST-18 was used for biparental mating, for which the medium was supplemented with 100 μg/ml 5-aminolevulinic acid (ALA). For

plasmid selection in *E. coli* donor strains, 12.5 µg/ml gentamicin was added to the growth medium. For plasmid selection in *P. aeruginosa* PA14 or LESB58, 50 µg/ml or 500 µg/ml gentamycin was added to the growth medium. Bacterial growth was monitored by measuring optical density at 600 nm (OD_{600}) with a spectrophotometer (Eppendorf, Mississauga).

2.2.2 General DNA manipulations

Primers used in polymerase chain reaction (PCR) assays are listed in Table A1. High-fidelity PCR was carried out using the Phusion DNA Polymerase (Thermo Scientific) in accordance with the manufacturer's specifications and employing optimized annealing temperatures. Oligomer sequences were based on the genome of *P. aeruginosa* UCBPP-PA14 (GenBank: NC_008463.1) available from NCBI. For PCR reactions, cells were boiled at 98°C with shaking (1,000 rpm) for 10 min and pelleted by centrifugation at 14,500 rpm for 3 min.

Restriction digests were performed using FastDigest restriction enzymes according to the manufacturer's specifications (Thermo Scientific). All ligation reactions were carried out at room temperature using T4 DNA ligase (Invitrogen). DNA purifications were performed using the GeneJET PCR purification kit or the GeneJET Gel extraction kit following the manufacturer's instructions (Thermo Scientific).

2.2.3 Recombinant DNA manipulations

Construction of the knockout vectors was based on the protocol described by Hmelo *et al.* (162). Briefly, 500 bp regions flanking the 5' and 3' ends of PA14 or LESB58 *ntrB*, *ntrC*, and *ntrBC* coding regions were PCR-amplified using respective primer pairs (Table A1). Reverse-complement sequences were added to primers to provide homology between flanking regions for continuous amplification in overlap-extension PCR. After each round of amplification, fragments were gel purified. The fusion product was ligated into the pEX18Gm vector and verified by sequencing (Eurofins, Toronto, ON).

Chromosomal deletions in PA14 or LESB58 (Δ*ntrB,* Δ*ntrC*, and Δ*ntrBC*) were obtained by conjugational transfer of the gene replacement vector into PA14. *E. coli* ST-18 was made electrocompetent by washing with 10% glycerol on ice (4°C). Gene replacement vectors were introduced by electroporation (1.8 kV, 25 µF, 200 Ω). Transformants were selected for with gentamicin (15 µg/ml), and donor as well as recipient strains were scratched from the surface of agar plates, resuspended in one ml of sterile water, and adjusted to an $OD_{600} = 0.1$. One hundred µl of *E. coli* ST-18 was mixed with 200 µl *P. aeruginosa* PA14 or LESB58 and spotted onto dYT

agar plates supplemented with 100 μg/ml ALA for overnight growth. The next day, spots were scratched from the surface of the plate, resuspended in one ml sterile water and diluted 1,000-fold. Dilute suspension (100 μl) was spread on LB agar plates with the appropriate antibiotic incorporated. The next day, single colonies were picked on LB agar plates containing 10% sucrose for counter-selection of mutants from single-crossovers. Gene deletion was confirmed by PCR and sequencing (Eurofins, Toronto, ON).

2.2.4 Construction of complementation plasmids

Construction of complementation vectors was based on the protocol of Kovach *et al.* (163). Briefly, the coding region of PA14 or LESB58 *ntrB*, *ntrC* and *ntrBC* was PCR amplified using appropriate complementation primer pairs (Table A1). PCR products were gel purified and digested with restriction enzymes *EcoRI* and *BamHI*. PCR products were subsequently cloned in *EcoRI*/*BamHI*-digested pBBR1MCS-5. *P. aeruginosa* PA14 or LESB58 were made electrocompetent by washing with 300 mM sucrose at room temperature (20°C) and plasmids were introduced by electroporation (2.5 kV, 25 μF, 200 Ω). Successful transformants were selected by picking on LB agar plates with antibiotic and confirmed by plasmid isolation followed by sequencing (Eurofins, Toronto, ON).

2.2.5 Biofilm formation

Biofilm formation was examined for the PA14 wild-type (WT) and mutants using a high-throughput microtitre assay as described elsewhere (117). Overnight cultures were diluted to a starting OD_{600} = 0.1 in BM2 containing 0.1% CAA and 0.4% glucose, then added to polypropylene 96-well plates (Falcon). Following 18-24 h static incubation at 37°C, biomass was stained with 0.1% crystal violet (CV) and dissolved in 70% ethanol. OD_{595} was read using a BioTek SynergyH1 microplate reader (BioTek, Winooski, VT). Three independent experiments containing three biological replicates each were performed.

2.2.6 Motility experiments

Swarming was examined on BM2 plates containing 0.1% CAA, 0.4% glucose and 0.5% agar. Surfing was examined on modified synthetic cystic fibrosis medium (MSCFM) plates containing 0.4% agar and 0.4% mucin, as previously described (11). Swimming and twitching of PA14 WT and mutants were examined on BM2 (containing 7 mM $(NH_4)_2SO_4$ and 0.4% glucose) or LB plates supplemented with 0.3% or 1.0% agar, respectively. Subcultures were adjusted to a starting OD_{600} = 0.1 in appropriate medium and grown to an OD_{600} = 0.4-0.6 for spot (swarming, swimming, surfing) or stab (twitching) inoculation. Plates were incubated for 18-24 h at 37°C and, in twitching

assays, another 24 h at room temperature (20°C). Plates were imaged with a BioRad ChemiDoc (BioRad, Montreal, QC) and surface area coverage of the plate was measured in ImageJ software (v1.52 q13, NIH: https://imagej.nih.gov/ij/). Three independent experiments containing three biological replicates each were performed.

2.2.7 Rhamnolipid precursor production

To explore the cellular mechanism underlying the motility phenotypes of mutants, rhamnolipid precursor production was analyzed by the agar plate method as previously described (164). The PA14 WT and mutants were grown overnight at 37°C, then spot inoculated onto iron-limited salt medium (0.7 g/l KH_2PO_4, 0.9 g/l $NaHPO_4$, 2.0 g/l $NaNO_3$, 0.4 g/l $MgSO_4$, 0.001 g/l $CaCl_2$, 0.001 g/l $FeSO_4$) supplemented with 0.1% glucose, 0.1% CAA, 0.02% cetyl trimethylammonium bromide (CTAB), 0.0005% methylene blue and 1.5% agar. Plates were incubated for 24 h at 37°C and another 96 h at room temperature. Rhamnolipid precursor production was measured by diameter of the zone of clearance around the colony. Two independent experiments containing three biological replicates each were performed.

2.2.8 Abscess model of infection in vivo

Animal experiments were performed in accordance with the CCAC guidelines and were approved by the University of British Columbia Animal Care Committee (certificate A19-0064). Pathogenesis of PA14 or LESB58 WT and mutants was assessed in vivo using a nuanced subcutaneous abscess model, as previously described (124). Bacterial cultures were grown to an OD_{600} = 1.0 in LB, washed twice in sterile PBS and resuspended to give a final inoculum of ~5 x 10^7 CFU (in 50 µl). Bacteria were injected subcutaneously into the left dorsum of CD-1 mice. Abscesses were formed for 18-72 h, visible dermonecrosis was measured using a caliper at the experimental endpoint and abscesses (or other organs, where applicable) were harvested in PBS for bacterial enumeration on LB agar.

2.2.9 RNA isolation and RNA-Seq

To characterize the molecular mechanism underlying adaptive phenotypes observed, I studied the transcriptomes of surface colonized PA14 WT and mutants. PA14 strains were sub-cultured to an OD_{600} = 0.4-0.6 and spot cultured on BM2 containing 0.4% glucose, 0.1% CAA and 0.5% agar for 18-24 h at 37°C. Cells were harvested from the tips of swarming tendrils in PBS and RNAProtect (2:1) reagent (Qiagen). RNA extraction was performed using the RNeasy Mini Kit (Qiagen) according to the manufacturer's specifications. Contaminating DNA was removed using the

TURBO DNA-free kit (Thermo Fisher) and rRNA was depleted by Reza Falsafi using the RiboZero Bacteria Kit (Illumina). Single-end cDNA libraries were constructed by Reza Falsafi using a KAPA stranded Total RNA Kit (KAPA Biosystems) and libraries were sequenced on an Illumina HiSeq 2500 platform in rapid run mode with 100 bp reads, excluding adapter/index sequences. Arjun Baghela performed RNA-Seq processing that included quality control using fastqc (v0.11.7) and multiqc (v1.6), alignment to the PA14 genome using STAR (v2.6.0a) and read counting using htseq-count (v0.10.0) (165-168). Genome assembly and gene annotations were taken from the *Pseudomonas* Genome Database (169). Genes with fewer than 10 counts in at least three samples were removed to increase detection power for differential expression (DE) analysis. The DESeq2 R package (v1.22.2) was used to perform DE analysis of PA14 mutants versus WT (170). Gene Ontology (GO) enrichment was assessed using the GOFuncR package using GO annotations for the PAO1 reference strain (171).

2.2.10 Real-time quantitative PCR

Real-time quantitative PCR (RT-qPCR) was used to validate expression of select dysregulated genes identified in mutants by RNA-Seq. Reaction samples were prepared using qScript one-step SYBR green RT-qPCR Kit (QuantaBio) with 0.2 ng/µl RNA. Amplification was performed using a LightCycler 96 instrument (Roche, Indianapolis, IN). Gene expression was quantified by the $\Delta\Delta C_t$ method with normalization to *rpoD* expression (172). Primers used for qRT-PCR are listed in Table A1.

2.3 Results

2.3.1 NtrBC was needed for full virulence of *P. aeruginosa* LESB58 in vivo

The murine cutaneous abscess model of chronic infection (124) was used to examine if NtrBC had a role in the pathology associated with infections. *P. aeruginosa* LESB58 is a well-characterized cystic fibrosis isolate that causes chronic lung infection and disseminates less than PA14 from localized infection (abscess) sites, apparently due to less efficient flagella-mediated motility (173). This strain was used to test in vivo growth and virulence of the Δ*ntrB,* Δ*ntrC* and Δ*ntrBC* mutants in longer-term (72 h) infections. Compared to LESB58 WT, abscess size as measured by visible dermonecrosis resulting from Δ*ntrBC* infection was significantly (~50%) reduced, but that of Δ*ntrB* and Δ*ntrC* was not significantly affected (Fig. 2-1A). Complementation of Δ*ntrBC* by introduction of the deleted gene fragment on the cloning vector pBBR1MCS-5 restored the abscess size to that of WT (Fig. 2-1B). In all cases, the number of bacteria recovered from abscesses was not different

between LESB58 strains (Figs. 2-1C,D).

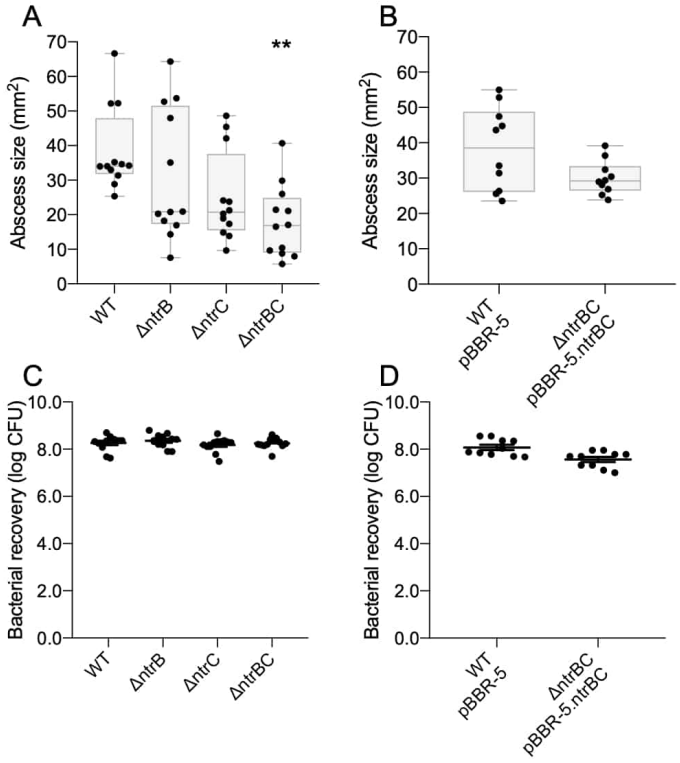

Figure 2-1. Virulence was reduced in LESB58 Δ*ntrBC* compared to the wild-type (WT) in a chronic model of CD-1 murine infection. Abscess size was significantly reduced in LESB58 Δ*ntrBC* compared to the WT (A), but no different than WT control when transformed with plasmid carrying the *ntrBC* gene (B). In contrast, bacterial recovery from abscesses formed by LESB58 mutants or WT were similar (C, D). Box and whiskers delineate interquartile range with geometric error from four independent experiments containing 3-4 biological replicates each (n = 10-12) (A, B). Otherwise, data were reported as mean ± standard error of the mean (SEM) (C, D). ** $P < 0.01$ compared to WT according to Kruskal-Wallis nonparametric test followed by Dunn's post-hoc analysis.

2.3.2 NtrBC was required for *P. aeruginosa* PA14 dissemination in vivo

P. aeruginosa PA14 WT and mutants were next examined for invasiveness in vivo using a shorter-term infection model since dissemination is associated with significant mortality of mice within 36 h (124). Since swarming motility has been associated with invasion of the heart, lungs, liver, spleen and kidneys of mice, and a prior study indicated PA14 Δ*ntrC* was swarming reduced (26), I collected appropriate organs distal to the site of localized abscesses and homogenized the tissues for bacterial enumeration to compare invasiveness between WT and mutants (Table 2-2, Fig. A1).

Bacteria less frequently infiltrated the heart and spleen from abscesses formed by Δ*ntrB,* Δ*ntrC* and Δ*ntrBC* mutants than from abscesses formed by the WT. In instances where mutant bacteria

infiltrated the heart, fewer mutant bacteria were recovered (43- to 275-fold differences); similarly, 13 times less Δ*ntrC* bacteria were recovered from the spleen (Figs. A1A,D). Bacterial infiltration and numbers of bacteria in the lungs were significantly reduced (150-fold) in infections by the Δ*ntrC* mutant (Fig. A1B). Both Δ*ntrC* and Δ*ntrBC* demonstrated reduced infiltration of the liver, but the number of bacteria recovered was only reduced for Δ*ntrBC* abscesses (1,440-fold) (Fig. A1C). Similarly, both Δ*ntrB* and Δ*ntrBC* demonstrated reduced infiltration of the kidneys, but the number of bacteria recovered was only reduced for the Δ*ntrBC* abscesses (17,500-fold) (Fig. A1E). Overall, invasiveness was most reduced in the PA14 Δ*ntrBC* double mutant relative to the WT.

Table 2-2. Invasiveness of PA14 *ntrBC* mutants was reduced in a murine infection model. Dissemination of PA14 wild-type (WT) and *ntrBC* mutant strains from abscess to organs is shown as the frequency of bacterial recovery, and range of bacterial counts in instances of recovery, from four independent experiments each including 1-3 individual mice per bacterial strain *(n* = 9*).* Mutants were significantly reduced for dissemination to some organs compared to WT according to Fisher's Exact Test (* $P < 0.05$).

Organ	Number of mice exhibiting bacteria in various organs (bacterial counts; CFU)			
	WT	**Δ*ntrB***	**Δ*ntrC***	**Δ*ntrBC***
Heart	8 (10^2-10^6)	2 (10^4-10^5) *	3 (10^2-10^3) *	0 *
Lungs	9 (10^2-10^6)	7 (10^2-10^5)	3 (10^2-10^4) *	7 (10^2-10^6)
Liver	8 (10^2-10^5)	5 (10^2-10^7)	3 (10^3-10^6) *	1 (10^2) *
Spleen	9 (10^2-10^6)	4 (10^2-10^5) *	4 (10^2-10^5) *	5 (10^3-10^4) *
Kidneys	7 (10^2-10^7)	2 (10^4-10^5) *	3 (10^3-10^5)	1 (10^3) *

2.3.3 *P. aeruginosa* Δ*ntrBC* had slightly reduced biofilm formation

P. aeruginosa biofilms represent a complex, adaptive sessile growth mode initiated by cell surface attachment to a substrate and switching of cellular physiological status (42,117). Klein et al. (117) revealed that NtrBC had a role in regulating the production of biofilms by *E. coli* under nitrogen limiting conditions. Although the role of NtrBC in biofilm formation has not been tested in more closely related bacteria, NtrC activation in nitrogen limiting conditions in proteobacteria has been shown (129,131). Biofilm formation of PA14 Δ*ntrB,* Δ*ntrC* and Δ*ntrBC* mutants was assessed relative to the WT (Fig. 2-2). Biofilm formation of the Δ*ntrBC* double mutant was significantly reduced (to ~60% that of WT) whereas biofilm formation of Δ*ntrB* and Δ*ntrC* was similar to WT (Fig. 2-2A). Biofilm formation was restored by complementation of Δ*ntrBC* with cloned *ntrBC* (Fig. 2-2B).

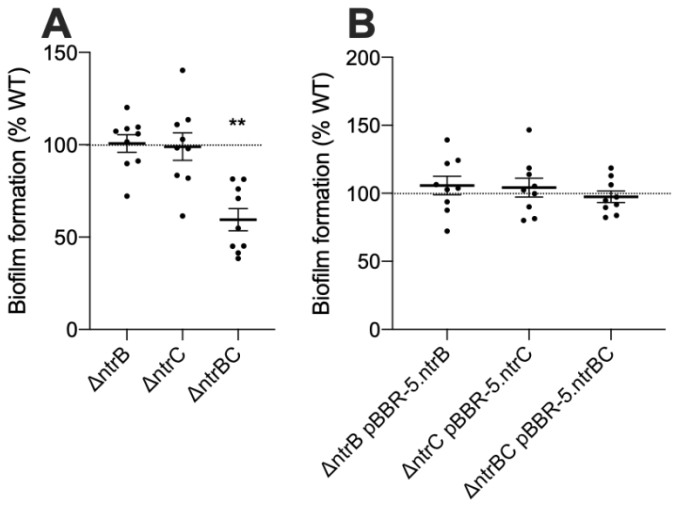

Figure 2-2. Biofilm formation was reduced in PA14 Δ*ntrBC* compared to the wild-type (WT). (A) Biofilm formation was significantly reduced in PA14 Δ*ntrBC* compared to the WT. (B) Biofilm formation was similar in PA14 Δ*ntrBC* transformed with plasmid containing *ntrBC* and WT transformed with plasmid. Biomass was stained with 0.1% crystal violet (CV), dissolved with 70% ethanol and measured (OD_{595}) then taken relative to the WT. Data reported as mean ± standard error of the mean (SEM) from three independent experiments containing three biological replicates each ($n = 9$). ** $P < 0.01$ according to Welch's t-test.

2.3.4 *P. aeruginosa* Δ*ntrBC* strains had altered metabolism of nitrogen

NtrBC has been described as a general nitrogen two-component regulatory system that is responsive to intracellular glutamine levels in various bacterial species (153,154,156). I sought to determine the influence of NtrBC on growth using other nitrogenous compounds such as $NaNO_2$ and $NaNO_3$ in the PA14 wild-type (WT) and Δ*ntrB,* Δ*ntrC* and Δ*ntrBC* mutants (Fig. 2-3, Table A2). There were no differences in overall growth between single deletions grown in BM2 minimal medium that utilized ammonium as a nitrogen source, although the growth kinetics of the double deletion mutant was altered, with a slower growth rate (~4-fold slower) (Fig. 2-3A). The double mutant also exhibited slightly reduced overall growth in BM2 supplemented with 0.1% CAA rather than $(NH_4)_2SO_4$ (Fig. 2-3B). No growth differences were observed between the WT and Δ*ntrB* or Δ*ntrC* under either of these conditions. In contrast, compared to the WT, each of Δ*ntrB,* Δ*ntrC* and Δ*ntrBC* were reduced for overall growth in BM2 supplemented with equimolar $NaNO_2$ or $NaNO_3$ instead of $(NH_4)_2SO_4$ (Figs. 2-3C,D). The growth of mutants was reduced 3- to 10-fold in $NaNO_2$ and 10- to 50-fold in $NaNO_3$ when compared to the WT. Complemented mutants grew like the WT.

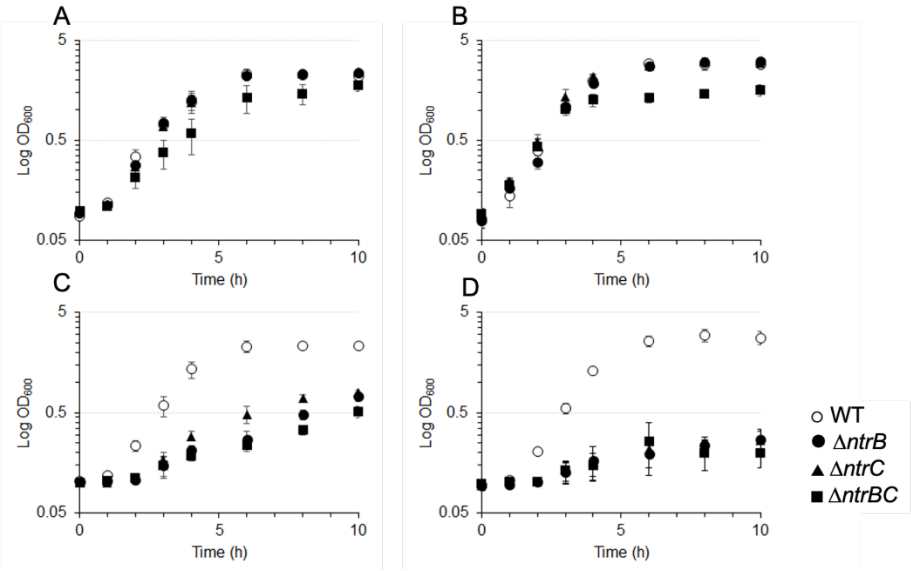

Figure 2-3. Growth of PA14 *ntrBC* mutant strains was influenced by nitrogen source. Bacteria were seeded in (A) basal medium (BM2), and BM2 in which $(NH_4)_2SO_4$ was replaced with (B) 0.1% casamino acids (CAA) (C) 14 mM $NaNO_2$ or (D) 14 mM $NaNO_3$. OD_{600} values were measured. The mean logarithmic OD_{600} ± standard error of the mean (SEM) from three independent experiments is shown (n = 3).

2.3.5 *P. aeruginosa* Δ*ntrBC* had altered swarming and surfing motilities

Rapid surface motilities of *P. aeruginosa,* such as swarming and surfing, represent complex adaptive lifestyles that are regulated by multiple transcription factors and are dependent on the nutrients and viscosity of the media (29,35,127,173). Since NtrBC contributes to *P. aeruginosa* responsiveness to nitrogen and has been implicated in swarming through transposon mutant screens (26), I investigated the ability of PA14 WT, Δ*ntrB*, Δ*ntrC* and Δ*ntrBC* to swarm under nitrogen-limiting conditions. Swarming of Δ*ntrB* and Δ*ntrC* was significantly reduced (~8% surface coverage), whereas swarming of the double deletion Δ*ntrBC* was completely inhibited (~1% surface coverage) relative to the WT (Figs. 2-4A,B).

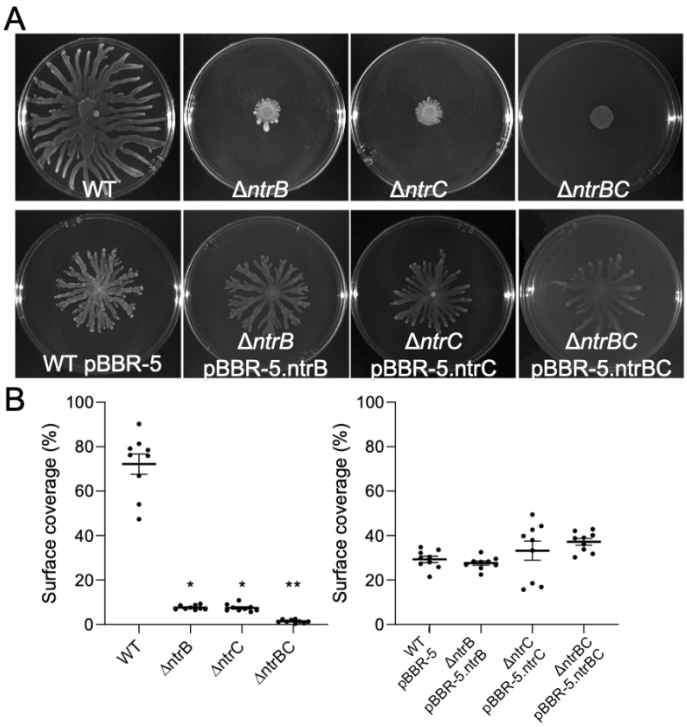

Figure 2-4. Swarming motility was dependent on both *ntrB* and *ntrC*. Shown are representative images of mutants and complemented strains. (A) Swarming motility was reduced or completely inhibited in PA14 mutant strains Δ*ntrB,* Δ*ntrC* and Δ*ntrBC* compared to WT. Swarming motility in PA14 mutant strains transformed with plasmid containing *ntrB*, *ntrC* or *ntrBC* genes was similar to WT transformed with plasmid. (B) Raw surface area coverage (%) of swarming colonies was assessed using ImageJ software. Data reported as mean ± standard error of the mean (SEM) from three independent experiments containing three biological replicates each ($n = 9$). * $P < 0.05$, ** $P < 0.01$ according to Kruskal-Wallis nonparametric test followed by Dunn's post-hoc analysis.

Surfing motility, which is quite different from swarming and occurs in the presence of mucin that is added to mimic the cystic fibrosis lung environment (12,17,36,38), was also investigated. It was found that surfing of PA14 Δ*ntrB* and Δ*ntrBC* mutants was significantly reduced when compared to the WT, although the effect was considerably less (13.5-17.0% reductions) than that observed for swarming (Figs. 2-5A,B). Additionally, the appearance of the Δ*ntrBC* mutant surfing colony was considerably different being thick throughout rather than just at the edge. Swimming and twitching motilities were unaffected by Δ*ntrB* or Δ*ntrC* mutations, with a modest but insignificant swimming effect observed only for the Δ*ntrBC* mutant (Table 2-3). Complementation of mutants by introduction of the respective deleted gene fragment restored swarming and surfing phenotypes to WT levels (Figs. 2-4,2-5).

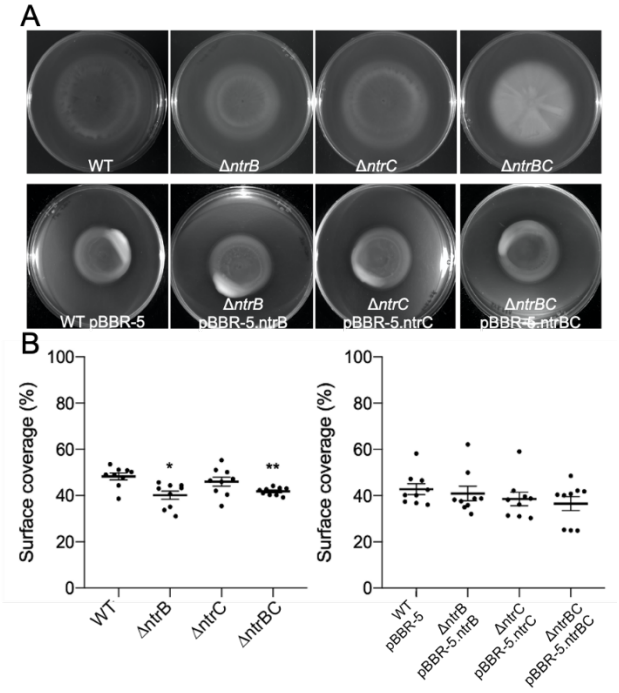

Figure 2-5. Surfing motility of PA14 was modestly reduced in mutants with *ntrB* deleted. (A) Surfing motility was reduced in PA14 mutant strains Δ*ntrB* and Δ*ntrBC* compared to WT. Surfing motility in PA14 mutant strains transformed with plasmid containing *ntrB*, *ntrC* or *ntrBC* genes was similar to WT transformed with plasmid. (B) Raw surface area coverage (%) of surfing colonies was assessed using ImageJ software. Data reported as mean ± standard error of the mean (SEM) from three independent experiments containing three biological replicates each ($n = 9$). * $P < 0.05$, ** $P < 0.01$ according to Kruskal-Wallis nonparametric test followed by Dunn's post-hoc analysis.

Table 2-3. Swarming and surfing motilities were reduced in PA14 *ntrBC* mutants. Motility of PA14 WT and *ntrBC* mutant*s* shown as mean surface area coverage ± standard error of the mean from three independent experiments containing three biological replicates each ($n = 9$). Mutants were significantly reduced for swarming and, more modestly, surfing motilities compared to WT according to a Kruskal-Wallis nonparametric test followed by Dunn's post-hoc analysis (* $P < 0.05$, ** $P < 0.01$).

Motility	**WT**	**Δ*ntrB***	**Δ*ntrC***	**Δ*ntrBC***
Swarming	72.2 ± 4.6%	7.66 ± 0.33% *	7.49 ± 0.54% **	1.45 ± 0.24% **
Swimming	9.87 ± 1.5%	7.85 ± 0.94%	9.97 ± 0.84%	9.24 ± 1.4%
Twitching	6.51 ± 0.42%	6.78 ± 0.55%	6.64 ± 0.47%	4.89 ± 0.63%
Surfing	48.3 ± 1.5%	40.1 ± 1.8% *	46.0 ± 2.0%	41.8 ± 0.55% **

Since I observed that NtrBC was important for growth on various nitrogen sources (Fig. 2-3) and prior research had implied a role for NtrBC in maintaining the carbon/nitrogen balance of *Pseudomonas* (174), I examined the influence of specific nitrogen and carbon growth substrates on the swarming phenotype of PA14 WT (Figs. A2,A3). Substitution of CAA in BM2 swarming media with ammonium sulfate and urea, but not with glutamate or $NaNO_2$, significantly reduced

swarming motility of PA14 WT by 70.8-74.4% (Figs. A2A,B). Although substitution of CAA for $NaNO_3$ caused a modest (23.3%) reduction in swarming, the effect was not statistically significant. Interestingly the swarming colony had quite different branching patterns on each of the permissive nitrogen sources suggesting that higher order features of swarming, not just area surface coverage, depend on nutritional composition of the environment. Similarly, substitution of glucose in BM2 swarming media with equimolar amounts of malate and succinate, but not citrate, significantly reduced swarming motility of PA14 WT by 8.6-46.8% and led to a change in the morphology of the swarming colony (Figs. A3A,B).

2.3.6 Mutants had reduced production of rhamnolipids

Rhamnolipids produced by *P. aeruginosa* reduce the surface tension between bacterial cells and growth medium and are necessary for swarming but not surfing motility (25). To determine whether rhamnolipid production was affected in Δ*ntrB,* Δ*ntrC* and Δ*ntrBC* mutants, I examined their ability to produce rhamnolipid precursors by a well-established agar plate method (164). Rhamnolipid precursor production was reduced on average 67% in the Δ*ntrBC* double mutant as indicated by the smaller zone of clearance surrounding colonies; however, precursor production in the Δ*ntrB* and Δ*ntrC* mutants was similar to WT levels (Fig. 2-6).

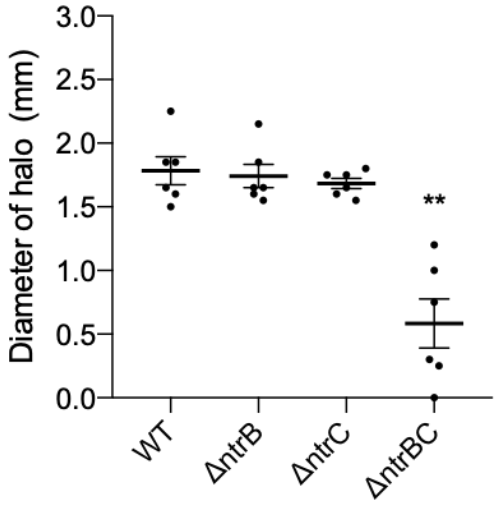

Figure 2-6. Rhamnolipid precursor production was significantly reduced in Δ*ntrBC* when compared to the wild-type (WT). Diameter of halo (mm) was measured following 120 h static incubation at room temperature (RT) on iron-limited salt medium. Data reported as mean ± standard error of the mean (SEM) from three independent experiments containing two biological replicates each (n = 6). ** $P < 0.05$ according to Kruskal-Wallis nonparametric test followed by Dunn's post-hoc analysis.

2.3.7 Mutant transcriptomes revealed massively dysregulated gene expression

To further characterize the molecular mechanisms by which NtrBC contributes to adaptive growth states, RNA-Seq was performed and the transcriptomes of PA14 Δ*ntrB* and Δ*ntrC* mutants were compared to WT under swarming conditions. These mutations substantially influenced the transcriptome of PA14, with 790 and 1184 genes dysregulated in Δ*ntrB* and Δ*ntrC* respectively, of which 682 genes were commonly dysregulated (e.g., Fig. 2-7).

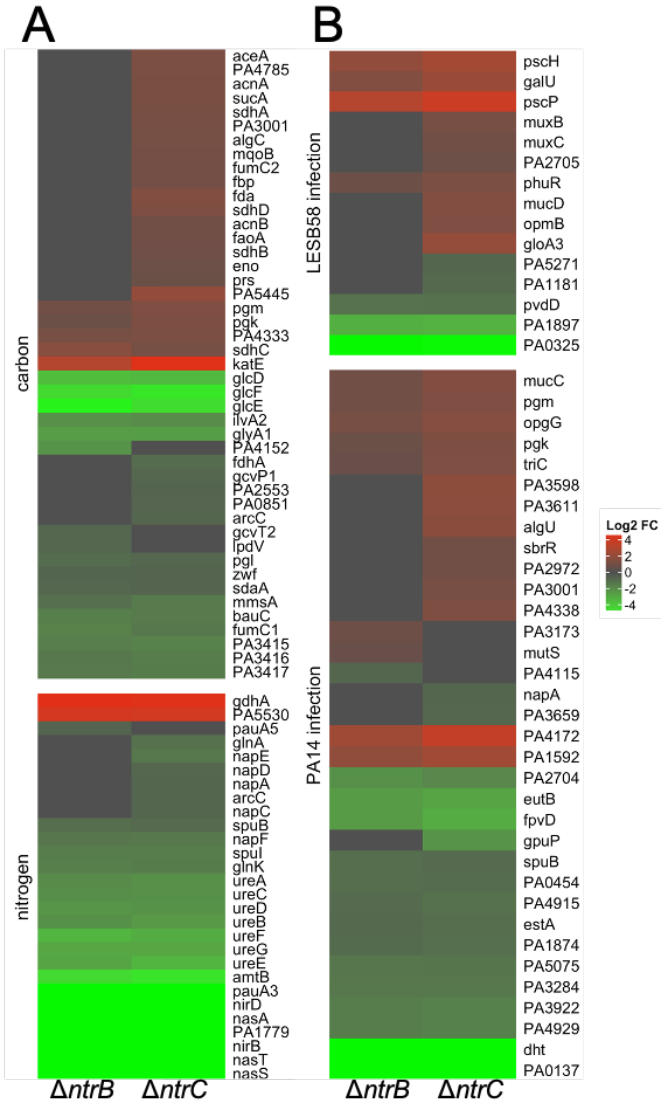

Figure 2-7. NtrBC was a global regulator that influenced expression of genes involved in physiological processes other than nitrogen metabolism. Heatmaps are shown for differentially expressed (DE) genes implicated in (A) carbon or nitrogen metabolism and (B) virulence during acute or chronic airway infection.

The large number of commonly dysregulated genes strongly indicated that in many cases NtrB and NtrC acted as a cognate pair. Conversely, the differences observed, somewhat weighted towards

the Δ*ntrC* mutant, were consistent with phenotypic differences between the two mutants (e.g., in surfing (Fig. 2-5)), and the observation that deletion of either *ntrB* or *ntrC* did not lead to the same phenotypes as deletion of both *ntrBC*, indicating potential cross talk with other regulators.

Several dysregulated genes are involved in general nitrogen and carbon metabolic processes according to the Kyoto Encyclopedia of Genes and Genomes (KEGG; https://www.genome.jp/kegg/) database (Fig. 2-7A, Table 2-4). Regarding nitrogen metabolism, genes involved in ammonium uptake, nitrate and nitrite assimilation, glutamine or glutamate synthesis and metabolism, and urea detoxification and assimilation were downregulated by 1.5- to 650-fold, generally in both mutants (Table 2-4A). Significant downregulation was also observed for many important carbon metabolism genes (Table 2-4B) including cognate pyruvate dehydrogenase genes PA3415-PA3417 and other pyruvate dehydrogenase genes such as PA4152 and *aceEF,* which encode proteins that convert pyruvate into acetyl-CoA for induction of the tricarboxylic acid (TCA) cycle (169). Nearly all enzymes involved in the TCA cycle were dysregulated; for example, fumarase (*fumC1*) and succinate dehydrogenase (*sdhABCD*), which catalyze the reduction of nicotinamide adenine nucleotide (NAD^+) for shuttling electrons to the ETC were upregulated, although other functionally redundant genes were downregulated (*fumC2*).

Table 2-4. Selected categories of genes were differentially expressed under swarming conditions in PA14 *ntrB* and/or *ntrC* mutants. Genes in four categories that were differentially expressed according to RNA-Seq in PA14 mutant strains. Gene expression for mutants is reported as fold-change (FC) relative to PA14 wild-type (WT). RNA was isolated using Qiagen RNEasy MiniPrep kit.

PAO1 Locus	Name	Annotation	FC Δ*ntrB*	FC Δ*ntrC*
A. Metabolic genes involved in Nitrogen Metabolism (KEGG)				
PA0296	*spuI*	glutamylpolyamine synthetase	-2.57	-2.56
PA0298	*spuB*	glutamylpolyamine synthetase	-1.87	-1.73
PA3356	*pauA5*	glutamine synthetase	-1.51	-1.47
PA1783	*nasA*	nitrate transporter	-16	-650
PA1781	*nirB*	assimilatory nitrite reductase large	-50	-137
PA1780	*nirD*	assimilatory nitrite reductase small	-64.2	-340
PA1779	-	assimilatory nitrate reductase	-39.9	-90.0
PA1566	*pauA3*	glutamylpolyamine synthetase	-42.6	-42.0
PA1172	*napC*	cytochrome c-type protein NapC	-1.08	-1.59
PA1174	*napA*	nitrate reductase catalytic subunit	-1.29	-1.60
PA1175	*napD*	NapD protein of periplasmic nitrate reductase	-1.13	-1.64
PA1176	*napF*	ferredoxin component of nitrate reductase	-2.29	-2.22
PA1177	*napE*	periplasmic nitrate reductase NapE	-1.62	-2.27
PA1785	*nasT*	regulation of nitrate assimilation	-92.8	-83.4

PA1786	*nasS*	Nitrate binding ABC transport protein	-121	-91.2
PA4588	*gdhA*	glutamate dehydrogenase	17.2	16.5
PA4864	*ureD*	urease accessory protein	-3.91	-4.13
PA4865	*ureA*	urease gamma subunit	-3.37	-3.72
PA4867	*ureB*	urease beta subunit	-3.80	-4.46
PA4868	*ureC*	urease alpha subunit	-3.60	-3.80
PA4891	*ureE*	urease accessory protein UreE	-7.86	-5.75
PA4892	*ureF*	urease accessory protein UreF	-6.70	-7.79
PA4893	*ureG*	urease accessory protein UreG	-5.89	-5.97
PA5119	*glnA*	glutamine synthetase	-1.92	-1.98
PA5173	*arcC*	carbamate kinase	-1.25	-1.58
PA5287	*amtB*	ammonium transporter AmtB	-19.2	-15.7
PA5288	*glnK*	nitrogen regulatory protein P-II	-2.51	-2.68
PA5530	-	C5-dicarboxylate transporter	13.3	12.4
B. Metabolic genes involved in Central Carbon Metabolism (KEGG)				
PA0130	*bauC*	aldehyde dehydrogenase	-2.67	-2.45
PA0552	*pgk*	phosphoglycerate kinase	1.57	2.19
PA0555	*fda*	fructose-1,6-bisphosphate aldolase	2.02	2.43
PA0851	-	hypothetical protein	-1.54	-1.56
PA0854	*fumC2*	fumarate hydratase	1.52	1.85
PA1326	*ilvA2*	threonine dehydratase	-3.84	-3.45
PA1562	*acnA*	aconitate hydratase	1.39	2.07
PA1581	*sdhC*	succinate dehydrogenase, cytochrome b556 subunit	2.71	1.91
PA1582	*sdhD*	succinate dehydrogenase (D subunit)	2.20	2.23
PA1583	*sdhA*	succinate dehydrogenase flavoprotein subunit	1.70	2.00
PA1584	*sdhB*	succinate dehydrogenase iron-sulfur subunit	1.55	1.68
PA1585	*sucA*	2-oxoglutarate dehydrogenase E1	1.93	2.06
PA1787	*acnB*	bifunctional aconitate hydratase	1.60	1.77
PA2147	*katE*	hydroperoxidase II	6.56	16.2
PA2250	*lpdV*	lipoamide dehydrogenase-Val	-1.62	-1.31
PA2442	*gcvT2*	glycine cleavage system protein T2	-1.62	-1.47
PA2443	*sdaA*	L-serine dehydratase	-1.64	-1.52
PA2553	-	acyl-CoA thiolase	-1.34	-1.53
PA2634	*aceA*	isocitrate lyase	2.00	2.10
PA3001	*gapA*	glyceraldehyde-3-phosphate dehydrogenase	1.75	1.96
PA3014	*faoA*	multifunctional fatty acid oxidation complex subunit α	1.74	1.75
PA3182	*pgl*	6-phosphogluconolactonase	-1.80	-1.63
PA3183	*zwf*	glucose-6-phosphate 1-dehydrogenase	-1.55	-1.52
PA3415	-	probable dihydrolipoamide acetyltransferase	-2.61	-2.80
PA3416	*pdhB*	Prob. pyruvate dehydrogenase E1 component, β chain	-2.28	-2.55
PA3417	-	pyruvate dehydrogenase E1 component subunit alpha	-2.39	-2.53
PA3570	*mmsA*	methylmalonate-semialdehyde dehydrogenase	-1.92	-2.44
PA3635	*eno*	phosphopyruvate hydratase	1.61	1.61
PA4152	-	branched-chain α-keto acid dehydrogenase subunit E2	-3.96	-1.81
PA4333	*fumA*	fumarase	2.00	2.13

PA4470	*fumC1*	fumarate hydratase	-2.84	-2.31
PA4640	*mqoB*	malate:quinone oxidoreductase	1.57	1.87
PA4670	*prs*	ribose-phosphate pyrophosphokinase	1.62	1.57
PA4785	*yfcY*	acetyl-CoA acetyltransferase	1.26	2.10
PA5110	*fbp*	fructose-1,6-bisphosphatase	1.36	1.83
PA5131	*pgm*	phosphoglyceromutase	1.75	2.31
PA5173	*arcC*	carbamate kinase	1.75	-1.58
PA5192	*pckA*	phosphoenolpyruvate carboxykinase	1.26	1.35
PA5213	*gcvP1*	glycine dehydrogenase	-1.48	-1.61
PA5322	*algC*	phosphomannomutase	1.58	1.90
PA5353	*glcF*	glycolate oxidase subunit GlcF	-15.6	-20.0
PA5354	*glcE*	glycolate oxidase subunit GlcE	-25.5	-16.5
PA5355	*glcD*	glycolate oxidase subunit GlcD	-9.09	-8.42
PA5415	*glyA1*	serine hydroxymethyltransferase	-4.76	-4.96
PA5421	*fdhA*	glutathione-independent formaldehyde dehydrogenase	-1.45	-1.79
PA5445	-	coenzyme A transferase	1.87	3.38
C. Pathogenicity genes required for virulence in rat acute lung infection				
PA0098	-	3-oxoacyl-ACP synthase	-112	-153
PA0158	*triC*	RND efflux transporter	1.51	2.22
PA0287	*gpuP*	sodium:solute symporter	-2.41	-4.01
PA0298	*spuB*	glutamine synthetase	-1.87	-1.73
PA0441	*dht*	phenylhydantoinase	-38.2	-48.4
PA0454	-	hypothetical protein	-1.83	-1.8
PA0552	*pgk*	phosphoglycerate kinase	1.57	2.19
PA0762	*algU*	RNA polymerase sigma factor AlgU	1.45	2.78
PA0765	*mucC*	positive regulator for alginate biosynthesis MucC	1.76	2.47
PA1174	*napA*	nitrate reductase catalytic subunit napA	-1.28	-1.60
PA1596	*htpG*	heat shock protein 90	3.14	4.47
PA1874	-	hypothetical protein	-1.75	-1.89
PA2408	*fpvD*	ABC transporter ATP-binding protein	-4.64	-6.59
PA2704	-	AraC family transcriptional regulator	-3.85	-3.15
PA2895	*sbrR*	SbrR	-1.08	1.76
PA2972	-	Maf-like protein	1.53	1.75
PA3001	-	glyceraldehyde-3-phosphate dehydrogenase	1.75	1.96
PA3173	-	short chain dehydrogenase	1.65	1.34
PA3284	-	hypothetical protein	-2.26	-2.27
PA3598	-	hypothetical protein	1.44	2.98
PA3611	-	hypothetical protein	2.17	2.93
PA3620	*mutS*	DNA mismatch repair protein MutS	1.50	1.39
PA3659	-	succinyldiaminopimelate transaminase	-1.41	-1.61
PA3922	-	hypothetical protein	-2.53	-2.75
PA4024	*eutB*	ethanolamine ammonia-lyase large subunit	-4.66	-5.59
PA4172	-	hypothetical protein	-1.58	8.93
PA4308	-	exonuclease III	-1.03	1.04
PA4338	-	hypothetical protein	1.49	2.26

PA4659	-	MerR family transcriptional regulator	2.72	1.96
PA4915	-	methyl-accepting chemotaxis protein	-1.72	-2.04
PA4929	-	hypothetical protein	-2.56	-2.77
PA5075	-	ABC transporter permease	-2.21	-2.18
PA5078	*opgG*	glucan biosynthesis protein G	1.94	2.57
PA5112	*estA*	esterase EstA	-1.7	-1.88
PA5131	*pgm*	phosphoglyceromutase	1.75	2.31
D. Pathogenicity genes required for virulence in rat chronic lung infection				
PA1695	*pscP*	translocation protein in type III secretion	6.67	10.7
PA2399	*pvdD*	pyoverdine synthetase D	-2.09	-2.00
PA2525	*opmB*	outer membrane protein	1.49	2.32
PA2526	*muxC*	efflux transporter	1.26	1.78
PA2527	*muxB*	RND efflux transporter	1.41	1.95
PA0325	-	ABC transporter permease	-36.4	-31.0
PA2705	-	hypothetical protein	1.20	1.62
PA2023	*galU*	UTP-glucose-1-phosphate uridylyltransferase	2.36	3.86
PA1897	-	hypothetical protein	-6.91	-7.42
PA1721	*pscH*	type III export protein PscH	3.24	4.79
PA1181	-	sensor protein	-1.62	-1.68
PA0766	*mucD*	serine protease MucD	1.75	2.40
PA4710	*phuR*	heme/hemoglobin uptake outer membrane receptor	1.60	2.16
PA5111	*hsiC3*	lactoylglutathione lyase	2.15	-2.71
PA5271	-	hypothetical protein	-1.04	-1.59

There was also differential expression of genes necessary for full virulence in acute (175) or chronic (176) lung infection models in rats (Fig. 2-7B, Tables 2-4C,D) consistent with our in vivo studies that indicated a role for NtrBC in *P. aeruginosa* pathogenicity (Figs. 2-1, A3, Table 2-3). Downregulated pathogenicity genes included a putative 3-oxoacyl-ACP synthase PA0098 (112 to 153-fold downregulated), an ABC transport permease PA0325 (36- to 31-fold downregulated), *dht* (38- to 48-fold downregulated), ferri-pyoverdine transporter *fpvD* (4.6- to 6.6-fold downregulated), pyoverdine synthase D (2-fold downregulated) ethanol ammonia lyase *eutB* (4.6- to 6.6-fold downregulated), hypothetical protein PA1897 (6.9- to 7.4-fold downregulated) and 16 others. Genes that intersect virulence and metabolism were the most downregulated including PA0098 and *dht*, which are involved in catabolism of fatty and amino acids respectively. Other downregulated genes that intersect metabolism and virulence included *gpuP*, *glnA*, *pgk* and *hsiC3*. Overall, genes involved in virulence were more upregulated than downregulated in Δ*ntrB* and Δ*ntrC*. Upregulated genes included *muxABC* and *opmB*, components of a resistance-nodulation-cell division (RND)-type multidrug efflux pump, as well as *pscH, pscP* and *phuR,* that encode extracellular membrane proteins involved in the T3SS and heme uptake, respectively (169). The DNA repair protein

exonuclease III (PA4172) was the most highly upregulated (by 4.2- to 8.9-fold) of these virulence genes of interest.

2.4 Discussion

In these experiments, the impact of NtrBC on in vivo invasiveness and virulence was examined, as well as surface colonization and growth in the presence of different nitrogen- and carbon-containing compounds. Deletion mutants Δ*ntrB*, Δ*ntrC* and Δ*ntrBC* exhibited significantly reduced growth in the presence of $NaNO_3$ or $NaNO_2$ and, for the double deletion only, moderately reduced growth in the presence of $(NH_4)_2SO_4$ or CAA as the sole nitrogen source (Fig. 2-4). Reduced growth in the presence of nitrate and nitrite was predicted since NtrC is known to activate the expression of several key genes involved in nitrate assimilation in other species of proteobacteria (153,154). Accordingly, the gene expression data presented here indicated that transcription of *nas* (nitrate assimilation), *nir* (assimilatory nitrite reductase) and PA1779 (assimilatory nitrate reductase) were downregulated by 92.8- to 650.6-fold in Δ*ntrB* and Δ*ntrC* mutants under swarming motility conditions that require weaker nitrogen sources (Fig. 2-7, Table 2-4).

These data reinforce the concept that many adaptive growth phenotypes of bacteria are at least partly dependent on the nutritional status of the environment (34,39,42,48), indicating it is important to improve our understanding of the sophisticated mechanisms underlying *P. aeruginosa* carbon and nitrogen metabolism. Consistent with this, a targeted screen of 113 PA14 mutants with transposons inserted in a gene encoding a two-component system sensor or regulator revealed that 44 mutants had a swarming phenotype distinct from the WT in a context-dependent fashion (177). Our experiments showed that swarming of PA14 WT was inhibited by the substitution of CAA in swarming media with equimolar urea or $(NH_4)_2SO_4$ but not $NaNO_3$, $NaNO_2$ or glutamate, all of which supported swarming (Fig. A2). These results are interesting when considered in the context of infection, since *P. aeruginosa* preferentially uses nitrate for efficient growth in anoxic environments (178) and nitrate is abundant in the airways of CF patients. Moreover, bacterial detoxification of nitrates and nitrites is essential for surviving host responses and contributes to redox homeostasis and fitness in situ (179).

Swarming of PA14 WT was also inhibited by substitution of glucose in swarming media for equimolar succinate or malate, but not citrate (Fig. A2). Succinate and malate are quickly converted to oxaloacetate or pyruvate through metabolic reactions in the oxidative portion of the TCA cycle (174). These metabolites positively regulate TCA cycle activity and prevent carbon flux through

the glyoxylate shunt, a competing metabolic pathway with a role in mediating bacterial oxidative stress (180). Reduced ability of *P. aeruginosa* to swarm in the presence of these nutrients suggested an adaptive role for carbon and nitrogen metabolism in pathogenesis. This argument is further strengthened by motility experiments that revealed swarming and surfing defects of PA14 Δ*ntrBC* mutants (Figs. 2-4,2-5). Since swimming and twitching motilities were unaffected, it is unlikely that modifications of the flagellum or type IV pili (bacterial appendages required for swimming and twitching, respectively) were the cause of mutant swarming defects (Table 2-3). Instead, motility defects of mutants could at least partially be explained by poorer production of rhamnolipids, which facilitate swarming motility by "lubrication" of the surface (i.e., reduction of surface tension between bacterial cells and the medium) (Fig. 2-6) (10,174). Mutant phenotypes exhibited for surfing motility were less drastic than for swarming motility, probably in part because surfing does not depend on rhamnolipid production, although the lower apparent dependence of surfing on a poor nitrogen source might also play a role (11).

Since NtrC is annotated as an enhancer of RpoN, which influences expression of approximately a fifth of the *P. aeruginosa* genome (128,131,132) and induces cascading transcription of numerous regulatory genes, I anticipated a greater number of genes to be dysregulated in Δ*ntrC* than Δ*ntrB* compared to the WT. Indeed, deletion of *ntrC* caused dysregulated expression of 1,192 genes, whereas deletion of *ntrB* caused dysregulation of 791 genes, 686 of which were commonly dysregulated in Δ*ntrB* and Δ*ntrC*. This result suggested divergence in the regulons of NtrB and NtrC, although further experiments are needed for validation. Nonetheless, the RNA-Seq results described support my hypothesis that NtrB and NtrC have overlapping but unique influences on adaptive lifestyles. The activity of NtrB and NtrC may be at least partly independent of RpoN since there are important differences in gene expression across Δ*ntrB*, Δ*ntrC* and Δ*rpoN* mutants studied independently (181,182). For example, published studies showed that *rpoN* mutation led to direct and substantial downregulation of the T6SS as well as QS signaling. More specifically, the Δ*rpoN* mutants exhibited dysregulated expression of the *pqs* and *lasRI* genes, but upregulation of *rhlAB* genes downstream of the *rhlRI* operon (181,182). The study described in this Chapter showed that while a few T6SS genes such as *vgrG* and *clpV* were modestly downregulated ~2-fold in *ntrC* mutants (Table A3), *pqs* and other quorum sensing genes were not affected and rhamnolipid production was suppressed in the double mutant.

Chapter 3: Development of a murine model of sinusitis for pre-clinical screening of immunomodulatory and antibacterial therapies

3.1 Introduction

Individuals with CF are highly susceptible to respiratory infections due to copious production of mucus in their lungs, which reduces ciliary function and the effectiveness of innate immune responses (183). One-third of *P. aeruginosa* CF infections occur within the first six months of life and, despite reports of transmission between patients, the majority are caused by environmental isolates (184,185), with few exceptions such as epidemic isolates (e.g., Liverpool Epidemic Strains) (176). Although many studies have examined changes in bacterial diversity associated with long-term adaptation to the lung environment during chronic infection, relatively little is known about the early stages of *P. aeruginosa* colonization and pathogenesis. Initial colonization of the nasopharynx and paranasal sinuses has been suggested to facilitate incremental adaptation and physiological optimization for the anoxic conditions characteristic of the CF lung (186,187). The genetic similarity of bacteria isolated from the upper and lower airways over time further suggests that the nasal cavity could be a reservoir for recurrent *P. aeruginosa* and *S. aureus* lung infections (188). Further, 60–80% of CF patients have radiographic evidence of rhinosinusitis, although less than 20% of patients report relevant symptoms (189,190).

Rhinosinusitis is a multifactorial disease characterized by inflammation of the sinus mucosa (191). Symptoms of this disease may include, but are not limited to, nasal congestion, discharge and obstruction, facial pain, edema, or obstruction of sinuses (192,193). The etiology of rhinosinusitis can involve host and/or environmental factors, including sinonasal anatomic abnormalities, scarring of the sinus cavity due to prior injuries, genetic disorders that cause immunodeficiency or autoimmune diseases, fungal or bacterial infection, allergy, and inhalation of pollutants (194). Since this disease is not well defined, diagnosing patients is very challenging. Chronic rhinosinusitis, characterized by persistent symptoms, is particularly troubling since it is often associated with bacterial biofilm infections (194), which are recalcitrant to therapy and recur even after surgical debridement or antibiotic therapy. Multiple immune mechanisms exist at the mucosal surface to influence host-pathogen interactions and may contribute to the aberrant inflammation associated with this condition (195). Thus, a diverse range of factors have been investigated as drivers of rhinosinusitis, including defects in innate immunity (191). Antibiotics are routinely prescribed upon suspicion of bacterial rhinosinusitis. However, antibiotics are only effective in a small subset of patients and inflammation triggered by fungal/viral infection or exposure to irritants

is symptomatically indistinguishable (194,195). Poor antimicrobial stewardship continues to burden the healthcare system and contributes to the increasing prevalence of multidrug resistance in opportunistic pathogens like *P. aeruginosa* and *S. aureus* (41,46). HDPs are promising alternatives to antibiotics since they play essential roles in providing protection against pathogens and modulating immune responses (42).

Pre-clinical animal studies are essential to our understanding of complex host-pathogen interactions and the efficacy of antimicrobial and immunomodulatory therapies. Unfortunately, current murine models of acute bacterial rhinosinusitis have contributed poorly to our understanding of early sinonasal colonization since such infections are often highly invasive and/or ethically or technically challenging (196). Here, I report a simple murine model utilizing bioluminescent and chemiluminescent imaging in live mice, allowing non-invasive monitoring of bacterial infections and the corresponding host response over time in the sinus cavity. This murine model overcomes certain limitations of those previously described since it is technically straightforward, reliable, reproducible and enables application of minimally invasive imaging technologies. The model was adapted for longer-term infections by using epidemic clinical isolates of *P. aeruginosa* (LESB58) or *S. aureus* (USA300 LAC) that persisted in the nasal cavities and elicited prolonged inflammation. This model enabled proof of concept studies to investigate the effectiveness of several HDPs (IDR-1018, DJK-5 and IDR-1002), showing that these peptides were able to provide protection against *P. aeruginosa* or *S. aureus* infections by reducing bacterial burden in the upper respiratory tract and/or modulating the immune response of the mice.

3.2 Materials and Methods

3.2.1 Bacterial strains and culture conditions

Bacterial strains used for the work described in this Chapter are listed in Table 3-1.

Table 3-1. Bacterial strains and plasmids used in Chapter 3.

Strain or plasmid	Relevant characteristics[a]	Ref
Strain		
S. aureus USA300 LAC	Community-acquired MRSA, parental strain	197
S. aureus USA300-*Lux*	pRP1190::*luxCDABE* (*gapA*-Pro, Cm^r)	198
P. aeruginosa LESB58	Liverpool Epidemic Strain (LES)B58, isolated from a CF patient	159
P. aeruginosa LESB58-*Lux*	pUCP::lux*CDABE* (*rpoZ*-Pro, Gm^r)	125
P. aeruginosa LESB65	Liverpool Epidemic Strain (LES)B65, isolated from a	199

	CF patient	
P. aeruginosa LESB65-*Lux*	Chromosomal::*luxCDABE* (*P1*-Pro, Gm^r)	This study
Plasmids		
pUC-mini-Gm-*lux*-*P1*-Pro	pUC18T::mini-Tn7T::*luxCDABE*::*P1*-Pro, Gm^r	200
pTNS2	pTNS::*lacI*-Pro::RSF, Kan^r	201

Bacterial strains were streaked onto LB agar plates from frozen stocks and grown overnight at 37°C. The following day, an individual colony was used to make an overnight culture in LB broth or dYT by incubating bacteria at 37°C with shaking (250 rpm) for no longer than 18 h. Bacterial growth was monitored by measuring OD_{600} with a spectrophotometer (Eppendorf, Mississauga, ON). Subcultures were obtained by diluting overnight cultures to OD_{600} = 0.1 and grown to an OD_{600} = 2.0 for *S. aureus* or 1.0 for *P. aeruginosa* strains. Bacterial cells were washed twice with sterile PBS and resuspended in the appropriate media to the concentrations indicated. For plasmid selection, the following antibiotics were used: 50 µg/ml chloramphenicol for *S. aureus* USA300-Lux, and 500 µg/ml gentamycin for *P. aeruginosa* strains LESB58-Lux.

3.2.2 Generation of *P. aeruginosa* bioluminescent strains

Plasmid pUC-mini-Gm-*lux*-*P1*-Pro (200), with the *P1* promoter driving constitutive expression of the *luxCDABE* operon, was co-electroporated with helper plasmid pTNS2 (201) into *P. aeruginosa* LESB58 or LESB65 cells as previously described (202). Briefly, bacteria were scraped from an agar plate grown overnight and resuspended in 300 mM sucrose prior to washing twice. After the last washing step, pellets were resuspended in 100 µl of 300 mM sucrose and mixed with 500 ng of each plasmid. Cells were transformed via electroporation using an Eppendorf Electroporator 2510 (2.5 kV, 25 µF, 200 Ω). All steps were carried out at room temperature. Cells were recovered for 3 h at 37°C in dYT broth with shaking at 220 rpm after electroporation. Positive clones, showing strong bioluminescence, were selected on LB agar plates containing gentamicin and further verified for correct chromosomal insertion via PCR of the flanking regions with chromosome-specific primers as described previously.

3.2.3 Animal care

Animal experiments were performed in accordance with the CCAC guidelines and were approved by the University of British Columbia Animal Care Committee (certificate A17-0253). Mice used in this study were inbred C57Bl/6 mice (female, aged 11-13 weeks) or outbred CD-1 mice (female, aged 7-9 weeks). All animals were purchased from Charles River Laboratories, Inc. (Wilmington, MA). C57Bl/6 mice weighed 20 ± 5 g at the time of experiment, whereas CD-1 mice weighed 25

± 5 g. Animals were group housed in cohorts of 4-5 littermates exposed to the same bacterial pathogen. Littermates of the same sex were randomly assigned to experimental groups. Standard animal husbandry protocols were employed.

3.2.4 Intranasal infection in vivo

Bacterial subcultures were washed twice with sterile PBS and resuspended at an OD_{600} = 1.0. For longer-term infection, performed by Dr. Grace Choi, LESB65 was washed twice with sterile PBS and then resuspended in sodium alginate (11 mg/ml) (203). Twenty µl of bacteria were instilled, dropwise, into the left naris of mice under anesthesia (2.5% isoflurane) yielding inocula of 10^6 CFU or 10^7 CFU for *P. aeruginosa* or *S. aureus* infections, respectively. Animals were monitored and given heat support immediately following the infection. All animals were allowed to recover from anesthesia before returning them to their cage. Experiments were repeated 2-4 times with 2-3 animals per group. The welfare of mice was monitored by recording clinical score, capturing changes in weight, fur, activity, hydration, breathing, and pain using a mouse grimace scale, at 3-, 24-, 48-, and 72-h post-infection for the acute infection model, while additional monitoring was provided at 120 h for the longer-term infection.

3.2.5 Tracking bioluminescent bacteria in vivo

Disease progression over time, was followed by acquiring bacterial bioluminescence images (60 or 90 s exposure, medium binning) under anesthesia (2.5% isofluorane) at 24- or 48-h intervals, up to 120 h post-infection, using a Lumina *in vivo* imaging system (IVIS) (PerkinElmer, Waltham, MA). Images were analyzed using Living Image software (v3.1) (PerkinElmer, Waltham, MA).

3.2.6 Tracking reactive oxidative species to the site of infection

To detect the production of ROS generated during the innate immune response of the host, a chemiluminescent probe, L-012 (25 mg/kg, Millipore Sigma, Burlington, MA) that has high sensitivity to superoxide and peroxynitrite anions, was used (204). The probe was subcutaneously injected between the ears of the mice at various time points during the infection. The detection of localized signal was optimal within 20 ± 2 min of probe injection. Background noise was indicated as the limit of detection (LOD). Representative images were acquired using a Lumina IVIS (60 s exposure, medium binning) and analyzed using Living Image software (v3.1).

3.2.7 Sample Collection

At the experimental endpoint, mice were euthanized by intraperitoneal injection of sodium

pentobarbital (120 mg/kg), followed by cardiac puncture for blood collection, nasal lavage, and excision of lungs and heads. For nasal lavage, an incision was made one-third of the way down the trachea and one ml of PBS was rinsed through the sinus cavity using an intravenous catheter. For lung tissues, whole lungs were collected in sterile PBS, and homogenized using a Mini Beadbeater-96 cell disrupter (BioSpec Products, Oklahoma, USA) for 5 min. Serial dilutions of nasal lavage fluid and lung homogenate were plated on LB agar for bacterial enumeration, and the remaining liquid was stored at -20°C for use in subsequent assays.

For histopathological studies of the nasal cavity, mice were decapitated, and the head was degloved for optimal perfusion of fixative (10% buffered formalin) into the tissue. Decalcification, cross-sectioning and histochemical staining with hematoxylin and eosin (H&E), as adapted from Lindsay et al. (205), were performed by Wax-It Histology Services Inc. (University of British Columbia, Vancouver, CA). Histological evaluation was performed on samples post-infection, and representative images are shown.

3.2.8 Peptide treatments

Peptides IDR-1018 (VRLIVAVRIWRR-NH_2) (206), DJK-5 (all D-amino acids vqwrairvrvir-NH_2) (104) and IDR-1002 (VQRWLIVWRIRK-NH_2) (207), were synthesized by CPC Scientific or Genscript using solid-phase 9-flurenylmethoxy carbonyl (Fmoc) chemistry and purified to >95% purity using reverse-phase high-performance liquid chromatography (HPLC). The lyophilized peptides were resuspended in endotoxin-free water.

All peptides used for treatment of intranasal infection were tested for toxicity prior to efficacy testing. Peptides were diluted in endotoxin-free water to their desired concentration with consideration of net peptide content (approximately 70% of dry weight). For shorter-term infection, peptides or water (10 µl) were instilled directly into the left naris of mice 24 h post-infection. For the longer-term infection, peptides or water (~10-13 µl) were delivered via Respimat® inhaler (Boehringer Ingelheim, Ridgefield, CT). Progression of disease was monitored, and sample collection was performed as described above.

3.2.9 Cytotoxicity of human bronchial epithelial cells

The SV40-transformed, immortalized human bronchial epithelial (HBE) cell line, 16HBE14o- (208) were cultured in minimum essential medium with Earle's salts (MEM, Gibco, Massachusetts, USA) containing 10% heat-inactivated fetal bovine serum (FBS) (Gibco) and 1% L-glutamine (Gibco), at 37°C in a 5% CO_2 humidified incubator. To passage cells, medium was removed, and

the cells were washed with PBS. Adherent cells were detached with 0.25% Trypsin-EDTA (Gibco, Massachusetts, USA) at 37°C in a 5% CO_2 humidified incubator for approximately 4-6 min. An equal volume of MEM containing 10% FBS and 1% L-glutamine was added to neutralize the reaction. Cells were centrifuged at 1,000 rpm for 5 min, and the supernatant was removed. Fresh media were used to resuspend the cells before seeding into new flasks or plates.

HBE cells were seeded into 96-well plates (~4 x 10^5 cells/well) and incubated at 37°C with 5% CO_2. Media were refreshed the next day, and cells were allowed to grow to confluency in a monolayer. On the day of infection, media were removed and replaced with MEM supplemented with 1% FBS and 1% L-glutamine, and cells were allowed to rest for at least one h. For each replicate, the number of HBE cells per well was determined on the day of the experiment, and the multiplicity of infection (MOI) was calculated.

Sub-cultures of *P. aeruginosa* LESB58 and LESB65 were grown to an OD_{600} = 1.0 in LB broth. Bacterial cells were washed twice with sterile PBS and resuspended in MEM containing 1% FBS and 1% L-glutamine. Pavneet Kalsi infected HBE cells with *P. aeruginosa* LESB58 or LESB65 at a MOI of 1, 5, 10 or 100 for 18-, 24- or 48-h. Cell free tissue culture supernatants were collected at experimental endpoints by centrifugation (4°C, 5 min at 1000 rpm to remove detached HBE cell and debris, supernatant was transferred to new tubes, follow by 5 min at 8000 rpm to remove bacterial cells). Cellular cytotoxicity was determined by monitoring the release of the enzyme lactate dehydrogenase (LDH) in the tissue culture supernatant, using a colorimetric detection assay from Roche Diagnostic (Laval, QC, Canada), according to the manufacturer's instructions. The remaining tissue culture supernatants were aliquoted and stored at -20°C for protein quantification.

3.2.10 Enzyme-linked immunosorbent assay

Nasal lavage fluid, lung homogenates and tissue culture supernatants were aliquoted and stored at -20°C until needed for enzyme-linked immunosorbent assays (ELISAs), as performed by Dr. Grace Choi. Levels of cytokines and chemokines were measured using eBioscience (San Diego, California, USA) antibodies for murine TNF-α and IL-1β and human IL-6. MIP-2 and KC (CXCL1) antibodies were from R&D Systems, Inc. (Minneapolis, MN, USA). Human IL-8 was purchased from Invitrogen (Carlsbad, California, USA). Serial dilutions of the recombinant cytokines or chemokines were used to establish a standard curve for evaluation of the protein concentration in tissue culture supernatants. ELISAs were performed following the manufacturer's protocols with optimization of antibody and sample dilutions, washes, and incubation times. They

were developed using 3,3',5,5'-tetramethylbenzidine (TMB) solution (eBioscience) and the reaction stopped with concentrated (2 N) sulfuric acid. The plates were read on a Power Wave X340 plate-reader (Bio-Tek Instruments) and fitted to a 4-parameter standard curve using KC4 software v3.0 (Bio-Tek Instruments).

3.3 Results

3.3.1 Bacterial bioluminescence could be monitored for up to 24 h in vivo

Development of murine models of rhinosinusitis has been hampered by the tendency of bacteria to disseminate or be aspirated into the lungs of the host to the extent where they cannot be reliably enumerated in the sinus cavity (208). To monitor this phenomenon in the acute rhinosinusitis model, I used bioluminescently tagged strains to follow the ability of clinical isolates *S. aureus* USA300 LAC and *P. aeruginosa* LESB58 to initiate and maintain intranasal infection. Luminescence signals were used to monitor bacterial burden in the nasal cavity in real time (Fig. S4). The bacterial burden over the course of the experiment was further quantified by obtaining CFU counts from the nasal lavage fluid (Fig. 3-1A). Local inflammatory responses were assessed 6 h post-infection by monitoring the production of ROS, expressed as radiance (Fig. 3-1B).

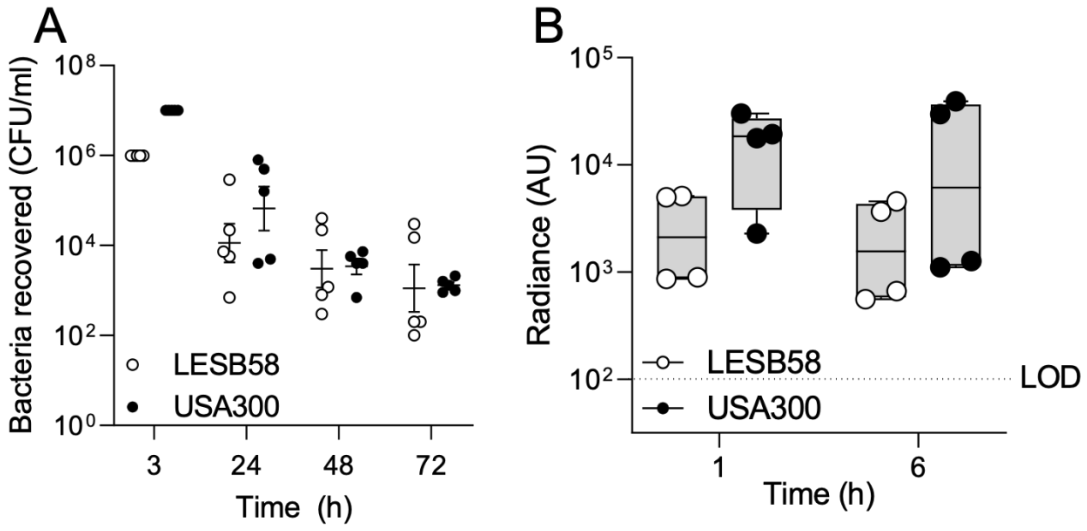

Figure 3-1. Clinically important species of bacteria established acute intranasal infection and elicited reactive oxygen species production. *P. aeruginosa* LESB58-Lux or *S. aureus* USA300-Lux were inoculated dropwise in the left naris of C57Bl/6 mice (10^6 or 10^7 CFU, respectively). (A) Bacteria were recovered up to 72 h post-infection by nasal lavage. (B) Localization of oxidative species to the site of infection was tracked using the chemiluminescent L-012 sodium salt probe (25 mg/kg). Radiance was quantified 1- and 6-h post-infection across species. The limit of detection (LOD) is shown as a dotted line at 10^2 counts. n = 4-5 per time point. Data are shown as mean ± SEM.

Luminescent signals were detected in the nasal cavities, but not in the lungs, of mice administered ~10^7 CFU *S. aureus* USA300-Lux, for up to 24 h post-infection (Fig. 3-2).

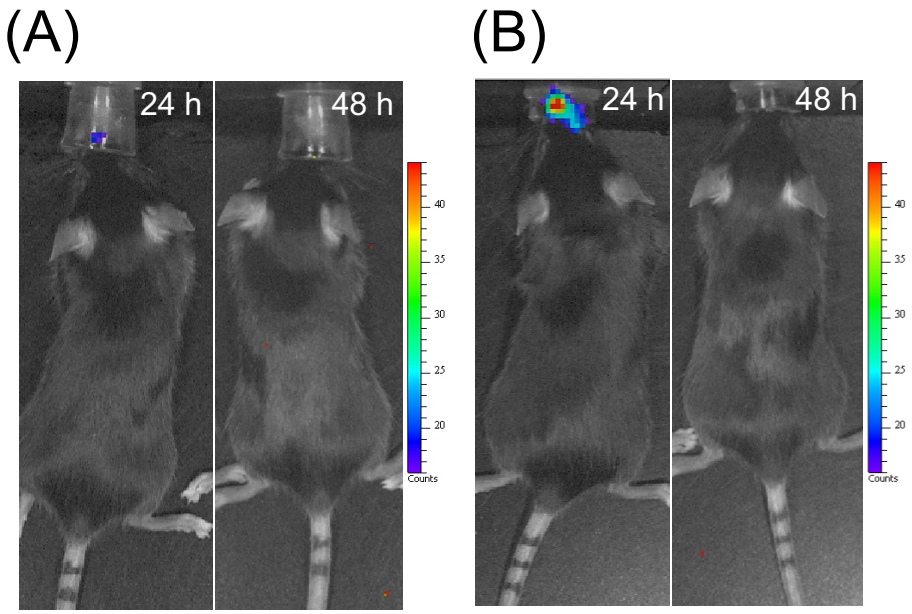

Figure 3-2. Clinically important species of bacteria established intranasal infection. (A) *S. aureus* USA300-Lux or (B) *P. aeruginosa* LESB58-Lux were inoculated dropwise in the left naris of C57Bl/6 mice (10^7 or 10^6 CFU, respectively). Mice were imaged using an *in vivo* imaging system (IVIS) for a maximum of 3 days, but no signal was detected after 24 h. $n = 4$ per time point. One representative image is shown.

The amount of *S. aureus* USA300-Lux recovered by nasal lavage 24 h post-infection was ~10^5 CFU (Fig. 3-1A). Although luminescence could not be detected beyond this time point, the number of bacteria in the nasal cavity was stable for up to 3 days post-infection ($8.4 \pm 1.2 \times 10^3$ CFU). It appears likely that the bacterial counts recovered, especially at 24 h post-infection, and that the numbers of bacteria present were underestimated, possibly due to biofilm formation/aggregation and/or tight adherence of bacteria to tissues. To determine whether aspiration or dissemination could account for the loss of luminescence, bacteria recovered from lung homogenates were examined (Fig. 3-3A).

Like the pattern observed for the nasal cavity, bacterial counts from the lungs were greatest at 24 h post-infection, with $6.2 \pm 3.2 \times 10^4$ CFU *S. aureus* USA300-Lux recovered (Fig 3-3A). Consistent weight loss in mice over time corroborated infection persistence for at least 3 days (Fig. 3-3B). Compared to *S. aureus* USA300-Lux, mice administered ~10^6 CFU *P. aeruginosa* LESB58-Lux expressed stronger bacterial luminescence 24 h post-infection (Fig. 3-2B) and 1.2 ± 2.1 10^4 CFU were recovered from nasal lavage at this time (Fig. 3-1A). Like *S. aureus*, *P. aeruginosa* LESB58-

Lux luminescence could not be detected beyond this time point (Fig. 3-2B), even though 7.2 ± 2.7 x 10^3 CFU *P. aeruginosa* were recovered from nasal lavage 3 days post-infection (Fig. 3-1A). From the lung homogenate, bacterial counts were greatest 24 h after *P. aeruginosa* infection (4.3 ± 2.4 x 10^3 CFU), and the number of bacteria declined thereafter. Mice infected with *P. aeruginosa* also consistently lost weight, but overall animal wellness was stable (Fig. 3-3B).

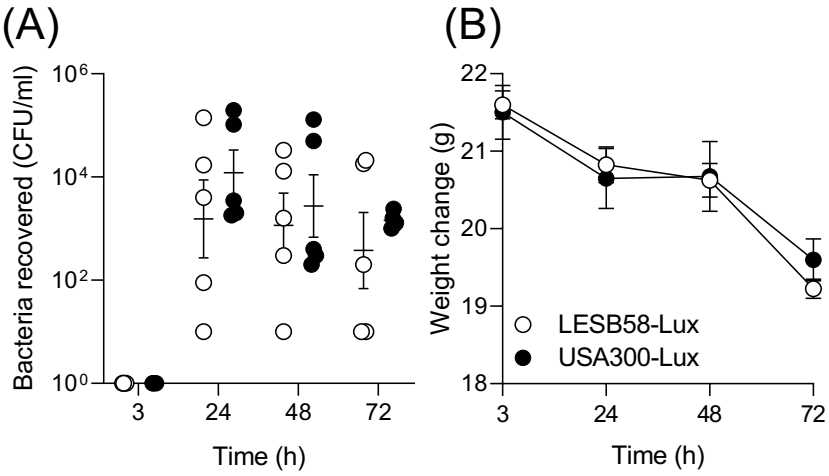

Figure 3-3. Aspiration or dissemination of bacteria from the nasal cavity did not account for loss of luminescence but could have contributed to weight loss following infection. *S. aureus* USA300-Lux or *P. aeruginosa* LESB58-Lux were inoculated dropwise in the left naris of C57Bl/6 mice (10^7 or 10^6 CFU, respectively). Weight was recorded each day following infection. (A) Lung tissue was harvested in 1 ml PBS, homogenized, diluted and plated on LB for enumeration. Bacterial recovery from the lungs was greatest 24 h post-infection. (B) Mice infected with bacteria experienced weight loss over the course of infection but overall animal welfare was stable. Data are shown as geometric mean ± SD.

Bacterial load in the lungs depended on the density of the inoculum used to establish an infection (Fig. 3-4A). Mice inoculated with *P. aeruginosa* LESB58-Lux at higher densities of 10^7 CFU and 10^8 CFU exhibited increased luminescence in the lungs after 24 h than mice inoculated with 10^6 CFU (Figs. 3-4A B). Additionally, mice that were inoculated at a greater density survived less (Fig. 3-4C).

Within 24 h of a higher dose infection, 25-50% of mice reached their clinical endpoint, whereas in the lower bacterial density cohort, all mice survived until the experimental endpoint at 72 h post-infection (Fig. 3-4C). Furthermore, the tendency for bacteria to be aspirated into the lungs of mice depended on host genotype (not shown). CD-1 mice treated with *P. aeruginosa* LESB58-Lux exhibited stronger luminescence in the lungs at 3 h and 24 h post-infection compared to C57Bl/6 mice treated with the same dose of bacteria. Moreover, no signal was detected in the nasal cavities

of CD-1 mice 24 h post-infection. This effect was also observed for *S. aureus* USA300-Lux infection in CD-1 mice.

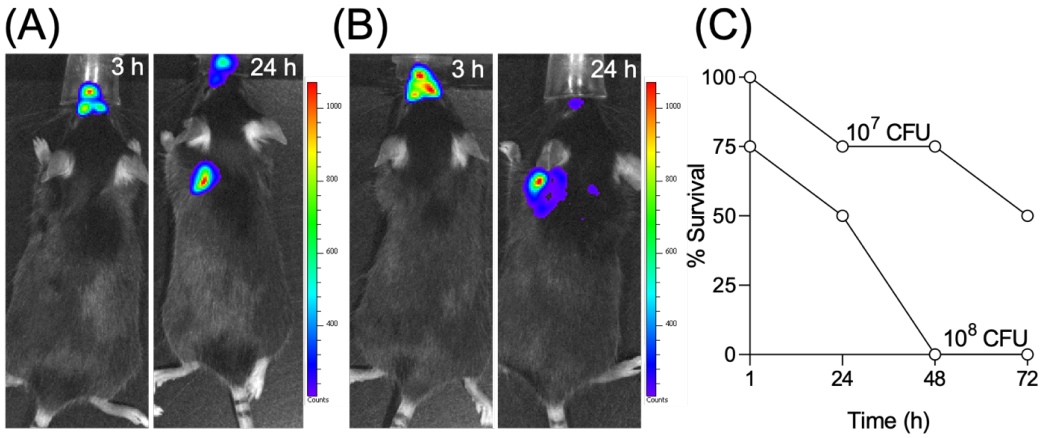

Figure 3-4. Aspiration or dissemination of bacteria from the nasal cavity depended on density of infection and contributed to mortality. (A) Lux-tagged *P. aeruginosa* LESB58 was inoculated dropwise in the left naris of C57Bl/6 mice at densities of (A) 10^7 or (B) 10^8 CFU. Mice were imaged using an in vivo imaging system (IVIS) for a maximum of 72 h. Extent of bacterial aspiration into the lungs was associated with density of infection. (C) Survival (%) of mice (to the humane endpoint) inoculated with bacteria at a lower dose was greater than that for mice inoculated with a higher dose of bacteria. 50% of mice in the lower density cohort, but no mice in the higher density cohort, survived to the experimental endpoint. $n = 4$. One representative image is shown.

3.3.2 *P. aeruginosa* LESB58 induced neutrophil-mediated inflammation

Since acute bacterial rhinosinusitis is associated with neutrophil and macrophage recruitment/activation to help eradicate invading pathogens, partially through an oxidative response, the chemiluminescent probe L-012 (8-amino-5-chloro-7-phenylpyrido[3,4-d]pyridazine-1,4(2H,3H)dione) was used to measure the production of ROS in live mice infected with non-luminescent bacteria (Fig. 3-1B). Strong radiance was detected one h post *S. aureus* USA300-Lux infection (~1.2 x 10^4 radiance), but the signal was more variable after 6 h (Figs. 3-1B, A4A). No signal was detected at 12 h (data not shown). The rapid decline of ROS indicated that the activation of neutrophils and macrophages recruited to the site of infection was transient. When compared to *S. aureus*, *P. aeruginosa* elicited a weaker oxidative response (~2.6 x 10^3 radiance), but ROS measurements were more consistent over-time (Figs. 3-1B, A4B).

Since I observed a rapid induction of ROS in the nasal cavities of infected mice, histological investigations were conducted following *S. aureus* USA300 (Fig. A5) or *P. aeruginosa* LESB58 infection (Fig. 3-5A).

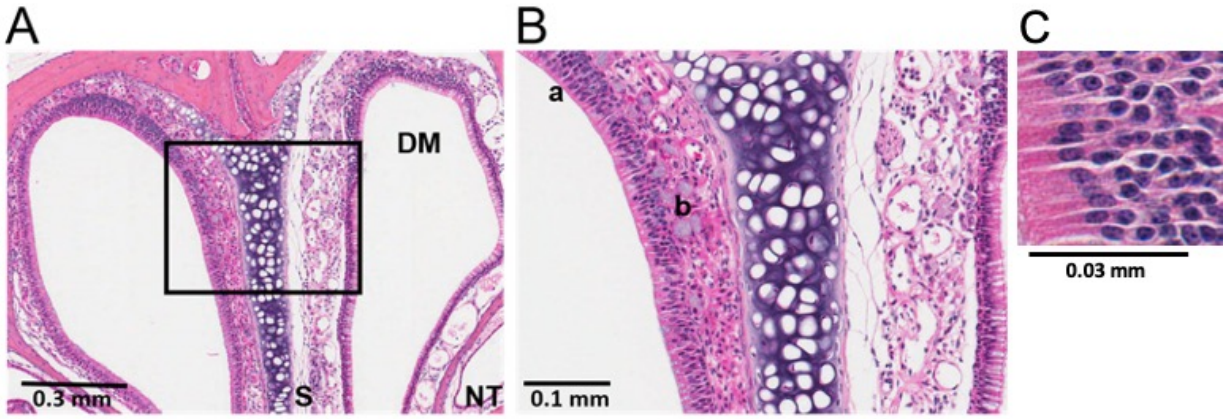

Figure 3-5. Bacterial induction of inflammation in the murine nasal cavity was partially mediated by neutrophils. Histological sections treated with hematoxylin and eosin (H&E) stain revealed reactive mucosa that was most pronounced at 24 h post-infection. *P. aeruginosa* LESB58 was inoculated dropwise in the left nare of C57Bl/6 mice (~10^6 CFU) providing a within-subject control in the right nare. (A) Focal neutrophil infiltration (30-40x more neutrophils per high power field) was observed at a 4 mm deep cross-section of the nasal cavity. Sinus secretions (mucus) with admixed cells were most abundant at 24 h post-infection. (B) Select areas of the field were expanded for visualization of (a) neutrophils and (b) mucus secreting cells. Abbreviations used: DM = dorsal meatus, NT = nasoturbinate, S = septum.

Examinations revealed that bacteria-mediated neutrophil infiltration was most pronounced at 24 h in tissues sectioned in 2 mm increments from the ventral nares, and was sustained for up to 72 h (Figs. 3-5A, A5). As indicated in the Figure, more neutrophils and mucus secreting cells were detected in the mucosa lining the dorsal meatus (DM) of the left nare, when compared to that of the right nare that was not exposed to infection, as early as 24 h post-infection (Fig. 3-5B). Indeed, 30-40x more neutrophils per high powered field were enumerated in the DM of the left nare of mice exposed to either *S. aureus* or *P. aeruginosa*. Similar reactivity was observed in other clinically relevant areas of the sinus cavity, including the ethmoid and maxillary sinuses (ES and MS, respectively) and the nasopharyngeal meatus (NPM) (Fig. A5). Disease progression was indicated by accumulation of mucosal secretions and epithelial damage resulting from persistent reactive mucosa in these regions at 48 h post-infection. Interestingly, the left olfactory bulb (OB) of mice, intranasally exposed to infection, was also inflamed.

3.3.3 Host-defense peptides reduced *P. aeruginosa* LESB58 burden

The increased prevalence of multi-drug resistant strains of pathogens implicated in acute bacterial rhinosinusitis, and the low effectiveness of conventional antibiotics, warrant efficacy assessment of alternative therapies in this context. Synthetic HDPs with known anti-biofilm or antimicrobial activities were administered to mice at the highest possible concentration that did not cause visible

lesioning in lung tissue or impact on animal welfare. HDPs tested were IDR-1018 (7.5 mg/kg), DJK-5 (2.5 mg/kg) and IDR-1002 (7.5 mg/kg). Each HDP reduced bacterial burden of the nasal cavity and improved the overall welfare of mice when administered dropwise into the naris one h after infection (Fig. 3-6).

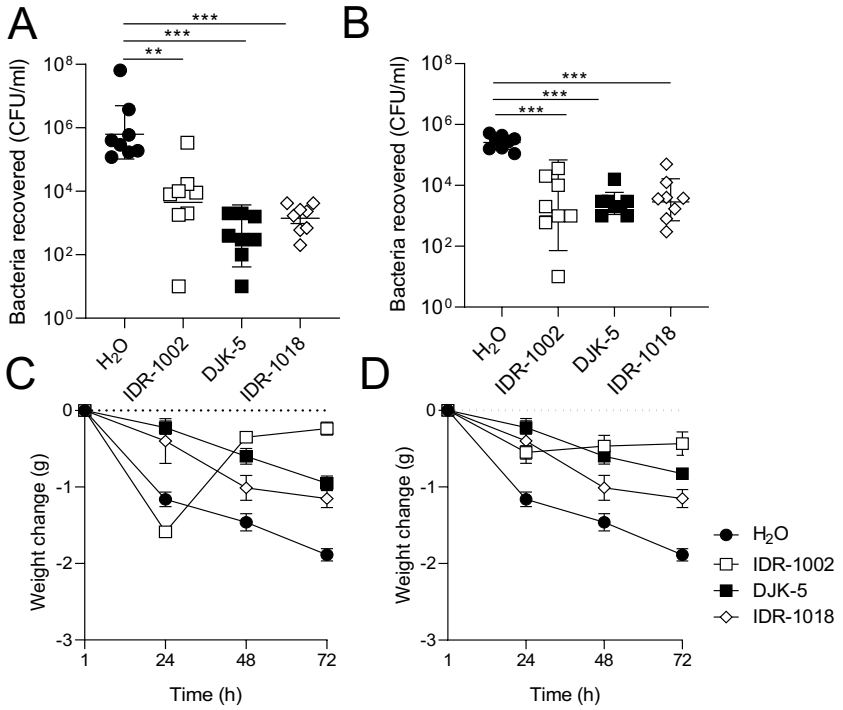

Figure 3-6. Host-defense peptides reduced bacterial load in the nasal cavity and stabilized weight loss following infection. (A, C) *S. aureus* USA300-Lux or (B, D) *P. aeruginosa* LESB58-Lux were inoculated dropwise in the left naris of C57Bl/6 mice (10^7 or 10^6 CFU, respectively). Mice were intranasally treated with endotoxin-free water (vehicle) or peptide (7.5 mg/kg or 2.5 mg/kg for DJK-5) 24 h post-infection. 48 h later, mice were euthanized and bacteria in the nasal cavity were collected by lavage. (A, B) All peptides reduced bacterial burden of the sinuses approximately 100-fold across species. (C, D) Peptide treatment stabilized weight loss or promoted weight gain following infection across species, whereas mice treated with endotoxin-free water continued to lose weight over time. $n = 8$. Data are presented as geometric mean ± SD. ** $P < 0.01$, *** $P < 0.001$ according to Mann-Whitney U-test.

Peptides IDR-1018 and DJK-5 exhibited more potent antibacterial activity than IDR-1002 in the context of *S. aureus* USA300 LAC infection (Fig. 3-6A). Peptides IDR-1018 and DJK-5 significantly decreased *S. aureus* bacterial burden by ~4,275-fold and ~10,500-fold, respectively, while IDR-1002 showed a lesser and non-significant decrease when compared to the vehicle control. Compared to the control group, IDR-1018 and DJK-5 treated mice showed reduced weight loss 72 h after infection with *S. aureus* (Fig. 3-6C). Interestingly, treatment with IDR-1002 caused gain of weight by 48 h post-infection. All peptide treatments exhibited similar antimicrobial activity in the context of *P. aeruginosa* infection, by significantly reducing bacterial burden by 25-

to 100-fold (Fig. 3-6B). In addition, all peptide treatments were able to reduce weight loss post-infection (Fig. 3-6D).

Intranasal administration of a small volume of peptides impacted on lung topology. Peptides (7.5 mg/kg for IDR peptides and 2.5 mg/kg for DJK-5) did not cause lesions or precipitation in the lungs of infected mice (Fig. A6), which were less punctate or discolored than the lungs of infected mice treated with water. These results indicated that peptides protected against bacterial mediated damage in the lungs of mice through antimicrobial and potentially immunomodulatory activity.

3.3.4 *P. aeruginosa* LESB65 persisted in the sinus cavity for up to 120 h

P. aeruginosa LESB65, another clinical isolate identified to persist in the respiratory tract of mice (199) in a distinct pneumonic infection model, was examined by Dr. Grace Choi and Pavneet Kalsi for HBE-directed cytotoxicity relative to that caused by LESB58 (Fig. A7). LESB58 mediated a significant amount of HBE cell death in a dose-dependent manner, in contrast to strain LESB65 that exhibited minimal cytotoxicity (Fig. A7A). LESB65 took 48 h to mediate approximately 45-50% host cell death (Fig. A7B), equivalent to the cytotoxicity cause by strain LESB58 in 18 h (Fig. A7A). ELISAs performed on cell supernatants revealed that LESB65 infection induced secretion of the pro-inflammatory cytokine IL-6 (Fig. A7C) and chemokine IL-8 (Fig. A7D) by HBE cells.

To mimic the alginate-containing biofilm environment during chronic infection, and to determine if the rhinosinusitis model described at present could be amended for longer-term infection, *P. aeruginosa* LESB65-Lux was encapsulated in sodium alginate (11 mg/ml) and inoculated in the left naris of mice (~10^6 CFU) and tracked for up to 120 h (Fig. 3-7) by Dr. Grace Ka-Yee Choi.

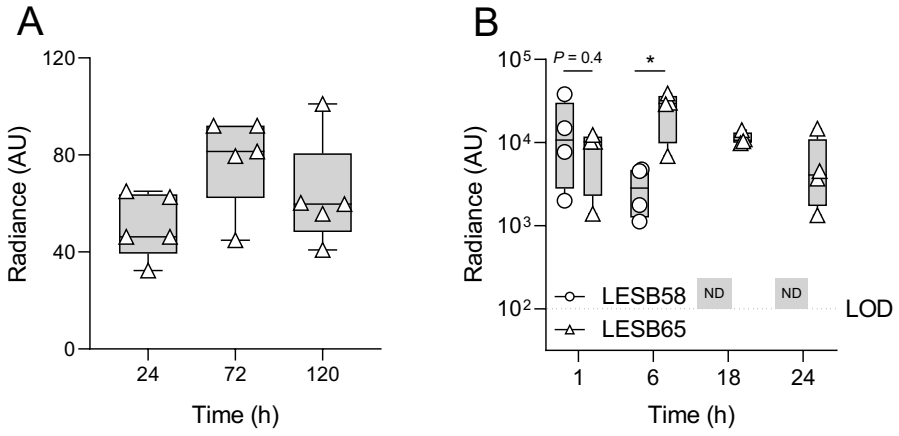

Figure 3-7. *P. aeruginosa* LESB65 persisted in the nasal cavity for up to 5 days and elicited a prolonged inflammatory response. *P. aeruginosa* LESB65-Lux encapsulated in sodium alginate (11 mg/ml) was inoculated dropwise in the left nare of C57Bl/6 mice (~10^6 CFU). (A) Bacterial load was highest 72 h post-infection but was maintained for up to 120 h. These experiments were

performed by Dr. Grace Ka-Yee Choi. (B) Localization of oxidative species to the site of LESB58 or LESB65 infection was tracked using the chemiluminescent L-012 sodium salt probe (25 mg/kg). The signal was not detected (ND) in mice treated with LESB58 beyond 6 h. n = 4-5. Data are shown as geometric mean ± SD. The limit of detection (LOD) is shown as a dotted line at 10^2 counts. These experiments were performed by me. * $P < 0.05$ according to Student's t-test.

Since bacteria were encapsulated in alginate, nasal lavage did not adequately rinse bacteria from the nasal cavity of mice. Instead, radiance was used to estimate the relative bacterial burden in the sinus cavity over time (Fig. 3-7A). The intensity of the radiance increased over time and was strongest at 72 h post-infection (Fig. 3-7A). Thereafter, radiance dissipated slightly, but was maintained for up to 120 h post-infection. The median radiance measured in mice 72 h post-infection (78.0 AU) was slightly higher than 24 h post-infection (50.5 AU) and 120 h post-infection (63.5 AU).

To determine whether *P. aeruginosa* strain LESB65 elicited prolonged inflammation in the nasal cavity compared to LESB58, I measured the production of ROS using the chemiluminescent L-012 probe in live mice (Fig. 3-7B). ROS in the nasal cavity of mice infected with strain LESB65 was like that of strain LESB58 one h post-infection (Fig. 3-7B), which indicated a rapid, robust host oxidative response. However, unlike *P. aeruginosa* strain LESB58, the signal obtained following strain LESB65 infection continued to increase for up to 6 h post-infection and could still be detected 24 h post-infection (Fig. 3-7B). Radiance detected in the nasal cavity of mice infected with LESB58 was stable for up to 6 h but could not be detected at later time points of 18 and 24 h (Fig. 3-7B). At 6 h post-infection, the intensity of the signal detected following LESB65 infection was significantly higher (~10-fold) than that following LESB58 infection. Overall, these results indicate that intranasal infection of LESB65 in alginate sustained a prolonged host inflammatory response.

Dr. Grace Ka-Yee Choi monitored murine weight change, bacterial titre in the lungs and bacteria-mediated immune responses were monitored in the presence and absence of HDPs administered by a Respimat device (Fig. A8). Mice treated with peptides lost weight more rapidly than mice treated with the vehicle during the first 72 h. Mice treated with IDR-1002 or DJK-5 recovered lost weight by 120 h, better than mice treated with IDR-1018 (Fig. A8A). Since nasal lavage did not adequately rinse bacteria from the nasal cavity of mice, only bacterial load from the lungs was enumerated. Like shorter-term infection, treatment with IDR-1018 and DJK-5 significantly reduced bacterial load in the lung, but IDR-1002 demonstrated no significant reduction (Fig. A8B). Last, peptides IDR-1002 and DJK-5, but not IDR-1018, significantly suppressed pro-inflammatory

cytokine IL-6, without effecting KC production (Figs. A8C,D). Taken together, these results suggested that peptides exerted unique activities during *P. aeruginosa* LESB65 infection.

3.4 Discussion

The multifactorial etiology of rhinosinusitis was inadequately understood until recent elucidation of the role of inflammation and likely microbial biofilms in more chronic cases, which are characterized by persistent sinonasal immune responses (195). The mucosal epithelium lining the sinus cavity plays an important role in rhinosinusitis, since it is the first point of contact between the host and pathogens in which various immune signaling cascades are initiated (191,196). Here, I described a preclinical murine model of acute bacterial sinusitis to study pathological mechanisms underlying rhinosinusitis and disease progression. Although the sinus anatomy of mice is not identical to that of humans, the epithelial architecture is the same (208). More specifically, the anterior naris is lined by a pseudostratified, non-ciliated epithelium whereas the rest of the nasal cavity is lined by a ciliated columnar epithelium in both mice and human. Thus, immune cell infiltration and inflammation of the nasal mucosa associated with rhinosinusitis, as well as efficacy of peptides at combatting these properties, can be examined in this model.

In the rhinosinusitis model established here, the C57Bl/6 murine nasal cavity was acutely colonized with clinical isolates of two common pathogens found in rhinosinusitis and in CF patients, *S. aureus* (USA300) and *P. aeruginosa* (LESB58) (Figs. 3-1,3-2). Both strains of bacteria were maintained in nasal cavity for at least 72 h, without compromising the wellbeing of the animals (Figs. 3-1,3-2). Moreover, strong inflammatory responses were elicited, and immune cell infiltration was sustained in the nasal epithelium of mice for the duration of the infection (Figs. 3-1,3-5,3-7). In models with alternate delivery of bacteria, inflammation could not be achieved by acute infection in the absence of nasal obstruction, immune system disturbance, or antibiotic therapy (196). The model described here is, therefore, more representative of the natural acquisition of bacteria from the environment via the nasal (inhaled) route and the early stages of disease pathogenesis. Moreover, this model is more straightforward to execute and less injurious to the host than those previously described. A combination of factors might have contributed to the differences observed in our model including the bacterial strains used, density of inoculant and mouse genotype. For example, *S. aureus* strain Newman is a different clinical isolate that is used extensively in animal models due to its robust virulence phenotypes (209). However, use of this strain was associated with rapid clearance from the nasal cavity, which was partially attributed to competition with resident nasal flora and clearance by immune cells stimulated by microbial

enterotoxins. Interestingly, *S. aureus* strains that were originally isolated from humans, including strains Newman and Reynolds, colonized the nares of mice no better than those originally isolated from mice such as strain DAK (210). Pre-exposure to agents that interfere with immune processes and community interactions enable stable colonization of the murine nasopharynx but limit the ability to subsequently test treatment efficacy. Thus, I turned to strains that have been successfully used in a chronic localized abscess model (124). *S. aureus* USA300 LAC is a less virulent community-acquired epidemic strain that can persist on mucosal surfaces without aberrant immune activation at low density (211), which might be one reason for the suitability of this strain in establishing nasal colonization. Compared to the common *P. aeruginosa* laboratory strains, PAO1 and PA14, epidemic CF clinical isolate LESB58 is less motile (173,212), leading to reduced dissemination from the nasal cavity to the lungs. Furthermore, the LESB58 strain produced more biofilm than PAO1 and PA14. These features might be particularly important in the context of respiratory disorders, especially in CF patients in which mucociliary defense mechanisms are compromised. Further work is needed to characterize the bacterial factors that influence nasal carriage of pathogenic strains and identify effectors of immunity that influence colonization patterns.

Towards this end, my model was amended to study a longer-term infection using a less virulent chronic infection CF isolate, *P. aeruginosa* LESB65 (Figs. 3-7,A7,A8) identified through studies performed in collaboration with Dr. Grace Ka-Yee Choi and Pavneet Kalsi. To mimic the matrix-protected biofilm environment, and to recapitulate mucus build-up in the airways of sinusitis and CF patients, LESB65 was encapsulated in sodium alginate. Others have reported that infections with LESB65 resuspended in PBS solution can last from four days (in BALB/c mice, with 60% of the mice surviving) up to 28 days (in BALB/c OlaHsd mice; survival rate not reported) (187,199). The model described herein allowed infections to persist for at least five days. Notably, all mice survived until the experimental endpoint and developed infections. Although special preparation of inoculant added complexity to the protocol, encapsulation of bacteria did not mitigate host immune responses (Figs. A7,A8). However, alginate interfered with recovery of bacteria by nasal lavage. To overcome this, bacterial load was estimated by measuring radiance arising from luminescent bacteria in situ (Fig. 3-7A). Interestingly, bacterial luminescence peaked 72 h following infection, and slightly decreased thereafter, but could be maintained for up to 120 h post-infection. *P. aeruginosa* LESB65-mediated inflammation in the nasal cavity, as indicated by ROS generation, pathology (not shown), and cytokine production, was also maintained.

Compared to other published models, the model described herein allowed non-invasive tracking of rhinosinusitis progression (Figs. 3-2,3-4). Time-course assessments of bacterial load and host response to acute bacterial rhinosinusitis have relied on progressive sacrifice of different animals and are limited by the instability of reactive metabolites in lavage fluid (196,208). The use of luminescence in this study not only reduced the variability associated with physiological differences between subjects, which in turn allowed more controlled analysis of disease progression, but also reduced costs and were arguably more ethical. ROS contributed to inflammatory disease progression with kinetics typical of what is observed with neutrophils and macrophages that rapidly infiltrate sites of infection to execute innate immune functions, peaking in the first hours following infection (Figs. 3-1,3-7). Bacterial retention in the nasal cavity, despite neutrophilic influx and an oxidative burst, suggested that the model could be applied to study infections longer than five days. Interestingly, the oxidative burst elicited by LESB65 infection was more pronounced and sustained at later time points than that elicited by LESB58 infection (Fig. 3-7).

HDPs and their synthetic analogs are promising antimicrobial and immunomodulatory agents that inhibit biofilm formation in vitro, reduce abscess size and modulate inflammation in vivo (42,65,203). Dr. Grace Ka-Yee Choi and I showed that the synthetic HDPs DJK-5, IDR-1002 and IDR-1018 effectively reduced bacterial load in the nasal cavities of mice exposed to USA300 LAC, LESB58 or LESB65 infections and prevented weight loss associated with disease progression without toxic side effects in the lungs (Figs. 3-6,A8). Interestingly, the peptides prevented extensive punctation and discoloration of the lungs associated with lesions caused by bacterial colonization (Fig. A6). Since bacteria rapidly form biofilms to cope with harsh conditions within the host, treatment administered 24 h post-infection via intranasal installation likely did not wash bacteria into the lungs. Administration of peptides IDR-1002 and DJK-5 reduced bacterial-mediated inflammatory responses in the lung (Fig. A8), while maintaining induced chemokine expression and promoting weight recovery. These data suggest that the peptides can reduce inflammation, while maintaining the ability to recruit immune cells to the lung.

Chapter 4: NtrBC selectively regulates host-pathogen interactions, virulence and ciprofloxacin susceptibility

4.1 Introduction

Eradication of *P. aeruginosa* infection has become very difficult due to its capacity to resist conventional antibiotic therapy through various intrinsic, acquired, and adaptive mechanisms (5,6). Adaptive resistance is often overlooked since it is not genetically encoded (i.e., not observed when organisms are cultured in normal lab media ex vivo), often influences the effectiveness of multiple antibiotics in vivo, and is induced by a wide array of environmental stimuli characteristic of the host milieu including altered pH, oxygen and/or nutrient limitation, as well as antibiotic exposure (6). Importantly, adaptive resistance is distinct from tolerance and persistence, which are characterized by metabolic dormancy that enables bacterial survival but not growth in the presence of antibiotics (213). In contrast, cells exhibiting adaptive resistance can actively divide and adopt 'social' lifestyles such as swarming or surfing motility and biofilm formation (13,14). Adding to their complexity, genetic determinants of adaptive lifestyles and the physical characteristics of swarming or biofilm-forming colonies differ according to the availability of nutrients (111). Consistent with this, I showed in Chapter 2 that *P. aeruginosa* swarming can occur on a variety of carbon and nitrogen sources, but phenotypically varies depending on the composition of the medium.

Similarly, antibiotic susceptibility is dependent on central metabolism and can be potentiated or inhibited by addition of dicarboxylates such as fumarate or glyoxylate, respectively (214,215). Tight regulation of gene expression through two-component regulatory system signaling allows *P. aeruginosa* to rapidly respond to environmental changes, contributing to its adaptability (177). Since the transcriptional profile of *P. aeruginosa* PA14 Δ*ntrB* and Δ*ntrC* demonstrated that genes involved in ciprofloxacin resistance were differentially expressed, I hypothesized that mutants would be more susceptible to ciprofloxacin in vitro. While confirming this data in vivo, I observed that, in the absence of ciprofloxacin, NtrBC mutants colonized the respiratory tracts, but not the skin, of mice to a lesser extent than WT. I hypothesized this effect was due to the different availability of nitrogen in tissues and explored the impact of nitrogenous species on biofilm formation in vitro. Furthermore, I demonstrated that NtrBC regulated host-directed cytotoxicity, virulence factor production and macrophage-mediated uptake, any of which might have contributed to differential colonization of host tissues.

4.2 Materials and Methods

4.2.1 Tissue culture, bacterial strains and growth conditions

Bacterial strains used in this Chapter are described in Table 4-1.

Table 4-1. Bacterial strains and plasmids used in Chapter 4.

Strain	Relevant characteristics	Ref. or Source
PA14	WT *P. aeruginosa* UCBPP-PA14	158
PA14 Δ*ntrB*	PA14 *ntrB* chromosomal deletion	This thesis
PA14 Δ*ntrC*	PA14 *ntrC* chromosomal deletion	This thesis
PA14 Δ*ntrBC*	PA14 *ntrBC* chromosomal deletion	This thesis
LESB58	WT *P. aeruginosa* Liverpool Epidemic Strain B58	159
LESB58 Δ*ntrB*	LESB58 *ntrB* chromosomal deletion	This thesis
LESB58 Δ*ntrC*	LESB58 *ntrC* chromosomal deletion	This thesis
LESB58 Δ*ntrBC*	LESB58 *ntrBC* chromosomal deletion	This thesis

Overnight cultures were routinely maintained in LB broth prepared according to the manufacturer's specifications (Thermo Scientific). Overnight and sub-cultures were incubated for no longer than 18 h at 37°C with shaking (250 rpm). Modified forms of BM2 (containing 62 mM potassium phosphate buffer (pH = 7.0), 0.1% CAA, 2 mM $MgSO_4$, 10 μM $FeSO_4$, 20 mM glucose) were used for biofilm assays, kill curves and minimal inhibitory concentration (MIC) assays. For testing the influence of nitrogen on biofilm formation and ciprofloxacin killing, NO_3^-, NO_2^-, Glu or urea replaced 0.1% CAA. Other media used in specific assays are described elsewhere. For plasmid selection in *P. aeruginosa* PA14 and LESB58, 50 μg/ml and 500 μg/ml gentamycin was added to growth media, respectively. Bacterial growth was monitored by measuring OD_{600} (Eppendorf, Mississauga, ON).

The Simian virus 40 (SV40)-transformed, immortalized HBE cell line 16HBE14o− was used for the cytotoxicity assay. Dr. Grace Choi cultured HBE cells in MEM with Earle's Salts supplemented with 10% FBS (Gibco) and 2 mM L-glutamine (Gibco). The cell line was routinely cultured to 85 to 90% confluence in 100% humidity and 5% CO_2 at 37°C and used between passages 9-15.

The human monocytic-like cell line THP-1 was obtained from the American Type Culture Collection (ATCC) and was routinely cultured by Beverlie Baquir in RPMI-1640 supplemented with 2 mM L-glutamine and 10% FBS. Cells were differentiated into mature macrophages by stimulation with 100 ng/ml phorbol-12-myristate-13-acetate (PMA [P1585; Sigma]) for 48 h and then replaced with fresh medium without PMA for 24 h prior to the assay. The cell line was routinely cultured to 85 to 90% confluence in 100% humidity and 5% CO2 at 37°C.

4.2.2 Minimal inhibitory concentration assays

Broth microdilution assays were performed according to the standard protocol outlined by the Clinical and Laboratory Standards Institute (CLSI) (216) with minor modifications. Bacteria were seeded at ~10^5 CFU/ml in a 2-fold concentration gradient of antibiotic in Mueller-Hinton Broth (MHB) or BM2, with N-source as indicated, at 200 µl/well in 96-well polystyrene flat bottom plates (Corning). Plates were incubated for 18 h at 37°C. The MIC of antibiotics was determined as the lowest concentration that visibly inhibited bacterial growth.

4.2.3 Kill curves

Overnight cultures were diluted to a starting OD_{600} = 0.1 in 5 ml MHB. Cultures were grown to mid-log phase (OD_{600} = 0.4-0.6) at 37°C with aeration, and then treated with a high concentration of ciprofloxacin (25 µg/ml). Aliquots were taken every 30 or 60 min for up to 240 min following inoculation, then diluted in PBS (pH = 7.4) and plated on LB agar plates for enumeration.

4.2.4 Animal care

Animal experiments were performed in accordance with the CCAC guidelines and were approved by the University of British Columbia Animal Care Committee (certificates A17-0253 and A19-0064). Mice used in this Chapter were inbred C57Bl/6 mice (female, aged 11-13 weeks) or outbred CD-1 mice (female, aged 5-7 weeks). All animals were purchased from Charles River Laboratories, Inc. (Wilmington, MA). C57Bl/6 and CD-1 mice weighed 20 ± 5 g and 25 ± 5 g, respectively, at the time of experiment and were group housed in cohorts of 4-5 littermates exposed to the same bacterial strain. Littermates were randomly assigned to experimental groups. Standard animal husbandry protocols were employed.

4.2.5 Subcutaneous (abscess) infection

Ciprofloxacin susceptibility of LESB58 WT and mutants was assessed in vivo using a nuanced subcutaneous abscess model, as previously described (124). Bacterial cultures were grown to an OD_{600} = 1.0 in LB, washed twice in sterile PBS and resuspended to give a final inoculum of ~5 x 10^7 CFU (in 50 µl). Bacteria were injected subcutaneously into the left dorsum of CD-1 mice and treated one h later with 50 µl of 0.2 mg/ml ciprofloxacin in endotoxin-free water. Abscesses were formed for 72 h, visible dermonecrosis was measured using a caliper at experimental endpoint and abscesses were harvested in PBS for bacterial enumeration on LB.

4.2.6 Sinusitis infection

Sinusitis infections were performed as described in Chapter 3. Briefly, bacterial subcultures of *P. aeruginosa* LESB58 WT and mutant strains were washed twice with sterile PBS and resuspended at an OD_{600} = 1.0. Bacteria were instilled (20 µl), dropwise, into the left naris of C57Bl/6 mice under anesthesia (2.5% isoflurane) at 10^6 CFU. At the experimental endpoint, mice were euthanized and nasal lavage as well as excision of lungs were performed for bacterial enumeration.

4.2.7 Biofilm formation

PA14 WT was examined for biofilm formation in the presence of different nitrogen sources using a high throughput microtitre assay as described elsewhere (117). Overnight cultures were diluted to a starting OD_{600} = 0.1 in BM2 medium with 20 mM glucose and nitrogen sources, then grown in polypropylene 96-well plates (Falcon). Following 18-24 h static incubation at 37°C, biomass was stained with 0.1% CV and dissolved in 70% ethanol. The OD_{595} was read using a BioTek SynergyH1 microplate reader (BioTek, Winooski, VT). Three independent experiments containing three biological replicates each were performed.

4.2.8 Virulence factor assays

Pyoverdine was assessed as previously described (217). Briefly, bacteria were incubated in casamino acid medium (0.5% CAA, 0.1 mM $MgSO_4$, 0.4% glucose, 7 mM potassium phosphate buffer, pH = 7.0) at 37°C (250 rpm). Turbid cultures were pelleted, and the supernatant was collected in a fresh microfuge tube. Five µl of supernatant was mixed with 995 µl 10 mM Tris-HCl (pH = 6.8). Fluorescence was measured at an excitation and emission wavelength of 400 nm and 460 nm (Synergy H1 Microplate Reader, Biotek). Pyocyanin concentrations were determined spectrophotometrically after extraction with chloroform and 0.2 M HCl as described elsewhere (218). Absorbance at 520 nm was read (Synergy H1 Microplate Reader, Biotek). Elastase was determined by proteolysis of the Elastin-Congo red complex (Sigma) as described elsewhere (219). Five hundred µl of supernatant from cultures grown for 16 h was collected, added to 10 mg/ml Elastin-Congo red in PBS (pH = 7.4) and incubated at 37°C (250 rpm) for 8 h. Absorbance of the aqueous fraction was examined at 495 nm (Synergy H1 Microplate Reader, Biotek).

4.2.9 Toxicity toward human bronchial epithelial cells

Toxicity assays described in this section were performed in collaboration with Dr. Grace Choi. Confluent HBE cells were washed once with PBS (pH = 7.4) (Gibco), removed by trypsinization

with 0.25% Trypsin-EDTA (Gibco) and counted. HBE cells were then seeded at ~7.5 x 10^5 cells/well in 500 µl in a 24-well plate and grown again to confluency (2-3 days). Then, medium (MEM, 1% FBS, 2 mM L-glutamine) was refreshed and cells were rested for one h. Bacterial cultures grown to mid-log phase were pelleted, washed once with PBS and resuspended in medium. Bacterial cells were added to host cells at an MOI = 10, and co-cultures were maintained at 37°C with 5% CO_2 for 12-16 h. HBE cell cytotoxicity was evaluated by measuring the release of LDH into the supernatant as previously described (220).

4.2.10 Macrophage uptake (gentamicin protection assay)

Macrophage-mediated uptake of PA14 WT and mutants was performed by Beverlie Baquir as described (221) with minor modifications. Briefly, cultures were grown to mid-log phase (OD_{600} = 0.4-0.6), then washed with RPMI-1640 and resuspended in one ml of medium. Mature macrophages were seeded in 24 well plates at ~3.5 × 10^5 cells/well. Bacteria were added at an MOI = 10 and incubated for one h at 37°C. Cells were washed with PBS and treated with 400 µg/ml gentamicin for 30 min at 37°C to remove residual bacteria from the well. Following treatment, macrophages were again washed, then left to rest for an additional 30-60 min or lysed with 0.1% Triton X-100. Macrophage lysate was plated onto LB agar for bacterial enumeration at 30- or 90-min post-infection.

4.3 Results

4.3.1 *P. aeruginosa* PA14 *ntrBC* mutants were more sensitive to ciprofloxacin

I assessed whether NtrB and NtrC directly impacted on susceptibility to antibiotics in MHB, a standard medium for determining their MIC (Table 4-2). The MIC of the fluoroquinolone ciprofloxacin (CIP) was 8-fold lower for Δ*ntrB* and Δ*ntrC* strains and ≥16-fold lower for Δ*ntrBC*. However, there were no statistically significant differences in the MICs of tobramycin (TM), chloramphenicol (CAP) or tetracycline (TC) between *P. aeruginosa* PA14 strains.

Table 4-2. *P. aeruginosa ntrBC* mutants were more susceptible to ciprofloxacin. The minimal inhibitory concentration (MIC) of antibiotics was expressed as the lowest concentration that inhibited growth in at least two of three independent experiments. Abbreviations: CIP, ciprofloxacin; TM, tobramycin; CAP, chloramphenicol; TC, tetracycline.

	MIC (µg/ml)			
Strain	**CIP**	**TM**	**CAP**	**TC**
PA14 WT	3.13	6.25	>200	1.56
PA14 *ΔntrB*	0.39	6.25	>200	0.78
PA14 *ΔntrC*	0.39	12.5	>200	1.56

PA14 *ΔntrBC*	<0.39	6.25	>200	0.78

I then tested whether NtrBC directly impacted on the rate of killing of *P. aeruginosa* PA14 by treating mid-log phase cultures with a high concentration (25 μg/ml) of ciprofloxacin in MHB (Fig. 4-1).

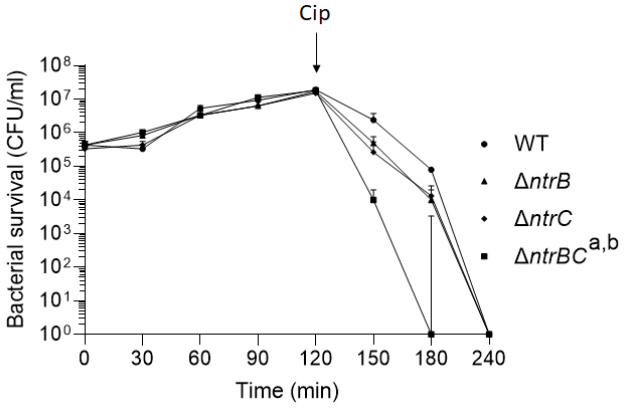

Figure 4-1. Mutation of the nitrogen regulatory two-component system, NtrBC, increased *P. aeruginosa* susceptibility to ciprofloxacin. Kill curves were performed in MHB after addition of 25 μg/ml ciprofloxacin at t = 120 min. Data are reported as mean ± standard error of the mean (SEM) from three independent experiments performed in duplicate. $^{a,b}P < 0.05$ different from WT at t = 150 min (a) and t = 180 min (b) according to Kruskal Wallis nonparametric test followed by Dunn's post-hoc analysis.

Deletion of the entire two-component system (Δ*ntrBC*) resulted in significantly reduced viability by 2-$\log_{10}$ within 30 min of ciprofloxacin treatment, and in most cases complete killing within 30-60 min of treatment, cf. WT that required 120 min for all bacteria to be killed. Deletion of just the response regulator (Δ*ntrB*) or the sensor kinase (Δ*ntrC*) from the chromosome of PA14 had no significant impact on the rate of killing. Consistent with this, the nitrogen source impacted on swarming-mediated resistance to ciprofloxacin (Fig. 4-2) exhibited by *P. aeruginosa*.

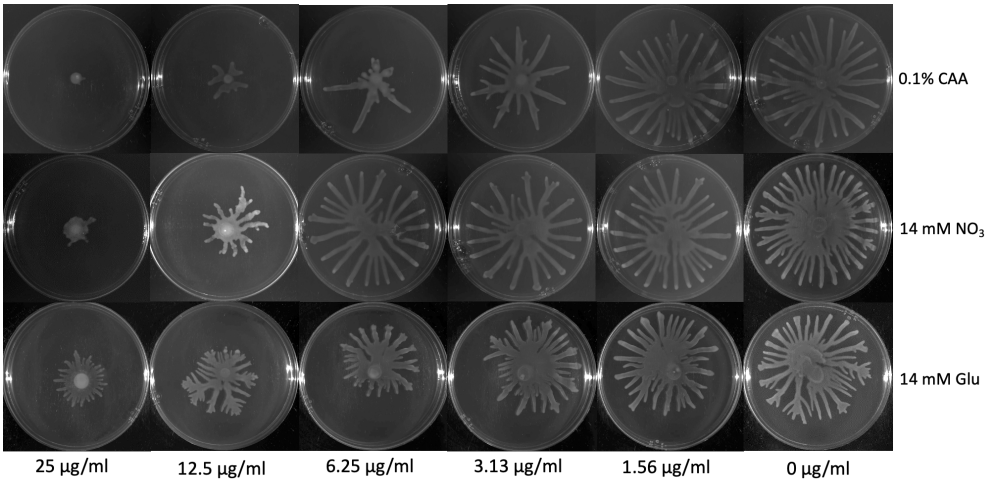

Figure 4-2. *P. aeruginosa* PA14 swarming-mediated resistance to ciprofloxacin depended on nitrogen source. Swarming assays were performed on BM2 supplemented with 0.4% glucose and 0.5% agar as well as casamino acids (CAA), nitrate (NO_3^-) or glutamate (Glu). Ciprofloxacin was titrated (0-25 µg/ml) into the plate, as indicated on the abscissa. Swarming in the presence of ciprofloxacin was greatest when Glu was used as the nitrogen source, and weakest when CAA were used. Data are representative images of three independent experiments (n = 3) captured with a BioRad ChemiDoc.

More specifically, the same high concentration (25 µg/ml) of ciprofloxacin that killed *P. aeruginosa* PA14 strains in mid-log phase (Fig. 4-1) completely inhibited swarming by the WT on standard swarming medium, in which 0.1% CAA are used as the nitrogen source (Fig. 4-2). With each 2-fold dilution of ciprofloxacin, PA14 WT swarmed more. Thus, there appeared to be a concentration-dependent impact of ciprofloxacin on swarming under standard conditions. A similar concentration-dependent effect of ciprofloxacin-mediated inhibition of swarming was observed when 14 mM NO_3^- or Glu were used as the nitrogen source. However, PA14 WT appeared more resistant to ciprofloxacin-mediated inhibition of swarming on alternative nitrogen sources, since more swarming tendrils were observed even at the highest concentration of ciprofloxacin used.

To explain the mechanism by which NtrBC influenced susceptibility to ciprofloxacin, I used the transcriptional data on the PA14 Δ*ntrB* and Δ*ntrC* strains to examine the differential expression of genes in mutants belonging to the ciprofloxacin resistome (Table 4-2). Compared to WT, 17 of 287 ciprofloxacin resistome genes were downregulated in Δ*ntrB* and/or Δ*ntrC* strains.

Table 4-3. Ciprofloxacin resistome genes were downregulated in PA14 *ntrB* and *ntrC* mutants. Fastq and count files for all samples are available on the NCBI Gene Expression Omnibus (GEO) under accession number GSE145591. Data are expressed as mean fold-change (FC) values from three biological replicates. Blank cells indicate no change in expression.

PA14 ID	Name	Annotation	FC Δ*ntrB*	FC Δ*ntr*C	Ref.
PA14_03760	*gpuP*	3-guanidinopropionate transport protein		-4	222

PA14_10770	PA4112	sensor/response regulator hybrid		-1.8	222
PA14_13110	PA3924	probable medium-chain acyl-CoA ligase	-2.2	-2.8	223
PA14_18120	*mmsA*	methylmalonate-semialdehyde dehydrogenase	-1.9	-2.4	224
PA14_18830	PA3517	probable lyase	-2.7	-2.8	222
PA14_29420	PA2682	conserved hypothetical protein	-2.2	-2.7	224
PA14_29640	*fhp*	flavohemoprotein	-6.2	-5.8	224
PA14_33630	*pvdJ*	pyoverdine biosynthesis gene J	-2.4	-2.4	223
PA14_33650	*pvdD*	pyoverdine synthetase D	-2.1	-2.0	224
PA14_37310	PA2110	hypothetical protein	-8.4	-6.7	222
PA14_38690	PA1997	probable AMP-binding enzyme	-1.8	-1.6	223
PA14_45580	PA1459	probable methyltransferase	-1.7	-1.6	224
PA14_47100	*ilvA2*	threonine dehydratase, biosynthetic	-3.8	-3.5	222
PA14_47930	*lhpH*	4-hydroxyproline catabolism LhpH	-16.9	-9.7	222
PA14_53800	*mntH2*	manganese transport protein MntH		-2.3	222
PA14_55220	PA0703	MFS family transporter		-1.7	224
PA14_58690	PA4523	hypothetical protein	-1.5		224

The most downregulated ciprofloxacin resistome gene was *lhpH*, the product of which is implicated in 4-hydroxyproline catabolism, that was expressed 16.9- and 9.7-fold less in Δ*ntrB* and Δ*ntrC* when compared to WT, respectively. Other substantially downregulated resistome genes encoded a putative allophanate hydrolase subunit with a carboxytransferase domain (PA14_37310/PA2110), a flavohemoprotein (*fhp*), a threonine dehydratase biosynthetic protein (*ilvA2*).

4.3.2 LESB58 mutants were more susceptible to ciprofloxacin in vivo

Since I observed that NtrBC was needed for resistance to ciprofloxacin in vitro, and ciprofloxacin was able to eradicate *P. aeruginosa* from the lungs of CF patients in a recent clinical trial (225), I tested the ability of ciprofloxacin to kill LESB58 WT and mutants in vivo (Fig. 4-3).

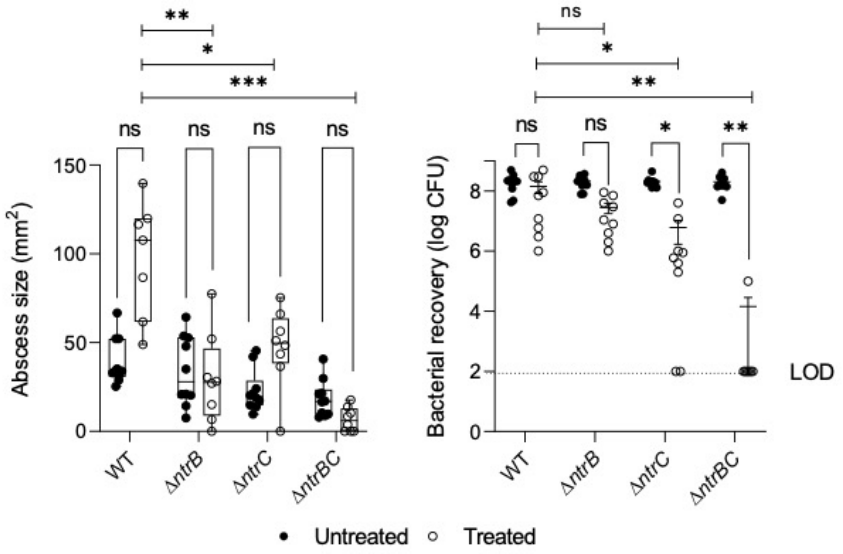

Figure 4-3. Mutation of the nitrogen regulatory two-component system, NtrBC, sensitized *P. aeruginosa* LESB58 to ciprofloxacin treatment in vivo. Box and whiskers delineate interquartile range with geometric error from three independent experiments containing 2-3 biological replicates each (n = 8-10). Bacterial recovery data are reported as geometric mean ± geometric standard deviation (SD). * $P < 0.05$, ** $P < 0.01$, *** $P < 0.001$ compared to WT according to two-way ANOVA followed by Dunnett's post-hoc analysis.

Treatment of WT with 0.1 mg ciprofloxacin did not significantly reduce abscess size when compared to untreated cells. Consistent with observations in Chapter 2 (Fig. 2-1), deletion of *ntrB*, *ntrC* or both also failed to significantly reduce bacterial load when compared to WT in the absence of treatment. However, mutants were more susceptible to ciprofloxacin in vivo. NtrBC mutants were reduced log 4-fold compared to WT following ciprofloxacin treatment. Ciprofloxacin treatment also reduced bacterial load of LESB58 deletion mutants when compared to untreated cells of the same strain and treated WT. Indeed, abscesses formed by LESB58 WT that were untreated or treated with ciprofloxacin contained 1.8 to 2.3 x 10^8 CFU, respectively. In contrast, abscesses formed by LESB58 Δ*ntrBC* after ciprofloxacin treatment contained an average of only 1.4 x 10^4 CFU (with bacteria being reduced below the LOD in all but one instance), even though the Δ*ntrBC* deletion did not affect counts in the absence of ciprofloxacin treatment (2.0 x 10^8 CFU recovered). Abscesses formed by LESB58 Δ*ntrC* exhibited a more moderate 30-fold decrease in bacterial load from 1.8 x 10^8 CFU to 6.1 x 10^6 CFU following ciprofloxacin treatment, while ciprofloxacin did not have a significant effect on LESB58 Δ*ntrB* colonization of abscesses.

4.3.3 LESB58 mutants were reduced for respiratory tract colonization

I wondered whether LESB58 NtrBC mutants would also colonize tissues other than the skin as

well as WT. To investigate this, *P. aeruginosa* LESB58 strains were tested for colonization and virulence in the upper respiratory tract of mice (Fig. 4-4).

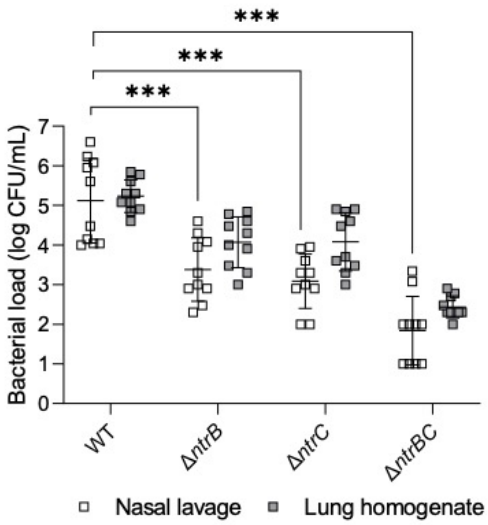

Figure 4-4. Mutation of the nitrogen regulatory two-component system, NtrBC, reduced bacterial load of *P. aeruginosa* in a murine model of sinusitis. Data are presented as geometric mean ± standard deviation for three independent experiments containing 3-4 biological replicates each ($n = 10$). * $P < 0.05$, ** $P < 0.01$ according to two-way ANOVA followed by Dunnett's post-hoc analysis.

In this model I determined that *ntrBC* deletion had a very substantial and significant effect when compared to WT, with significantly fewer Δ*ntrB,* Δ*ntrC* or Δ*ntrBC* isolated from the nasal cavity and lungs of mice, 72 h post-infection. Thus 96- to 298-fold fewer bacteria were isolated from the nasal cavity, while 8- to 10-fold less bacteria were found in the lungs of mice, infected with LESB58 Δ*ntrB* or Δ*ntrC* mutants. Moreover, the LESB58 Δ*ntrBC* double mutant demonstrated an even more profound effect with 2,155-fold and 766-fold fewer bacteria isolated from the nasal cavity and lungs respectively, although the latter was not significant. Conversely, no significant differences were detected for bacterial load of the same strain between nasal cavity and lungs, suggesting that these differences were consistent in these different areas of the respiratory tract. Importantly, *ntrBC* mutation reduced *P. aeruginosa* LESB58 colonization of the respiratory tract to a far greater extent than was observed in the high-density skin abscess model. This effect could be reversed by complementation of the mutants with the cloned *ntrBC* coding region (Fig. A9).

4.3.4 Nitrogen source impacted on biofilm formation by PA14 WT

I hypothesized that the influence of infection site on NtrBC-mediated colonization might be reflective of different nutrient (e.g., nitrogen) availability in tissues. For example, it has been

proposed that urea might be the predominant nitrogen source in skin (226), while amino acids are the major nitrogen source in the lung (227). Thus, I examined the influence of nitrogen source on biofilm formation (Fig. 4-5), which is important for bacterial survival during chronic infection, and susceptibility of *P. aeruginosa* PA14 to ciprofloxacin killing *in vitro*.

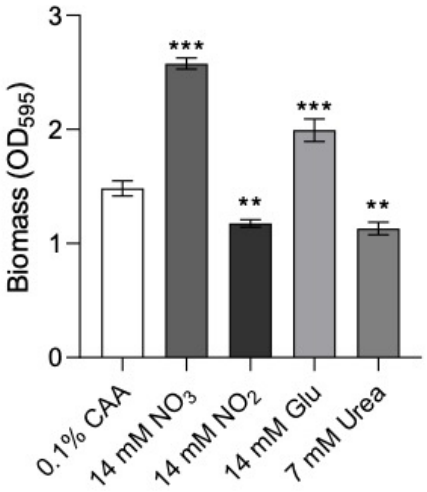

Figure 4-5. Biofilm formation of *P. aeruginosa* PA14 was influenced by nitrogen source. Biofilm was formed in BM2 medium containing casamino acids (CAA), nitrate (NO_3^-), nitrite (NO_2^-) glutamate (Glu), or urea. Data reported as mean ± standard error of the mean (SEM) from three independent experiments containing 2-3 biological replicates each (n = 6-9). ** $P < 0.01$, *** $P < 0.001$ according to Kruskal-Wallis nonparametric test followed by Dunn's post-hoc analysis.

Relative to that in CAA, biofilm biomass staining (OD_{595}) was significantly increased to 174% and 130% when NO_3^- and Glu replaced CAA in the growth medium. In contrast, when NO_2^- or Urea replaced CAA, OD_{595} was decreased to 79.2% and 76.3% respectively.

4.3.5 PA14 mutants produced less virulence factors in vitro

Since pyoverdine synthesis genes were expressed 2.0- to 2.5-fold less in Δ*ntrB* and Δ*ntrC* strains when compared to WT (Table 4-3, Table A4), and because mutants were less capable of colonizing the respiratory tract, I measured the production of virulence factors including pyoverdine, pyocyanin and elastase by PA14 strains grown overnight for 16 h (Fig. 4-6).

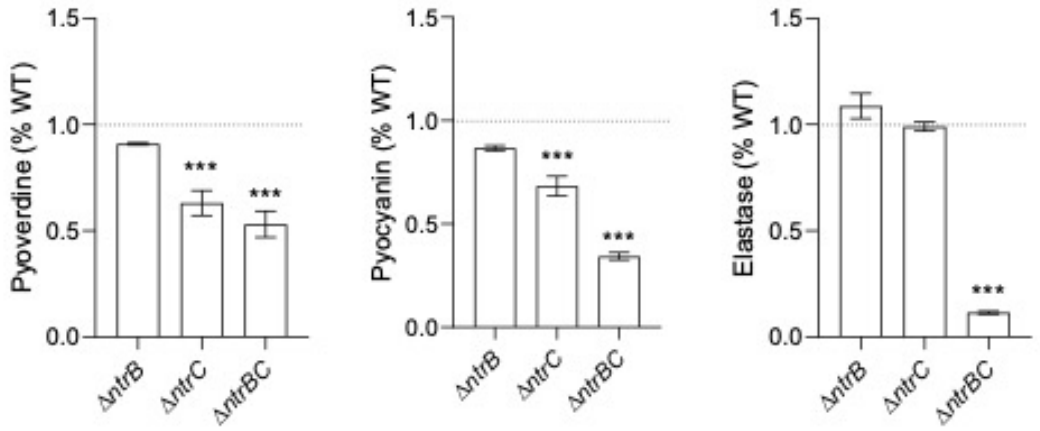

Figure 4-6. Mutation of the nitrogen regulatory two-component system, NtrBC, reduced production of virulence factors by *P. aeruginosa.* The supernatants of overnight cultures of similar density were assessed for pyoverdine, pyocyanin and elastase. Data were reported as mean ± standard error of the mean (SEM) from three independent experiments each containing three biological replicates (n = 9). *** $P < 0.001$ different from WT according to one-way ANOVA followed by Dunn's post-hoc analysis.

Although there were no statistically significant differences between PA14 WT and Δ*ntrB,* production of pyoverdine and pyocyanin in Δ*ntrC* was significantly reduced by 38.2% and 31.7%, respectively. Production of all virulence factors was significantly and substantially reduced in the Δ*ntrBC* double mutant, by 48.2%, 65.2% and 89.8% for pyoverdine, pyocyanin and elastase, respectively. This coincided with the downregulated expression of 19 genes involved in the production of siderophores or phenazines in Δ*ntrB* and/or Δ*ntrC* (Table A8). Substantial reductions in virulence determinants might be expected to reduce *P. aeruginosa* mutants colonization of select tissues.

4.3.6 PA14 mutants induced more robust host-cell response

Since virulence factor production is a key determinant of *P. aeruginosa* pathogenesis (39), and NtrBC directly impacted on the levels of secreted virulence factors including cytotoxins like elastase (Fig. 4-6) and rhamnolipids (Fig. 2-6), I studied whether NtrBC modulated host-directed cytotoxicity in vitro (Fig. 4-7).

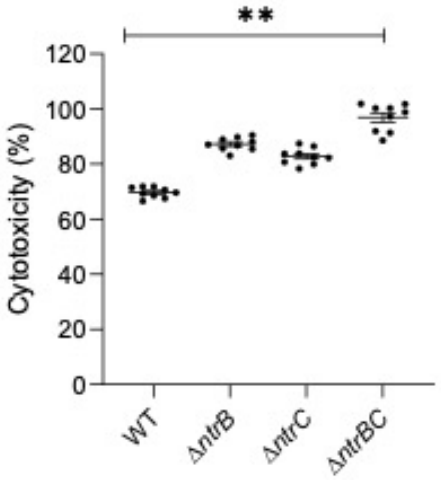

Figure 4-7. Mutation of the nitrogen regulatory two-component system, NtrBC, increased host-directed cytotoxicity of *P. aeruginosa*. Data are presented as mean ± standard error of the mean from four independent experiments containing three biological replicates each (n = 12). ** $P < 0.01$ according to one-way ANOVA followed by Dunn's post-hoc analysis.

A modest but non-significant increase in cytotoxicity of HBE cells was observed following infection with Δ*ntrB* or Δ*ntrC* (13.2% and 7.03% greater than WT, respectively) at an MOI = 10, and a modest but significant 21.5% increase in cytotoxicity was observed following infection with Δ*ntrBC*.

I next tested susceptibility to non-opsonic phagocytosis by examining macrophage-mediated uptake and clearance of pathogens at an MOI = 10 (Fig. 4-8).

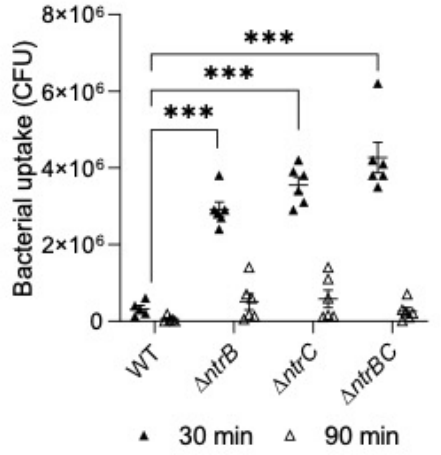

Figure 4-8. Mutation of the nitrogen regulatory two-component system, NtrBC, increased uptake of *P. aeruginosa* by macrophages. Cell lysates at t = 30, 90 min were plated for bacterial enumeration following serial dilution. Data are presented as geometric mean ± standard deviation for three independent experiments containing 2 biological replicates each (n = 6). *** $P < 0.001$ different from WT according to two-way ANOVA followed by Dunnett's post-hoc analysis.

Using the gentamicin-protection assay to record bacteria taken up by macrophages, lysates from infections with Δ*ntrB,* Δ*ntrC* or Δ*ntrBC* contained 9.0- to 13.2-fold more bacteria than lysates from infections with WT at 30 min, indicating substantially greater uptake of these mutants. This coincided with significant upregulation of 38 genes important for macrophage uptake (Table A4). There were no statistically significant differences between mutants and WT at 90 min. Nonetheless, each strain was reduced, on average, by ~10-fold at the later time point, indicating similar rates of clearance. In contrast, pilot studies showed that neutrophil-mediated uptake of PA14 WT and mutants was not significantly different (not shown).

4.4 Discussion

NtrBC is a two-component system of *P. aeruginosa* that is essential for sensing environmental nitrogen levels and responding to nitrogen starvation through the upregulation of genes involved in nitrate assimilation (131,154). NtrC is known to activate a variety of other physiological processes, including histidine utilization (228) and, in *E. coli*, the stringent stress response (136), in part by catalyzing open-complex formation by RNAP comprised by the alternative sigma factor RpoN/σ^{54}. The results described in this Chapter are distinct from those shown in Chapter 2, since NtrBC regulated colonization in a tissue-specific manner by affecting certain host-pathogen interactions and production of virulence factors. I also explored the role of nitrogen in adaptive phenotypes, including biofilm formation and swarming-mediated antibiotic resistance.

Adding to our knowledge of NtrBC as a global regulator, the results shown here indicate that the activity of this two-component system directly impacted on ciprofloxacin resistance of *P. aeruginosa* (Fig. 4-1, Table 4-2) without influencing susceptibility to tobramycin, tetracycline, or chloramphenicol. This was recapitulated in an abscess model of high-density infection (Fig. 4-3). Ciprofloxacin is one of the most important antibiotics used for the treatment of CF lung infections of both children and adults (225). However, ciprofloxacin resistance is on the rise, with 40% of CF isolates sampled in one study exhibiting resistance (229). Ciprofloxacin resistance is usually multifactorial, involving expulsion by the multidrug efflux-porin systems (223,224), as well as mutations in the DNA gyrase (*gyrAB*) or topoisomerase (*parCE*) that are targeted by ciprofloxacin (230). I identified other, non-canonical effectors of ciprofloxacin resistance downstream of NtrBC that spanned multiple physiological categories (Table 4-3). Some of the most significantly dysregulated effectors included the intracellular protease PfpI (169), which has been shown to affect swarming and biofilm formation as well as resistance (231), and the acyl-CoA ligase PA3924 (169), which is needed for nutrient acquisition in the murine lung (232). Effectors of ciprofloxacin

resistance implicated in metabolic pathways, including *fhp* and LhpH (169), were also highly dysregulated, indicating that the NtrBC regulatory system intersects metabolism and resistance of *P. aeruginosa*.

In the airways of CF patients, *P. aeruginosa* undergoes a broad metabolic rewiring (59) to accommodate the needs of the cell according to the diversity and availability of nutrients, such as free amino acids and NO_3^- that are not detected in abundance in other bodily niches (227). Thus, interference with metabolism of these nitrogen sources could inhibit colonization ability in a tissue-specific manner. In support of this, I showed that *P. aeruginosa* LESB58 Δ*ntrB* and/or Δ*ntrC* mutants, which are deficient for metabolism of nitrogenous species including NO_3^- (Fig. 2-3), and glutamate but not urea (not shown), colonized the skin to a similar extent as WT in the absence of ciprofloxacin treatment (Fig. 4-3), but did not colonize the respiratory tract of mice as well as WT (Fig. 4-4). This effect could be mitigated by complementation of the *ntrBC* coding region back into mutants (Fig. A9). This contributes to our understanding of the complex physiological processes assumed by bacteria during infection that impacts on pathogenesis and antimicrobial intervention (39) and indicates that NtrBC is important for metabolic adaptation in the nasal cavity and lungs, but not the skin. This data also implicates NtrBC in recurrent CF infection, since *P. aeruginosa* may persist in the sinus cavity of patients, representing a reservoir where it can adapt and disseminate into the lower respiratory tract over time (187). As well, increased susceptibility to ciprofloxacin was conferred by the LESB58 Δ*ntrB* and/or Δ*ntrC* mutation in vivo (Fig. 4-3), validating in vitro MIC results under physiologically relevant conditions, which is meaningful since bacterial susceptibility to antimicrobials is heavily dependent on environmental conditions.

Indeed, pathoadaptivity and metabolism are intrinsically associated, and nutritional cues in CF sputum impact on multicellular behaviours such as biofilm formation and swarming motility (227). I previously showed that nitrogen source impacted on swarming motility of *P. aeruginosa* (Figs. A2,A3) and that certain nitrogen-containing compounds, including ammonium and urea, did not support swarming motility as did CAA and NO_3^-. Here I provided further evidence showing that nitrogen source impacts on biofilm formation (Fig. 4-5), and that the effects on biofilm and swarming phenotypes are associated, which taken together could partially explain the distinct tissue colonization patterns of *P. aeruginosa* LESB58 strains. More specifically, the nitrogen sources that promoted biofilm formation and swarming (NO_3^- and the free amino acid glutamate, relative to CAA) are those that are abundant in the respiratory tract but not the skin (226,227). Also, Δ*ntrB* and/or Δ*ntrC* mutants did not grow well in these nitrogen sources, nor did they undergo biofilm

formation or swarming motility as well as WT in BM2 containing CAA as the nitrogen source. Furthermore, nitrogen source influenced the ability of *P. aeruginosa* to swarm in the presence of a high concentration of ciprofloxacin (Fig. 4-2). At ~8x its MIC, ciprofloxacin inhibited swarming of PA14 on BM2 containing CAA as the nitrogen source. However, swarming was still observed in the presence of this concentration of ciprofloxacin following substitution of CAA for glutamate and NO_3^-. Thus, PA14 exhibited swarming-associated resistance to ciprofloxacin in a nitrogen-dependent manner. This data might have implications for the development of metabolism-based therapeutics. For instance, compounds that antagonise NO_3^- and glutamate metabolism may be explored as possible therapies to prevent *P. aeruginosa* adaptations in situ since provision of NO_3^- and glutamate as the sole nitrogen source promoted adaptive phenotypes across the board. This data shows the importance of considering experimental conditions and bacterial lifestyle when determining the activity of emerging antibacterial compounds (39,42). Further, therapies targeting adaptive lifestyles of bacteria could be developed as antimicrobial agents with potential for limiting bacterial dissemination in vivo (14).

Since genes implicated in the production of pyoverdine (*pvdD*, *pvdJ*) were also significantly downregulated in Δ*ntrB* and Δ*ntrC* mutants (Table 4-3, Table A4), I assessed PA14 strains for their production of virulence factors (Fig. 4-6). I showed that strains defective for nitrogen metabolism produced less pyocyanin, pyoverdine and elastase. Although pathoadapted strains of *P. aeruginosa* isolated from chronic CF lung infections are characterized by reduced virulence overall, a recent study identified significant within-patient phenotypic diversity of isolates (233) characterized by co-existence of strains that under-produce or overproduce pyoverdine and elastase. This might be caused by mutations affecting nitrogen metabolism or differential availability of nutrients in distinct niches of the lung, since virulence factor production is associated with core metabolic activity of *P. aeruginosa* (234) and is inhibited following perturbation of metabolism during biofilm formation (235).

Though production of select virulence factors was downregulated in *ntrBC* mutants, I noted significantly more HBE-directed cytotoxicity by PA14 Δ*ntrBC* than WT (Fig. 4-7). The first step in establishing *P. aeruginosa* infection of the airway is receptor-mediated binding to the apical surface of the epithelium, which depends on type IV pili and the T3SS (29,30). Type IV pili are functional in the PA14 Δ*ntrB,* Δ*ntrC* and Δ*ntrBC* strains since they twitched normally, indicating epithelial stimulation by the type IV pili could partially explain the cytotoxicity observed. On the other hand, upregulated expression of T3SS components (Table A4) could also play a role. Indeed,

expression of the type III apparatus encoded by *pscBCEP* (52) was upregulated 3.0- to 7.5-fold in Δ*ntrB* or Δ*ntrC* compared to WT, and expression of type III effectors encoded by *pcr1* and *pcr3* were upregulated 6.1-fold and 12-fold, respectively. Innate immunity mediated by phagocytic clearance by neutrophils and macrophages is key to the endogenous control of *P. aeruginosa* (79) and could be stimulated by release of epithelial cell contents following cytotoxicity. Therefore, I studied whether uptake by macrophages was affected by mutation of *ntrBC* (Fig. 4-8). Indeed Δ*ntrB,* Δ*ntrC* and Δ*ntrBC* mutants were more susceptible to phagocytosis by mature macrophages, and demonstrated similar rates of clearance following uptake compared to PA14 WT. In this regard, it is worth noting that *ntrBC* mutants have functional flagella (since they swim normally) given that both flagella and type IV pili are involved in non-opsonic phagocytosis by macrophages (79). Production of type III toxins such as *exoSTY* has been shown to limit uptake of *P. aeruginosa* by macrophages, and the expression of these is modestly downregulated in *ntrBC* mutants. Type III toxin (*exoSTY*) secretion by mutants should be assessed in future studies, particularly since genes encoding type III apparatus (*pscBEP*) and other effectors (*pcr1* and *pcr3*) were not all consistently upregulated or downregulated in mutants (i.e., exhibited different patterns of dysregulated expression).

Chapter 5: NtrBC regulates the production of anti-Staphylococcal virulence factors

5.1 Introduction

P. aeruginosa is often co-isolated with *S. aureus* from chronic wound infections (236,237) and the expectorated sputum of adults with CF (238). Various studies have examined the relationship between *P. aeruginosa* and *S. aureus* growth in CF lung infection models (3,74). During childhood, CF lungs are readily colonized by *S. aureus*, which is associated with a higher likelihood of colonization by *P. aeruginosa* in mid- to late-teenage years (239). Once present, *P. aeruginosa* rapidly takes over, indicating a competitive exclusion of *S. aureus* in the context of CF.

Less is known about the relationship between these species in other bodily niches. However, recent data indicates that the competitive advantage of *P. aeruginosa* over *S. aureus* is muted in the presence of certain host factors (74). For example, acute wound infection models that incorporate serum into the growth medium allow *P. aeruginosa* and *S. aureus* to co-exist (3,237), at least in the early stages of infection. Thus, interspecific interactions appear to be highly regulated and dependent on environmental conditions. Over time, *P. aeruginosa* and *S. aureus* may partition into different areas of the skin and soft tissues, similar to what is observed in CF lungs. Accordingly, chronic wound biopsies revealed that *S. aureus* preferentially colonized the surface of the skin, whereas *P. aeruginosa* was predominantly found in deeper layers (240). This could be prompted by interspecies signaling during the early stages of infection, representing a determinant of virulence, since interspecific interactions have bilateral impacts on the production of tissue-damaging molecules including pyoverdine, pyocyanin and elastases of *P. aeruginosa* (241).

Here, I aimed to elucidate the role of NtrBC signaling in interspecies competition between *P. aeruginosa* and *S. aureus*, since it was shown to be induced in the early stages of co-culture (242). I confirmed that *P. aeruginosa* LESB58 *ntrBC* promoter activity was induced by *S. aureus* USA300 LAC and the small molecule N-acetylglucosamine. The LESB58 WT and the isogenic Δ*ntrB* mutant outgrew and induced lysis of *S. aureus* USA300 in competition assays in vitro, but LESB58 Δ*ntrC* and Δ*ntrBC* strains did not. This could be complemented by overexpression of the QS signaling genes *lasI* and *pqsH*, but not *rhlI*, at least partially by restoring the production of anti-Staphylococcal virulence factors. Importantly, the *ntrBC*-dependent competitive phenotypes were maintained, albeit somewhat muted, during biofilm formation in more complex human and mouse models of co-infection. Based on these data, I propose a model by which NtrBC activity could

shape interspecies interactions between *P. aeruginosa* and *S. aureus* during the early stages of co-culture.

5.2 Materials and Methods

5.2.1 Bacterial strains and culture conditions

Bacterial strains and plasmids used in this Chapter are presented in Table 5-1.

Table 5-1. Bacterial strains and plasmids used in Chapter 5.

Strain	Characteristics	Reference
Pseudomonas aeruginosa		
LESB58	WT *P. aeruginosa* Liverpool Epidemic Strain B58	159
LESB58 Δ*ntrB*	LESB58 *ntrB* chromosomal deletion	This thesis
LESB58 Δ*ntrC*	LESB58 *ntrC* chromosomal deletion	This thesis
LESB58 Δ*ntrBC*	LESB58 *ntrBC* chromosomal deletion	This thesis
LESB58 *ntrBC*-pro	LESB58 *ntrBC*-pro-*luxCDABE*	This thesis
LESB58 Δ*ntrB ntrBC*-pro	LESB58 *ntrB* mutant, *ntrBC*-pro-*luxCDABE*	This thesis
LESB58 Δ*ntrC ntrBC*-pro	LESB58 *ntrC* mutant, *ntrBC*-pro-*luxCDABE*	This thesis
LESB58 Δ*ntrBC ntrBC*-pro	LESB58 *ntrBC* mutant, *ntrBC*-pro-*luxCDABE*	This thesis
Staphylococcus aureus		
USA300 LAC	Community-acquired MRSA, parental strain	197
Plasmids		
pUC18-Tn7T-lux-Gm	pUC18T::mini-Tn7T::*luxCDABE*, Gm^r	200
pTNS2	pTNS::*lacI*-Pro::RSF, Kan^r	201
pUC-Tn7T-*ntrBC*-pro-lux	pUC18-Tn7T-lux derivative, 0.5 kbp *ntrBC*-pro, Gm^r	This thesis
pBBR1MCS-5	Broad host range cloning vector, Gm^r	161
pBBR.*rhlI*	Cloned 0.61 kbp *rhlI* gene, Gm^r	This thesis
pBBR.*lasI*	Cloned 0.61 kbp *lasI* gene, Gm^r	This thesis
pBBR.*pqsH*	Cloned 1.15 kbp *pqsH* gene, Gm^r	This thesis

Overnight cultures were routinely maintained in LB broth or dYT prepared according to the manufacturer's specifications (Thermo Scientific). Overnight and sub-cultures were incubated for no longer than 18 h at 37°C with shaking (250 rpm). Modified forms of BM2 (containing 62 mM potassium phosphate buffer (pH = 7.0), 2 mM $MgSO_4$, 10 µM $FeSO_4$, 20 mM glucose and 0.1% CAA and/or 7 mM $(NH_4)_2SO_4$,) were used for promoter induction assays, competition assays and biofilm induction assays in vitro. Other media used in specific assays are described in subsequent subsections. Gentamicin (500 µg/ml) was added to growth media for plasmid selection in *P. aeruginosa* LESB58 strains. Kanamycin (30 µg/ml) or gentamicin (15 µg/ml) was added to growth media for plasmid selection in *E. coli*. Bacterial growth was monitored by measuring OD_{600} with a spectrophotometer (Eppendorf, Mississauga, Canada).

5.2.2 General DNA manipulations

High-fidelity PCR was carried out using the Phusion DNA Polymerase (Thermo Scientific) in accordance with the manufacturer's specifications and optimized annealing temperatures. Oligomer sequences were based on the genome of *P. aeruginosa* UCBPP-PA14 or LESB58 available from NCBI. For colony PCR reactions performed on LESB58, cells were boiled at 98°C with shaking (1,000 rpm) for 10 min and pelleted by centrifugation at 14,500 rpm for 3 min. Restriction digests were performed using FastDigest restriction enzymes according to the manufacturer's specifications (Thermo Scientific). All ligation reactions were carried out at room temperature using T4 DNA ligase (Invitrogen). DNA purifications were performed using the GeneJET PCR purification kit or the GeneJET Gel extraction kit following the manufacturer's instructions (Thermo Scientific).

5.2.3 Generation of recombinant strains

Coding sequences of LESB58 *rhlI*, *lasI* and *pqsH* were PCR amplified, gel purified and digested with restriction enzymes EcoRI and BamHI. PCR products were subsequently cloned in the EcoRI/BamHI digested low copy number vector pBBR1MCS-5. LESB58 were scraped from an agar plate and resuspended in 300 mM sucrose. After washing twice, pelleted cells were resuspended in 100 µl of 300 mM sucrose and mixed with 500 ng of plasmid. Cells were transformed via electroporation (2.5 kV, 25 µF, 200 Ω). All steps were carried out at room temperature. Cells were recovered for 3 h at 37°C in dYT broth with shaking at 220 rpm after electroporation.

Plasmid pUC18T-min-Tn7T-lux (200) was modified by cloning the *EcoR*I/*BamH*I digested *ntrBC*-promoter PCR product into the multiple cloning site. The derivative pUC-Tn7T-*ntrBC*-Pro-lux was co-electroporated with the helper plasmid pTNS2 (201) into electrocompetent *P. aeruginosa* LESB58 strains, as described above. Positive clones, showing strong bioluminescence, were selected on LB agar plates containing gentamicin and further verified for correct chromosomal insertion via PCR of the flanking regions with transposon- and chromosome-specific primers as described previously (201,202).

5.2.4 Promoter induction assays in vitro

Luminescent bacteria were seeded at a density of ~1.5 x 10^7 CFU/ml in flat-bottomed 96-well plates (Corning) containing BM2 with or without USA300 or signaling molecules, as indicated in the Figure legends. Plates were incubated at 37°C with continuous shaking (250 rpm). OD_{600} and

luminescence measurements were taken at one h increments for 20 h (Synergy H1, BioTek). Experiments were performed three times with at least three technical replicates.

The ammonium concentration in the medium was measured, in parallel, using an ammonia assay kit (Sigma) on centrifuged (8,000 rpm for 5 min) and filtered (0.2 μm pore size) cell supernatants, according to the manufacturer's specifications.

5.2.5 Competition assays

Each species of bacteria was adjusted to an OD_{600} = 0.1 in batch cultures (ratio of 1:1). Competition assays with LESB58 and USA300 were grown for 24 h with shaking (250 rpm) at 37°C. Samples were taken for serial dilution and bacterial enumeration on selective media (salt agar and *Pseudomonas* isolation agar) following 18-34 h incubation. Experiments were performed three times.

5.2.6 Biofilm formation in vitro

Biofilm assays were performed as previously described (243), with minor modifications. Briefly, bacteria were scraped from a plate, resuspended in PBS (pH = 7.4) and mixed at OD_{600} = 0.1 (ratio of 1:1). Polymicrobial cultures were seeded into round-bottomed 96-well polypropylene plates (Corning) and incubated at 37°C for 24-28 h. Planktonic cells were removed and biofilms were washed prior to staining with CV (0.1%) or resuspension and serial dilution for bacterial enumeration on selective media in parallel. Experiments were performed three times with three technical replicates in each.

5.2.7 Biofilm formation ex vivo

A recently developed human organoid model (101) was used, with minor modifications, to monitor polymicrobial biofilm formation ex vivo with the technical assistance of Noushin Akhoundsadegh. Ker-CT cells (ATCC CRL_4048) were routinely cultured in Keratinocyte-SFM medium (Gibco) at 37°C, 5% CO_2. Human skin equivalents were then formed by seeding cells on transfer filter inserts (0.4 μm pore size) in deep 12-well ThinCert™ plates containing DermaLife K Keratinocyte Complete Medium (Lifeline Cell Technology) that was prepared according to the manufacturer's specifications. Plates were incubated for 2-3 days until cells reached confluency with media replacement every other day. Prior to infection, K0 medium (DMEM (Gibco) supplemented with Ham's F-12 (Gibco), hydrocortisone, isopreterenol, insulin, selenious acid, L-serine and L-carnitine) was added to the wells.

Bacteria were sub-cultured from overnight cultures in BM2 with 0.4% glucose and 0.1% CAA to mid-log phase (OD_{600} = 0.4-0.6) prior to infection. Bacteria were then washed twice in PBS and resuspended to an OD_{600} = 0.1 for each species (1:1 ratio). Polymicrobial cultures were added to the apical surface of human skin equivalents for biofilm formation. Infected human skin equivalents were incubated at 37°C, 5% CO_2 for 24 h. Uninfected controls were treated with triton X-100 (Sigma) and skins were incubated for an additional one h. Transfer inserts were removed from wells and skins were extracted for homogenization followed by serial dilution and bacterial enumeration on selective media. Supernatants were screened for LDH using an assay kit as previously described (220). Experiments were performed three times with three technical replicates in each.

5.2.8 Bacterial colonization in vivo

Animal experiments were performed in accordance with the CCAC guidelines and were approved by the University of British Columbia Animal Care Committee (certificate A19-0064). Mice used in this Chapter were outbred CD-1 mice (female, aged 5-7 weeks). All animals were purchased from Charles River Laboratories, Inc. (Wilmington, MA). CD-1 mice weighed 25 ± 5 g at the time of experiment and were group housed in cohorts of 4-5 littermates exposed to the same bacterial strains. Littermates were randomly assigned to experimental groups. Standard animal husbandry protocols were employed.

Bacterial colonization in vivo was assessed using a subcutaneous abscess model, as previously described (124). Briefly, luminescent LESB58 and non-luminescent USA300 subcultures were grown to stationary phase, then washed twice with sterile PBS and resuspended at an OD_{600} = 1.0. Species were mixed (for a ratio of 1:2) and 50 µl were injected subcutaneously into the right dorsum of mice. Abscesses were formed for 72 h prior to measurement of visible dermonecrosis. Luminescence was monitored in 24 h increments using an in vivo imaging system (IVIS; Perkin Elmer, Waltham, MA, USA). Then, abscesses were harvested for bacterial enumeration following homogenization and serial dilution. Experiments were repeated three times with two biological replicates in each.

5.2.9 Virulence factor assays

Pyoverdine was assessed as previously described (217). Briefly, bacteria were incubated in CAA medium (0.5% CAA, 0.1 mM $MgSO_4$, 0.4% glucose, 7 mM potassium phosphate buffer, pH = 7.0) at 37°C (250 rpm). Turbid cultures were pelleted, and the supernatant was collected in a fresh

microfuge tube. Five µl of supernatant was mixed with 995 µl 10 mM Tris-HCl (pH = 6.8). Fluorescence was measured at an excitation wavelength of 400 nm and emission 460 nm using a microplate reader (Synergy H1, Biotek). Pyocyanin concentrations were determined spectrophotometrically after extraction with chloroform and 0.2 M HCl as described elsewhere (218). Absorbance at 520 nm was read (Synergy H1, Biotek). Elastase was determined by proteolysis of the Elastin-Congo red complex (Sigma) as described elsewhere (219). Five hundred µl of supernatant from cultures grown for 16 h was collected, added to 10 mg/ml Elastin-Congo red in PBS (pH = 7.4) and incubated at 37°C (250 rpm) for 8 h. Absorbance of the aqueous fraction was examined at 495 nm (Synergy H1, Biotek). Experiments were performed three times with three biological replicates in each.

5.2.10 RNA isolation and RT-qPCR

LESB58 strains were sub-cultured to an OD_{600} = 0.4-0.6 and spot cultured on BM2 plates for 18-24 h at 37°C. Surface colonized cells were harvested from the plate in PBS and RNAProtect (at a 1:2 ratio) reagent (Qiagen). RNA extraction from three biological replicates was performed using the RNeasy Mini Kit (Qiagen) according to the manufacturer's specifications. Deoxyribonucleases were removed using the TURBO DNA-free kit (Thermo Fisher). RT-qPCR was used to validate expression of select dysregulated genes identified by RNA-Seq described in Chapter 2. Reaction samples were prepared using qScript one-step SYBR green RT-qPCRKit (QuantaBio) with 0.2 ng/µl RNA. Amplification was performed using a LightCycler 96 instrument (Roche, Indianapolis, IN). Gene expression was quantified by the $\Delta\Delta C_t$ method with normalization to *rpoD* expression (172). Primers used for qRT-PCR are listed in Table A5.

5.3 Results

5.3.1 Co-culture of *P. aeruginosa* and *S. aureus* induced *ntrBC* expression

To confirm the finding that *P. aeruginosa ntrBC* expression was stimulated in the early stages of co-culture with *S. aureus* (242) LESB58 *ntrBC* promoter activity was monitored by luminescence detection in the presence or absence of USA300 LAC (Fig. 5-1A). Ammonium concentration in the medium was measured in parallel (Fig. 5-1B), since depletion of extracellular ammonium was correlated with low intracellular nitrogen availability and induction of *ntrBC* in other reference strains of *P. aeruginosa* (150,228).

The luminescence (i.e., *ntrBC* promoter activity) detected from co-culture increased rapidly six h after inoculation. At six and seven h post-inoculation, *ntrBC* promoter activity in co-culture was

2.6- and 4.7-fold greater, respectively, than the promoter activity in monoculture (Fig. 5-1A). The maximum luminescence detected during co-culture was 5.1-fold greater than during monoculture at 12 h post-inoculation (7.2 versus 2.1). Ammonium depleted slowly and at similar rates during both mono- and co-culture of species (Fig. 5-1B), indicating that LESB58 *ntrBC* promoter activity was independent of extracellular ammonium levels. Indeed, ammonium was only reduced by 32.6% during monoculture, from 0.92 µg/ml at the time of inoculation to 0.62 µg/ml 12 h post-inoculation. Similarly, ammonium was reduced by 31.9% during co-culture, from 0.91 µg/ml at the time of inoculation to 0.62 µg/ml 12 h post-inoculation.

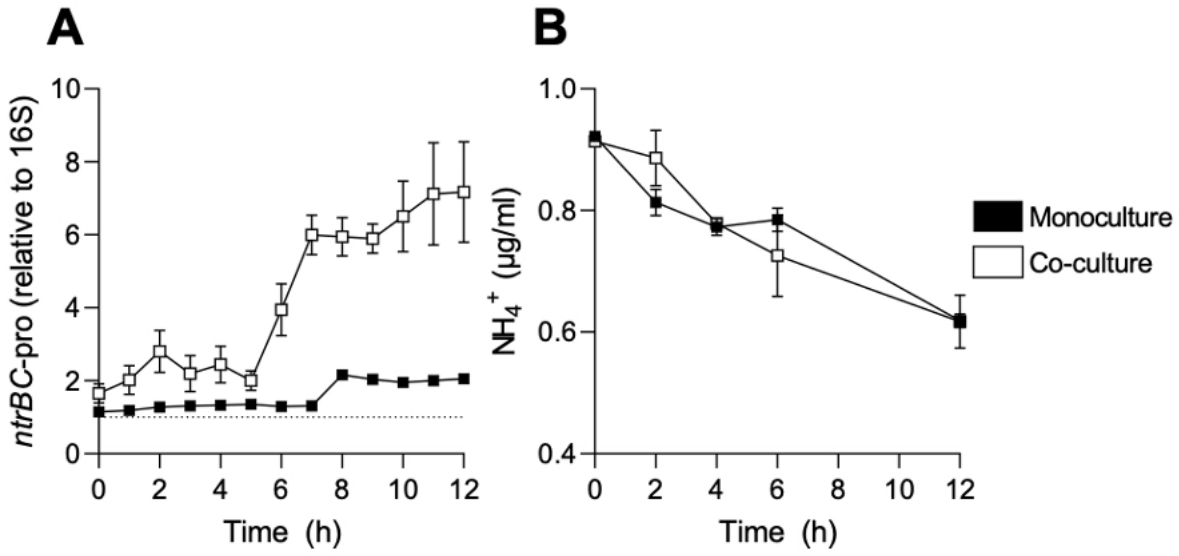

Figure 5-1. *P. aeruginosa* LESB58 *ntrBC*-promoter activity was stimulated during co-culture and was independent of ammonium depletion from the medium. (A) *P. aeruginosa* LESB58 was seeded in the absence (shown as monoculture in black) or presence (shown as co-culture in white) of *S. aureus* USA300 at a total bacterial density of ~5 x 10^5 CFU/ml and luminescence due to the activation of the *ntrBC* promoter was monitored every h for up to 20 h. (B) Extracellular concentration of ammonium (NH_4+) was monitored in parallel using an ammonia assay kit (Sigma).

N-acetylglucosamine is a component of peptidoglycan that can be liberated following bacterial (e.g., *S. aureus*) lysis, and D-ribose is an analogue of the autoinducer-2 QS molecule produced by Gram-positive pathogens (e.g., *S. aureus*) (74). To determine whether these signaling molecules had a potential role in inducing *ntrBC* promoter activity during co-culture, I examined the impact of N-acetylglucosamine and D-ribose on luminescence of LESB58 WT, Δ*ntrB*, Δ*ntrC* and Δ*ntrBC* mutants (Fig. 5-2).

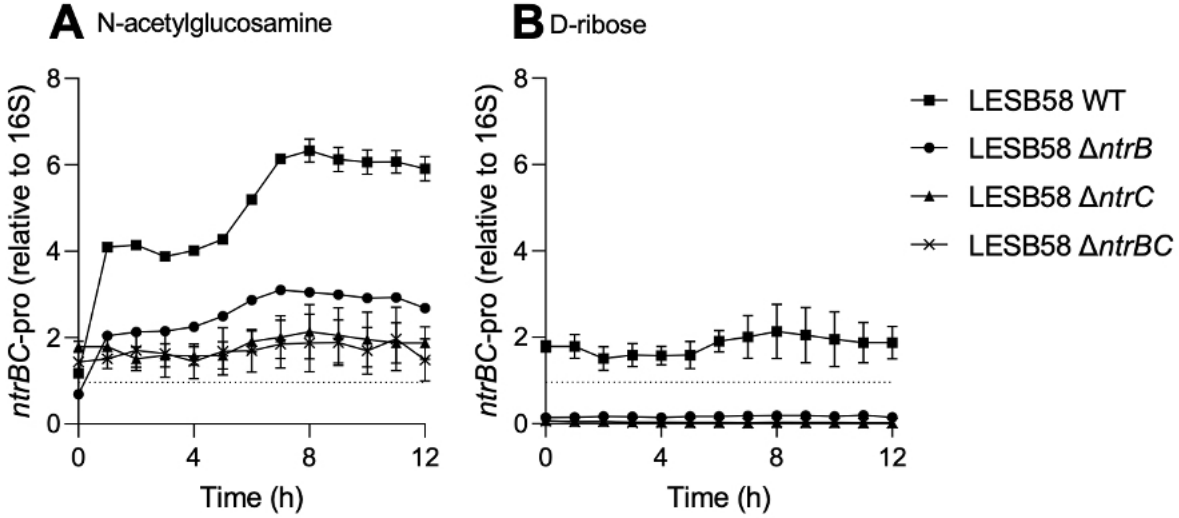

Figure 5-2. N-acetylglucosamine and D-ribose caused the induction of *P. aeruginosa* LESB58 *ntrBC* promoter activity in a self-amplification dependent manner. *P. aeruginosa* LESB58 strains were seeded at a density of ~5 x 10^5 CFU/ml and treated with (A) N-acetylglucosamine (20 μM) or (B) D-ribose (20 μM) prior to luminescence detection for up to 20 h.

N-acetylglucosamine treatment stimulated *ntrBC* promoter activity of LESB58 WT by 2.9-fold one h post-inoculation, relative to t = 0 h, rising to 5.2-fold eight h post-inoculation. The promoter activity of *ntrBC* began to decline thereafter, although was still 4.7-fold greater 12 h post-inoculation (Fig. 5-2A). Only a 0.35- to 0.45-fold increase in promoter activity was observed in Δ*ntrC* or Δ*ntrBC* mutants at the peak level at t = 8 h, although they always exhibited *ntrBC* promoter activity that was greater than 16S promoter activity. In contrast, the Δ*ntrB* mutant had an activity that was intermediate between these mutants and WT, demonstrating a 2.4-fold induction of *ntrBC* promoter activity in the presence of N-acetylglucosamine eight h post-inoculation. D-ribose induced the expression of *ntrBC* in the LESB58 WT only, which exhibited a 0.34-fold increase in luminescence at t = 8 h than t = 0 h (Fig. 5-2B) though *ntrBC* promoter activity was always greater than 16S promoter activity under these conditions. In the mutants there was no induction of *ntrBC* promoter activity, indicating that the effect of ribose was dependent on NtrBC. These data were consistent with at least a partial requirement of NtrB and NtrC for the induction of *ntrBC* promoter activity by *S. aureus* metabolites.

5.3.2 Anti-Staphylococcal activity of *P. aeruginosa* depends on NtrBC in vitro

Next, I confirmed the observation (74) that *P. aeruginosa* competitively displaces *S. aureus* using clinical isolates in batch culture growth experiments (Fig. 5-3). Since NtrBC promoter activity was stimulated during co-culture with *S. aureus* USA300 LAC, it was hypothesized that NtrB and/or

NtrC activity was important for the competitive advantage of *P. aeruginosa* over *S. aureus*. It was observed that *P. aeruginosa* LESB58 Δ*ntrC* and Δ*ntrBC* mutants were outcompeted by *S. aureus* USA300 LAC during batch culture in BM2 (Fig. 5-3C,D), whereas the WT and Δ*ntrB* mutant maintained a competitive edge during co-culture (Fig. 5-3A,B).

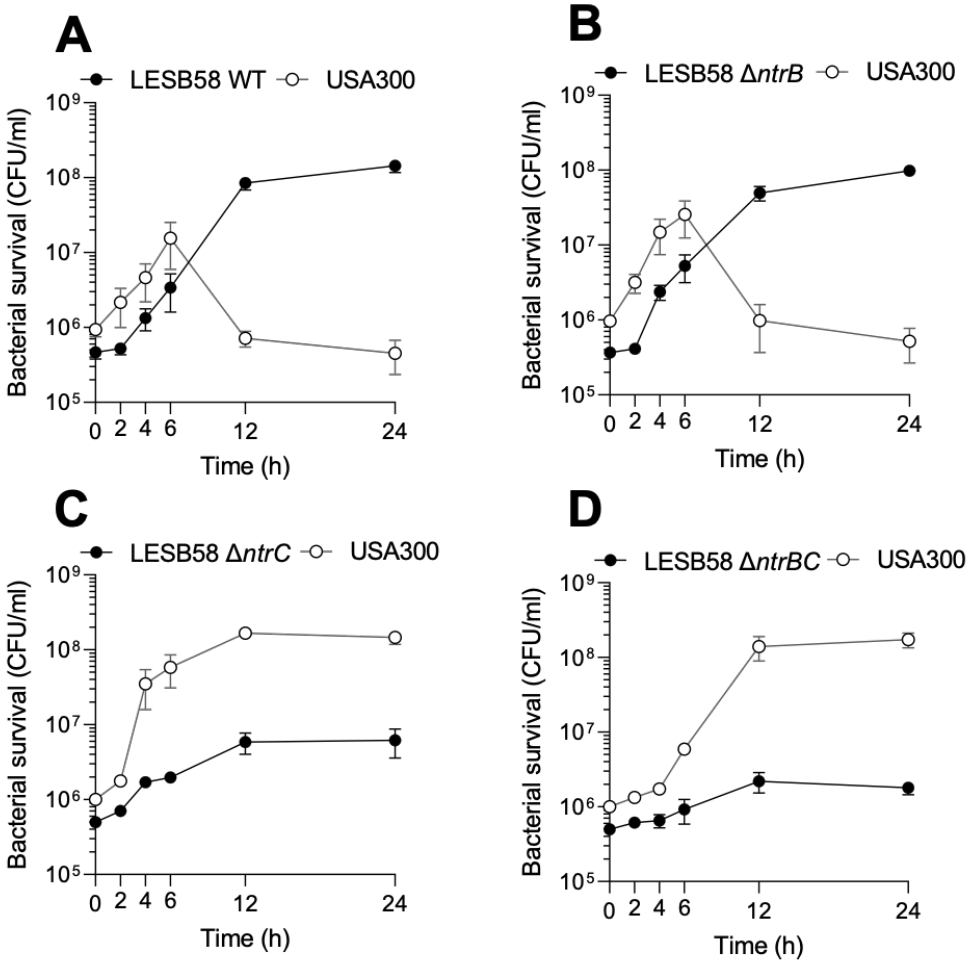

Figure 5-3. *P. aeruginosa* LESB58 outcompeted *S. aureus* USA300 in an NtrC-dependent manner. *P. aeruginosa* LESB58 (A) WT, (B) Δ*ntrB*, (C) Δ*ntrC* or (D) Δ*ntrBC* mutant strains were seeded at a starting OD_{600} = 0.1 in batch cultures that were sampled at two-, six- or twelve-h intervals and plated on selective media for bacterial enumeration. Data are presented as mean ± standard error of the mean (SEM) for three independent experiments (n = 3).

During co-culture with either *P. aeruginosa* LESB58 WT or Δ*ntrB* strains, *S. aureus* USA300 LAC grew steadily until six h post-inoculation (Fig. 5-3A,B). However, between six and 12 h, death of USA300 LAC was observed, since the number of USA300 LAC recovered from co-culture with LESB58 WT and Δ*ntrB* at the 12 h time point was 21.7-and 26.0-fold less than at six h, respectively. During this period, the growth rate of LESB58 WT was exponential and constant,

although LESB58 Δ*ntrB* had a slight reduction in growth rate. In contrast, the growth rate of the Δ*ntrC* and Δ*ntrBC* mutants was greatly reduced after the two h time point when compared to LESB58 WT or Δ*ntrB* strains. Furthermore, LESB58 Δ*ntrC* and Δ*ntrBC* mutants never overtook USA300 LAC. *S. aureus* USA300 LAC grew to a total density of 1.4-1.6 x 10^8 CFU/ml by 12 h post inoculum during co-culture with LESB58 Δ*ntrC* and Δ*ntrBC* mutants, respectively, whereas their density was reduced to 7.2 or 9.8 x 10^5 CFU/ml during co-culture with WT and Δ*ntrB*, respectively. Differences between the strains were ameliorated by complementation of the deleted gene (Fig. A10). This showed that interspecies inhibition of *S. aureus* USA300 LAC by *P. aeruginosa* LESB58 was dependent on NtrBC.

5.3.3 Anti-Staphylococcal activity depends on NtrBC in host-like conditions

I was next interested to determine whether the competitive advantage conferred on *P. aeruginosa* LESB58 by NtrBC depended on environmental conditions since, for example, it had been previously observed that interspecies competition was muted in the presence of host factors (74). Thus, I tested interspecies competition between LESB WT and mutant strains co-cultured with USA300 in biofilm formation assays in vitro (Figs. 5-4A,B) and, in collaboration with Noushin Akhoundsadegh in a model of biofilm infection formed on a human skin organoid model (Figs. 5-4C,D).

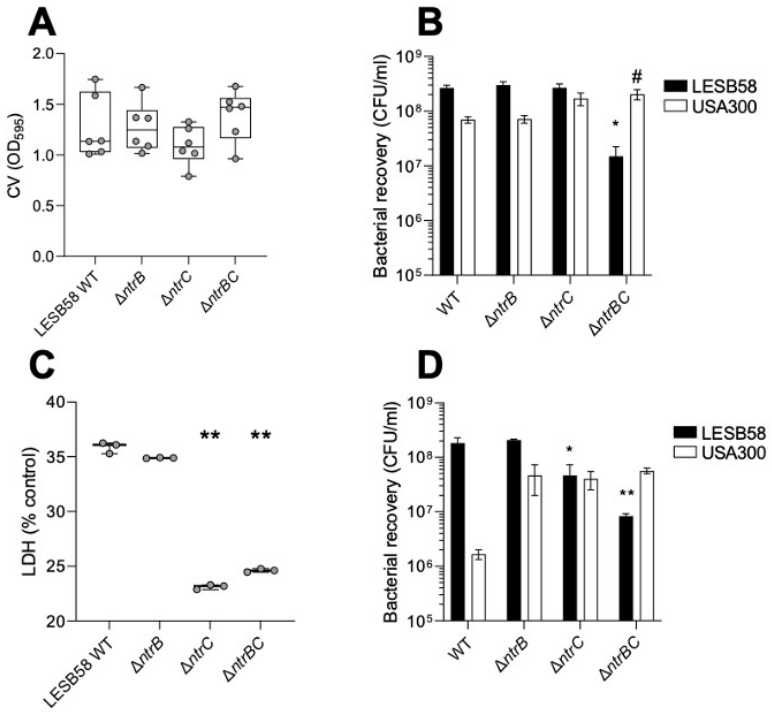

Figure 5-4. NtrBC-dependent competitive advantage of *P. aeruginosa* LESB58 over *S. aureus* USA300 was muted in host-like conditions. Biofilms were formed with *P. aeruginosa* LESB58 strains in host-like media on (A,B) polypropylene plates or (C,D) human skin organoids, formed by Noushin Akhoundsadegh. Biofilms were (A) stained with CV and (B) scraped for bacterial enumeration on selective media, or in the case of skin equivalents (C) assessed for LDH release or (D) bacteria were enumerated. Data are presented as mean ± standard error of the mean (SEM) and box and whiskers delineate interquartile range for data from three independent experiments with one or two biological replicates in each (n = 3-6). * $P < 0.05$, ** $P < 0.01$ different than biofilms formed with LESB58 WT or # $P < 0.05$ different than USA300 formed with LESB58 WT according to two-way ANOVA followed by Dunnett's post-hoc analysis.

The total amount of biomass that was formed by mixed species biofilms in polypropylene 96-well plates containing DMEM supplemented with FBS and glucose was not significantly different between strains (Fig. 5-4A), although the number (CFU/ml) of LESB58 or USA300 recovered from biofilms varied depending on which strain of LESB58 was co-inoculated (Fig. 5-4B). In the WT mixed species biofilms, there was much lower competition between *P. aeruginosa* LESB58 and *S. aureus* USA300 with only a 3.6-fold advantage for *P. aeruginosa* (Fig. 4), cf. the >100-fold difference in broth co-culture (Fig. 5-3). More specifically, the number of LESB58 Δ*ntrBC* was significantly reduced by 218-fold from 2.4 x 10^8 CFU/ml to 1.1 x 10^7 CFU/ml, on average. Accordingly, the number of USA300 LAC increased 3-fold from 6.2 x 10^7 CFU/ml (recovered from biofilms formed with LESB58 WT) to 1.9 x 10^8 CFU/ml (recovered from biofilms formed with LESB58 Δ*ntrBC*). The *P. aeruginosa* LESB58 mutants might have exhibited different competition toward *S. aureus* USA300 LAC in biofilm or planktonic growth assays due to the reduced ability of Δ*ntrBC* to form biofilms even in the absence of competition (see Chapter 2) or due to different composition of the medium, possibly containing a metabolite that impacts on Δ*ntrBC* fitness.

Compared to biofilms formed on skin organoids with either USA300 LAC and LESB58 WT, mixed biofilms formed by USA300 LAC and either LESB58 Δ*ntrC* or Δ*ntrBC* caused 12.8% (23.1% cf. 35.9% relative to control) and 11.3% (24.6% cf. 35.9% relative to control) less cytotoxicity in human skin organoids models (Fig. 5-4C). In contrast, mixed biofilms formed with USA300 LAC and LESB58 Δ*ntrB* were comparable to that of WT (34.9% cf. 35.9% relative to control). *P. aeruginosa* LESB58 WT was recovered in 100-fold larger numbers than *S. aureus* USA300 LAC (Fig. 5-4D) similar to observations in broth co-culture (Fig. 5-3). Recovery of LESB58 Δ*ntrC* was significantly decreased by 2.8-fold from 1.9 x 10^8 CFU/ml to 6.9 x 10^7 CFU/ml, whereas recovery of LESB58 Δ*ntrBC* was reduced even more by 232-fold to 8.2 x 10^6 CFU/ml (Fig. 5-4D). In co-culture with all mutant strains, the number of *S. aureus* USA300 LAC was significantly increased

by nearly 800-fold from 1.1 x 10^6 CFU/ml to approximately 8 x 10^8 CFU/ml (Fig. 5-4D). Thus, while in vitro biofilms showed somewhat different interspecies competition effects than those observed in batch culture, biofilms on skin organoids showed rather similar effects with modest differences.

To determine the importance of NtrBC on competition in vivo, the abscess model of high-density infection (124) was modified by co-inoculating LESB58 strains and USA300 LAC (Fig. 5-5). The induction of *ntrBC* promoter activity was first assessed in vivo (Figs. 5-5A,B). Relative to 16S rRNA expression, there was a 2.9-fold greater *ntrBC* promoter activity observed during polymicrobial infection than monomicrobial infection at 24 h post-infection. Thereafter, the *ntrBC* promoter activity observed during polymicrobial infection declined, but was still higher than the activity observed during mono-species infection, though promoter activity during multi-species infection was only significantly greater than mono-species infection at the 48 h time-point (Fig. 5-5B).

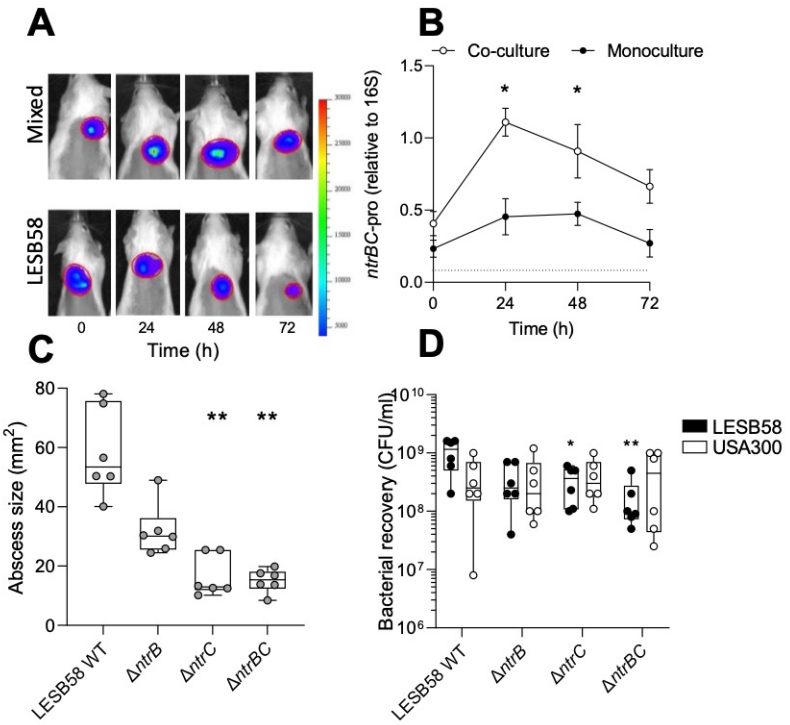

Figure 5-5. *P. aeruginosa* LESB58 *ntrBC* promoter activity was induced during co-culture in vivo and Δ*ntrC* and Δ*ntrBC* mutants were slightly outcompeted by *S. aureus* USA300. Bacteria were inoculated in the right dorsum of mice and (A,B) luminescence was imaged with an in vivo imaging system (IVIS) prior to euthanasia 72 h post infection followed by (C) measurement of the abscess and (D) bacterial enumeration following homogenization on selective media. Data are presented as mean ± standard error of the mean (SEM) and box and whiskers delineate interquartile

range for data from three independent experiments containing two biological replicates in each (n = 6). * $P < 0.05$, ** $P < 0.01$ different from mixed infections with LESB58 WT according to One-Way or Two-Way Kruskal Wallis test followed by Dunn's correction.

The area of abscesses formed with USA300 LAC mixed with LESB58 WT were, on average, 58.3 mm^2, whereas polymicrobial abscesses formed with the mutants were only 31.1, 19.2 or 19.3 mm^2 (Fig. 5-5C), but were only statistically significant for Δ*ntrC* and Δ*ntrBC*. There were no statistically significant differences between the numbers of bacteria recovered from polymicrobial abscesses formed with LESB58 WT and Δ*ntrB* (Fig. 5-5D). However, in mixed infections the average numbers of LESB58 Δ*ntrC* were reduced 3-fold from 1.0 x 10^9 CFU/ml to 3.4 x 10^8 CFU/ml, and 5.3-fold for LESB58 Δ*ntrBC,* to 1.9 x 10^8 CFU/ml (Fig. 5-5D).

5.3.4 Genes involved in production of anti-Staphylococcal virulence factors

To begin to unravel the mechanism(s) by which NtrBC confers a competitive advantage on *P. aeruginosa* LESB58 over *S. aureus* USA300, the regions upstream of all coding sequences in *P. aeruginosa* were scanned for the recently published NtrC binding motif (244) (Fig. A11) using Find Individual Motif Occurrences (FIMO) software (245). FIMO detected 259 binding targets (Table A6), some having more than one non-redundant binding site; 36 of the downstream genes were differentially expressed in PA14 Δ*ntrB* or Δ*ntrC* strains (Table A3). A literature search identified strong possibilities from initial hits that were involved in the production of anti-Staphylococcal virulence factors and were expressed from RpoN-dependent promoters, and differential expression of these genes was confirmed using RT-qPCR on RNA isolated from LESB58 WT and mutants (Table 5-2).

Table 5-2. Differential expression of selected genes involved in the production of anti-Staphylococcal virulence factors. Gene expression is shown as fold-change (FC) from WT using the ΔΔCt method. Dysregulated expression was considered significant when FC was greater than ±2. Data are shown as the mean from three independent experiments containing three technical replicates in each (n = 3).

LESB58 Locus Tag	Gene Name	Annotation	Fold Change cf. WT		
			Δ*ntrB*	Δ*ntrC*	Δ*ntrBC*
PALES_07171	*phzA1*	Phenazine biosynthesis protein	-10.1	-9.8	-9.2
PALES_41691	*pyS2*	Pyocin S2	-6.6	-6.3	-6.8
PALES_45811	*algU*	RNA Polymerase sigma factor AlgU	-5.4	-5.6	-5.4
PALES_28691	*pvdS*	Extracytoplasmic function sigma factor	-4.5	-4.1	-4.3
PALES_39841	*lasR*	Transcriptional regulator LasR	-3.9	-4.1	-4.0
PALES_44741	*plcH*	Hemolytic phospholipase C precursor	2.1	2.0	2.4

According to RT-qPCR, the most significantly downregulated hit was *phzA1*, a phenazine biosynthesis protein (169), which was -9.2 to -10.1 fold downregulated when compared to WT.

The next most downregulated hit was *pyS2*, a pyocin with antibacterial impacts on competitors (169), which was -6.3 to -6.8 fold downregulated. Other downregulated genes included transcriptional regulators such as *algU*, *pvdS* and *lasR*, the last of which is a master regulator of QS in the hierarchical regulatory network of *P. aeruginosa* (73), and has impacts on production of virulence factors with anti-Staphylococcal activity (182).

5.3.5 Anti-Staphylococcal activity depended on quorum sensing

To validate whether dysregulated expression of QS systems contributed to NtrBC-dependent competitive exclusion of *S. aureus* USA300 by *P. aeruginosa* LESB58, I investigated the competitive phenotype of LESB58 Δ*ntrBC* strains transformed with an overexpression vector containing the coding sequence of QS molecules including *lasI*, *rhlI* and *pqsH* (Fig. 5-6).

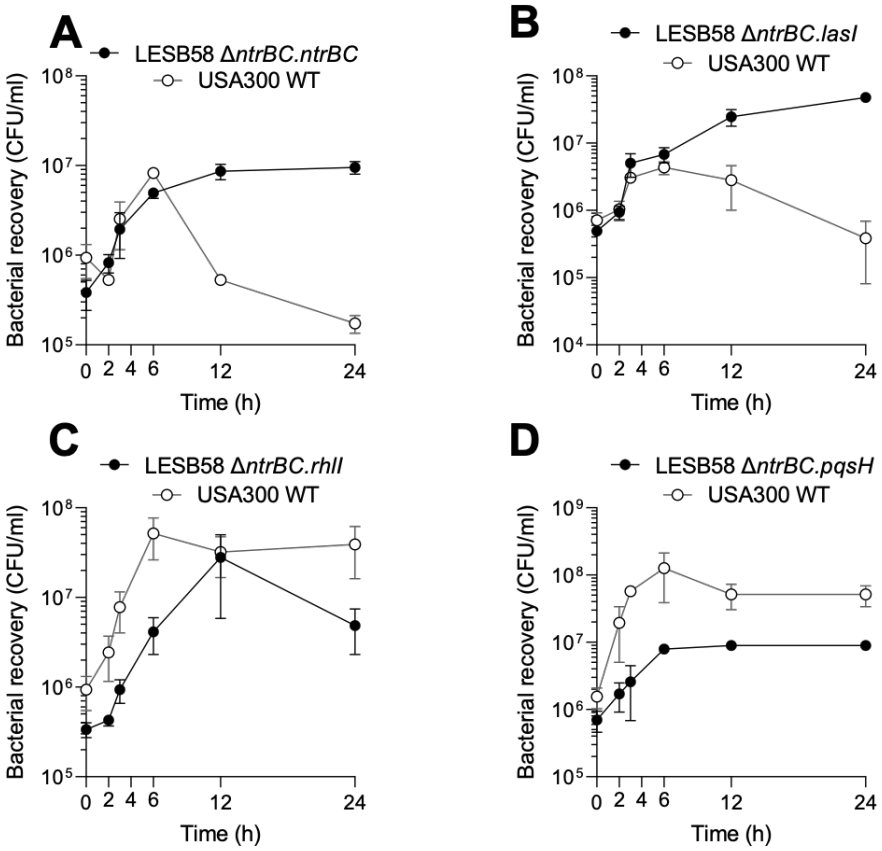

Figure 5-6. Competitive phenotype of *P. aeruginosa* LESB58 Δ*ntrBC* could be phenotypically complemented by both *ntrBC* and *lasI*, but not *rhlI* or *pqsH*. *P. aeruginosa* LESB58 Δ*ntrBC* strains were seeded with *S. aureus* USA300 at starting OD_{600} = 0.1 in cultures that were sampled in two, six or 12 h intervals and plated on selective media for bacterial enumeration. Data are presented as mean ± standard error of the mean (SEM) for three independent experiments (n = 3).

As was observed for batch cultures seeded with LESB58 WT and USA300 (Fig. 5-3A), the density

of LESB58 Δ*ntrBC/ntrBC*$^{+}$ and USA300 increased from the time of inoculation to 6 h post-inoculation, when USA300 LAC numbers sharply declined from 8.2 x 10^6 CFU/ml to 5.3 x 10^5 CFU/ml (Fig. 5-6A), much as had been observed for WT LESB58 (Fig. 5-3A). LESB58 Δ*ntrBC/lasI*$^{+}$, when co-cultured with *S. aureus* USA300, showed partial phenotypic complementation, in that the LasI expressing strain was able to at least partially outcompete USA300 by 12 h post-inoculation (Fig. 5-6B), with the number of USA300 declining beyond 6 h post-inoculation, as also observed for LESB58 Δ*ntrBC/ntrBC*$^{+}$, but not to the same extent. In contrast, neither LESB58 Δ*ntrBC/rhlI*$^{+}$ (Fig. 5-6C) nor LESB58 Δ*ntrBC/pqsH*$^{+}$ (Fig. 5-6D) was able to outcompete USA300 at any time point. The growth rate of LESB58 Δ*ntrBC/pqsH*$^{+}$ was the lowest of all the strains examined in this experiment, reaching a maximum bacterial density of 7.9 x 10^6 CFU/ml around six h post-inoculation, then remaining at this density until the experimental endpoint. Regardless of the LESB58 growth rate, no staphylolytic activity by either of the latter two complemented strains was apparent, since the density of USA300 LAC did not decline at any point (Figs. 5-6C,D).

To confirm that the overexpression of specific QS determinants phenotypically complemented the decrease in *P. aeruginosa* virulence factors with known anti-Staphylococcal activity (65), virulence factor secretion was examined in LESB58 strains (Fig. 5-7).

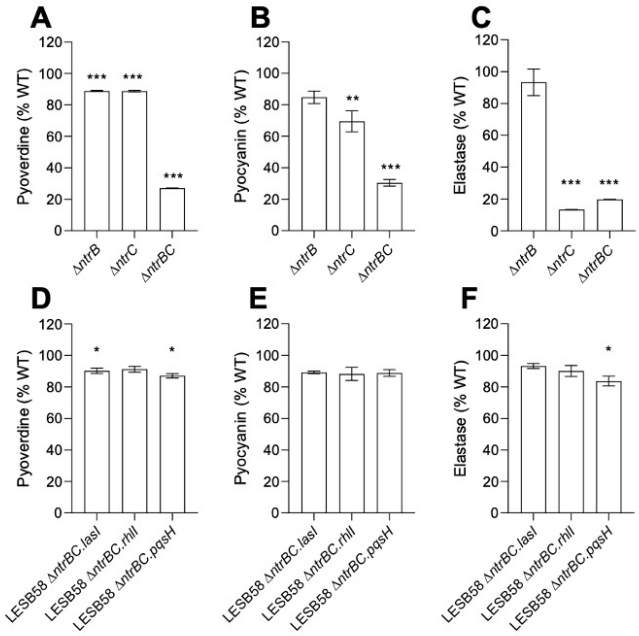

Figure 5-7. Virulence factor production could be restored in *P. aeruginosa* LESB58 Δ*ntrBC* by overexpression of *ntrBC*, *lasI*, *rhlI* and *pqsH*. Levels of (A,D) pyoverdine, (B,E) pyocyanin and (C,F) elastase produced by mutants (A-C) or complements (D-F) were quantified using well established methods. Data are presented as mean ± standard error of the mean (SEM) for three

independent experiments containing three biological replicates in each ($n = 9$). * $P < 0.05$, ** $P < 0.01$, *** $P < 0.001$ different from control according to one-way ANOVA followed by Dunnett's post-hoc analysis.

As was observed for PA14 mutant strains (Fig. 4-5), virulence factor production was significantly downregulated in LESB58 Δ*ntrBC* and/or Δ*ntrC* strains (Figs. 5-7A-C), depending on the virulence factor. While statistically significant, reduced production of pyoverdine by LESB58 (Δ*ntrB* and) Δ*ntrC* was not strong (~87% of WT). However, LESB58 Δ*ntrBC* only produced only 22% of the level of pyoverdine cf. WT. Similarly, great reduction for pyocyanin (to 34% WT levels) and elastase (to 19% WT levels). LESB58 Δ*ntrB* produced ~82% of WT levels for the latter virulence factors, which was not significantly different, whereas LESB58 Δ*ntrC* produced only 71% and 17% as much pyocyanin and elastase as WT. In this case, the production of virulence factors by LESB58 Δ*ntrBC* could be restored by overexpression of QS determinants, including *lasI*, *rhlI* and *pqsH* (Figs. 5-7D-F).

5.4 Discussion

I examined the importance of NtrBC in interspecies competition between clinical isolates of *S. aureus* and *P. aeruginosa*, pathogens that are highly comorbid in skin wound infections as well as upper respiratory tract infections of CF patients (236,238). Induction of *P. aeruginosa* LESB58 *ntrBC* promoter activity was greater in the presence of *S. aureus* USA300 LAC than in monoculture, which was independent of ammonium concentration of the supernatant (Fig. 5-1). Extracellular ammonium is usually correlated with intracellular nitrogen availability of laboratory reference strains of *S. aureus* and *P. aeruginosa* (246,247) since ammonium is their preferred source of nitrogen. However, clinical isolates may exhibit auxotrophy for essential amino acids, which limits protein synthesis, adaptation and growth unless that amino acid is abundant in the environment (248,249). Thus, the extracellular concentration of ammonium may not be the best indicator of intracellular nitrogen status for the strains of *S. aureus* and *P. aeruginosa* used in this Chapter, at least partially explaining why ammonium was not rapidly depleted from the medium, did not correlate with *ntrBC* promoter activity and did not differ between mixed culture and monoculture conditions (Fig. 5-1). However, *ntrBC* could be induced by stimuli other than low intracellular nitrogen status. Indeed, induction of *ntrBC* promoter activity could be recapitulated by addition of specific *S. aureus* extracellular signaling molecules (Fig. 5-2), including N-acetylglucosamine, a component of peptidoglycan that can be liberated following bacterial lysis, and D-ribose, an analogue of the autoinducer-2 QS molecule (74). Future studies should examine

whether these molecules are abundant in the supernatant of competing species (USA300 and LESB58) to determine whether they are the molecules triggering the induction of *ntrBC* promoter activity during co-culture (Fig. 5-1). Interestingly, D-ribose only slightly stimulated *ntrBC* promoter activity in LESB58 WT, but not mutant strains (LESB58 Δ*ntrB*, Δ*ntrC*, or Δ*ntrBC*) (Fig. 5-2). This indicated that NtrBC is required for *ntrBC* promoter activity following stimulation by D-ribose during co-culture. While N-acetylglucosamine also did not induce *ntrBC* promoter activity in mutant strains (since the amount of luminescence detected at $t = 0$ h was not significantly different from luminescence detected at later time points in mutant strains), *ntrBC* promoter activity was detected (Fig. 5-2). This provided evidence that NtrBC was not essential for *ntrBC* promoter activity following stimulation by N-acetylglucosamine. Still, induction of *ntrBC* promoter activity of LESB58 WT was (at its peak) ~6-fold greater than at the point of inoculation. Taken together, these data indicate that self amplification of NtrBC and/or amplification by exogenous molecules released in co-culture may play a role in NtrBC signaling downstream of interspecies competition with *S. aureus* USA300 LAC. Overall, the data presented (Figs. 5-1,5-2) supported my hypothesis that NtrBC was important for conferring a competitive advantage on LESB58 over USA300 LAC, and that NtrBC self amplification of promoter activity, dependent in part on molecules released into the environment by *S. aureus*, may be needed for full responsiveness to interspecies signaling molecules.

P. aeruginosa LESB58 WT and Δ*ntrB* strains outcompeted *S. aureus* USA300 in the planktonic competition assay, performed in LB, whereas Δ*ntrC* and Δ*ntrBC* strains did not (Fig. 5-3). The anti-Staphylococcal activity of *P. aeruginosa* in in vitro culture systems has been described previously (reviewed in ref 74) and attributed to the production of various molecules including 4-hydroxy-2-heptylquinolone N-oxide (HQNO), which is regulated by the PQS signaling system, and other virulence factors (such as those described in Chapter 4, Fig. 5-4) with anti-Staphylococcal activity (74). Some molecules produced by *P. aeruginosa* that are not typically considered to be virulence factors, such as long-chain AHL molecules normally involved in LasRI and RhlRI QS signaling systems, can also interfere with the fitness of *S. aureus* by inhibiting respiratory (ETC) activity and preventing planktonic growth (74). The anti-Staphylococcal activity of *P. aeruginosa* is influenced by environmental factors, including the presence of host factors such as serum or mediators of immune signaling (74). Accordingly, it has been observed that competitive inhibition by *P. aeruginosa* of *S. aureus* can be muted in host-like conditions characteristic of, for example, animal models of disease and biofilm formation in host-mimicking media (3,237,240). This could

partially explain why different patterns of competitive exclusion were exhibited by strains of *P. aeruginosa* LESB58 (WT, Δ*ntrB*, Δ*ntrC*, or Δ*ntrBC*) in biofilm assays in vitro (Fig. 5-4A,B) and air-liquid interface skin organoid models (Fig. 5-4C,D). Generally, LESB58 and USA300 LAC co-existed better during in vitro biofilm growth, suggesting that either *S. aureus* USA300 LAC was producing fewer molecules that primed *P. aeruginosa* LESB58 strains, or that production of anti-Staphylococcal molecules was muted.

To further explore this issue, I interrogated the mechanism(s) possibly underlying inhibition of *S. aureus* USA300 LAC by different strains of *P. aeruginosa* LESB58 during planktonic or biofilm competition assays. I searched upstream regions of coding sequences of *P. aeruginosa* LESB58 by inputting a prior defined position weight matrix (244) to FIMO software (245) for identifying potential binding locations (Table A6). The number of hits identified was likely an underestimate, since the binding motif of NtrC was not well conserved (Fig. A12), and since NtrC can bind to RpoN directly from solution (129,130,250), making it difficult to identify members of the NtrBC regulon by this approach. Leads identified by FIMO included the alternative sigma factor PvdS (252), implicated in iron scavenging and pyoverdine synthesis for iron acquisition as well as in exotoxin A production, and expression of the transcriptional regulator LasR (72,73,76), the master regulator of the hierarchical QS regulatory network of *P. aeruginosa*. Differential expression of strong leads was confirmed by RT-qPCR (Table 5-2). LasR was considered a strong lead due to its expression from an RpoN-dependent promoter (76), global regulation of processes including synthesis of virulence factors with anti-Staphylococcal activity (74), and differential expression in PA14 Δ*ntrB* and Δ*ntrC* mutants (Table A3). Thus, I examined the impact of overexpression of QS molecules on competitive and virulence phenotypes of LESB58 Δ*ntrB,* Δ*ntrC* and Δ*ntrBC* mutants (Figs. 5-6,5-7). Overexpression of *lasI* in the LESB58 Δ*ntrBC* genetic background restored competition with USA300 LAC (Fig. 5-6) and production of pyoverdine, pyocyanin and elastase production (Fig. 5-7). However, *rhlI* and *pqsH* did not restore the competitive advantage of LESB58 Δ*ntrBC* (Fig. 5-6), despite improving pyoverdine, pyocyanin and elastase production (Fig. 5-7), indicating that other anti-Staphylococcal molecules such as C12-HSL itself (253) might be regulated by the LasRI QS system but not other QS systems lower in the hierarchical QS regulatory network.

Chapter 6: Regulatory activity of NtrBC was partly independent of RpoN

6.1 Introduction

NtrC has been proposed to enhance the transcriptional activity of the RNAP holoenzyme associated with the alternative sigma factor RpoN (129), which cannot catalyze open complex formation and transcription initiation without bEBPs such as NtrC. NtrC has been suggested to promote the activity of RpoN through binding to a poorly conserved motif ~100-200 bp upstream of RpoN-dependent promoters (132) or by binding RpoN directly (251). NtrC is one of 28 bEBPs in the *P. aeruginosa* PA14 proteome with an annotated RpoN binding site (252). Some of these are two-component system response regulators, including CbrB (169,174), which is a global regulator involved in carbon catabolism, virulence and resistance of *P. aeruginosa*. Recently, it was shown that CbrAB regulates the expression of the small RNAs (sRNAs) *crcZ* and *crcY,* which regulate catabolite repression control independently of RpoN (254,255). However, whether NtrC and other bEBPs encoded by *P. aeruginosa* have RpoN-independent regulatory functions remains unexplored. Furthermore, whether RpoN has a direct role in adaptive surface colonization phenotypes in vitro or in vivo is unknown, although many CF isolates of *P. aeruginosa* are *rpoN*$^-$ (256). Here, I phenotypically screened *P. aeruginosa* PA14 or LESB58 Δ*rpoN* mutants for surface colonization phenotypes in vitro and in vivo. I characterized the transcriptional profiles of surface colonized Δ*ntrBC* and Δ*rpoN* mutants for a more comprehensive comparison of regulons and examination of potential RpoN-independent regulatory functions of NtrBC.

6.2 Materials and Methods

6.2.1 Bacterial strains and culture conditions

Bacterial strains and plasmids used in this Chapter are described in Table 6-1.

Table 6-1. Bacterial strains and plasmids used in Chapter 6.

Strain or plasmid	Relevant characteristics	Ref.
Escherichia coli		
XL-1 Blue	*recA1 endA1 gyrA96 thi*- 1 *hsdR17* (rK- mK+) *supE44 relA1 lac* [*F'proAB laclq ZΔM15Tn10*(Tc^r)]	Stratagene
ST-18	*pro thi hsdR*$^+$ Tp^r Sm^r; chromosome::RP4-2 Tc::Mu-Km::Tn7/λ*pir ΔhemA*	157
Pseudomonas aeruginosa		
PA14	WT *P. aeruginosa* UCBPP-PA14	158
PA14 Δ*rpoN*	PA14 *rpoN* chromosomal deletion	215
LESB58	WT *P. aeruginosa* Liverpool Epidemic Strain (LES)B58	159

LESB58 Δ*rpoN*	LESB58 *rpoN* chromosomal deletion	This thesis
Plasmid		
pEX18Gm	Gene replacement vector, suicide plasmid carrying *sacB*, Gm^r	160
pEX18Gm.Δ*rpoN*	Cloned 0.94 kbp fusion fragment flanking *rpoN,* Gm^r	This thesis

Overnight cultures were routinely maintained in Luria-Bertani (LB) broth. Overnight and sub-cultures were incubated for no longer than 18 h at 37°C with shaking (250 rpm). Modified forms of BM2 (62 mM potassium phosphate buffer (pH = 7.0), 2 mM $MgSO_4$, 10 µM $FeSO_4$), containing 0.4% glucose and 0.1% CAA or 7 mM $(NH_4)_2SO_4$ were used for assays unless noted otherwise.

E. coli strains were routinely cultured in dYT medium at 37°C with shaking (250 rpm). *E. coli* XL-1 Blue was used as the cloning host and ST-18 for biparental mating where the medium was supplemented with 100 µg/ml ALA. For plasmid selection in *E. coli* donor strains, 12.5 µg/ml gentamycin was added to growth media. For plasmid selection in *P. aeruginosa* PA14 or LESB58, 50 µg/ml or 500 µg/ml gentamycin was added to growth media. Bacterial growth was monitored by measuring OD_{600} with a spectrophotometer (Eppendorf, Mississauga, ON).

6.2.2 General DNA manipulations

Primers used in PCR assays are listed in Table A7. High-fidelity PCR was carried out using the Phusion DNA Polymerase (Thermo Scientific) in accordance with the manufacturer's specifications and optimized annealing temperatures. Oligomer sequences were based on the genome of *P. aeruginosa* LESB58 (GenBank: NC_008463.1) available from NCBI. For PCR reactions, cells were boiled at 98°C with shaking (1,000 rpm) for 10 min and pelleted by centrifugation at 14,500 rpm for 3 min.

Restriction digests were performed using FastDigest restriction enzymes according to the manufacturer's specifications (Thermo Scientific). All ligation reactions were carried out at room temperature using T4 DNA ligase (Invitrogen). DNA purifications were performed using the GeneJET PCR Purification kit or the GeneJET Gel Extraction kit following the manufacturer's instructions (Thermo Scientific).

6.2.3 Generation of recombinant strains

Construction of the knockout vector was based on a previously described protocol (162) and performed by Christina Wiesmann. Briefly, 500 bp regions flanking the 5' and 3' ends of LESB58 *rpoN* were PCR amplified. Reverse-complement sequences were added to primers to provide

homology between flanking regions for continuous amplification in overlap extension PCR. After amplification, fragments were gel purified. The fusion product was ligated into the pEX18Gm vector and transformed (1.8 kV, 25 μF, 200 Ω) into electrocompetent *E. coli* XL-1 Blue. Cells were made electrocompetent by washing with 10% glycerol on ice (4°C). Transformants were recovered in dYT for 1 h (37°C, 220 rpm) prior to blue-white screening. Successful ligation was verified by sequencing (Eurofins, Toronto, ON).

A chromosomal deletion in LESB58 was obtained by conjugational transfer of the gene replacement vector from *E. coli* ST-18 that was made electrocompetent as described above. One hundred μl of *E. coli* ST-18 was mixed with 200 μl *P. aeruginosa* LESB58 and spotted onto dYT agar plates supplemented with 100 μg/ml ALA for overnight growth. On the next day, spots were scratched from the surface of the plate, resuspended in one ml sterile water, and diluted 1,000-fold. Dilute suspension was spread on LB agar plates with gentamicin. Single colonies were picked on LB agar plates containing 10% sucrose for counter-selection of mutants from single-crossovers. Gene deletion was confirmed by PCR and sequencing (Eurofins, Toronto, ON).

6.2.4 Biofilm formation assay

I examined PA14 WT and Δ*rpoN* for biofilm formation using a high-throughput microtitre assay as described elsewhere (117). Overnight cultures were diluted to a starting OD_{600} = 0.1 in BM2 containing 0.1% CAA and 0.4% glucose, then added to polypropylene 96-well plates (Falcon). Following 18-24 h static incubation at 37°C, biomass was stained with 0.1% CV and dissolved in 70% ethanol. OD_{595} was read using a BioTek SynergyH1 microplate reader (BioTek, Winooski, VT).

6.2.5 Motility experiments

Swarming was examined on BM2 plates containing 0.1% CAA, 0.4% glucose and 0.5% agar. Surfing was examined on MSCFM supplemented with 0.4% agar and 0.4% mucin, as previously described (11). Swimming and twitching of PA14 WT and Δ*rpoN* were examined on BM2 (containing 7 mM $(NH_4)_2SO_4$ and 0.4% glucose) or LB plates supplemented with 0.3% or 1.0% agar, respectively. Subcultures were adjusted to a starting OD_{600} = 0.1 in the appropriate medium and grown to an OD_{600} = 0.4-0.6 for spot (swarming, swimming, surfing) or stab (twitching) inoculation. Plates were incubated for 18-24 h at 37°C and, in twitching assays, another 24 h at room temperature (20°C). Plates were imaged with a BioRad ChemiDoc (BioRad, Montreal, QC) and surface area coverage of the plate was measured in ImageJ software (v1.52 q13, NIH:

https://imagej.nih.gov/ij/).

6.2.6 Abscess model of infection in vivo

Animal experiments were performed in accordance with the CCAC guidelines and were approved by the University of British Columbia Animal Care Committee (certificate A19-0064). Pathogenesis of PA14 or LESB58 WT and Δ*rpoN* was assessed in vivo using a subcutaneous abscess model, as previously described (125). Bacterial cultures were grown to an OD_{600} = 1.0 in LB, washed twice in sterile PBS and resuspended to give a final inoculum of ~5 x 10^7 CFU (in 50 µl). Bacteria were injected subcutaneously into the left dorsum of CD-1 mice. Abscesses were formed for 72 h, visible dermonecrosis was measured using a caliper at experimental endpoint and abscesses were harvested in PBS for bacterial enumeration on LB.

6.2.7 RNA Isolation and RNA-Seq

To characterize the molecular mechanism underlying adaptive phenotypes observed, I studied the transcriptomes of surface colonized PA14 WT, Δ*ntrBC* and Δ*rpoN*. PA14 strains were sub-cultured to an OD_{600} = 0.4-0.6 and spot cultured on BM2 containing 0.4% glucose, 0.1% CAA and 0.5% agar for 18-24 h at 37°C. Cells were harvested from the center of the colony, in PBS and RNAProtect (2:1) reagent (Qiagen). RNA extraction was performed using the RNeasy Mini Kit (Qiagen) according to the manufacturer's specifications. Contaminating DNA was removed using the TURBO DNA-free kit (Thermo Fisher). Reza Falsafi depleted rRNA using the RiboZero Bacteria Kit (Illumina). Single-end cDNA libraries were constructed using a KAPA stranded Total RNA Kit (KAPA Biosystems) and libraries were sequenced on an Illumina HiSeq 2500 platform in rapid run mode with 100 bp reads, excluding adapter/index sequences. Arjun Baghela processed RNA-Seq data, which included quality control using fastqc (v0.11.7) and multiqc (v1.6), alignment to the PA14 genome using STAR (v2.6.0a) and read counting using htseq-count (v0.10.0) (165-168). Genome assembly and gene annotations were taken from the *Pseudomonas* Genome Database (169). Genes with fewer than 10 counts in at least three samples were removed to increase detection power for DE analysis. The DESeq2 R package (v1.22.2) was used to perform DE analysis of PA14 mutants versus WT (170). Gene Ontology (GO) enrichment was assessed using the GOFuncR package using GO annotations for the PAO1 reference strain (171).

6.3 Results

6.3.1 *P. aeruginosa* Δ*rpoN* produced more biofilm than WT in different media

To assess whether RpoN had a role in biofilm formation of *P. aeruginosa* PA14, I screened the Δ*rpoN* mutant for biomass production in different media (Fig. 6-1).

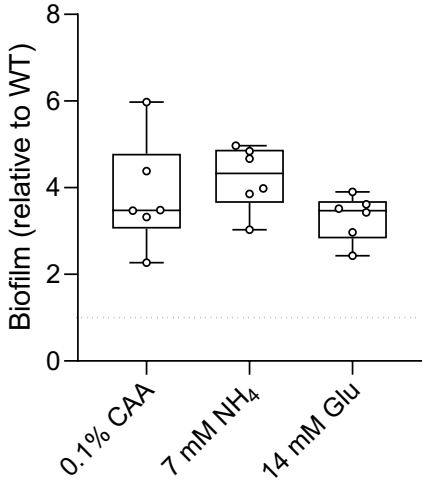

Figure 6-1. *P. aeruginosa* PA14 Δ*rpoN* produced more biofilm than wild-type (WT) in media supplemented with different nitrogen sources. Bacteria were adjusted to a starting OD_{600} = 0.01 in modified forms of BM2 containing 0.1% casamino acids (CAA), 7 mM ammonium (NH_4) or 14 mM glutamate (Glu). Biomass was stained and expressed relative to wild-type (WT).

P. aeruginosa PA14 Δ*rpoN* produced 3.8-fold more biofilm as WT in the presence of CAA, 4.2-fold more biofilm in the presence of ammonium and 3.7-fold more biofilm in the presence of glutamate. Thus, the impact of RpoN on biofilm formation was maintained in nitrogen sources abundant in different tissues.

6.3.2 *P. aeruginosa* Δ*rpoN* was not motile

To determine whether RpoN had a role in other surface colonization phenotypes, I screened the *P. aeruginosa* PA14 Δ*rpoN* mutant for different motilities (Fig. 6-2).

PA14 Δ*rpoN* was defective for each of the motilities. More specifically, mutants inoculated on swarming plates covered only 4.1% of the plate, whereas the WT covered 72.1% of the plate (Fig. 6-2A), a 17.5-fold reduction. Similarly, surfing (Fig. 6-2B), swimming (Figs. 6-2C) and twitching

(Figs. 6-2D) motilities were reduced by to 4.4-, 8.1- and 3.2-fold, respectively.

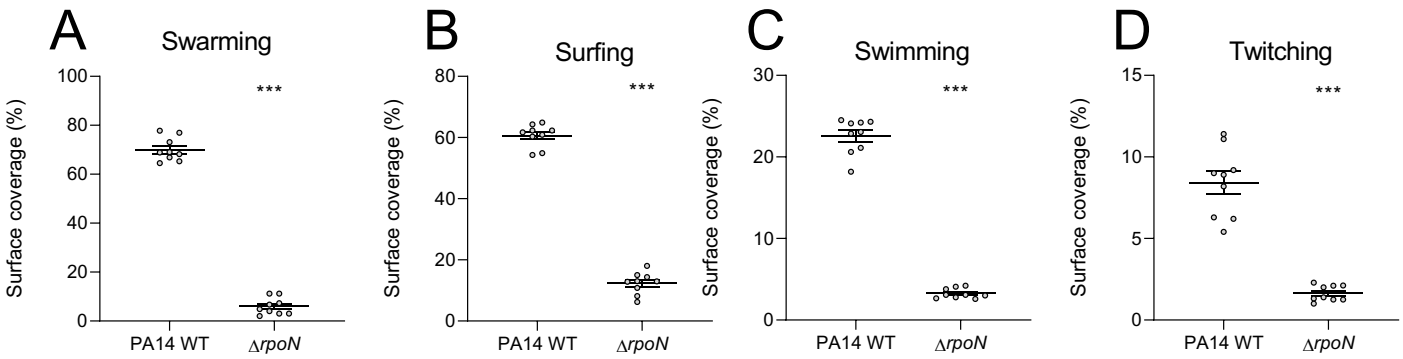

Figure 6-2. *P. aeruginosa* PA14 Δ*rpoN* was deficient for swarming, surfing, swimming and twitching motilities. Bacteria were grown to mid-log phase (OD_{600} = 0.4-0.6) prior to spot inoculation on (A-C) swarming, surfing or swimming plates and stab inoculation on (D) twitching plates. Data are presented as mean ± standard error of the mean (SEM) from three independent experiments containing three biological replicates in each (n = 9). *** $P < 0.001$ different from WT according to Student's unpaired t-test.

6.3.3 *P. aeruginosa* Δ*rpoN* was less invasive and virulent

Prior studies showed that flagella-mediated motility (swarming in particular) was needed for dissemination from localized infections in vivo (16). Thus, I examined invasiveness of the non-motile PA14 Δ*rpoN* strain in a murine model of abscess infection (Table 6-2).

Table 6-2. Invasiveness of PA14 Δ*rpoN* was reduced in comparison to the wild-type (WT) in a high-density infection model. Dissemination of PA14 wild-type (WT) and Δ*rpoN* from abscess to organs is shown as the frequency of bacterial recovery, and range of bacterial counts in instances of recovery, from three independent experiments each including 1-2 individual mice per bacterial strain *(n = 3-5).* Mutants were significantly reduced for dissemination to some organs compared to WT according to Fisher's Exact Test (* $P < 0.05$).

Organ	Number of mice exhibiting bacteria in various organs (bacterial counts; CFU)	
	WT (n = 3)	**Δ*rpoN* (n = 5)**
Heart	3 (10^4)	0 *
Lungs	3 (10^5)	0 *
Liver	3 (10^6)	1 (10^2)
Spleen	3 (10^4-10^5)	0 *
Kidneys	3 (10^4-10^5)	2 (10^2)

In line with prior observations, the non-motile PA14 Δ*rpoN* disseminated to organs from the abscess in fewer instances than WT. For all mice tested, PA14 Δ*rpoN* was never recovered from the heart, lungs, or spleen of mice, which represented a significant difference from the WT. The WT disseminated to these organs in all instances and was recovered at a high density (depending on the organ, 10^4-10^6 CFU were recovered, on average). PA14 Δ*rpoN* was recovered from the

liver in one instance and from the kidneys in two instances. Regardless, the number of mutant bacteria recovered was reduced by at least 2-log orders (10^2 CFU cf. 10^6 CFU for the liver and 10^2 CFU cf. 10^4-10^5 CFU for the kidneys).

Next, I examined whether the same trend was observed between *P. aeruginosa* LESB58 WT and Δ*rpoN* strains in the longer-term subcutaneous infection model (Fig. 6-3).

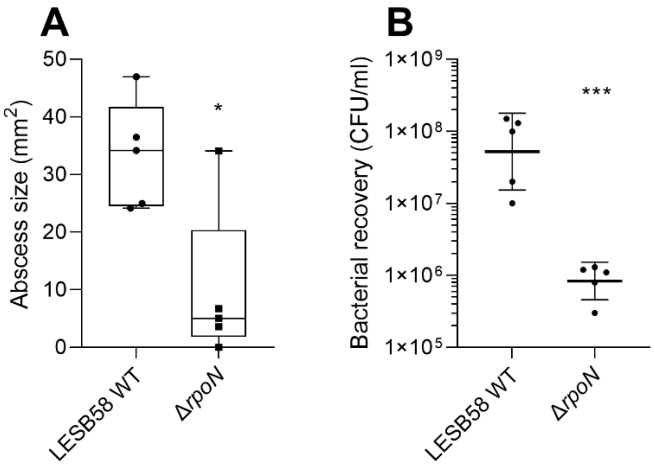

Figure 6-3. *P. aeruginosa* LESB58 Δ*rpoN* colonized the skin of mice less well than wild-type (WT). (A) Abscess size and (B) bacterial recovery was significantly reduced in LESB58 Δ*rpoN* compared to the WT. Box and whiskers delineate interquartile range with geometric error from three independent experiments containing 1-2 biological replicates each (n = 5) (A). Otherwise, data reported as mean ± standard error of the mean (SEM) (B). * $P < 0.05$, *** $P < 0.001$ compared to WT according to Mann-Whitney U-test.

Abscesses formed by LESB58 Δ*rpoN* were 8.1-fold smaller than for WT, the former covering 4.2 mm^2 while the WT abscesses covered 34.1 mm^2, on average (Fig. 6-3A). Correspondingly, there was a ~72-fold difference in CFU/ml between LESB58 WT and Δ*rpoN* bacterial recovery rates (Fig. 6-3B).

6.3.4 Transcriptional profiles of *P. aeruginosa* Δ*rpoN* and Δ*ntrBC*

To further characterize the molecular mechanisms by which NtrBC might contribute to adaptive growth states independently of RpoN, RNA-Seq was performed on RNA extracted from PA14 WT, Δ*ntrBC* and Δ*rpoN* mutants growing on the surface of swarming motility plates cultured on BM2 containing 0.4% glucose, 0.1% CAA and 0.5% agar for 20 h at 37°C. Cells were sampled from the center of the colonies. Deletion of *ntrBC* and *rpoN* drastically influenced the transcriptome of PA14, as reflected by the large number of dysregulated genes (3,229 for Δ*ntrBC* and 3,757 for Δ*rpoN*) with absolute FC in expression ≥ 2 (Fig. A12). A significant subset (2,514;

66.9-77.9%) of differentially expressed (DE) genes were common between the two mutant strains. This indicated a great amount of overlap in the NtrBC and RpoN regulons, as expected. However, there were also 715 genes that were DE in PA14 Δ*ntrBC* but not Δ*rpoN* mutants (Table A8). Genes that were uniquely dysregulated in PA14 Δ*ntrBC* spanned biological processes including translation, protein transport, peptide metabolism and biosynthesis, production of ATP and cilium or flagellum-dependent motility, as well as 30 involved in transcriptional regulation (Table 6-3).

Table 6-3. Regulatory genes that were uniquely DE in PA14 *ntrBC* but not *rpoN* mutants. Gene expression for mutants is reported as fold-change (FC) relative to PA14 WT. RNA was isolated using Qiagen RNEasy MiniPrep kit.

PAO1 Locus	Name	Annotation	FC Δ*ntrBC* cf. WT
PA1363	-	ECF sigma factor	-2.17
PA1456	*cheY*	two-component response regulator CheY	-2.34
PA1544	*anr*	transcriptional regulator Anr	2.34
PA1603	-	probable transcriptional regulator	2.03
PA1636	*kdpD*	two-component sensor KdpD	2.25
PA1853	-	probable transcriptional regulator	8.05
PA1864	-	probable transcriptional regulator	-5.12
PA1884	-	probable transcriptional regulator	2.26
PA2121	-	probable transcriptional regulator	2.48
PA2127	*cgrA*	cupA gene regulator A, CgrA	-2.03
PA2489	-	probable transcriptional regulator	2.11
PA2809	*copR*	two-component response regulator, CopR	2.4
PA3271	-	probable two-component sensor	5.71
PA3704	*wspE*	probable chemotaxis sensor/effector fusion protein	2.73
PA3965	-	probable transcriptional regulator	-2.29
PA3995	-	probable transcriptional regulator	2.48
PA4021	-	probable transcriptional regulator	-3
PA4070	-	probable transcriptional regulator	-2.38
PA4094	-	probable transcriptional regulator	-3.8
PA4275	*nusG*	transcription antitermination protein NusG	-3.39
PA4464	*ptsN*	nitrogen regulatory IIA protein	-2.8
PA4508	-	probable transcriptional regulator	-2.12
PA4547	*pilR*	two-component response regulator PilR	2.38
PA4659	*cupE4*	probable transcriptional regulator	4.09
PA4776	*pmrA*	PmrA: two-component response regulator	2.12
PA4777	*pmrB*	PmrB: two-component sensor kinase	2.02
PA5157	-	probable transcriptional regulator	2.62
PA5324	*sphR*	Sphingosine-responsive regulator, SphR	-2.24
PA5483	*algB*	two-component response regulator AlgB	-2.32
PA5550	*glmR*	GlmR transcriptional regulator	-2.87

Of the 30 regulatory genes exclusively DE in PA14 Δ*ntrBC*, 16 were annotated as probable

transcriptional regulators (or similar), representing 53.3% of those detected. The remaining 14 regulatory genes have been well described (169). CheY, for example, is a two-component transcriptional regulator involved in chemotaxis (257) that is encoded in the che I gene cluster of the *P. aeruginosa* chromosome. When a chemoattractant binds to a methyl-accepting chemotaxis protein (MCP), it undergoes a conformational change and stimulate phosphorylation of CheA, the cognate sensor kinase for CheY, which in turn can bind to the flagellar motor (encoded by *fliM*) and induce rotational switching to orient the bacterium toward the chemoattractant. Since expression of *cheY* is downregulated 2.3-fold in PA14 Δ*ntrBC*, it is possible that chemotaxis of this strain was impacted. Other *ntrBC*-dependent, *rpoN*-independent regulators involved in chemotaxis and functionality of bacterial appendages implicated in surface colonization and motile phenotypes included PilR (258) and the surface responsive regulator WspE (259), which were upregulated 2.4-fold and 2.7-fold, respectively. Other transcriptional regulators with large regulons were dysregulated in PA14 Δ*ntrBC*, including *nusG*, which encodes a transcription elongation factor that is needed for efficient transcription termination by Rho factor (260) and *anr*, which encodes an oxygen responsive regulator of anaerobiosis downstream of the stringent stress response (34), likely contributing strongly to the divergence of transcriptional profiles between PA14 Δ*ntrBC* and Δ*rpoN*. The gene encoding the nitrogen regulatory IIA protein (*ptsN*) was only differentially expressed in PA14 Δ*ntrBC*, which was surprising due to its predicted occurrence in an operon with *rpoN* (169). Other regulators that were upregulated included PA1853 (8.1-fold), which is 80% similar to a protein from the denitrification cluster of *P. stutzeri* (261), PA3271/*mxtR* (5.7-fold), an orphan sensor kinase that controls quinolone signal production via MexT (262) and PA4651/*cupE4* (4.1-fold), a pilus assembly chaperone (263).

Several genes that were dysregulated in either PA14 Δ*ntrBC*, Δ*rpoN* or both were involved in general nitrogen and carbon metabolic processes according to the Kyoto Encyclopedia of Genes and Genomes (KEGG; https://www.genome.jp/kegg/) database (Table 6-4A,B). Numerous genes involved in virulence during acute lung infection (175) were also dysregulated in PA14 Δ*ntrBC* and/or Δ*rpoN* mutants (Table 6-4C). The large number of metabolic genes found to be DE in only one of these strains argues against NtrBC working only through RpoN. However, several metabolic genes were DE in both mutant strains, consistent with the partial role of NtrC as an enhancer of RpoN activity (129). The majority (50 of 90; ~56%) of DE genes involved in carbon metabolism were common, although 17 genes (19%) were DE only in Δ*ntrBC* and 23 (26%) were DE in only Δ*rpoN*. Of the genes involved in nitrogen metabolism, *ntrB* was the most significantly

downregulated gene across mutant strains, downregulated by 369- and 227- fold in Δ*ntrBC* and Δ*rpoN,* respectively. Surprisingly, *ntrC* was only significantly downregulated (by 359-fold) in the Δ*ntrBC* mutant strain. This might indicate that transcription of *ntrC* can be uncoupled from *ntrB* and does not always depend on RpoN.

Table 6-4. Selected categories of genes were differentially expressed under swarming conditions in PA14 *ntrBC* and/or *rpoN* mutants. Genes in four categories that were differentially expressed according to RNA-Seq in PA14 mutant strains. Gene expression for mutants is reported as fold-change (FC) relative to PA14 WT. RNA was isolated using Qiagen RNEasy MiniPrep kit.

PAO1 Locus	Name	Annotation	FC Δ*ntrBC*	FC Δ*rpoN*
A. Genes involved in nitrogen metabolism				
PA0102	-	probable carbonic anhydrase		-2.22
PA0298	*spuB*	glutamylpolyamine synthetase	-2.73	
PA0519	*nirS*	nitrite reductase precursor		5.69
PA0523	*norC*	nitric-oxide reductase subunit C	-4.15	
PA0524	*norB*	nitric-oxide reductase subunit B	-4.50	-2.33
PA0660	-	hypothetical protein	3.50	3.47
PA4202	*nmoA*	nitronate monooxygenase NmoA	2.13	2.05
PA3877	*narK1*	nitrite extrusion protein 1	-7.08	
PA3876	*narK2*	nitrite extrusion protein 2	-2.55	
PA3392	*nosZ*	nitrous-oxide reductase precursor	-4.02	-2.18
PA1781	*nirB*	assimilatory nitrite reductase large subunit	-2.83	-3.73
PA1174	*napA*	periplasmic nitrate reductase protein NapA		-64.3
PA1173	*napB*	cytochrome c-type protein NapB precursor		-32.7
PA5119	*glnA*	glutamine synthetase		2.02
PA5124	*ntrB*	two-component sensor NtrB	-369	-273
PA5125	*ntrC*	two-component response regulator NtrC	-359	
PA5173	*arcC*	carbamate kinase		-4.97
PA5522	*pauA6*	glutamylpolyamine synthetase	-2.03	
PA5530	-	C5-dicarboxylate transporter	-2.68	3.23
B. Genes involved in carbon metabolism				
PA0330	*rpiA*	ribose 5-phosphate isomerase		2.00
PA0331	*ilvA1*	threonine dehydratase, biosynthetic		3.56
PA0430	*metF*	5,10-methylenetetrahydrofolate reductase	2.11	1.98
PA0482	*glcB*	malate synthase G	3.64	
PA0548	*tktA*	transketolase	2.60	2.63
PA0552	*pgk*	phosphoglycerate kinase		3.19
PA0555	*fda*	fructose-1,6-bisphosphate aldolase		1.66
PA0607	*rpe*	ribulose-phosphate 3-epimerase		2.43
PA4236	*katA*	catalase		-3.12
PA4152	-	probable hydrolase	-10.7	-5.14
PA3687	*ppc*	phosphoenolpyruvate carboxylase	2.12	
PA3639	*accA*	acetyl-coenzyme A carboxylase carboxyl transferase (α SU)		2.83
PA3628	-	putative esterase	2.14	

PA3471	-	probable malic enzyme	2.13	3.10
PA3452	*mqoA*	malate:quinone oxidoreductase		2.24
PA3417	-	pyruvate dehydrogenase E1 component, alpha subunit	-13.6	-243
PA3416	-	pyruvate dehydrogenase E1 component, beta chain	-13.5	-443
PA3415	-	probable dihydrolipoamide acetyltransferase	-10.8	-162
PA3195	*gapA*	glyceraldehyde 3-phosphate dehydrogenase	5.38	6.38
PA3194	*edd*	phosphogluconate dehydratase	2.45	2.68
PA3193	*glk*	glucokinase	3.66	4.20
PA3183	*zwf*	glucose-6-phosphate 1-dehydrogenase	3.46	6.24
PA3182	*pgl*	6-phosphogluconolactonase	5.69	7.07
PA3181	-	2-keto-3-deoxy-6-phosphogluconate aldolase	3.88	5.33
PA3167	*serC*	3-phosphoserine aminotransferase		2.51
PA2796	*tal*	transaldolase	2.54	
PA2624	*idh*	isocitrate dehydrogenase	10.8	5.37
PA2623	*icd*	isocitrate dehydrogenase	2.51	
PA2555	-	probable AMP-binding enzyme	5.02	3.92
PA2553	-	probable acyl-CoA thiolase	5.39	4.27
PA2446	*gcvH2*	glycine cleavage system protein H2		16.0
PA2445	*gcvP2*	glycine cleavage system protein P2	-3.61	19.2
PA2444	*glyA2*	serine hydroxymethyltransferase	-6.53	16.8
PA2443	*sdaA*	L-serine dehydratase		2.02
PA2442	*gcvT2*	glycine cleavage system protein T2		4.41
PA2323	*gapN*	GapN	9.33	35.0
PA2321	*gntK*	GntK	9.14	20.3
PA2250	*lpdV*	lipoamide dehydrogenase-Val	2.46	4.45
PA2147	*katE*	catalase HPII	-10.7	-19.6
PA2001	*atoB*	acetyl-CoA acetyltransferase	12.27	4.38
PA1796	*folD*	5,10-methylene-tetrahydrofolate dehydrogenase		2.08
PA1787	*acnB*	aconitate hydratase 2	3.05	3.69
PA1737	-	probable 3-hydroxyacyl-CoA dehydrogenase	-3.34	-3.21
PA1736	-	probable acyl-CoA thiolase	-2.67	
PA1589	*sucD*	succinyl-CoA synthetase alpha chain	2.23	2.48
PA1588	*sucC*	succinyl-CoA synthetase beta chain	2.28	2.58
PA1587	*lpd*	dihydrolipoamide dehydrogenase Lpd	2.46	
PA1586	*sucB*	dihydrolipoamide succinyltransferase (E2 subunit)	2.25	
PA1585	*sucA*	2-oxoglutarate dehydrogenase (E1 subunit)	3.27	2.06
PA1584	*sdhB*	succinate dehydrogenase (B subunit)	2.01	
PA1583	*sdhA*	succinate dehydrogenase (A subunit)	3.36	3.20
PA1582	*sdhD*	succinate dehydrogenase (D subunit)	4.78	3.88
PA1580	*gltA*	citrate synthase	5.27	3.61
PA1562	*acnA*	aconitate hydratase 1		-6.26
PA1499	-	conserved hypothetical protein	-4.08	-2.47
PA1326	*ilvA2*	threonine dehydratase, biosynthetic	-2.09	
PA0887	*acsA*	acetyl-coenzyme A synthetase	2.12	2.36
PA0854	*fumC2*	fumarate hydratase		-6.40

PA0836	*ackA*	acetate kinase	3.74	4.82
PA0835	*pta*	phosphate acetyltransferase	2.03	
PA0747	-	probable aldehyde dehydrogenase		-3.14
PA4329	*pykA*	pyruvate kinase II	2.90	5.74
PA4333	-	probable fumarase		3.55
PA4640	*mqoB*	malate:quinone oxidoreductase	2.67	
PA4670	*prs*	ribose-phosphate pyrophosphokinase	-2.02	
PA4733	*acsB*	acetyl-coenzyme A synthetase	-2.85	-2.00
PA4785	-	probable acyl-CoA thiolase		-2.39
PA4810	*fdnI*	nitrate-inducible formate dehydrogenase, gamma subunit	-2.99	
PA4811	*fdnH*	nitrate-inducible formate dehydrogenase, beta subunit	-2.23	-6.40
PA4829	*lpd3*	dihydrolipoamide dehydrogenase 3		-3.25
PA4847	*accB*	biotin carboxyl carrier protein (BCCP)		4.80
PA4848	*accC*	biotin carboxylase	2.40	4.46
PA4960	-	probable phosphoserine phosphatase		2.00
PA5015	*aceE*	pyruvate dehydrogenase	2.69	6.55
PA5016	*aceF*	dihydrolipoamide acetyltransferase	2.05	3.22
PA5020	-	probable acyl-CoA dehydrogenase		-2.91
PA5046	-	malic enzyme	-3.43	2.33
PA5110	*fbp*	fructose-1,6-bisphosphatase		2.21
PA5173	*arcC*	carbamate kinase		-4.97
PA5192	*pckA*	phosphoenolpyruvate carboxykinase	-2.09	
PA5213	*gcvP1*	glycine cleavage system protein P1	-2.47	-12.8
PA5353	*glcF*	glycolate oxidase subunit GlcF	-41.8	-16.4
PA5354	*glcE*	glycolate oxidase subunit GlcE	-14.7	-9.92
PA5355	*glcD*	glycolate oxidase subunit GlcD	-40.1	-11.1
PA5379	*sdaB*	L-serine dehydratase		-2.33
PA5415	*glyA1*	serine hydroxymethyltransferase	-2.31	
PA5421	*fdhA*	glutathione-independent formaldehyde dehydrogenase		-2.80
PA5435	-	probable transcarboxylase subunit		2.37
PA5436	-	probable biotin carboxylase subunit of a transcarboxylase	2.69	
PA5445	-	probable coenzyme A transferase	6.29	2.04
C. Genes involved in PA14 virulence				
PA0041	-	probable hemagglutinin	-3.26	-2.31
PA0073	*tagT1*	TagT1		-4.72
PA0077	*icmF1*	IcmF1		-2.80
PA0082	*tssA1*	TssA1		-2.34
PA0090	*clpV1*	ClpV1		-2.42
PA0098	-	hypothetical protein	-2.27	
PA0141	-	conserved hypothetical protein	3.24	
PA0298	*spuB*	Glutamylpolyamine synthetase	-2.73	
PA0375	*ftsX*	cell division protein FtsX		2.53
PA0410	*pilI*	twitching motility protein PilI	2.69	3.71
PA0428	-	probable ATP-dependent RNA helicase	2.13	2.44
PA0441	*dht*	dihydropyrimidinase	-17.7	-13.6

PA0447	*gcdH*	glutaryl-CoA dehydrogenase	2.40	2.33
PA0454	-	conserved hypothetical protein		2.30
PA0455	*dbpA*	RNA helicase DbpA	3.63	
PA0459	-	probable ClpA/B protease ATP binding subunit	2.22	-5.16
PA0552	*pgk*	phosphoglycerate kinase	3.19	
PA0605	*agtC*	AgtC	2.15	2.86
PA0620	-	probable bacteriophage protein	-5.23	-4.17
PA4172	-	probable nuclease	-5.92	-6.36
PA4024	*eutB*	ethanolamine ammonia-lyase large subunit	2.05	
PA3922	-	conserved hypothetical protein	-2.45	
PA3893	-	conserved hypothetical protein	3.22	
PA3876	*narK2*	nitrite extrusion protein 2	-2.55	
PA3831	*pepA*	leucine aminopeptidase	3.46	4.17
PA3763	*purL*	Phosphoribosyl formyl glycinamidine synthase		3.01
PA3735	*thrC*	threonine synthase		3.04
PA3683	-	conserved hypothetical protein	3.45	3.21
PA3663	-	hypothetical protein	2.06	
PA3659	-	probable aminotransferase	3.67	2.32
PA3620	*mutS*	DNA mismatch repair protein MutS	2.18	3.63
PA3607	*potA*	polyamine transport protein PotA	-3.82	
PA3598	-	conserved hypothetical protein	-5.00	-5.02
PA3524	*gloA1*	lactoylglutathione lyase	-3.15	-2.66
PA3308	*hepA*	RNA helicase HepA		3.90
PA3298	-	hypothetical protein	-5.92	
PA3291	*tli1*	Tli1	-12.2	-14.1
PA3284	-	hypothetical protein	-3.52	
PA3191	*gtrS*	glucose transport sensor, GtrS	2.10	
PA2998	*nqrB*	Na+-translocating NADH:ubiquinone oxidoreductase subunit		3.03
PA2895	*sbrR*	SbrR	-2.83	-6.56
PA2462	-	hypothetical protein	-2.91	
PA2439	-	hypothetical protein	-3.28	
PA2408	*fpvD*	ferripyoverdine	29.1	13.6
PA1981	-	hypothetical protein	-5.11	-17.7
PA1927	*metE*	5-methyltetrahydropteroyltriglutamate-homocysteine S-methyltransferase	-2.20	-2.46
PA1874	-	hypothetical protein		-90.8
PA1596	*htpG*	heat shock protein HtpG	-2.93	9.41
PA1592	-	hypothetical protein	-4.40	-10.7
PA1436	-	probable Resistance-Nodulation-Cell Division (RND) efflux transporter		-2.93
PA1248	*aprF*	Alkaline protease secretion outer membrane protein	3.75	-10.4
PA1174	*napA*	periplasmic nitrate reductase protein NapA		-64.3
PA1157	-	probable two-component response regulator	2.82	
PA1054	*shaA*	ShaA		
PA1009	-	hypothetical protein	4.67	6.39
PA0895	*aruC*	N2-Succinylornithine 5-aminotransferase (SOAT)	-2.11	

PA0806	-	hypothetical protein	-2.02	-12.3
PA0779	*asrA*	AsrA		5.37
PA0762	*algU*	sigma factor AlgU	-5.36	-5.18
PA4338	-	hypothetical protein	-3.54	
PA4434	-	probable oxidoreductase	2.95	
PA4528	*pilD*	type 4 prepilin peptidase PilD	2.67	
PA4543	-	conserved hypothetical protein	2.72	2.40
PA4620	-	hypothetical protein	3.73	3.61
PA4625	*cdrA*	cyclic diguanylate-regulated TPS partner A, CdrA	-17.8	-55.7
PA4659	-	probable transcriptional regulator	4.09	
PA4692	-	conserved hypothetical protein	-2.50	-2.19
PA4764	*fur*	ferric uptake regulation protein		-2.92
PA4834	*cntI*	CntI	-2.87	-2.94
PA4852	-	conserved hypothetical protein	-2.69	
PA4854	*purH*	phosphoribosylaminoimidazolecarboxamide formyltransferase	2.75	
PA4855	*purD*	phosphoribosylamine-glycine ligase	4.04	
PA4886	-	probable two-component sensor	2.08	2.35
PA4915	-	probable chemotaxis transducer	-3.39	-22.7
PA4929	-	hypothetical protein	-2.93	
PA5075	-	probable permease of ABC transporter		4.52
PA5084	*dguA*	DguA	-21.0	-18.7
PA5167	*dctP*	DctP	-4.55	-3.27
PA5201	-	conserved hypothetical protein	3.87	
PA5295	-	hypothetical protein	2.56	
PA5327	*sphC*	SphC		-3.15
PA5347	-	hypothetical protein	-3.42	
PA5437	-	probable transcriptional regulator		4.65
PA5441	-	hypothetical protein		2.82
PA5449	*wbpX*	glycosyltransferase WbpX	2.13	3.13

Other metabolic genes that were similarly dysregulated across mutants (Table 6-4) included *norB*, *nosZ* and *nirB*, each of which play a distinct role in the transformation of nitrogen through its various oxidation states (137). Of the genes implicated in carbon metabolism, pyruvate dehydrogenase genes PA3416 and PA3417 (169) were the most downregulated by 13.5- to 13.6-fold in the Δ*ntrBC* mutant strain and 223- to 443-fold in the Δ*rpoN* mutant strain. Of the genes implicated in virulence, *cdrA* (encoding a biofilm matrix protein/adhesin) (267) was the most consistently downregulated (by 17.8- and 55-fold in Δ*ntrBC* and Δ*rpoN* strains, respectively). The alternative sigma factor *algU* was also significantly downregulated (by 5.36- and 5.18-fold in Δ*ntrBC* and Δ*rpoN* strains, respectively). Similarly, the *katE* enzyme involved in detoxification of ROS was downregulated (10.7- and 19.6-fold) across mutants. In contrast, several genes were upregulated across mutants, representing a negative regulatory function of NtrBC and/or RpoN that

has not been emphasized previously. For example, several key genes involved in glycolysis and the TCA cycle, including *pgl*, *zwf*, *glk* and *edd* (169), were more than 2-fold upregulated in both the PA14 Δ*ntrBC* and Δ*rpoN* mutants. Similarly, the *fpvD* gene involved in iron scavenging was upregulated 29.1- and 13.6-fold across mutants. In contrast, *glyA2* and *gcvP2* were regulated in different directions in mutant strains. These genes, both important for amino acid metabolism, were downregulated in the Δ*ntrBC* mutant (6.53- and 6.32-fold, respectively) but upregulated in the Δ*rpoN* mutant (16.8- and 19.2- fold, respectively). Other genes regulated in different directions in Δ*ntrBC* and Δ*rpoN* included PA5046 (downregulated 3.43-fold or upregulated 2.33-fold in mutants), PA0459, a probable ATP binding subunit of *clp* protease (upregulated 2.22-fold or downregulated 5.16-fold in mutants), *htpG,* a heat shock protein (downregulated 2.93-fold and upregulated 9.41-fold in mutants), and the alkaline protease secretion molecule *aprF* (upregulated 3.75-fold or downregulated 10.4-fold in mutants) (169).

There were many instances of dysregulated expression of genes involved in metabolism or virulence by Δ*ntrBC* or Δ*rpoN* only. With respect to nitrogen metabolism, the genes involved in nitrite extrusion, *narK1* and *narK2*, were downregulated only in Δ*ntrBC* (7.08- and 2.55-fold, respectively). In contrast, genes involved in periplasmic metabolism of nitrate, *napA* and *napB*, were dysregulated only in Δ*rpoN* (64.3- and 32.7-fold, respectively). Genes DE in only one mutant were not enriched for any particular metabolic pathway involved in carbon metabolism. With respect to virulence during acute airway infection (175), some exotoxins were dysregulated only in Δ*rpoN*, including *tagT1* (downregulated 4.7-fold), *icmF1* (downregulated 2.8-fold), *tssA1* (downregulated 2.34-fold) and *clpV1* (downregulated 2.42-fold). In contrast, *tli1* was downregulated in both Δ*ntrBC* and Δ*rpoN* (12.2- and 14.1-fold, respectively).

6.4 Discussion

Here, I screened the *P. aeruginosa* PA14 Δ*rpoN* mutant for adaptive phenotypes that were shown to be regulated by NtrBC in previous Chapters. The PA14 Δ*rpoN* mutant was an overproducer of biofilm (Fig. 6-1) in BM2 containing ammonium, CAA or glutamate as the nitrogen source. This contrasted with the biofilm phenotypes exhibited by PA14 Δ*ntrB,* Δ*ntrC* and Δ*ntrBC* (Chapter 2), which produced WT levels of biofilm in BM2 containing CAA or, for the double mutant, slightly less (~65%) biofilm than WT. Forty genes important for biofilm formation (51) were significantly dysregulated in the PA14 Δ*rpoN* mutant, which could provide insights into the mechanism(s) by which biofilm was overproduced. Some of these genes were regulated in opposite directions in

PA14 Δ*ntrBC* and Δ*rpoN,* including the quinone signaling *pqqE* (169) that was upregulated 2.51-fold and downregulated 4.10-fold, and the oxidoreductase PA1881 (169) that was upregulated 2.62-fold and downregulated 6.40-fold, in the respective mutants. Another study that assessed longer-term biofilm formation found that *P. aeruginosa* PAO1 Δ*rpoN* mutants formed fewer microcolonies and formed biofilms that were structurally distinct from that of *P. aeruginosa* PAO1 WT (264). Dysregulated expression of genes involved in flagellar motility and type IV pili function, known to be important for microcolony formation and early-stage biofilm formation (45), could perhaps explain these findings.

The PA14 Δ*rpoN* mutant was completely defective for all forms of motility (Fig. 6-2), which indicated that the mutant did not produce functional bacterial appendages upon which twitching and swimming depend, including type IV pili and the flagellum (18), respectively. Several genes involved in flagellar synthesis or function were DE in the PA14 Δ*rpoN* mutant, including the flagellar motor switch proteins *fliN* and *fliM*, downregulated 3.0- and 2.4-fold, respectively, as well as the flagellar capping protein *fliD* (downregulated 2.2-fold). Genes involved in synthesis or function of the type IV pili that were downregulated included *pilC* (2.4-fold), *pilG* (2.9-fold), *pilV2* and *pilM2* (both 2.1-fold), *fimV* (2.1-fold), *tadD* (16.9-fold), *rcpC* (30.6-fold) and the cup cluster of genes (*cupE1-cupE6*). Microscopy or other phenotypic assays could be performed to confirm the absence of bacterial appendages on the PA14 Δ*rpoN* mutant. Toward this end, a prior study reported that a *P. aeruginosa* PAK *rpoN* null strain lacked type IV pili, adhesins and flagella (265) and was not phagocytosed well by macrophages. PA14 Δ*ntrB,* Δ*ntrC* and Δ*ntrBC* were also reduced or completely defective for swarming motility (Chapter 2), similar to PA14 Δ*rpoN* (Fig. 6-2). However, PA14 Δ*ntrB,* Δ*ntrC* and Δ*ntrBC* mutants were not significantly reduced for surfing, swimming, or twitching motilities, indicating that mutants produced functional flagella and type IV pili in contrast to PA14 Δ*rpoN*. It is also likely that reduced production of rhamnolipids contributed to the motility defects observed for PA14 Δ*rpoN*, similar to that for PA14 Δ*ntrB,* Δ*ntrC* and Δ*ntrBC* mutants, since *rhl* genes were significantly downregulated in PA14 Δ*rpoN.* More specifically, *rhlA* and *rhlB* were downregulated 48.8- and 15.0-fold, respectively. Defective QS signaling could have also contributed to motility defects, since regulators including *rhlR* and *lasR* were downregulated 37.8- and 17.8-fold, respectively.

Since we know that swarming motility, and flagellum-dependent motilities in general, contribute to invasiveness and virulence in vivo (16), I hypothesized that the PA14 and LESB58 Δ*rpoN*

mutant would exhibit less invasiveness and virulence than WT in murine models of abscess infection. Accordingly, the PA14 Δ*rpoN* mutant was far less invasive than WT, infiltrating only the liver and kidneys of mice in one or two (of five) instances, respectively (Table 6-2). In contrast, PA14 Δ*ntrB* and Δ*ntrC* mutants infiltrated all organs examined at least twice, and bacterial recovery of these mutants from organs was more like WT (Chapter 2). Like PA14 Δ*rpoN,* the Δ*ntrBC* mutant did not infiltrate the heart in any instances, infiltrated the liver and kidneys in only one instance (of nine) and the bacterial recovery from all organs where bacteria were found was much lower than WT on average, except in the instance of the lungs. Thus, although the Δ*ntrBC* double mutant was more like PA14 Δ*rpoN* than single mutants Δ*ntrB* and Δ*ntrC*, important differences were observed. Another important difference was observed in the longer-term abscess model, since LESB58 Δ*rpoN* colonized the skin less well than WT (as shown by the ~100-fold difference in bacterial recovery) (Fig. 6-3). Like the LESB58 Δ*ntrBC* mutant, there was also a statistically significant difference in the size of abscesses formed by LESB58 Δ*rpoN* when compared to WT*,* though the size of abscesses formed by LESB58 Δ*ntrBC* (Chapter 2) was more than double that of LESB58 Δ*rpoN* (13.2 mm^2 vs. 4.2 mm^2). Reduced invasiveness and virulence of the PA14 Δ*rpoN* mutant could likely be explained by the complete loss of motilities and dysregulated expression of genes involved in production and functionality of their associated appendages that have moonlighting roles in adherence to surfaces, as well as the greater downregulation of genes important for infection (Table 6-4C). The latter included greater downregulation of the *fur r*egulon, which is important for virulence and metabolism in iron-restricted environments (71,266) due to regulation of iron sequestering mechanisms and detoxification of pyochelin. For example, effectors implicated in iron scavenging that are downstream of *fur*, including *pvdS*, were downregulated in PA14 Δ*rpoN,* as well as pyoverdine biosynthesis proteins (*pvdD*, *pvdE*, *pvdF*). Another gene important for infection that was more significantly downregulated in the Δ*rpoN* mutant compared to the Δ*ntrBC* mutant was *cdrA*, which is important for persistence in the presence of host proteases (267) and has a role in biofilm formation.

Interestingly, 715 genes were uniquely dysregulated in the Δ*ntrBC* mutant, including many genes encoding ribosomal proteins (including *rpm, rps*, *rpl*), receptors involved in iron acquisition (including *pirA, hitA*), T6SS proteins (including *tss*, *tli*, *xcp*, *tsi*), exoenzymes (including *exsC*, *exoT*), T3SS apparatus or effectors (including *pcrV*, *psc*, *ptrA*) and transcriptional regulators (such

as *pchR*, *anr*, *pilR*, *nrtR*, *cgrR*, *cheY*) highlighted in Table 6-3. Clearly, NtrBC and RpoN are global regulators with overlapping but also diverse functions in physiological and pathological processes that are triggered to cope with environmental conditions. Though there was significant overlap between the functions of NtrBC and RpoN, aligning with the role of NtrC as a bEBP of transcription initiation from RpoN-dependent promoters, significant regulatory activity of NtrBC occurred independently of RpoN. Since I observed a significant downregulation of *rpoN* (>20-fold) in the PA14 Δ*ntrBC* mutant but did not find an NtrC binding site upstream of *rpoN* promoters, future studies should determine whether NtrC can bind directly to RpoN for enhancement of its autoregulatory functions, or if the impact of *ntrBC* deletion on *rpoN* expression was due to indirect regulation downstream of other dysregulated regulators.

Chapter 7: Conclusions

Data presented in this thesis revealed a major and multifactorial role for NtrBC in adaptive lifestyles and virulence of the environmentally ubiquitous, opportunistic pathogen *P. aeruginosa*. The role of NtrB and NtrC in adaptive lifestyles including swarming and surfing motilities (Figs. 2-4,2-5), as well as biofilm formation (Fig. 2-2) and infection in vivo (Figs. 2-1,A1, Table 2-2), appeared to be additive. Since NtrC has been shown to sometimes phosphorylate independently of NtrB (130), possibly mitigating some of the impact of *ntrB* mutation on phenotypes of interest, I hypothesized that the PA14 or LESB58 Δ*ntrC* mutants would have phenotypes more different from WT than the Δ*ntrB* mutants. However, I did not hypothesize that the Δ*ntrBC* mutants would have phenotypes more significantly different from WT than the Δ*ntrC* mutants. This was surprising since canonical two-component system signaling is highly specific and, theoretically, mutation of the response regulator should manifest in the same phenotype as mutation of both the response regulator and sensor kinase, even if the response regulator can auto-phosphorylate. Comparison of the transcriptional profiles of single Δ*ntrB* and Δ*ntrC* mutants to the double Δ*ntrBC* mutant could shed insight on this phenomenon. Overall, there were 790 genes dysregulated in the PA14 Δ*ntrB* mutant (Chapter 2), 1,184 genes dysregulated in the PA14 Δ*ntrC* mutant (Chapter 2) and 3,229 genes dysregulated in the PA14 Δ*ntrBC* mutant (Chapter 6) isolated from swarming plates. Importantly, RNA from the Δ*ntrB* or Δ*ntrC* mutants were isolated from cells that were actively swarming, whereas RNA from the Δ*ntrBC* mutant was isolated from cells in the center of the colony (since this mutant had no actively swarming cells). Although the expression of genes was determined relative to WT cells picked from the same area of the swarming plate (i.e., from tips of swarming tendrils or the center of the swarming colony), transcriptional differences between the Δ*ntrBC* double mutant and Δ*ntrB* or Δ*ntrC* single mutants could be confounded. As well, genes that had an absolute FC ≥1.5 were considered differentially expressed during analysis of the transcriptional profiles of Δ*ntrB* or Δ*ntrC* single mutants, whereas due to the much larger impact, genes that had an absolute FC ≥2 were considered differentially expressed during analysis of the transcriptional profile of the Δ*ntrBC* double mutant (and Δ*rpoN*). Nonetheless, the observation that Δ*ntrBC* double mutants were transcriptionally more different from WT than Δ*ntrB* or Δ*ntrC* single mutants coincided with phenotypic analyses.

There were 837 genes that overlapped between the transcriptional profiles of Δ*ntrB* or Δ*ntrC* and Δ*ntrBC*, consistent in part with the role of NtrB and NtrC acting as a cognate pair with insulated

signal transduction (i.e., undergoing canonical two-component system signaling without crosstalk). More specifically, 677 of the 790 genes differentially expressed in the Δ*ntrB* mutant were also differentially expressed in the Δ*ntrBC* mutant, representing ~86% overlap. Similarly, 1023 of the 1184 genes that were differentially expressed in the Δ*ntrC* mutant were also differentially expressed in the Δ*ntrBC* mutant, also representing ~86% overlap. Genes that overlapped between mutants spanned functional categories, including nitrogen and carbon metabolism as well as genes involved in phenotypes of interest. For example, the flagellar gene *flgF* was downregulated 2.71-, 2.05- and 22.8-fold in Δ*ntrB*, Δ*ntrC*, and Δ*ntrBC* respectively. Another flagellar gene, *fliF*, was downregulated 2.55-, 1.97- and 14.4- fold in Δ*ntrB*, Δ*ntrC*, and Δ*ntrBC* respectively. Other flagellar genes that were significantly downregulated in single mutants, but more significantly downregulated in the double mutant, corresponding to more different phenotypes in which flagellar function is implicated (including motilities as well as virulence and biofilm formation, as discussed in Chapters 2, 4 and 6) included *flgJ* and *fliK*. Interestingly, *fliI* and *fliJ* were dysregulated in single mutants, but not in the double mutant. Further, genes involved in synthesis and function of type IV pili, including *pilP* and *pilU*, were downregulated in the Δ*ntrC* and Δ*rpoN* mutants only. In PA14 Δ*ntrC,* these genes were downregulated 1.61- and 1.55-fold, whereas in Δ*rpoN* they were downregulated 2.10- and 2.50-fold, respectively. The closer agreement of gene expression in Δ*ntrC* and Δ*rpoN* mutants, when compared to the divergent levels of expression of genes involved in appendage synthesis or function observed for e.g., Δ*ntrC* and Δ*ntrBC*, might indicate that these processes are regulated by NtrC acting as a bEBP that facilitates transcription from RpoN-promoters (268). Towards this end, I detected conserved NtrC binding sites upstream of RpoN-dependent promoters for *fliC*, a gene that encodes the monomeric subunit of flagella that is implicated in immunogenicity (77-81) of *P. aeruginosa* PA14, the *flgFGHIJK* operon, involved in flagella functionality (23) and the *pil-chp* operon (che IV cluster of genes) (22), providing further evidence for the potential role of NtrC as an enhancer of RpoN-dependent expression of bacterial appendages or signaling mechanisms involved in chemotactic motilities.

Since the transcriptional profiles between Δ*ntrB*, Δ*ntrC*, and Δ*ntrBC* did not completely overlap, it is possible that the NtrBC two-component system was engaged in non-linear signal transmission (i.e., crosstalk with other two-component systems). Crosstalk is loosely defined as activation (i.e., phosphorylation) of a response regulator by a sensor kinase other than its cognate pair. Although two-component systems have significant sequence homology at the primary and secondary sequence levels (269), crosstalk does not often occur. It is difficult to predict crosstalk between

two-component systems since there are numerous variables (nutrient availability, temporal distribution of two-component system activation, spatial distribution of phosphorylated response regulators and sensor kinases, etc.) (reviewed in refs 269,270). Nonetheless, integration of information from different stimuli enables cells to generate a concerted response to multiple stimuli or diversify the physiological outcome of activation by a single stimulus. Crosstalk between the NtrBC and the CheAY two-component systems, integrating nitrogen metabolism and (during times of nutrient limitation) scavenging through chemotaxis, has been observed in vitro (271). Although CheA could phosphorylate NtrC, phosphorylation by NtrB was much more efficient, suggesting partial selectivity despite promiscuity between these two-component signaling systems. The crosstalk between systems is in part due to the conservation of the phosphate-accepting residue (Asp54) between the response regulators of respective signaling cascades (271). Likewise, NtrC could be phosphorylated by AmgS (272) of the AmgRS two-component system involved in aminoglycoside resistance (273) and sometimes referred to as EnvZ-OmpR in the literature. Similar to what has been observed for CheA-NtrC crosstalk, EnvZ phosphorylation of NtrC in vitro is much less efficient than phosphorylation by NtrB (273). Interestingly, I identified an NtrC binding site upstream of the *cheA* promoter (Table A6), suggesting that NtrC could regulate transcription of the che I cluster of genes. However, *cheY* was only significantly dysregulated in the PA14 Δ*ntrBC* mutant (downregulated 2.34-fold) (Table A14). Future studies should be performed to determine whether the NtrBC two-component system exhibits non-linear signaling (i.e., crosstalk with other two component systems) in the media used for examining phenotypes of interest, and to determine whether crosstalk occurs with other (not previously identified) two-component systems, such as the CbrAB regulatory system involved in central carbon metabolism, swarming and virulence of *P. aeruginosa* PA14 in vivo (26,38,221,255). CbrB, similar to NtrC, is a bacterial enhancer binding protein (bEBP) of RpoN-mediated transcription (274). Although crosstalk of CbrAB and NtrBC has not been studied explicitly, studies have shown that they function in a coordinated manner to regulate the carbon and nitrogen metabolic flow in *Pseudomonas* spp. (274,275). Interestingly, when histidine was supplied to *P. fluorescens* as the sole carbon source, transcription of the *hutU* operon (involved in catabolism of histidine) was initiated from an RpoN-dependent promoter and required only CbrAB (275). However, when histidine was supplied as the sole nitrogen source, transcription was initiated from a σ^{70}-type promoter and required both NtrBC and CbrAB. Accordingly, I observed that *hutU* was downregulated across PA14 Δ*ntrB*, Δ*ntrC*, Δ*ntrBC* and Δ*rpoN* (Chapters 2,6). Integration of

signaling between the NtrBC and CbrAB two-component systems might help to explain the expanded role for NtrBC in metabolism of carbon- and nitrogen-containing compounds documented in this thesis (Chapter 2).

I showed that PA14 Δ*ntrB*, Δ*ntrC*, and Δ*ntrBC* mutants grew less well than WT in the presence of nitrate and nitrite (Fig. 2-3), which could be at least partly explained by dysregulated expression of numerous genes involved in nitrogen metabolism. PA1779, an assimilatory nitrate reductase (169), was downregulated 39.9- and 90-fold in PA14 Δ*ntrB* and Δ*ntrC*, respectively, but not in the Δ*ntrBC* double mutant. Genes involved in nitrite reduction were downregulated, e.g., *nirB* (169), downregulated 50.4-, 137- and 2.83-fold across mutants. Other regulators of nitrogen metabolism including *glnK* and *ptsN* were also significantly downregulated across mutants. GlnK is a PII-like protein that regulates the phosphatase activity of NtrB and is, in turn, regulated by NtrC (since expression of *glnK* is driven by an RpoN-dependent promoter that is enhanced by NtrC) (276). PtsN, on the other hand, is a phosphotransferase protein involved in selective assimilation of glucose (277) that is regulated by NtrC (since an NtrC binding motif was identified upstream). However, numerous genes involved in nitrogen and carbon metabolism (Tables 2-4,6-4) that were DE in PA14 Δ*ntrB*, Δ*ntrC*, and Δ*ntrBC* (as well as Δ*rpoN*) could be indirect and mediated by dysregulated expression of other regulators, since NtrC enhancer elements were not found proximal to all DE genes. Nonetheless, direct influence of NtrC on key branches of central carbon metabolism is possible, since NtrC binding sites were found upstream of genes involved in catabolism of various carbon and/or nitrogen sources, including phosphogluconate (*edd*), ornithine (*argF*), glycine (*gcvH2*), aspartate (*nadB*), isocitrate (*aceA*), ammonia or glutamate (*glnA*), and methionine (*metN*).

I showed that swarming occurred on a range of nitrogen and carbon sources, including nitrate, urea, glutamate, and malate (Figs. A2,A3) and that the morphology of swarming colonies was medium-dependent. Previously, plasticity of swarming motility has been observed with regards to genetic determinants including two-component systems (177). These data reinforce the concept that many adaptive growth states of bacteria are at least partly dependent on the nutritional status of the environment (34,39,42,48). Toward this end, I showed that colonization of LESB58 Δ*ntrB*, Δ*ntrC*, and Δ*ntrBC* exhibited different ability to colonize distinct niches of the murine respiratory tract (Fig. 4-4) in a newly developed murine model of sinusitis (Chapter 3) and the skin (Fig. 2-1), where abundance of and types of nutrients vary (59,227). In the airways of patients with CF, for example, *P. aeruginosa* adapts to the abundant nitrate and free amino acids present in the sputum (59,227).

Since nitrate promoted swarming (Fig. A2), swarming-mediated resistance to ciprofloxacin (Fig. 4-2), biofilm formation (Fig. 4-5) and the NtrBC two-component system was important for growth in nitrate (Fig. 2-3), therapies that target NtrB and/or NtrC and perturb nitrate assimilation could have significant potential for treating infections by *P. aeruginosa*. Although perturbation of nitrate assimilation has not yet been therapeutically explored, potentiation of aminoglycoside lethality by fumarate and other C_4-dicarboxylates has (215). Fumarate was taken up by transporters (expression of which are regulated by RpoN) and metabolized, stimulating ETC activity and cellular respiration, which improved uptake of the antibiotic tobramycin and overall antimicrobial effects of therapy. In another study, a hydrocarbon stapled peptide, capable of penetrating Gram-negative bacteria and binding RpoN-dependent promoters, reduced virulence of the pathogen *E. coli* (277). These specific strategies, or strategies including peptide therapies that inhibit the regulatory role of NtrC rather than RpoN, might be particularly helpful for treating infections of the respiratory tract, where NtrC and RpoN activity are likely upregulated due to the environmental presence of nitrate. Further, I observed that *ntrC*-promoter activity was stimulated in the abscess model of skin infection in mice (Fig. 5-5), suggesting this to be a promising therapeutic approach in several clinical indications. In addition, stapled peptides that target NtrC binding motifs and inhibit expression of genes from NtrC enhanced promoters might limit the production of virulence factors including elastase, pyoverdine and pyocyanin that were reduced in PA14 (Chapter 4) and LESB58 (Chapter 5) Δ*ntrB*, Δ*ntrC*, and Δ*ntrBC* mutants by a QS-dependent mechanism. Accordingly, the transcription of genes involved in pyoverdine synthesis such as *pvdL*, *pvdP*, *pvdD*, *pvdE*, *pvdS*, was downregulated across mutant strains (Chapters 2,6). However, the transcription of phenazine biosynthesis genes involved in production of pyocyanin was downregulated only in the Δ*ntrBC* and Δ*rpoN* mutant strains (Chapter 6). Furthermore, *lasA* and *lasB* elastases were downregulated (67.8- and 267-fold, respectively) only in the Δ*rpoN* mutant (Chapter 6). In contrast, *lasA* was upregulated in PA14 Δ*ntrB* and Δ*ntrC* (2.22- and 2.45-fold, respectively) (Chapter 2).

Promoter activity of *ntrC* was stimulated to an even greater extent during polymicrobial abscess infection, caused by co-inoculation of *P. aeruginosa* and *S. aureus*, than during monomicrobial infection. *S. aureus* is the most common pathogen co-morbid to *P. aeruginosa* in chronic infections of skin wounds and the respiratory tract (3,221). Since polymicrobial infections are clinically very common, and there are bilateral impacts on antibiotic resistance and virulence of competing species during polymicrobial infection, the efficacy of emerging antimicrobials should be screened in pre-clinical models amenable to co-culture of highly comorbid species. In Chapter 5, I showed that *P.*

aeruginosa NtrBC was important for sensing and responding to *S. aureus*. I focused on determining the role of NtrBC in production of anti-Staphylococcal virulence factors produced by *P. aeruginosa*. A prior study that showed *ntrC* expression was upregulated in the early stages of co-culture (242), presumably contributing to metabolic rewiring necessary for co-existence or competitive exclusion of *S. aureus* by *P. aeruginosa*. Other genes previously identified to contribute to metabolic rewiring of *P. aeruginosa* during co-culture with *S. aureus* (242), which were dysregulated in PA14 mutants, spanned nitrogen (*glnA*, *narK1*, *pauA5*) and carbon (*mmsA*, *glcE*, *gapA*, *glcF*, *lpdV*, *edd*, *pgl*, *acsA*, *zwf*, *fdnI*) metabolism. I determined that pyoverdine, pyocyanin and elastase, each of which have a role in biofilm dispersion or inhibition of cellular respiration by *S. aureus* (74), were reduced in mutants and that this effect could be complemented by complementation of the QS molecules *lasI* and (partially) *pqsH* or *rhlI* (Figure 5-7). Further studies should assess whether *P. aeruginosa ntrBC* mutant strains are sensitive to virulence factors produced by *S. aureus* and if N-acetylglucosamine, D-ribose, or other small signaling molecules liberated from *S. aureus* during infection can impact on adaptive phenotypes (such as swarming or surfing motilities and biofilm formation) of *P. aeruginosa* in monoculture. Further studies should also be performed to determine whether interspecies competition in vivo impacts on efficacy of antibiotics, and to predict compensatory mechanisms that could be triggered by inhibition of NtrB and NtrC by emerging therapies during mono- or polymicrobial infections.

Animal models that closely resemble human diseases are needed for efficacy testing of pre-clinical antibacterial or immunomodulatory therapies and will contribute to clinical development of drug candidates for infectious diseases. This is particularly important in the context of polymicrobial infections, since I saw that interspecies competition is muted in the presence of physiological factors (Fig. 5-5). The murine model of bacterial rhinosinusitis described in Chapter 3 can be used to assess the antibacterial, antibiofilm and/or immunomodulatory activity of promising therapeutic candidates during monomicrobial infection, which could result in better translation of candidate therapies (e.g., stapled peptides or HDPs) to human treatment. Moreover, the model can easily be adapted for the study of chronic infections in both the sinuses and the lungs to aid in our understanding of pathogenic mechanisms associated with initial rhinosinusitis infection or recurrent pulmonary exacerbations in CF. Future studies should focus on optimizing the model for polymicrobial infections and examining recurrent lung infections.

Overall, the data presented in this Thesis shows, for the first time, a major role for the NtrBC two-component system in adaptation and virulence of *P. aeruginosa* across in vitro and in vivo

conditions. The data presented in Chapters 2, 4, 5 and 6 could inform therapeutic development of emerging treatment options for recurrent or recalcitrant infections occurring in different bodily niches. Animal studies, and particularly the new model of rhinosinusitis infection described in Chapter 3, should be performed to provide proof-of-concept for new therapies in conditions that mimic the host environment and trigger clinically relevant pathological or physiological processes in *P. aeruginosa*. More work should be done to determine the direct regulatory role of NtrB and NtrC (i.e., regulation of gene expression independent of gene expression from RpoN-dependent promoters) in adaptive lifestyles that confer antibiotic resistance in situ. This is particularly important, since *rpoN*$^{-}$ isolates of *P. aeruginosa* are clinically common and exhibit resistance to front-line antibiotics including tobramycin and gentamycin. Better definition of NtrBC direct activities could also help us predict compensatory mechanisms that might be selected for in the presence of NtrB or NtrC targeted therapies. Nonetheless, the work described here shows that NtrBC intersects metabolism, adaptation and virulence and is a viable target for emerging therapies that could be developed to combat the antimicrobial resistance crisis.

References

1. Diggle SP, Whiteley M. 2020. *Pseudomonas aeruginosa*: opportunistic pathogen and lab rat. Microbiology (Reading). 166(1): 30-33.
2. Crone S, Vives-Flórez M, Kvich L, Saunders AM, Malone M, Nicolaisen MH, et al. 2020. The environmental occurrence of *Pseudomonas aeruginosa*. APMIS. 128(3): 220-31.
3. Serra R, Grande R, Butrico L, Rossi A, Settimio UF, Caroleo B, et al. 2015. Chronic wound infections: the role of *Pseudomonas aeruginosa* and *Staphylococcus aureus*. Expert Rev. Anti Infect. Ther. 13(5): 605-13.
4. Hoo ZH, Edenborough FP, Curley R, Prtak L, Dewar J, Allenby MI, et al. 2018. Understanding *Pseudomonas* status among adults with cystic fibrosis: a real-world comparison of the Leeds criteria against clinicans' decision. Eur. J. Clin. Microbiol. Infect. Dis. 37(4): 735-43.
5. Poole K. 2011. *Pseudomonas aeruginosa*: resistance to the max. Front. Microbiol. 2: 65.
6. Bredeinstein EBM, Fuente-Nūnez C, Hancock REW. 2011. *Pseudomonas aeruginosa*: all roads lead to resistance. Trends Microbiol. 19(8): 419-26.
7. World Health Organization. 2017. Prioritization of pathogens to guide discovery, research and development of new antibiotics for drug-resistant bacterial infections, including tuberculosis. ISBN: 978-92-4-002643-8
8. Kaier K, Heister T, Götting T, Wolkewitz M, Mutters NT. 2019. Measuring the in-hospital costs of *Pseudomonas aeruginosa* pneumonia: methodology and results from a German teaching hospital. BMC Infect. Dis. 19, 1028.
9. Nelson RE, Hatfield KM, Wolford H, Samore MH, Scott RD, Reddy SC. 2021. National estimates of healthcare costs associated with multidrug-resistant bacterial infections among hospitalized patients in the United States. Clin. Infect. Dis. 72: S17-26.
10. Overhage J, Bains M, Brazas MD, Hancock REW. 2008. Swarming of *Pseudomonas aeruginosa* is a complex adaptation leading to increased production of virulence factors and antibiotic resistance. J. Bacteriol. 190(8): 2671-9.
11. Sun E, Liu S, Hancock REW. 2018. Surfing motility: a conserved yet diverse adaptation among motile bacteria. J. Bacteriol. 200(23): e00394-18.
12. Taylor PK, Yeung ATY, Hancock REW. 2014. Antibiotic resistance in *Pseudomonas aeruginosa* biofilms: towards the development of novel anti-biofilm therapies. J. Biotechnol. 191: 121-30.
13. Moradali MF, Ghods S, Rehm BHA. 2017. *Pseudomonas aeruginosa* lifestyle: a paradigm for adaptation, survival and persistence. Front. Cell. Infect. Microbiol. 7: 39.
14. Coleman SR, Blimkie T, Falsafi R, Hancock REW. 2020. Multidrug adaptive resistance of *Pseudomonas aeruginosa* swarming cells. Antimicrob. Agents Chemother. 64(3): e01999-19.
15. Parsek MR, Singh PK. 2003. Bacterial biofilms: an emerging link to disease pathogenesis. Annu. Rev. Microbiol. 57: 677-701.
16. Coleman SR, Pletzer D, Hancock REW. 2020. Contribution of swarming motility to dissemination in a *Pseudomonas aeruginosa* murine skin abscess infection model. J. Infect. Dis. 224(4): 726-33.
17. Pletzer D, Sun E, Ritchie C, Wilkinson L, Lio LT, Trimble MJ, et al. 2020. Surfing motility is a complex adaptation dependent on the stringent stress response in *Pseudomonas aeruginosa* LESB58. PLoS Pathog. 16(3): e1008444.
18. Henrichsen J. 1972. Bacterial surface translocation: a survey and classification. Bacteriol. Rev. 36(4): 478-503.
19. Harshey RM. 2003. Bacterial motility on a surface: many ways to a common goal. Annu. Rev. Microbiol. 57: 249-73.

20. Hölscher T, Kovács ÁT. 2017. Sliding on the surface: bacterial spreading without an active motor. Environ. Microbiol. 19(7): 2537-45.
21. Ha D-G, Kuchma SL, O'Toole GA. 2014. Plate-based assay for swimming motility in *Pseudomonas aeruginosa*. Methods Mol. Biol. 1149: 59-65.
22. Sampedro I, Parales RE, Krell T, Hill JE. 2015. *Pseudomonas* chemotaxis. FEMS Microbiol. Rev. 39(1): 17-46.
23. Köhler T, Curty LK, Barja F, Delden C, Pechère J-C. 2000. Swarming of *Pseudomonas aeruginosa* is dependent on cell-to-cell signaling and requires flagella and pili. J. Bacteriol. 182: 5990–5996.
24. Kearns DB. 2010. A field guide to bacterial swarming motility. Nat. Rev. Microbiol. 8: 634–44.
25. Caiazza NC, Shanks RMQ, O'Toole GA. 2005. Rhamnolipids modulate swarming motility patterns of *Pseudomonas aeruginosa*. J. Bacteriol. 187: 7351–7361.
26. Yeung ATY, Torfs ECW, Jamshidi F, Bains M, Wiegand I, Hancock REW, et al. 2009. Swarming of *Pseudomonas aeruginosa* is controlled by a broad spectrum of transcriptional regulators, including MetR. J. Bacteriol. 191(18): 5592-602.
27. Klausen M, Heydorn A, Ragas P, Lambertsen L, Aaes-Jørgensen A, Molin S, et al. 2003. Biofilm formation by *Pseudomonas aeruginosa* wild type, flagella and type IV pili mutants. Mol. Microbiol. 48: 1511–1524.
28. Nogales J, Vargas P, Farias GA, Olmedilla A, Sanjuán J, Gallegos M-T. 2015. FleQ coordinates flagellum-dependent and -independent motilities in *Pseudomonas syringae* pv. tomato DC3000. Appl. Environ. Microbiol. 81: 7533–7545.
29. Brown II, Häse CC. 2001. Flagellum-independent surface migration of *Vibrio cholerae* and *Escherichia coli*. J. Bacteriol. 183: 3784–90.
30. Anyan ME, Amiri A, Harvey CW, Tierra G, Morales-Soto N, Driscoll CM, et al. 2014. Type IV pili interactions promote intercellular association and moderate swarming of *Pseudomonas aeruginosa*. Proc. Natl. Acad. Sci. USA. 111(50): 18013-8.
31. Alifano P, Fani R, Liò P, Lazcano A, Bazzicalupo M, Carlomagno MS, et al. 1996. Histidine biosynthetic pathway and genes: structure, regulation and evolution. Microbiol. Rev. 60(1): 44-69.
32. Hayashi NR, Arai H, Kodama T, Igarashi Y. 1998. The *nirQ* gene, which is required for denitrification of *Pseudomonas aeruginosa*, can activate the RubisCO from *Pseudomonas hydrogenothermophila*. Biochim. Biophys. Acta. 1381(3): 347-50.
33. Arai H, Mizutani M, Igarashi Y. 2003. Transcriptional regulation of the *nos* genes for nitrous oxide reductase in *Pseudomonas aeruginosa*. Microbiology (Reading). 149: 29-36.
34. Wilkinson LV, Alford MA, Coleman SR, Wu BC, Lee AHY, Blimkie TM, et al. 2021. Peptide 1018 inhibits swarming and influences Anr regulated gene expression downstream of the stringent stress response in *Pseudomonas aeruginosa*. PLoS One. 16(4): e0250977.
35. Yeung ATY, Parayno A, Hancock REW. 2012. Mucin promotes rapid surface motility in *Pseudomonas aeruginosa*. mBio. 3: e00073-12.
36. Sun E, Gill EE, Falsafi R, Yeung A, Liu S, Hancock REW. 2018. Broad-spectrum adaptive antibiotic resistance associated with *Pseudomonas aeruginosa* mucin-dependent surfing motility. Antimicrob. Agents Chemother. 62(9): e00848-18.
37. Ehre C, Ridley C, Thornton DJ. 2014. Cystic fibrosis: an inherited disease affecting mucin-producing organs. Int. J. Biochem. Cell Biol. 52: 136-45.
38. Yeung ATY. 2012. Complex regulations of swarming and surfing motilities in *Pseudomonas aeruginosa*. Doctoral dissertation, University of British Columbia, Vancouver, BC. https://open.library.ubc.ca/cIRcle/collections/ubctheses/24/items/1.0073189.

39. Alford MA, Pletzer D, Hancock REW. 2019. Dismantling the bacterial virulence program. Microb. Biotechnol. 12(3): 409-13.
40. Rossi E, La Rosa R, Bartell JA, Marvig RL, Haagensen JAJ, Sommer LM. 2020. *Pseudomonas aeruginosa* adaptation and evolution in patients with cystic fibrosis. Nat. Rev. Microbiol. 19: 331-42.
41. Ciofu O, Tolker-Nielsen T. 2019. Tolerance and resistance of *Pseudomonas aeruginosa* biofilms to antimicrobial agents – how *P. aeruginosa* can escape antibiotics. Front. Microbiol. 10: 913.
42. Hancock REW, Alford MA, Haney EF. 2021. Antibiofilm activity of host defence peptides: complexity provides opportunities. Nat. Rev. Microbiol. Online ahead of print.
43. Hall-Stoodley L, Costerton JW, Stoodley P. 2014. Bacterial biofilms: from the natural environment to infectious diseases. Nat. Rev. Microbiol. 2: 95-108.
44. Rumbaugh KP, Sauer K. 2020. Biofilm dispersion. Nat. Rev. Microbiol. 18(10): 571-86.
45. O'Toole GA, Kolter R. 1998. Flagellar and twitching motility are necessary for *Pseudomonas aeruginosa* biofilm development. Mol. Microbiol. 30: 295–304.
46. Fernández L, Breidenstein EBM, Hancock REW. 2011. Creeping baselines and adaptive resistance to antibiotics. Drug Resist. Updat. 14: 1-21.
47. Bryers JD. 2008. Medical biofilms. Biotechnol. Bioeng. 100: 1-18.
48. Malone M, Bjarnsholt T, McBain AJ, James GA, Stoodley P, Leaper D, et al. 2017. The prevalence of biofilms in chronic wounds: a systematic review and meta-analysis of published data. J. Wound Care. 26: 20-25.
49. Flemming H-C, Wingender J, Szewzyk U, Steinberg P, Rice SA, Kjelleberg SK. 2016. Biofilms: an emergent form of bacterial life. Nat. Rev. Microbiol. 14: 563-75.
50. Cornforth DM, Dees JL, Ibberson CB, Huse HK, Mathieson IH, Kirketerp-Møller K, et al. 2018. *Pseudomonas aeruginosa* transcriptome during human infection. Proc. Natl. Acad. Sci. USA. 115(22): E5125-34.
51. Dötsch A, Eckweiler D, Schniederjans M, Zimmerman A, Jensen V, Scharfe M, et al. 2012. The *Pseudomonas aeruginosa* transcriptome in planktonic cultures and static biofilms using RNA sequencing. PLoS One. 7(2): e31092.
52. Mikkelsen H, Bond NJ, Skindersoe ME, Givskov M, Lilley KS, Welch M. 2009. Biofilms and type III secretion are not mutually exclusive in *Pseudomonas aeruginosa*. Microbiology. 155: 687–698.
53. Waite RD, Paccanaro A, Papakonstantinopoulou A, Hurst JM, Saqi M, Littler E, et al. 2006. Clustering of *Pseudomonas aeruginosa* transcriptomes from planktonic cultures, developing and mature biofilms reveals distinct expression profiles. BMC Genomics. 7: 162.
54. Mah TF, O'Toole GA. 2001. Mechanisms of biofilm resistance to antimicrobial agents. Trends Microbiol. 9(1): 34-9.
55. Hall CW, Mah TF. 2017. Molecular mechanisms of biofilm-based antibiotic resistance and tolerance in pathogenic bacteria. FEMS Microbiol. Rev. 41: 276-301.
56. Goltermann L, Tolker-Nielsen T. 2017. Importance of the exopolysaccharide matrix in antimicrobial tolerance of *Pseudomonas aeruginosa* aggregates. 61(4): e02696-16.
57. Tseng BS, Zhang W, Harrison JJ, Quach TP, Song JL, Penterman J, et al. 2013. The extracellular matrix protects *Pseudomonas aeruginosa* biofilms by limiting the penetration of tobramycin. Environ. Microbiol. 15(10): 2865-78.
58. Sharma D, Misba L, Khan AU. 2019. Antibiotics versus biofilm: an emerging battleground in microbial communities. Antimicrob. Resist. Infect. Control. 8: 76.
59. La Rosa R, Rossi E, Feist AM, Johansen HK, Molin S. 2021. Compensatory evolution of *Pseudomonas aeruginosa*'s slow growth phenotype suggests mechanisms of adaptation in cystic fibrosis. Nat. Commun. 12: 3186.

60. Podlesek Z, Bertok DZ. 2020. The DNA damage inducible SOS response is a key player in the generation of bacterial persister cells and population wide tolerance. Front. Microbiol. 11: 1785.
61. Blanchard AC, Waters VJ. 2019. Microbiology of cystic fibrosis airways. Semin. Repir. Crit. Care Med. 40(6): 727-36.
62. Hogardt M, Heesemann J. 2010. Adaptation of *Pseudomonas aeruginosa* during persistence in the cystic fibrosis lung. Int. J. Med. Microbiol. 300(8): 557-62.
63. Jurado-Martín I, Sainz-Mejías M, McClean S. 2021. *Pseudomonas aeruginosa*: an audacious pathogen with an adaptable arsenal of virulence factors. Int. J. Mol. Sci. 22(6): 3128.
64. Veesenmeyer JL, Hauser AR, Lisboa T, Rello J. 2009. *Pseudomonas aeruginosa* virulence and therapy: evolving translational strategies. Crit. Care Med. 37(5): 1777-86.
65. Gellatly SL, Hancock REW. 2013. *Pseudomonas aeruginosa*: new insights into pathogenesis and host defenses. Pathog. Dis. 67: 159-73.
66. Filloux A. 2011. Protein secretion systems in *Pseudomonas aeruginosa*: an essay on diversity, evolution and function. Front. Microbiol. 2: 155.
67. Hauser AR. 2009. The type III secretion system of *Pseudomonas aeruginosa*: infection by injection. Nat. Rev. Microbiol. 7: 654-65.
68. Hood RD, Singh P, Hsu F, Güvenger T, Carl MA, Trinidad RRS, et al. 2010. A type VI secretion system of *Pseudomonas aeruginosa* targets a toxin to bacteria. Cell Host Microbe. 7(1): 25-37.
69. Kang D, Revtovich AV, Chen Q, Shah KN, Cannon CL, Kirienko NV. 2019. Pyoverdine-dependent virulence of *Pseudomonas aeruginosa* isolates from cystic fibrosis patients. Front. Microbiol. 10: 2048.
70. Leoni L, Orsi N, de Lorenzo V, Visca P. 2000. Functional analysis of PvdS, an iron starvation sigma factor of *Pseudomonas aeruginosa*. J. Bacteriol. 182(6): 1481-91.
71. Bonneau A, Roche B, Schalk IJ. 2020. Iron acquisition in *Pseudomonas aeruginosa* by the siderophore pyoverdine: an intricate interacting network including periplasmic and membrane proteins. Sci. Rep. 10: 120.
72. Pena RT, Blasco L, Ambroa A, González-Pedrajo B, Fernández-García L, López M, et al. 2019. Relationship between quorum sensing and secretion systems. Front. Microbiol. 10: 1100.
73. Lee J, Zhang L. 2015. The hierarchy quorum sensing network in *Pseudomonas aeruginosa*. Protein Cell. 6(1): 26-41.
74. Hotterbeekx A, Kumar-Singh S, Goossens H, Malhotra-Kumar S. 2017. In vivo and in vitro interactions between *Pseudomonas aeruginosa* and *Staphylococcus* spp. Front. Cell. Infect. Microbiol. 7: 106.
75. Kariminik A, Baseri-Salehi M, Kheirkhah B. 2017. *Pseudomonas aeruginosa* quorum sensing modulates immune responses: an updated review article. Immunol. Lett. 190: 1–6.
76. Lavoie EG, Wangdi T, Kazmierczak BI. 2011. Innate immune responses to *Pseudomonas aeruginosa* infection. Microbes Infect. 13: 1133-45.
77. Descamps D, Le Gars M, Balloy V, Barbier D, Maschalidi S, Tohme M, et al. 2012. Toll-like receptor 5 (TLR5), IL-1β secretion, and asparagine endopeptidase are critical factors for alveolar macrophage phagocytosis and bacterial killing. Proc. Natl. Acad. Sci. USA. 109(5): 1619–24.
78. Anas AA, van Lieshout MHP, Claushuis TAM, de Vos AF, Florquin S, de Boer OJ, et al. 1995. Lung epithelial MyD88 drives early pulmonary clearance of *Pseudomonas aeruginosa* by a flagellin dependent mechanism. Am. J. Physiol. 311(2): 219-28.
79. Lovewell RR, Hayes SM, O'Toole GA, Berwin B. 2014. *Pseudomonas aeruginosa* flagellar motility activates the phagocyte PI3K/Akt pathway to induce phagocytic engulfment. Am. J. Physiol. 306(7): 698-707.

80. Floyd M, Winn M, Cullen C, Sil P, Chassaing B, Yoo D-G, et al. 2016. Swimming motility mediates the formation of neutrophil extracellular traps induced by flagellated *Pseudomonas aeruginosa*. PLoS Pathog. 12(11): e1005987.
81. Mahenthiralingam E, Campbell ME, Speert DP. 1994. Nonmotility and phagocytic resistance of *Pseudomonas aeruginosa* isolates from chronically colonized patients with cystic fibrosis. Infect. Immun. 62(2): 596–605.
82. Leighton TL, Buensuceso RNC, Howell PL, Burrows LL. 2015. Biogenesis of *Pseudomonas aeruginosa* type IV pili and regulation of their function. Environ. Microbiol. 17(11): 4148–63.
83. Kelly NM, Kluftinger JL, Pasloske BL, Paranchych W, Hancock REW. 1989. *Pseudomonas aeruginosa* pili as ligands for nonopsonic phagocytosis by fibronectin-stimulated macrophages. Infect. Immun. 57(12): 3841–5.
84. Moser C, Jensen PØ, Thomsen K, Kolpen M, Rybtke M, Lauland AS, et al. 2021. Immune responses to *Pseudomonas aeruginosa* biofilm infections. Front. Immunol. 12: 625597.
85. Fazli M, Bjarnsholt T, Kirketerp-Møller K, Jørgensen A, Andersen CB, Giskov M, et al. 2011. Quantitative analysis of the cellular inflammatory response against biofilm bacteria in chronic wounds. Wound Repair Regen. 19: 387-91.
86. Hancock REW, Sahl H-G. 2006. Antimicrobial and host-defense peptides as new anti-infective therapeutic strategies. Nat. Biotechnol. 24(12): 1551-7.
87. Meneguetti BT, dos Santos Machado L, Oshiro KGN, Nogueira ML, Carvalho CME, Franco OL. 2016. Antimicrobial peptides from fruits and their potential use as biotechnological tools – a review and outlook. Front. Microbiol. 7: 2136.
88. Fjell CD, Hiss JA, Hancock REW, Schneider G. 2011. Designing antimicrobial peptides: form follows function. Nat. Rev. Drug. Discov. 11(1): 37-51.
89. Nguyen LT, Haney EF, Vogel HJ. 2011. The expanding scope of antimicrobial peptide structures and their modes of action. Trends Biotechnol. 29(9): 464-72.
90. Magana M, Pushpanathan M, Santos AL, Leanse L, Fernandez M, Ioannidis A, et al. 2020. The value of antimicrobial peptides in the age of resistance. Lancet Infect. Dis. 20(9): e216-30.
91. Hancock REW, Haney EF, Gill EE. 2016. The immunology of host defence peptides: beyond antimicrobial activity. Nat. Rev. Immunol. 16(5): 321-34.
92. Mookherjee N, Anderson MA, Haagsman HP, Davidson DJ. 2020. Antimicrobial host defence peptides: functions and clinical potential. Nat. Rev. Drug Discov. 19(5): 311-32.
93. Di L. 2015. Strategic approaches to optimizing peptide ADME properties. AAPS J. 17(1): 134-43.
94. Kang J, Dietz MJ, Li B. 2019. Antimicrobial peptide LL-37 is bactericidal against *Staphylococcus aureus* biofilms. PLoS One. 14(6): e0216676.
95. Overhage J, Campisano A, Bains M, Torfs ECW, Rehm BHA, Hancock REW. 2008. Human host defense peptide LL-37 prevents bacterial biofilm formation. Infect. Immun. 76(9): 4176-82.
96. Parducho KR, Beadell B, Ybarra TK, Bush M, Escalara E, Trejos AT, et al. 2020. The antimicrobial peptide human beta-defensin 2 inhibits biofilm production of *Pseudomonas aeruginosa* without compromising metabolic activity. Front. Immunol. 11: 805.
97. Zhu C, Tan H, Cheng T, Shen H, Shao J, Guo Y, et al. 2013. Human beta-defensin 3 inhibits antibiotic-resistance *Staphylococcus* biofilm formation. 183(1): 204-13.
98. Loutet SA, Valvano MA. 2011. Extreme antimicrobial peptide and polymyxin B resistance in the genus *Burkholderia*. Front. Microbiol. 2: 159.
99. Pletzer D, Coleman SR, Hancock REW. 2016. Anti-biofilm peptides as a new weapon in antimicrobial warfare. Curr. Opin. Microbiol. 33: 35-40.

100. Pfalzgraff A, Brandenburg K, Weindl G. 2018. Antimicrobial peptides and their therapeutic potential for bacterial skin infections and wounds. Front. Pharmacol. 9: 281.
101. Wu B, Haney EF, Akhoundsadegh N, Pletzer D, Trimble MJ, Adriaans AE, et al. 2021. Human organoid biofilm model for assessing antibiofilm activity of novel agents. NPJ Biofilms Microbiomes. 7(1): 8.
102. Lebeaux D, Chauhan A, Rendueles O, Beloin C. 2013. From in vitro to in vivo models of bacterial biofilm-related infections. Pathogens. 2(2): 288-356.
103. Koo HB, Seo J. 2019. Antimicrobial peptides under clinical investigation. Peptide Science. 111(5): e24122.
104. de la Fuente-Nūnez C, Reffuveille F, Mansour SC, Reckseidler-Zenteno SL, Hernandez D, Brackman G, et al. 2015. D-enantiomeric peptides that eradicate wild-type and multi-drug resistant biofilms and protect against lethal *Pseudomonas aeruginosa* infections. Chem. Biol. 22(2): 196-205.
105. Haney EF, Wuerth KC, Rahanjam N, Nikouei NS, Ghassemi A, Noghani MA, et al. 2018. Identification of an IDR peptide formulation candidate that prevents peptide aggregation and retains immunomodulatory activity. Peptide Science. 111(1): e24077.
106. Bos JD, Meinardi MM. 2000. The 500 dalton rule for the skin penetration of chemical compounds and drugs. Exp. Dermatol. 9(3): 165-9.
107. Bolouri H, Sävman K, Wang W, Thomas A, Maurer N, Dullaghan E, et al. 2014. Innate defense regulator peptide 1018 protects against perinatal brain injury. Ann. Neurol. 75(3): 395-410.
108. de Breij A, Riool M, Cordfunke RA, Malanovic N, de Boer L, Koning RI, et al. 2018. The antimicrobial peptide SAAP-148 combats drug-resistant bacteria and biofilms. Sci. Transl. Med. 10(423): eaan4044.
109. Wuerth K, Lee AHY, Falsafi R, Gill EE, Hancock REW. 2018. Characterization of host responses during *Pseudomonas aeruginosa* acute infection in the lungs and blood and after treatment with the synthetic immunomodulatory peptide IDR-1002. Infect. Immun. 87(1): e00661-18.
110. Riquelme SA, Ahn D, Prince A. 2018. *Pseudomonas aeruginosa* and *Klebsiella pneumoniae* adaptation to innate immune clearance mechanisms in the lung. J. Innate Immune. 10: 442-54.
111. Rivas-Santiago B, Castañeda-Delgado JE, Rivas-Santiago CE, Waldbrook M, González-Curiel I, León-Contreras JC, et al. 2013. Ability of innate defence regulator peptides IDR-1002, IDR-HH2 and IDR-1018 to protect against *Mycobacterium tuberculosis* infections in animal models. PLoS One. 8(3): e59119.
112. Chen C, Deslouches B, Montelaro RC, Di YP. 2017. Enhanced efficacy of the engineered antimicrobial peptide WLBU2 via direct airway delivery in a murine model of *Pseudomonas aeruginosa* pneumonia. Clin. Microbiol. Infect. 24: 1-8.
113. Lebeaux D, Ghigo J-M, Beloin C. 2014. Biofilm-related infections: bridging the gap between clinical management and fundamental aspects of recalcitrance toward antibiotics. Microbiol. Mol. Biol. Rev. 78(3): 510-43.
114. Haisma EM, Göblyös A, Ravensbergen B, Adriaans AE, Cordfunke RA, Schrumpf J, et al. 2016. Antimicrobial peptide P60.4Ac-containing creams and gel for eradication of methicillin-resistant *Staphylococcus aureus* from cultured skin and airway epithelial surfaces. Antimicrob. Agents Chemother. 60(7): 4063-72.
115. Peek NFAW, Nell MJ, Brand R, Jansen-Werkhoven T, van Hoogdalem EJ, Verrijk R, et al. 2020. Ototopical drops containing a novel antibacterial synthetic peptide: safety and efficacy in adults with chronic suppurative otitis media. PLoS One. 15(4): e0231573.

116. Riool M, de Breij A, Drijfhout JW, Nibbering PH, Zaat SAJ. 2017. Antimicrobial peptides in biomedical device manufacturing. Front. Chem. 5: 63.
117. Haney EF, Trimble MJ, Cheng JT, Vallé Q, Hancock REW. 2018. Critical assessment of methods to quantify biofilm growth and evaluate antibiofilm activity of host defence peptides. Biomolecules. 8(2): 29.
118. Ceri H, Olson ME, Stremick C, Read RR, Morck D, Buret A. 1999. The Calgary biofilm device: new technology for rapid determination of antibiotic susceptibilities of bacterial biofilms. J. Clin. Microbiol. 37(6): 1771-6.
119. Locke LW, Shankaran K, Gong L, Stoodley P, Vozar SL, Cole SL, et al. 2020. Evaluation of peptide-based probes toward in vivo diagnostic imaging of bacterial biofilm-associated infections. ACS Infect. Dis. 6(8): 2086-98.
120. Cieplik F, Zaura E, Brandt BW, Buijs MJ, Buchalla W, Crielaard W, et al. 2018. Microcosm biofilms cultured from different oral niches in periodontitis patients. 11(1): 1551596.
121. Silviera GGOS, Torres MDT, Ribiero CFA, Meneguetti BT, Carvalho CME, de la Fuente-Nuñez C, et al. 2021. Antibiofilm peptides: relevant preclinical animal infection models and translational potential. ACS Pharmacol. Transl. Sci. 4(1): 55-73.
122. Knomtchouk KM, Kouhi A, Xia A, Bekale LA, Massa SM, Sweere JM, et al. 2020. A novel mouse model of chronic suppurative otitis media and its preclinical antibiotic evaluation. Sci. Adv. 6(33): eabc1828.
123. Starr CG, Ghimire J, Guha S, Hoffmann JP, Wang Y, Sun L, et al. 2020. Synthetic molecular evolution of host cell-compatible, antimicrobial peptides effective against drug-resistant, biofilm-forming bacteria. Proc. Natl. Acad. Sci. USA. 117(15): 8437-48.
124. Pletzer D, Mansour SC, Wuerth K, Rahanjam N, Hancock REW. 2017. New mouse model for chronic infections by Gram-negative bacteria enabling the study of anti-infective efficacy and host-microbe interactions. mBio. 8: e00140-17.
125. Pletzer D, Mansour SC, Hancock REW. 2018. Synergy between conventional antibiotics and peptides in a murine, sub-cutaneous abscess model caused by recalcitrant *ESKAPE* pathogens. PLoS Pathog. 14(6): e1007084.
126. Bondí R, Messina M, de Fino I, Bragonzi A, Rampioni G, Leoni L. 2014. Affecting *Pseudomonas aeruginosa* phenotypic plasticity by quorum sensing dysregulation hampers pathogenicity in murine chronic lung infection. PLoS One. 9(11): e112105.
127. Rodrigue A, Quentin Y, Lazdunski A, Mejean V, Foglino M. 2000. Two-component systems in *Pseudomonas aeruginosa*: why so many? Trends Microbiol. 8: 498-504.
128. Francis VI, Stevenson EC, Porter SL. 2017. Two-component systems required for virulence in *Pseudomonas aeruginosa*. FEMS Microbiol. Lett. 364(11): fnx104.
129. Yan D, Cho HS, Hastings CA, Igo MM, Lee SY, Pelton JG, et al. 1999. Beryllofluoride mimics phosphorylation of NtrC and other bacterial response regulators. Proc. Natl. Acad. Sci. USA 96(26):14789-94.
130. Desai SK, Kenney LJ. 2017. To ~P or not to ~P? Non-canonical activation by two-component response regulators. Mol. Microbiol. 103(2): 203-13.
131. Massimelli MJ, Sanchez DG, Buchieri MV, Olvera L, Beassoni PR, Schweizer HP, et al. 2011. Choline catabolism, σ^{54} factor and NtrC are required for the full expression of the *Pseudomonas aeruginosa* phosphorylcholine phosphatase gene. Microbiol. Res. 166: 380-390.
132. Colland F, Barth M, Hengge-Aronis R, Kolb A. 2000. Sigma factor selectivity of *Escherichia coli* RNA polymerase: role for CRP, IHF and Irp transcription factors. EMBO J. 19(12): 3028-37.
133. Mascher T, Helmann JD, Unden G. 2006. Stimulus perception in bacterial signal-transducing histidine kinases. Microbiol. Mol. Biol. Rev. 70(4): 910-38.

134. Vrede K, Heldal M, Norland S, Bratbak G. 2002. Elemental composition (C, N, P) and cell volume of exponentially growing and nutrient-limited bacterioplankton. Appl. Environ. Microbiol. 68(6): 2965-71.
135. Reitzer L. 2003. Nitrogen assimilation and global regulation in *Escherichia coli*. Annu. Rev. Microbiol. 57: 155-76.
136. Brown DR, Barton G, Pan Z, Buck M, Wigneshweraraj S. 2014. Nitrogen stress response and stringent response are coupled in *Escherichia coli*. Nat. Commun. 5: 4115.
137. Romeo A, Sonnleitner E, Sorger-Domenigg T, Nakano M, Eisenhaber B, Bläsi U. 2012. Transcriptional regulation of nitrate assimilation in *Pseudomonas aeruginosa* occurs via transcriptional antitermination within the *nirBD*-PA1779-*cobA* operon. Microbiology (Reading). 158: 1543-52.
138. Dolan SK, Kohlstedt M, Trigg S, Ramirez PV, Kaminski CF, Wittmann C, et al. 2020. Contextual flexibility in *Pseudomonas aeruginosa* central carbon metabolism during growth in single carbon sources. mBio. 11(2): e02684-19.
139. Muse WB, Bender RA. The *nac* (nitrogen assimilation control) gene from *Escherichia coli*. J. Bacteriol. 180(5): 1166-73.
140. Suh S-J, Silo-Suh L, Woods DE, Hassett DJ, West SHE, Ohman DE. 1999. Effect of *rpoS* mutation on the stress response and expression of virulence factors in *Pseudomonas aeruginosa*. J. Bacteriol. 181(13): 3890-97.
141. Poole K. Bacterial stress responses as determinants of antimicrobial resistance. J.Antimicrob. Chemother. 67(9): 2069-89.
142. Latifi A, Foglino M, Tanaka K, Williams P, Lazdunski A. 1996. A hierarchical quorum-sensing cascase in *Pseudomonas aeruginosa* links the transcriptional activators LasR and RhlR (VsmR) to expression of the stationary-phase sigma factor RpoS. Mol. Microbiol. 21: 1137-46.
143. Kim Y, Watrud LS, Matin A. 1995. A carbon starvation survival gene of *Pseudomonas putida* is regulated by sigma 54. J. Bacteriol. 177(7): 1850-9.
144. Miura K, Inouye S, Nakazawa A. 1998. The *rpoS* gene regulates OP2, an operon for the lower pathway of xylene catabolism on the TOL plasmid, and the stress response in *Pseudomonas putida* mt-2. Mol. Gen. Genet. 259(1): 72-8.
145. Irving SE, Corrigan RM. 2018. Triggering the stringent response: signals responsible for activating (p)ppGpp synthesis in bacteria. Microbiology (Reading). 164: 268-76.
146. Jishage M, Kvint K, Shingler V, Nyström T. 2002. Regulation of sigma factor competition by the alarmone ppGpp. Genes Dev. 16(10): 1260-70.
147. Turner KH, Everett J, Trivedi U, Rumbaugh KP, Whiteley M. 2014. Requirements for *Pseudomonas aeruginosa* acute burn and chronic surgical wound infection. PLoS Gen. 10: e1004743.
148. Rohmer L, Hocquet D, Miller SI. 2011. Are pathogenic bacteria just looking for food? Metabolism and microbial pathogenesis. Trends Microbiol. 19: 341–8.
149. Johnson PT, Townsend AR, Cleveland CC, Gilbert PM, Howarth RW, McKenzie VJ, et al. 2010. Linking environmental nutrient enrichment and disease emergence in humans and wildlife. Ecol. Appl. 20: 16–29.
150. Vicente EJ, Dean DR. 2017. Keeping the nitrogen-fixation dream alive. PNAS 114: 3009–11.
151. Arat S, Bullerjahn GS, Laubenbacher R. 2015. A network biology approach to denitrification in *Pseudomonas aeruginosa*. PLoS One 10: e0118235.
152. Galán-Vásquez E, Luna B, Martínez-Antonio A. 2011. The regulatory network of *Pseudomonas aeruginosa*. Micro. Inform. Exp. 1: 3.

153. Bhagirath AY, Li Y, Patidar R, Yerex K, Ma X, Kumar A, et al. 2019. Two component regulatory systems and antibiotic resistance in Gram-negative pathogens. Int. J. Mol. Sci. 20: 1781.
154. Luque-Almagro VM, Gates AJ, Moreno-Vivian C, Ferguson SJ, Richardson DJ, Roldan MD. 2011. Bacterial nitrate assimilation: gene distribution and regulation. Biochem. Soc. Trans. 39(6): 1838-43.
155. Fazeli H, Akbari R, Moghim S, Narimani T, Arabestani MR, Ghoddousi AR. 2012. *Pseudomonas aeruginosa* infections in patients, hospital means, and personnel's specimens. J. Res. Med. Sci. 17(4): 332-7.
156. Van Alst NE, Picardo KF, Iglewski BH, Haidaris CG. 2007. Nitrate sensing and metabolism modulate motility, biofilm formation, and virulence in *Pseudomonas aeruginosa*. Infect. Immun. 75: 3780-90.
157. Thoma S, Schobert M. 2009. An improved *Escherichia coli* donor strain for diparental mating. FEMS Microbiol. Lett. 294(2): 127-32.
158. Rahme LG, Stevens EJ, Wolfort SF, Shao J, Tompkins RG, Ausubel FM. 1995. Common virulence factors for bacterial pathogenicity in plants and animals. Science. 268(5219): 1899-902.
159. Cheng K, Smyth RL, Govan JR, Doherty C, Winstanley C, Denning N, et al. 1996. Spread of beta-lactam-resistant *Pseudomonas aeruginosa* in a cystic fibrosis clinic. Lancet. 348(9028): 639-42.
160. Hoang TT, Karkhoff-Schweizer RR, Kutchma AJ, Schweizer HP. 1998. A broad-host-range Flp-FRT recombination system for site-specific excision of chromosomally-located DNA sequences: application for isolation of unmarked *Pseudomonas aeruginosa* mutants. Gene. 212: 77-86.
161. Kovach ME, Elzer PH, Hill DS, Robertson GT, Farris MA, Roop RM, et al. 1995. Four new derivatives of the broad-host-range cloning vector pBBR1MCS, carrying different antibiotic-resistant cassettes. Gene. 166: 175-6.
162. Hmelo LR, Borlee BR, Almblad H, Love ME, Randall TE, Tseng BS, et al. 2015. Precision-engineering the *Pseudomonas aeruginosa* genome with two-step allelic exchange. Nat. Protoc. 10: 1820-41.
163. Kovach ME, Phillips RW, Elzer PH, Roop RM, Peterson KM. 1994. pBBR1MCS: a broad-host-range cloning vector. Biotechniques. 16(5): 800-802.
164. Pinzon NM, Ju L-K. 2009. Improved detection of rhamnolipid production using agar plates containing methylene blue and cetyl trimethylammonium bromide. Biotechnol. Lett. 31(10): 1583-8.
165. Anders S, Pyl PT, Huber W. 2015. HTSeq – a python framework to work with high-throughput sequencing data. Bioinformatics. 31(2): 166-169.
166. Dobin A, Davis CA, Schlesinger F, Drenkow J, Zaleski C, Jha S, et al. 2014. STAR: ultrafast universal RNA-seq aligner. Bioinformatics. 29(1): 15-21.
167. Ewels P, Magnusson M, Lundin S, Kaller M. 2016. MultiQC: summarize analysis results for multiple tools and samples in a single report. Bioinformatics. 32(19): 3047-3048.
168. Wingett SW, Andrews S. 2018. FastQ Screen: a tool for multi-genome mapping and quality control. F1000Res. 7: 1338.
169. Winsor GL, Griffiths EJ, Lo R, Dhillon BK, Shay JA, Brinkman FSL. 2016. Enhanced annotations and features for comparing thousands of *Pseudomonas* genomes in the *Pseudomonas* genomes database. Nucleic Acids Res. 44(D1): D646-653.
170. Love MI, Huber W, Anders S. (2014). Moderated estimation of fold change and dispersion for RNA-seq data with DESeq2. Genome Biol. 15(12): 550.
171. Grote S. 2019. GofuncR: Gene ontology enrichment using FUNC. R package version 1.4.0.

172. Schmittgen TD, Livak KJ. 2001. Analysis of relative gene expression data using real-time quantitative PCR and the 2(-Delta Delta C(T)) method. Methods. 25(4): 402-408.
173. Sousa AM, Pereira MO. 2014. *Pseudomonas aeruginosa* diversification during infection development in cystic fibrosis lungs – a review. Pathogens. 3(3): 680-703.
174. Zhang XX, Rainey PB. 2008. Dual involvement of CbrAB and NtrBC in the regulation of histidine utilization in *Pseudomonas fluorescens* SBW25. Genetics. 178(1): 185-95.
175. Potvin E, Lehoux DE, Kukavica-Ibrulj I, Richard KL, Sanschagrin F, Lau GW, et al. 2003. In vivo functional genomics of *Pseudomonas aeruginosa* for high-throughput screening of new virulence factors and antibacterial targets. Environ. Microbiol. 5(12): 1294-1308.
176. Winstanley C, Langille MGI, Fothergill JL, Kukavica-Ibrulj I, Paradis-Bleau C, Sanschagrin F, et al. 2009. Newly introduced genomic prophage islands are critical determinants of in vivo competitiveness in the Liverpool Epidemic Strain of *Pseudomonas aeruginosa*. Genome Res. 19(1): 12-23.
177. Kollaran AM, Joge S, Kotian HS, Badal D, Prakash D, Mishra A et al. 2019. Context-specific requirement of forty-four two-component loci in *Pseudomonas aeruginosa* swarming. iScience. 13: 305-17.
178. Toyofuku M, Yoon SS. 2018. Nitric oxide, an old molecule with noble functions in *Pseudomonas aeruginosa* biology. Adv. Microb. Physiol. 72: 117-45.
179. Vasquez-Torres A, Baumler A. 2017. Nitrate, nitrite and nitric oxide reductases: from the last universal common ancestor to modern bacterial pathogens. Curr. Opin. Microbiol. 29: 1-8.
180. Crousilles A, Dolan SK, Brear P, Chirgadze DY, Welch M. 2018. Gluconeogenic precursor availability regulates flux through the glyoxylate shunt in *Pseudomonas aeruginosa*. J. Biol. Chem. 293(37): 14260-9.
181. Damron FH, Owings JP, Okkotsu Y, Varga JJ, Schurr JR, Goldberg JB et al. 2012. Analysis of the *Pseudomonas aeruginosa* regulon controlled by the sensor kinase KinB and sigma factor RpoN. J. Bacteriol. 194(6): 1317-30.
182. Cai Z, Liu Y, Chen Y, Yam JKH, Chew SC, Chua SL et al. 2015. RpoN regulates virulence factors of *Pseudomonas aeruginosa* via modulating the PqsR quorum sensing regulator. Int. J. Mol. Sci. 16(12): 28311-9.
183. Winstanley C, O'Brien S, Brockhurst MA. 2016. *Pseudomonas aeruginosa* evolutionary adaptation and diversification in cystic fibrosis chronic lung infections. Trends Microbiol. 24 (5): 327–37.
184. Jelsbak L, Johansen HK, Frost AL, Thogersen R, Thomsen LE, Ciofu O, et al. 2007. Molecular epidemiology and dynamics of *Pseudomonas aeruginosa* populations in lungs of cystic fibrosis patients. Infect. Immun. 75(5): 2214-24.
185. Li Z, Kosorok MR, Farrell PM, Laxova A, West SE, Green CG, et al. 2005. Longitudinal development of mucoid *Pseudomonas aeruginosa* infection and lung disease progression in children with cystic fibrosis. JAMA. 293(5): 581-5.
186. Aanaes K, Rickelt LF, Johansen HK, von Buchwald C, Pressler T, Hoiby N, Jensen PO. 2011. Decreased mucosal oxygen tension in the maxillary sinuses in patients with cystic fibrosis. J. Cyst. Fibros. 10(2): 114-20.
187. Fothergill JL, Neill DR, Loman N, Winstanley C, Kadioglu A. 2014. *Pseudomonas aeruginosa* adaptation in the nasopharyngeal reservoir leads to migration and persistence in the lungs. Nat Commun. 5: 4780.
188. Mainz JG, Naehrlich L, Schien M, Kading M, Schiller I, Mayr S, et al. 2009. Concordant genotype of upper and lower airways of *P. aeruginosa* and *S. aureus* isolated in cystic fibrosis. Thorax. 64(6): 535-40.

189. Berkhout MC, van Rooden CJ, Rijntjes E, Fokkens WJ, el Bouazzaoui LH, Heijerman HG. 2014. Sinonasal manifestations of cystic fibrosis: a correlation between genotype and phenotype? J. Cyst. Fibros. 13(4): 442-8.
190. Tipirneni KE, Woodworth BA. 2017. Medical and surgical advancements in the management of cystic fibrosis chronic rhinosinusitis. Curr. Otorhinolaryngol. Rep. 5(1): 24-34.
191. Hoggard M, Mackenzie BW, Jain R, Taylor MW, Biswas K, Douglas RG. 2017. Chronic rhinosinusitis and the evolving understanding of microbial ecology in chronic inflammatory mucosal disease. Clin. Microbiol. Rev. 30(1): 321-348.
192. Fokkens WJ, Lund VJ, Mullol J, Bachert C, Alobid I, Baroody F, et al. 2012. European position paper on rhinosinusitis and nasal polyps: a summary for otorhinolaryngologists. Rhinology. 50(1): 1-12.
193. Orlandi RR, Kingdom TT, Hwang PH, Smith TL, Alt JA, Baroody FM, et al. 2016. International consensus statement on allergy and rhinology: rhinosinusitis. Int. Forum Allergy Rhinol. 1: S22-209.
194. Fastenberg JH, Hsueh WD, Mustafa A, Akbar NA, Abuzeid WM. 2016. Biofilms in chronic rhinosinusitis: pathophysiology and therapeutic strategies. World J. Otorhinolaryngol. Head Neck Surg. 2(4): 219-229.
195. Lee S, Lane AP. 2011. Chronic rhinosinusitis as a multifactorial inflammatory disorder. Curr. Infect. Dis. Rep. 13(2): 159-68.
196. Lux CA, Douglas RG, Cho DY, Taylor MW, Biswas K. 2019. Animal models for inflammatory mucosal disease and their potential for studying the microbiome in chronic rhinosinusitis. Rhinology Online. 2(2): 69-80.
197. Centers for Disease Control and Prevention (CDC). 2003. Outbreaks of community-associated methicillin-resistant *Staphylococcus aureus* skin infections – Los Angeles County, California, 2002-2003. MMWR Morb. Mortal. Wkly. Rep. 52(5): 88.
198. Plaut RD, Mocca CP, Prabhakara R, Merkel TJ, Stibitz S. 2013. Stably luminescent *Staphylococcus aureus* clinical strains for use in bioluminescent imaging. PLoS One. 8(3): e59232.
199. Carter ME, Fothergill JL, Walshaw MJ, Rajakumar K, Kadioglu A, Winstanley C. 2010. A subtype of a *Pseudomonas aeruginosa* cystic fibrosis epidemic strain exhibits enhanced virulence in a murine model of acute respiratory infection. J. Infect. Dis. 202(6): 935-42.
200. Damron FH, McKenney ES, Barbier M, Liechti GW, Schweizer HP, Goldberg JB. 2013. Construction of mobilizable mini-Tn7 vectors for bioluminescent detection of gram-negative bacteria and single-copy promoter lux reporter analysis. Appl. Environ. Microbiol. 79(13): 4149-53.
201. Choi KH, Gaynor JB, White KG, Lopez C, Bosio CM, Karkhoff-Schweizer RR, et al. 2005. A Tn7-based broad-range bacterial cloning and expression system. Nat. Methods. 2(6): 443-8.
202. Choi KH, Schweizer HP. 2006. Mini-Tn7 insertion in bacterial with single attTn7 sites: example *Pseudomonas aeruginosa*. Nat. Protoc. 1(1): 153-61.
203. Wuerth KC, Falsafi R, Hancock REW. 2017. Synthetic host defense peptide IDR-1002 reduces inflammation in *Pseudomonas aeruginosa* lung infection. PLoS One. 12(11): e0187565.
204. Kielland A, Blom T, Nandakumar KS, Holmdahl R, Blomhoff R, Carlsen H. 2009. In vivo imaging of reactive oxygen and nitrogen species in inflammation using the luminescent probe L-012. Free Radic. Biol. Med. 47(6): 760-6.
205. Lindsay R, Slaughter T, Britton-Webb J, Mog SR, Conran R, Tadros M, et al. 2006. Development of a murine model of chronic rhinosinusitis. Otolaryngol. Head Neck Surg. 134(5): 724-30.

206. Achtman AH, Pilat S, Law CW, Lynn DJ, Janot L, Mayer ML, et al. 2012. Effective adjunctive therapy by an innate defense regulatory peptide in a preclinical model of severe malaria. Sci. Transl. Med. 4(135): 135ra64.
207. Nijnik A, Madera L, Ma S, Waldbrook M, Elliott MR, Easton DM, et al. 2010. Synthetic cationic peptide IDR-1002 provides protection against bacterial infections through chemokine induction and enhanced leukocyte recruitment. J. Immunol. 184(5): 2539-50.
208. Jin M, Gu Z, Bian Z, Yang J, Cao Z, Yu X, Guo G. 2011. Developing a mouse model of acute bacterial rhinosinusitis. Eur. Arch. Otorhinolaryngol. 268(6): 857-61.
209. Sakr A, Bregeon F, Mege JL, Rolain JM, Blin O. 2018. *Staphylococcus aureus* nasal colonization: an update on mechanisms, epidemiology, risk factors, and subsequent infections. Front. Microbiol. 9: 2419.
210. Kiser KB, Cantey-Kiser JM, Lee JC. 1999. Development and characterization of a *Staphylococcus aureus* nasal colonization model in mice. Infect. Immun. 67(10): 5001-6.
211. Brown AF, Leech JM, Rogers TR, McLoughlin RM. 2014. *Staphylococcus aureus* colonization: modulation of host immune response and impact on human vaccine design. Front. Immunol. 4: 507.
212. Jeukens J, Boyle B, Kukavica-Ibrulj I, Ouellet MM, Aaron SD, Charette SJ, et al. 2014. Comparative genomics of isolates of a *Pseudomonas aeruginosa* epidemic strain associated with chronic lung infections of cystic fibrosis patients. PLoS One. 9(2): e87611.
213. Brauner A, Fridman O, Gefen O, Balaban NQ. 2016. Distinguishing between resistance, tolerance, and persistence to antibiotic treatment. Nat. Rev. Microbiol. 14:320-30.
214. Meylan S, Porter CBM, Yang JH, Belenky P, Gutierrez A, Lobritz MA et al. 2017. Carbon sources tune antibiotic susceptibility in *Pseudomonas aeruginosa* via tricarboxylic acid cycle control. Cell Chem. Biol. 24(2): 195-206.
215. Hall CW, Farkas E, Zhang L, Mah TF. 2019. Potentiation of aminoglycoside lethality by C_4-dicarboxylates requires RpoN in antibiotic-tolerant *Pseudomonas aeruginosa*. Antimicrob. Agents Chemother. 63(10): e01313-19.
216. Clinical and Laboratory Standards Institute (CLSI). Performance standards for antimicrobial susceptibility testing. 30th ed. CLSI supplement M100. ISBN 978-1-68440-067-6.
217. Imperi F, Ciccosanti F, Perdomo AB, Tiburzi F, Mancone C, Alonzi T, et al. 2009. Analysis of the periplasmic proteome of *Pseudomonas aeruginosa*, a metabolically versatile opportunistic pathogen. Proteomics. 9(7):1901-15
218. Essar DW, Eberly L, Hadero A, Crawford IP. 1990. Identification and characterization of genes for a second anthranilate synthase in *Pseudomonas aeruginosa*: interchangeability of the two anthranilate synthases and evolutionary implications. J. Bacteriol. 172: 884–900.
219. Ohman DE, Cryz SJ, Iglewski, BH. 1980. Isolation and characterization of *Pseudomonas aeruginosa* PAO mutant that produces altered elastase. J. Bacteriol. 142: 836–42.
220. Kumar P, Nagarajan A, Uchil PD. 2018. Analysis of cell viability by the lactate dehydrogenase assay. Cold Spring Harb. Protoc. 6.
221. Yeung ATY, Janot L, Pena OM, Neidig A, Kukavica-Ibrulj I, Hilchie A, et al. 2014. Requirement of the *Pseudomonas aeruginosa* CbrA sensor kinase for full virulence in a murine acute lung infection model. Infect. Immun. 82(3): 1256-67.
222. Fajardo A, Martínez-Martín N, Mercadillo M, Galán JC, Ghysels B, Matthijs S, et al. 2008. The neglected instrinsic resistome of bacterial pathogens. PLoS One. 3(2): e1619.
223. Brazas MD, Breidenstein EBM, Overhage J, Hancock REW. 2007. Role of lon, an ATP-dependent protease homolog, in resistance of *Pseudomonas aeruginosa* to ciprofloxacin. Antimicrob. Agents Chemother. 51(12): 4276-83.

224. Breidenstein EBM, Khaira BK, Wiegand I, Overhage J, Hancock REW. 2008. Complex ciprofloxacin resistome revealed by screening a *Pseudomonas aeruginosa* mutant library for altered susceptibility. Antimicrob. Agents Chemother. 52(12): 4486-91.
225. Hewer SCL, Smyth AR, Brown M, Jones AP, Hickey H, Kenna D, et al. 2020. Intravenous versus oral antibiotics for eradication of *Pseudomonas aeruginosa* in cystic fibrosis (TORPEDO-CF): a randomised controlled trial. Lancet Respir. Med. 8(10): 975-86.
226. Grice EA, Segre JA. 2011. The skin microbiome. Nat. Rev. Microbiol. 9(4): 244-53.
227. Palmer KL, Mashburn LM, Singh PK, Whiteley M. 2005. Cystic fibrosis sputum supports growth and cues key aspects of *Pseudomonas aeruginosa* physiology. J. Bacteriol. 187(15): 5267-77.
228. Naren N, Zhang X-X. 2021. Role of a local transcription factor in governing cellular carbon/nitrogen homeostasis in *Pseudomonas fluorescens*. Nucleic Acids Res. 49(6): 3204-16.
229. Landman D, Bratu S, Kochar S, Panwar M, Trehan M, Doymaz M, et al. 2007. Evolution of antimicrobial resistance among *Pseudomonas aeruginosa*, *Acinetobacter baumannii* and *Klebsiella pneumoniae* in Brooklyn, NY. J. Antimicrob. Chemother. 60: 78–82.
230. Feng X, Zhang, Z, Li X, Song Y, Kang J, Yin D, et al. 2019. Mutations in *gyrB* play an important role in ciprofloxacin-resistant *Pseudomonas aeruginosa*. Infect. Drug Resist. 12: 261–72.
231. Fernández L, Breidenstein EBM, Song D, Hancock REW. 2012. Role of intracellular proteases in the antibiotic resistance, motility and biofilm formation of *Pseudomonas aeruginosa*. Antimicrob. Agents Chemother. 56(2): 1128-32.
232. Zarzycki-Siek J, Norris MH, Kang Y, Sun Z, Bluhm AP, McMillan IA, et al. 2013. Elucidating the *Pseudomonas aeruginosa* fatty acid degradation pathway: identification of additional fatty acyl-CoA synthetase homologues. PLoS One. 8(5): e64554.
233. O'Brien S, Williams D, Fothergill JL, Paterson S, Winstanley C, Brockhurst MA. 2017. High virulence sub-populations in *Pseudomonas aeruginosa* long-term cystic fibrosis airway infections. BMC Microbiol. 17(1): 30.
234. Panayidou S, Georgiades K, Christofi T, Tamana S, Promponas VJ, Apidianakis Y. 2020. *Pseudomonas aeruginosa* core metabolism exerts a widespread growth-independent control on virulence. Sci. Rep. 10: 9505.
235. Perinbam K, Chacko JV, Kannan A, Digman MA, Siryaporn A. 2020. A shift in central metabolism accompanies virulence activation in *Pseudomonas aeruginosa*. mBio. 11(2): e0273018.
236. DeLeon S, Clinton A, Fowler H, Everett J, Horswill AR, Rumbaugh KP. 2014. Synergistic interactions of *Pseudomonas aeruginosa* and *Staphylococcus aureus* in an in vitro wound model. Infect. Immun. 82(11): 4718-28.
237. Alves PM, Al-Badi E, Withycombe C, Jones PM, Purdy KJ, Maddocks SE. 2018. Interaction between *Staphylococcus aureus* and *Pseudomonas aeruginosa* is beneficial for colonisation and pathogenicity in a mixed biofilm. Pathog. Dis. 76(1): fty003
238. Briaud P, Camus L, Bastein S, Doléans-Jordheim A, Vandenesch F, Moreau K. 2019. Coexistence with *Pseudomonas aeruginosa* alters *Staphylococcus aureus* transcriptome, antibiotic resistance and internalization into epithelial cells. Sci. Rep. 9: 16564.
239. Limoli DH, Yang J, Khansaheb MK, Helfman B, Peng L, Stecenko AA, et al. 2016. *Staphylococcus aureus* and *Pseudomonas aeruginosa* co-infection is associated with cystic fibrosis-related diabetes and poor clinical outcomes. Eur. J. Clin. Micro. Infect. Dis. 35: 947-53.

240. Fazli M, Bjarnsholt T, Kirketerp-Møller K, Jørgensen B, Andersen AS, et al. 2009. Nonrandom distribution of *Pseudomonas aeruginosa* and *Staphylococcus aureus* in chronic wounds. J. Clin. Microbiol. 47(12): 4084-9.
241. Tay WH, Chong KKL, Kline KA. 2016. Polymicrobial-host interactions during infection. J. Mol. Biol. 428(17): 3355-71.
242. Tognon M, Köhler T, Luscher A, van Delden C. 2019. Transcriptional profiling of *Pseudomonas aeruginosa* and *Staphylococcus aureus* during in vitro co-culture. BMC Genomics. 20: 30.
243. Nielson JE, Alford MA, Yung DBY, Molchanova N, Fortkort JA, Lin JS, et al. 2021. Self-assembly of antimicrobial peptoids impacts their biological effects on ESKAPE bacterial pathogens. ACS Infect. Dis. Submitted.
244. Wang T, Sun W, Fan L, Hua C, Wu N, Fan S, et al. 2021. An atlas of the binding specificities of transcription factors in *Pseudomonas aeruginosa* directs prediction of novel regulators in virulence. eLife. 10: e61885.
245. Grant CE, Bailey TL, Noble WS. 2011. FIMO: Scanning for occurrences of a given motif. Bioinformatics. 27(7): 1017-18.
246. Somerville GA, Proctor RA. 2009. At the crossroads of bacterial metabolism and virulence factor synthesis in Staphylococci. Microbiol. Mol. Biol. Rev. 73(2): 233-48.
247. Janssen DB, op den Camp HJ, Leenen PJ, van der Drift C. 1980. The enzymes of ammonia assimiliation in *Pseudomonas aeruginosa*. Arch. Microbiol. 124: 197-203.
248. La Rosa R, Johansen HK, Molin S. 2019. Adapting to the airways: metabolic requirements of *Pseudomonas aeruginosa* during the infection of cystic fibrosis patients. Metabolites. 9(10): 234.
249. Kaiser JC, King AN, Grigg JC, Sheldon JR, Edgell DR, Murphy MEP, et al. 2018. Repression of branched-chain amino acid synthesis in *Staphylococcus aureus* is mediated by isoleucine via CodY, and by a leucine-rich attenuator peptide. PLoS Genet. 14(1): e1007159.
250. Shingler V. Signal sensory systems that impact σ^{54}-dependent transcription. FEMS Microbiol. Rev. 35(3): 425-40.
251. Korgaonkar AK, Whiteley M. 2011. *Pseudomonas aeruginosa* enhances production of an antimicrobial in response to N-acetylglucosamine and peptidoglycan. J. Bacteriol. 193(4): 909-17.
252. Hunt TA, Peng W-T, Loubens I, Storey DG. The *Pseudomonas aeruginosa* alternative sigma factor PvdS controls exotoxin A expression and is expressed in lung infections associated with cystic fibrosis. Microbiology (Reading). 148: 3183-93.
253. Hare NJ, Solis N, Harmer C, Marzook NB, Rose B, Harbour C, et al. 2012. Proteomic profiling of *Pseudomonas aeruginosa* AES-1R, PAO1 and PA14 reveals potential virulence determinants associated with a transmissible cystic fibrosis-associated strain. BMC Microbiol. 12: 16.
254. La Rosa R, Nogales J, Rojo F. 2015. The Crc/CrcZ-CrcYglobal regulatory system helps the integration of gluconeogenic and glycolytic metabolism in *Pseudomonas putida*. Environ. Microbiol. 17: 3362-78.
255. Yeung ATY, Bains M, Hancock REW. 2011. The sensor kinase CbrA is a global regulator that modulates metabolism, virulence, and antibiotic resistance in *Pseudomonas aeruginosa*. J. Bacteriol. 193(4): 918.
256. Mahenthiralingam E, Campbell ME, Speert DP. 1994. Nonmotility and phagocytic resistance of *Pseudomonas aeruginosa* isolates from chronically colonized patients with cystic fibrosis. Infect. Immun. 62(2): 596-605.
257. Shimizu TS, Le Novère N, Beavil AJ, Sutton BJ, Bray D. 2000. Molecular model of a lattice of signalling proteins involved in bacterial chemotaxis. 2(11): 792-6.

258. Kilmury SLN, Burrows LL. 2018. The *Pseudomonas aeruginosa* PilSR two-component system regulates both twitching and swimming motilities. mBio. 9(4): e01310-18.
259. Change C-Y. 2017. Surface sensing for biofilm formation in *Pseudomonas aeruginosa*. Front. Microbiol. 8: 2671.
260. Li J, Mason SW, Greenblatt J. 1993. Elongation factor NusG interacts with termination factor rho to regulate termination and antitermination of transcription. Genes Dev. 7(1): 161-72.
261. Glockner AB, Zumft WG. 1996. Sequence analysis of an internal 9.72-kb segment from the 30-kb denitrification gene cluster of *Pseudomonas stutzeri*. Biochim. Biophys. Acta. 1277: 6-12.
262. Zaoui C, Overhage J, Löns D, Zimmerman A, Müsken M, Bielecki P, et al. 2011. An orphan sensor kinase controls quinolone signal production via MexT in *Pseudomonas aeruginosa*. 83(3): 536-47.
263. Giraud C, Bernard CS, Calderon V, Yang L, Filloux A, Molin S, et al. 2011. The PprA-PprB two-component system activates CupE, the first non-archetypal *Pseudomonas aeruginosa* chaperon-usher pathway system assembling fimbriae. Environ. Microbiol. 13(3): 666-83.
264. Thompson LS, Webb JS, Rice SA, Kjelleberg S. 2003. The alternative sigma factor RpoN regulates the quorum sensing gene *rhlI* in *Pseudomonas aeruginosa*. FEMS Microbiol. Lett. 220(2): 187-195.
265. Mahenthiralingam E, Speert DP. 1995. Nonopsonic phagocytosis of *Pseudomonas aeruginosa* by macrophages and polymorphonuclear leukocytes requires the presence of the bacterial flagellum. Infect. Immun. 63(11): 4519-23.
266. Pasqua M, Visaggio D, Sciuto AL, Genah S, Banin E, Visca P, et al. 2017. Ferric uptake regulator Fur is conditionally essential in *Pseudomonas aeruginosa*. J. Bacteriol. 199(22): e00472-17.
267. Reichhardt C, Wong C, da Silva DP, Wozniak DJ, Parsek MR. 2018. CdrA interactions within the *Pseudomonas aeruginosa* biofilm matrix safeguard it from proteolysis and promote cellular packing. mBio. 9(5): e01376-18.
268. Totten PA, Lara JC, Lory S. 1990. The *rpoN* gene product of *Pseudomonas aeruginosa* is required for expression of diverse genes, including the flagellin gene. 172(1): 389-96.
269. Agrawal R, Sahoo BK, Saini DK. 2016. Cross-talk and specificity in two-component signal transduction pathways. Future Microbiol. 11: 685-97.
270. Laub MT, Goulian M. 2007. Specificity in two-component signal transduction pathways. Annu. Rev. Genet. 41: 121-45.
271. Ninfa AJ, Ninfa EG, Lupas AN, Magasanik B, Stock J. 1988. Crosstalk between bacterial chemotaxis signal transduction proteins and regulators of transcription of the Ntr regulon: evidence that nitrogen assimilation and chemotaxis are controlled by a common phosphotransfer mechanism. Proc Natl Acad Sci USA. 85(15): 5492-5496
272. Igo MM, Ninfa AJ, Stock JB, Silhavy TJ. 1989. Phosphorylation and dephosphorylation of a bacterial transcriptional activator by a transmembrane receptor. Genes Dev. 3(11): 1725-34.
273. Lee S, Hinz A, Bauerle E, Angermeyer A, Juhaszova K, Kaneko Y, et al. 2009. Targeting a bacterial stress response to enhance antibiotic action. Proc. Natl. Acad. Sci. USA. 106(34): 14570-75.
274. Li W, Lu C-D. 2007. Regulation of carbon and nitrogen utilization by CbrAB and NtrBC two-component systems in *Pseudomonas aeruginosa*. J. Bacteriol. 189(15): 5413-20.
275. Zhang X-X, Rainey PB. 2008. Dual involvement of CbrAB and NtrBC in the regulation of histidine utilization in *Pseudomonas fluorescens* SBW25. Genetics. 178(1): 185-95.
276. Hervás AB, Canosa I, Little R, Dixon R, Santero E. 2009. NtrC-dependent regulatory network for nitrogen assimilation in *Pseudomonas putida*. J. Bacteriol. 191(19): 6123-25.

277. Payne SR, Pau DI, Whiting AL, Kim YJ, Pharoah BM, Moi C, et al. 2018. Inhibition of bacterial gene transcription with an RpoN-based stapled peptide. 25(9): 1059-66.

Appendix

Table A1. Primers used for experiments described in Chapter 2.

Primer	Sequence (5' – 3')
Knockout primers	
ntrB outA	AGCTACTGCGCATCCTCTTC
ntrB up_fwd	AGAGGATCCTGCTCGACGGCAAGCCTG
ntrB up_rev	CGGTCTCTGATCGGCTCATGGGGCGGGCAGCTGTTCCAA
ntrB down_fwd	TTGGAACAGCTGCCCGCCCCATGAGCCGATCAGAGACCG
ntrB down_rev	TGCAAGCTTCGCCTCGCCGATGATCTC
ntrB outB	TCCATCAGGTCCTTGGGGAT
ntrC outA	ACGAGATCAAGAACCCGCTC
ntrC up_fwd	AGAGGATCCGAACCTGGCGCCGACCAACAT
ntrC up_rev	TCGCTCATGGGAGCAGTGGCGCTGGTCAATGCACTCCTTGTTCCAGGGGC
ntrC down_fwd	GCCCCTGGAACAAGGAGTGCATTGACCAGCGCCACTGCTCCCATGAGCGA
ntrC down_rev	TGCAAGCTTGGGCGAGCTGGTGATGAATGCCTC
ntrC outB	AAGGGGGAATTCTCAGCCTG
ntrBC up_rev	TCGCTCATGGGAGCAGTGGCGCTGGCGGGCAGCTGTTCCAA
ntrBC down_fwd	TTGGAACAGCTGCCCGCCAGCGCCACTGCTCCCATGAGCGA
Complementation	
ntrB fwd	GCAGGAATTCATGCCGACCGATACCCTGCA
ntrB rev	GGGGGATCCTCAATGCACTCCTTGTTCCAGGGGC
ntrC fwd	GAATTCGATAATGAGCCGATCAGAGACCGT
ntrC rev	GGGGGATCCTCAGTCGTCGCCTTCGT
RT-qPCR	
ntrB fwd	GATACCCTGCACCGACTGTT
ntrB rev	TGCGCCTGGAGTACATGA
ntrC fwd	ATCAGAGACCGTCTGGATCG
ntrC rev	TGCAGCAGGAAGGCATGA
algR fwd	TTCGGTCGCGAGGCTTTCTT
algR rev	TGACGAATTCGCCTGGAAG
lasR fwd	AGCTGGAACGCTCAAGTGGA
lasR rev	TGGCTGTCCTTAGGCAACAG
rhlA fwd	GGGTTGATCACCAAGGACGA
rhlA rev	AATCACCTGGTCTCCGCGT
rhlB fwd	CCTGTCGGCGTTTCATGGAA
rhlB rev	GAACGTTGTCATAGGGAGGG

Table A2. Growth rates of PA14 *ntrBC* mutant strains was influenced by nitrogen source and significantly reduced in the presence of nitrate or nitrite as well as casamino acids for the double mutant. Briefly, bacteria were seeded from overnight cultures into batch cultures at low density (OD_{600} = 0.1) and incubated at 37ºC for 10 h with shaking in (A) basal medium (BM2) in which $(NH_4)_2SO_4$ was replaced with (B) 0.1% casamino acids (CAA) (C) 14 mM $NaNO_2$ or (D) 14 mM $NaNO_3$. Growth rates were calculated by taking the slope of the curve during exponential growth. Mean growth rate ± standard error of the mean (SEM) from three independent experiments is shown (n = 3). * $P < 0.05$, ** $P < 0.01$ different from WT according to Welch's t-test.

Medium	**WT**	**Δ*ntrB***	**Δ*ntrC***	**Δ*ntrBC***
BM2	0.38 ± 0.06	0.36 ± 0.02	0.34 ± 0.08	0.09 ± 0.01*
BM2 (0.1% CAA)	0.37 ± 0.08	0.39 ± 0.05	0.35 ± 0.07	0.09 ± 0.02*
BM2 (14 mM $NaNO_2$)	0.34 ± 0.05	0.07 ± 0.01**	0.11 ± 0.01**	0.04 ± 0.01**
BM2 (14 mM $NaNO_3$)	0.48 ± 0.08	0.03 ± 0.01**	0.04 ± 0.02**	0.01 ± 0.007**

Table A3. All genes differentially expressed under swarming conditions in PA14 *ntrB* and *ntrC* mutant strains. Gene expression for mutants is expressed as fold-change (FC) relative to PA14 wild-type (WT). Briefly, swarm plates were inoculated with 5 µl of planktonic cells suspended at OD600 = 0.4-0.6 in basal medium (BM2) supplemented with 0.1% casamino acids and 0.4% glucose, then incubated for 18-24 h at 37°C. Swarming cells were harvested from the tip of the swarm tendrils and RNA was isolated using Qiagen RNEasy MiniPrep kit.

PA14 Locus	PAO1 Locus	Name	Annotation	FC Δ*ntrB*	FC Δ*ntrC*
PA14_00080	PA0007	PA0007	hypothetical protein	-1.95	-2.36
PA14_00100	PA0009	glyQ	glycyl-tRNA synthetase alpha chain	1.66	
PA14_00470	PA0038	PA0038	hypothetical protein	1.72	1.83
PA14_00560	PA0044	exoT	exoenzyme T	4.92	9.39
PA14_00600	PA0048	PA0048	probable transcriptional regulator	-4.06	-4.04
PA14_00620	PA0049	PA0049	hypothetical protein	-3.44	-5.58
PA14_00650	PA0052	PA0052	hypothetical protein	-1.89	-2.25
PA14_00670	PA0055	PA0055	hypothetical protein	1.90	1.76
PA14_00710	PA0059	osmC	osmotically inducible protein OsmC	3.21	5.92
PA14_00720	PA0060	PA0060	conserved hypothetical protein	2.45	4.19
PA14_00740	PA0062	PA0062	hypothetical protein	2.99	5.07
PA14_01250	PA0103	PA0103	probable sulfate transporter	-2.80	-2.69
PA14_01270	PA0104	PA0104	hypothetical protein	-1.95	-1.67
PA14_01290	PA0105	coxB	cytochrome c oxidase, subunit II	-1.75	-2.03
PA14_01330	PA0109	PA0109	hypothetical protein	-1.72	-1.91
PA14_01340	PA0110	PA0110	hypothetical protein	-2.10	-2.30
PA14_01360	PA0112	PA0112	hypothetical protein	-2.05	-2.61
PA14_01410	PA0116	PA0116	hypothetical protein	-1.76	-1.94
PA14_01580	PA0129	bauD	Amino acid permease	-2.82	-2.58
PA14_01600	PA0130	bauC	3-Oxopropanoate dehydrogenase	-2.67	-2.45
PA14_01610	PA0131	bauB	BauB	-2.57	-1.87
PA14_01620	PA0132	bauA	Beta-alanine:pyruvate transaminase	-5.60	-4.65
PA14_01670	PA0136	PA0136	probable ATP-binding component of ABC transporter	-36.6	-37.6
PA14_01680	PA0137	PA0137	probable permease of ABC transporter	-112	-154
PA14_01690	PA0138	PA0138	probable permease of ABC transporter	-22.2	-29.7
PA14_01750	PA0142	PA0142	hypothetical protein	1.74	
PA14_01770	-	-	-	-11.3	-11.5
PA14_01780	PA0144	PA0144	hypothetical protein	-9.12	-9.86
PA14_01800	PA0146	PA0146	conserved hypothetical protein	-33.1	-31.3
PA14_01810	PA0147	PA0147	probable oxidoreductase	-5.47	-5.55
PA14_01830	PA0148	PA0148	adenine deaminase	-1.84	-2.05
PA14_01970	PA0158	triC	Resistance-Nodulation-Cell Division (RND) triclosan efflux transporter, TriC	1.51	2.22
PA14_02060	PA0165	PA0165	hypothetical protein	-8.22	-10.72
PA14_02070	PA0166	PA0166	probable transporter	-41.9	-244
PA14_02090	PA0167	PA0167	probable transcriptional regulator	-1.57	-1.64
PA14_02100	PA0168	PA0168	conserved hypothetical protein	-1.79	-1.60
PA14_02180	PA0173	PA0173	probable methylesterase	-2.88	-3.40
PA14_02190	PA0174	PA0174	conserved hypothetical protein	-2.43	-2.67

PA14_02200	PA0175	PA0175	probable chemotaxis protein methyltransferase	-2.15	-2.71
PA14_02220	PA0176	aer2	aerotaxis transducer Aer2	-2.38	-2.62
PA14_02230	PA0177	PA0177	probable purine-binding chemotaxis protein	-2.43	-2.72
PA14_02250	PA0178	PA0178	probable two-component sensor	-2.69	-3.02
PA14_02260	PA0179	PA0179	probable two-component response regulator	-2.03	-2.55
PA14_02270	PA0180	cttP	chemotactic transducer for trichloroethylene [positive chemotaxis], CttP	-1.70	-1.80
PA14_02450	PA0195	pntAA	putative NAD(P) transhydrogenase, SU α1	-1.87	-2.88
PA14_02450	PA0195	pntAB	putative NAD(P) transhydrogenase, SU α2	-1.87	-2.88
PA14_02470	PA0196	pntB	pyridine nucleotide transhydrogenase, beta subunit	-1.64	-2.31
PA14_02550	PA0208	mdcA	malonate decarboxylase alpha subunit	-10.3	-9.26
PA14_02560	PA0209	PA0209	conserved hypothetical protein	-19.2	-21.9
PA14_02570	PA0210	mdcC	malonate decarboxylase delta subunit	-14.8	-29.7
PA14_02580	PA0211	mdcD	malonate decarboxylase beta subunit	-32.0	-27.1
PA14_02590	PA0212	mdcE	malonate decarboxylase gamma subunit	-14.0	-9.63
PA14_02610	PA0213	PA0213	hypothetical protein	-13.7	-9.25
PA14_02620	PA0214	PA0214	probable acyl transferase	-11.3	-10.8
PA14_02630	PA0215	PA0215	malonate transporter MadL	-3.64	-4.13
PA14_02640	PA0216	PA0216	malonate transporter MadM	-3.72	-2.48
PA14_02660	PA0218	PA0218	probable transcriptional regulator	-2.71	-2.51
PA14_02680	PA0219	PA0219	probable aldehyde dehydrogenase	-3.24	-3.66
PA14_02690	PA0220	PA0220	amino acid APC family transporter	-7.50	-6.26
PA14_02700	PA0221	PA0221	probable aminotransferase	-7.29	-11.6
PA14_02720	PA0222	PA0222	hypothetical protein	-9.53	-6.41
PA14_03560	PA0274	PA0274	hypothetical protein	-2.50	-2.79
PA14_03710	PA0284	PA0284	hypothetical protein	1.81	
PA14_03770	PA0288	gpuA	3-guanidinopropionase	-2.70	-3.28
PA14_03800	PA0291	oprE	Anaerobically-induced outer membrane porin	1.85	1.81
PA14_03860	PA0296	spuI	Glutamylpolyamine synthetase	-2.57	-2.56
PA14_03870	PA0297	spuA	probable glutamine amidotransferase	-2.23	-2.95
PA14_03880	PA0298	spuB	Glutamylpolyamine synthetase	-1.87	-1.73
PA14_03900	PA0299	spuC	Polyamine:pyruvate transaminase	-3.33	-3.69
PA14_03920	PA0300	spuD	polyamine transport protein	-3.14	-3.33
PA14_03930	PA0301	spuE	polyamine transport protein	-3.30	-3.27
PA14_03940	PA0302	spuF	polyamine transport protein PotG	-3.46	-3.49
PA14_03950	PA0303	spuG	polyamine transport protein PotH	-3.23	-3.45
PA14_03960	PA0304	spuH	polyamine transport protein PotI	-4.04	-3.47
PA14_04010	-	-	-	1.63	
PA14_04190	PA0321	PA0321	acetylpolyamine amidohydrolase	-3.45	-3.43
PA14_04210	PA0322	PA0322	probable transporter	-3.04	-3.18
PA14_04220	PA0323	PA0323	Prob. binding protein component of ABC transporter	-17.7	-19.2
PA14_04230	PA0324	PA0324	probable permease of ABC transporter	-95.4	-189
PA14_04240	PA0325	PA0325	probable permease of ABC transporter	-36.4	-31.0
PA14_04250	PA0326	PA0326	Prob. ATP-binding component of ABC transporter	-15.6	-25.6
PA14_04290	PA0328	aaaA	arginine-specific autotransporter	-3.14	-3.13
PA14_04300	PA0329	PA0329	conserved hypothetical protein	1.71	
PA14_04760	PA0363	coaD	phosphopantetheine adenylyltransferase	1.61	1.59
PA14_05430	PA0417	chpE	probable chemotaxis protein	-4.47	-4.09
PA14_05630	PA0433	PA0433	hypothetical protein	2.75	7.68
PA14_05640	PA0434	PA0434	hypothetical protein	6.63	21.9

PA14_05690	PA0437	codA	cytosine deaminase	-3.75	-3.94
PA14_05700	PA0438	codB	cytosine permease	-3.75	-5.28
PA14_05740	PA0439	PA0439	probable oxidoreductase	-28.2	-40.6
PA14_05750	PA0440	PA0440	probable oxidoreductase	-33.1	-25.9
PA14_05770	PA0441	dht	dihydropyrimidinase	-38.2	-48.4
PA14_05790	PA0443	PA0443	probable transporter	-36.7	-42.0
PA14_05810	PA0444	PA0444	N-carbamoyl-beta-alanine amidohydrolase	-27.8	-23.5
PA14_05920	PA0454	PA0454	conserved hypothetical protein	-1.83	-1.80
PA14_06230	PA0476	PA0476	probable permease	-14.0	-13.5
PA14_06310	PA0484	PA0484	conserved hypothetical protein	-1.57	-1.92
PA14_06960	PA0534	pauB1	FAD-dependent oxidoreductase	-2.83	-2.29
PA14_07040	PA0542	PA0542	conserved hypothetical protein	1.60	
PA14_07090	PA0546	metK	methionine adenosyltransferase	2.23	2.15
PA14_07170	PA0551	epd	D-erythrose 4-phosphate dehydrogenase	1.78	2.01
PA14_07190	PA0552	pgk	phosphoglycerate kinase	1.57	2.19
PA14_07260	PA0558	PA0558	conserved hypothetical protein	1.70	1.71
PA14_07370	PA0567	PA0567	conserved hypothetical protein	2.50	3.12
PA14_07770	PA0595	lptD	LPS-assembly protein LptD	1.70	1.62
PA14_07850	PA0602	PA0602	probable binding protein component of ABC transporter	-1.98	-1.95
PA14_07860	PA0603	agtA	AgtA	1.80	1.84
PA14_08450	PA0659	PA0659	hypothetical protein	1.53	
PA14_08540	PA0667	PA0667	conserved hypothetical protein	1.83	1.87
PA14_09220	PA4230	pchB	salicylate biosynthesis protein PchB	1.84	1.90
PA14_09260	PA4227	pchR	transcriptional regulator PchR	1.72	1.70
PA14_09440	PA1903	phzE2	phenazine biosynthesis protein PhzE	1.89	1.65
PA14_09440	PA4214	phzE1	phenazine biosynthesis protein PhzE	1.89	1.65
PA14_09550	PA4204	ppgL	periplasmic gluconolactonase, PpgL	2.13	3.76
PA14_09880	PA4177	PA4177	hypothetical protein	-3.00	-3.58
PA14_09900	PA4175	piv	protease IV	-2.68	-3.75
PA14_09920	PA4173	PA4173	conserved hypothetical protein	-6.18	-4.84
PA14_09930	PA4172	PA4172	probable nuclease	4.24	8.94
PA14_09940	PA4171	PA4171	probable protease	4.64	9.02
PA14_10180	PA4158	fepC	ferric enterobactin transport protein FepC	-5.65	
PA14_10220	PA4154	PA4154	conserved hypothetical protein	2.91	4.45
PA14_10240	PA4152	PA4152	probable hydrolase	-3.96	
PA14_10280	PA4148	PA4148	probable short-chain dehydrogenase	-58.2	-16.6
PA14_10290	PA4147	acoR	transcriptional regulator AcoR	-2.15	-2.46
PA14_10340	PA4143	PA4143	probable toxin transporter	1.72	1.52
PA14_10360	PA4141	PA4141	hypothetical protein	2.38	1.82
PA14_10370	PA4140	PA4140	hypothetical protein	4.46	4.29
PA14_10380	PA4139	PA4139	hypothetical protein	6.30	5.50
PA14_10480	PA4135	PA4135	probable transcriptional regulator	1.66	
PA14_10730	PA4115	PA4115	conserved hypothetical protein	-1.58	
PA14_10750	PA4113	PA4113	probable major facilitator superfamily (MFS) transporter	1.89	1.74
PA14_10820	PA4108	PA4108	cyclic di-GMP phosphodiesterase	-1.67	-1.86
PA14_11240	PA4070	PA4070	probable transcriptional regulator	-3.74	-3.21
PA14_11310	PA4064	PA4064	Prob. ATP-binding component of ABC transporter	2.09	
PA14_11490	PA4048	PA4048	hypothetical protein	-1.57	-1.82
PA14_11580	PA4041	PA4041	hypothetical protein	-1.67	-1.89

PA14_11690	PA4031	ppa	inorganic pyrophosphatase	1.59	
PA14_11730	-	-	-	-29.1	-28.4
PA14_11740	PA4027	PA4027	hypothetical protein	-1.81	-2.02
PA14_11750	PA4026	PA4026	probable acetyltransferase	-2.12	-2.43
PA14_11760	PA4025	PA4025	probable ethanolamine ammonia-lyase light chain	-5.97	-6.32
PA14_11770	PA4024	eutB	ethanolamine ammonia-lyase large subunit	-4.66	-5.59
PA14_11790	PA4023	PA4023	probable transport protein	-11.9	-16.5
PA14_11810	PA4022	hdhA	hydrazone dehydrogenase, HdhA	-2.76	-3.64
PA14_11940	PA4012	PA4012	hypothetical protein	-1.96	-1.81
PA14_12180	PA3990	PA3990	conserved hypothetical protein	1.78	
PA14_12260	PA3986	PA3986	hypothetical protein	-1.70	-2.15
PA14_12270	PA3985	PA3985	conserved hypothetical protein	-1.87	-2.07
PA14_12620	PA3962	PA3962	hypothetical protein	2.11	2.98
PA14_12650	PA3959	PA3959	hypothetical protein	2.00	
PA14_12680	PA3957	PA3957	probable short-chain dehydrogenase	-2.55	-2.89
PA14_13110	PA3924	PA3924	probable medium-chain acyl-CoA ligase	-2.22	-2.77
PA14_13130	PA3923	PA3923	hypothetical protein	-2.36	-2.65
PA14_13140	PA3922	PA3922	conserved hypothetical protein	-2.53	-2.75
PA14_13170	PA3920	PA3920	probable metal transporting P-type ATPase	-2.40	-4.34
PA14_13490	PA3897	PA3897	hypothetical protein	-2.41	-2.83
PA14_14040	PA3861	rhl	ATP-dependent RNA helicase RhlB	1.50	
PA14_14330	PA3842	spcS	specific Pseudomonas chaperone for ExoS, SpcS	9.55	13.3
PA14_14660	PA3819	PA3819	conserved hypothetical protein	1.76	3.13
PA14_14680	PA3818	PA3818	extragenic suppressor protein SuhB	1.50	1.55
PA14_14810	PA3808	PA3808	conserved hypothetical protein	-1.58	-1.56
PA14_14820	PA3807	ndk	nucleoside diphosphate kinase	1.62	
PA14_14990	PA3795	PA3795	probable oxidoreductase	2.66	4.14
PA14_15070	PA3790	oprC	Putative copper transport outer membrane porin OprC precursor	11.5	65.4
PA14_15120	PA3785	PA3785	conserved hypothetical protein	2.96	4.42
PA14_15130	PA3784	PA3784	hypothetical protein	1.80	3.39
PA14_15290	PA3771	PA3771	probable transcriptional regulator	-3.63	-3.09
PA14_15790	PA3760	PA3760	N-Acetyl-D-Glucosamine phosphotransferase system transporter	-1.64	
PA14_15970	PA3745	rpsP	30S ribosomal protein S16	1.74	
PA14_16110	-	-	-	1.80	2.48
PA14_16390	PA3710	PA3710	probable GMC-type oxidoreductase	-2.18	-2.78
PA14_16410	PA3709	PA3709	probable major facilitator superfamily (MFS) transporter	-3.50	-4.45
PA14_16830	PA3675	PA3675	hypothetical protein	1.76	1.67
PA14_16860	PA3673	plsB	glycerol-3-phosphate acyltransferase	1.78	1.83
PA14_16920	PA3668	PA3668	conserved hypothetical protein	-1.94	-1.91
PA14_16970	PA3664	PA3664	conserved hypothetical protein	2.19	
PA14_17080	PA3654	pyrH	uridylate kinase	1.61	
PA14_17150	PA3648	opr86	outer membrane protein Opr86	1.81	1.68
PA14_17170	PA3647	PA3647	probable outer membrane protein precursor	1.76	1.57
PA14_17290	PA3637	pyrG	CTP synthase	1.76	
PA14_17500	PA3620	mutS	DNA mismatch repair protein MutS	1.50	
PA14_17930	PA3584	glpD	glycerol-3-phosphate dehydrogenase	-1.88	-3.02
PA14_17940	PA3583	glpR	glycerol-3-phosphate regulon repressor	-1.68	-1.89
PA14_17960	PA3582	glpK	glycerol kinase	-2.00	-3.05

PA14_17980	PA3581	glpF	glycerol uptake facilitator protein	-1.84	-2.49
PA14_18050	PA3576	PA3576	hypothetical protein	-2.18	-1.74
PA14_18070	-	-	-	-2.17	-5.34
PA14_18120	PA3570	mmsA	methylmalonate-semialdehyde dehydrogenase	-1.92	-2.44
PA14_18140	PA3569	mmsB	3-hydroxyisobutyrate dehydrogenase	-2.54	-2.94
PA14_18150	PA3568	PA3568	probable acetyl-coa synthetase	-3.14	-2.07
PA14_18250	PA3562	fruI	phosphotransferase system transporter enzyme I, FruI	-2.19	-1.62
PA14_18580	PA3540	algD	GDP-mannose 6-dehydrogenase AlgD	-6.52	-4.38
PA14_18690	PA3529	PA3529	alkylhydroperoxide reductase C	2.17	2.03
PA14_18720	PA3526	motY	MotY	-2.04	-1.62
PA14_18760	PA3523	mexP	MexP	-5.51	-5.27
PA14_18780	PA3522	mexQ	MexQ	-2.73	-3.34
PA14_18790	PA3521	opmE	OpmE	-5.18	-3.45
PA14_18810	PA3519	PA3519	hypothetical protein	-3.33	-6.63
PA14_18820	PA3518	PA3518	hypothetical protein	-2.90	-4.97
PA14_18830	PA3517	PA3517	probable lyase	-2.73	-2.80
PA14_18860	PA3515	PA3515	hypothetical protein	-1.89	
PA14_18880	PA3495	nth	endonuclease III	1.88	
PA14_19110	PA3478	rhlB	rhamnosyltransferase chain B	-2.18	-1.98
PA14_19170	PA3472	PA3472	hypothetical protein	1.79	1.84
PA14_19490	PA3450	lsfA	1-Cys peroxiredoxin LsfA	2.10	2.29
PA14_19650	PA3436	PA3436	hypothetical protein	-144	-294
PA14_19660	PA3435	PA3435	conserved hypothetical protein	1.61	1.55
PA14_19700	PA3430	PA3430	probable aldolase	-1.79	-1.56
PA14_19710	PA3429	PA3429	probable epoxide hydrolase	-2.44	-1.96
PA14_19850	PA3420	PA3420	probable transcriptional regulator	-2.37	-2.24
PA14_19870	PA3418	ldh	leucine dehydrogenase	-1.54	-2.16
PA14_19900	PA3417	PA3417	Prob. pyruvate dehydrogenase E1 component, α	-2.39	-2.53
PA14_19910	PA3416	PA3416	probable pyruvate dehydrogenase E1 component, β	-2.28	-2.55
PA14_19920	PA3415	PA3415	probable dihydrolipoamide acetyltransferase	-2.61	-2.80
PA14_20000	PA3409	hasS	HasS	-6.74	-7.74
PA14_20030	PA3406	hasD	transport protein HasD	-30.34	-22.23
PA14_20040	PA3405	hasE	metalloprotease secretion protein	-23.30	-8.47
PA14_20060	-	-	-	-5.94	-3.57
PA14_20070	PA3403	PA3403	hypothetical protein	-25.83	-25.04
PA14_20080	PA3402	PA3402	hypothetical protein	-2.06	-2.25
PA14_20270	PA3387	rhlG	beta-ketoacyl reductase	-2.42	
PA14_20570	PA3365	PA3365	probable chaperone	-3.32	-3.07
PA14_20580	PA3364	amiC	aliphatic amidase expression-regulating protein	-2.64	-1.92
PA14_20590	PA3363	amiR	aliphatic amidase regulator	-2.56	-1.91
PA14_20620	PA3360	PA3360	probable secretion protein	-2.74	-2.56
PA14_20670	PA3356	pauA5	Glutamylpolyamine synthetase	-1.51	
PA14_20690	PA3354	PA3354	hypothetical protein	-1.92	-1.69
PA14_20740	PA3350	PA3350	hypothetical protein	-2.11	-2.23
PA14_20760	PA3348	PA3348	probable chemotaxis protein methyltransferase	-1.51	
PA14_20780	PA3346	hsbR	HptB-dependent secretion and biofilm regulator	-1.74	-1.78
PA14_20860	PA3340	PA3340	hypothetical protein	-1.71	-1.86
PA14_20960	PA3332	PA3332	conserved hypothetical protein	1.92	
PA14_20970	PA3331	PA3331	cytochrome P450	1.73	1.52
PA14_21000	PA3329	PA3329	hypothetical protein	1.70	-

PA14_21120	PA3318	PA3318	hypothetical protein	8.02	6.75
PA14_21440	PA3295	PA3295	probable HIT family protein	1.78	
PA14_21550	PA3285	PA3285	probable sigma-70 factor, ECF subfamily	-1.57	
PA14_21570	PA3284	PA3284	hypothetical protein	-2.26	-2.27
PA14_21580	PA3283	PA3283	conserved hypothetical protein	-3.60	-2.77
PA14_21680	PA3273	PA3273	hypothetical protein	1.62	3.39
PA14_21820	PA3262	PA3262	Prob. peptidyl-prolyl cis-trans isomerase, FkbP-type	1.91	1.68
PA14_21910	PA3254	PA3254	Prob. ATP-binding component of ABC transporter	-2.17	-2.60
PA14_21920	PA3253	PA3253	probable permease of ABC transporter	-2.33	-3.66
PA14_21930	PA3252	PA3252	probable permease of ABC transporter	-2.60	-3.23
PA14_21940	PA3251	PA3251	hypothetical protein	-2.64	-3.29
PA14_21960	PA3250	PA3250	hypothetical protein	-2.22	-3.11
PA14_22010	PA3245	minE	cell division topological specificity factor MinE	1.55	1.64
PA14_22330	PA3236	betX	BetX	-2.96	-2.77
PA14_22480	PA3224	PA3224	hypothetical protein	1.62	
PA14_22570	PA3221	csaA	CsaA protein	2.42	
PA14_22940	PA3192	gltR	two-component response regulator GltR	-1.59	
PA14_23060	PA3184	PA3184	probable transcriptional regulator	-1.53	
PA14_23070	PA3183	zwf	glucose-6-phosphate 1-dehydrogenase	-1.55	-1.52
PA14_23080	PA3182	pgl	6-phosphogluconolactonase	-1.80	-1.63
PA14_23200	PA3173	PA3173	probable short-chain dehydrogenase	1.65	
PA14_23500	PA3139	PA3139	probable amino acid aminotransferase	1.82	1.60
PA14_24210	PA3089	PA3089	hypothetical protein	-1.65	-1.95
PA14_24480	PA3064	pelA	PelA	1.89	
PA14_24490	PA3063	pelB	PelB	1.69	
PA14_24780	PA3039	PA3039	probable transporter	-6.56	-7.71
PA14_24880	PA3031	PA3031	hypothetical protein	1.63	1.63
PA14_25040	PA3017	PA3017	conserved hypothetical protein	-3.70	-3.69
PA14_25090	PA3013	faoB	fatty-acid oxidation complex beta-subunit	1.89	1.96
PA14_25180	PA3006	psrA	transcriptional regulator PsrA	-2.63	-2.82
PA14_25430	PA2988	lolE	lipoprotein localization protein LolE	1.66	1.92
PA14_25440	PA2987	lolD	lipoprotein localization protein LolD	1.63	2.12
PA14_25450	PA2986	lolC	lipoprotein localization protein LolC	2.34	
PA14_25520	PA2980	PA2980	conserved hypothetical protein	1.75	
PA14_26280	PA2920	PA2920	probable chemotaxis transducer	-2.35	-2.25
PA14_26910	PA2875	PA2875	conserved hypothetical protein	-1.61	-1.65
PA14_26940	PA2872	PA2872	hypothetical protein	-1.83	-1.62
PA14_27100	PA2862	lipA	lactonizing lipase precursor	-2.06	
PA14_27120	PA2860	PA2860	hypothetical protein	1.72	
PA14_27210	PA2851	efp	translation elongation factor P	1.60	
PA14_27630	-	-	-	9.78	8.53
PA14_27640	-	-	-	10.5	10.8
PA14_27650	-	-	-	7.08	4.91
PA14_27660	-	-	-	6.64	4.93
PA14_27675	-	-	-	3.31	3.67
PA14_27680	-	-	-	4.06	4.58
PA14_27690	-	-	-	6.92	
PA14_27710	PA2817	PA2817	hypothetical protein	1.56	1.75
PA14_27830	PA2808	ptrA	Pseudomonas type III repressor A	-3.60	-8.97
PA14_27840	PA2807	PA2807	hypothetical protein	-4.94	-14.4

PA14_28140	PA2779	PA2779	hypothetical protein	-1.81	-2.16
PA14_28150	PA2778	PA2778	hypothetical protein	-3.34	-2.70
PA14_28180	PA2776	pauB3	FAD-dependent oxidoreductase	-1.86	-1.77
PA14_28220	PA2773	PA2773	hypothetical protein	2.52	4.51
PA14_28250	-	-	-	1.82	1.51
PA14_28280	PA2770	PA2770	hypothetical protein	-1.62	-1.57
PA14_28490	PA2754	PA2754	conserved hypothetical protein	1.83	3.08
PA14_28650	PA2744	thrS	threonyl-tRNA synthetase	1.75	
PA14_29180	PA2704	PA2704	probable transcriptional regulator	-3.85	-3.15
PA14_29240	PA2698	PA2698	probable hydrolase	1.75	1.60
PA14_29420	PA2682	PA2682	conserved hypothetical protein	-2.24	-2.72
PA14_29640	PA2664	fhp	flavohemoprotein	-6.23	-5.77
PA14_29650	PA2663	ppyR	psl and pyoverdine operon regulator, PpyR	-4.13	-4.80
PA14_29660	PA2662	PA2662	conserved hypothetical protein	-4.98	-4.39
PA14_29710	PA2659	PA2659	hypothetical protein	2.73	1.87
PA14_29760	PA2654	PA2654	probable chemotaxis transducer	-2.20	-1.93
PA14_30240	PA2619	infA	initiation factor	1.94	1.51
PA14_30980	-	-	-	2.71	2.23
PA14_31070	-	-	-	-2.54	-2.22
PA14_31430	-	-	-	1.95	2.68
PA14_31450	-	-	-	-2.53	-3.09
PA14_32140	PA2514	antC	anthranilate dioxygenase reductase	-45.8	-30.8
PA14_32150	PA2513	antB	anthranilate dioxygenase small subunit	-94.5	-100
PA14_32160	PA2512	antA	anthranilate dioxygenase large subunit	-10.4	-13.4
PA14_32190	PA2511	antR	AntR	-7.68	-8.12
PA14_32220	PA2509	catB	muconate cycloisomerase I	-10.4	-10.5
PA14_32230	PA2508	catC	muconolactone delta-isomerase	-3.88	-3.93
PA14_32240	PA2507	catA	catechol 1,2-dioxygenase	-7.54	-7.35
PA14_32280	PA2504	PA2504	hypothetical protein	-1.87	-1.90
PA14_32490	PA2485	PA2485	hypothetical protein	1.88	2.92
PA14_32530	PA2482	PA2482	probable cytochrome c	-2.44	-2.60
PA14_32540	PA2481	PA2481	hypothetical protein	-3.21	-2.31
PA14_33030	PA2443	sdaA	L-serine dehydratase	-1.64	-1.52
PA14_33040	PA2442	gcvT2	glycine cleavage system protein T2	-1.62	
PA14_33050	PA2441	PA2441	hypothetical protein	2.78	1.68
PA14_33060	PA2440	PA2440	hypothetical protein	1.95	1.66
PA14_33160	PA2433	PA2433	hypothetical protein	2.80	5.81
PA14_33250	PA2427	PA2427	hypothetical protein	-4.68	-3.77
PA14_33270	PA2425	pvdG	PvdG	-4.02	-7.59
PA14_33280	PA2424	pvdL	PvdL	-4.29	-6.11
PA14_33450	PA2416	treA	periplasmic trehalase precursor	2.67	5.83
PA14_33460	PA2415	PA2415	hypothetical protein	3.05	4.55
PA14_33530	PA2410	fpvF	FpvF	-2.49	-4.03
PA14_33540	PA2409	fpvE	FpvE	-8.13	-6.50
PA14_33550	PA2408	fpvD	FpvD	-4.64	-6.59
PA14_33560	PA2407	fpvC	FpvC	-3.41	-5.75
PA14_33570	PA2406	fpvK	FpvK	-6.44	-8.01
PA14_33590	PA2404	fpvH	FpvH	-5.47	-5.86
PA14_33600	PA2403	fpvG	FpvG	-2.65	-4.23
PA14_33610	PA2402	PA2402	probable non-ribosomal peptide synthetase	-2.99	-3.04
PA14_33630	PA2400	pvdJ	PvdJ	-2.42	-2.35

PA14_33650	PA2399	pvdD	pyoverdine synthetase D	-2.09	-2.00
PA14_33680	PA2398	fpvA	ferripyoverdine receptor	-1.92	-2.83
PA14_33710	PA2395	pvdO	PvdO	-5.12	-3.66
PA14_33810	PA2386	pvdA	L-ornithine N5-oxygenase	-2.54	-3.49
PA14_33820	PA2385	pvdQ	3-oxo-C12-homoserine lactone acylase PvdQ	-4.08	-5.90
PA14_33830	PA2384	PA2384	hypothetical protein	-3.73	-4.05
PA14_33980	-	-	-	-2.02	-4.54
PA14_34190	PA2356	msuD	methanesulfonate sulfonatase MsuD	-6.16	-5.84
PA14_34210	PA2354	PA2354	probable transcriptional regulator	-3.33	-3.14
PA14_34540	PA2326	PA2326	hypothetical protein	-3.53	-2.46
PA14_34820	PA2304	ambC	AmbC	1.72	1.63
PA14_34830	PA2303	ambD	AmbD	1.89	1.73
PA14_34870	PA2300	chiC	chitinase	1.69	
PA14_35240	PA2268	PA2268	hypothetical protein	-2.17	
PA14_35270	PA2266	PA2266	probable cytochrome c precursor	-1.73	-1.66
PA14_35490	PA2250	lpdV	lipoamide dehydrogenase-Val	-1.62	
PA14_35840	-	-	-	1.55	
PA14_35880	-	-	-	-1.79	
PA14_35940	-	-	-	-4.37	-2.89
PA14_35950	-	-	-	-4.48	-2.45
PA14_35970	-	-	-	-4.39	-2.78
PA14_35990	-	-	-	-4.02	-2.70
PA14_36200	PA2204	PA2204	probable binding protein component of ABC transporter	2.44	
PA14_36330	PA2193	hcnA	hydrogen cyanide synthase HcnA	1.82	
PA14_36345	PA2191	exoY	adenylate cyclase ExoY	3.03	4.52
PA14_36360	PA2187	PA2187	hypothetical protein	2.29	5.32
PA14_36375	PA2180	PA2180	hypothetical protein	2.76	6.46
PA14_36480	-	-	-	3.95	9.15
PA14_36490	PA2173	PA2173	hypothetical protein	3.04	10.2
PA14_36530	PA2169	PA2169	hypothetical protein	3.06	5.16
PA14_36570	PA2165	PA2165	probable glycogen synthase	2.39	5.33
PA14_36670	PA2157	PA2157	hypothetical protein	2.09	5.71
PA14_36690	PA2155	PA2155	probable phospholipase	1.72	4.98
PA14_36710	PA2153	glgB	1,4-alpha-glucan branching enzyme	2.67	7.25
PA14_36730	PA2152	PA2152	probable trehalose synthase	2.79	7.63
PA14_36740	PA2151	PA2151	conserved hypothetical protein	2.71	6.66
PA14_36790	-	-	-	3.46	7.68
PA14_36810	PA2147	katE	catalase HPII	6.56	16.2
PA14_36820	PA2146	PA2146	conserved hypothetical protein	2.89	2.78
PA14_36980	PA2134	PA2134	hypothetical protein	3.66	7.39
PA14_37210	PA2116	PA2116	conserved hypothetical protein	-2.91	-3.39
PA14_37220	PA2115	PA2115	probable transcriptional regulator	-3.79	-4.04
PA14_37250	PA2114	PA2114	probable major facilitator superfamily (MFS) transporter	-3.46	-4.82
PA14_37260	PA2113	opdO	pyroglutamate porin OpdO	-6.21	-6.41
PA14_37270	PA2112	PA2112	conserved hypothetical protein	-6.17	-6.24
PA14_37290	PA2111	PA2111	hypothetical protein	-4.61	-5.95
PA14_37310	PA2110	PA2110	hypothetical protein	-8.42	-6.73
PA14_37350	PA2107	PA2107	hypothetical protein	2.29	4.99
PA14_37660	PA2076	PA2076	probable transcriptional regulator	-1.63	-1.59

PA14_37790	PA2065	pcoA	copper resistance protein A precursor	-2.13	-3.96
PA14_37810	PA2064	pcoB	copper resistance protein B precursor	-3.45	-6.64
PA14_37830	PA2062	PA2062	probable pyridoxal-phosphate dependent enzyme	1.67	1.79
PA14_38050	PA2046	PA2046	hypothetical protein	2.09	3.63
PA14_38160	PA2039	PA2039	hypothetical protein	-1.99	-2.43
PA14_38200	PA2035	PA2035	probable decarboxylase	-1.50	-1.51
PA14_38210	PA2034	PA2034	hypothetical protein	-2.49	-
PA14_38260	PA2031	PA2031	hypothetical protein	-2.81	-3.08
PA14_38270	PA2030	PA2030	hypothetical protein	-3.63	-2.96
PA14_38310	PA2027	PA2027	hypothetical protein	-4.60	-4.61
PA14_38340	PA2024	PA2024	probable ring-cleaving dioxygenase	-1.66	-2.01
PA14_38350	PA2023	galU	UTP--glucose-1-phosphate uridylyltransferase	2.36	3.86
PA14_38690	PA1997	PA1997	probable AMP-binding enzyme	-1.84	-1.61
PA14_38740	PA1992	ercS	ErcS	-1.66	
PA14_38825	PA1985	pqqA	pyrroloquinoline quinone biosynthesis protein A	2.17	1.66
PA14_39070	PA1969	PA1969	hypothetical protein	1.74	2.11
PA14_39090	PA1967	PA1967	hypothetical protein	-2.34	-2.75
PA14_39240	PA1954	fapC	FapC	-2.75	-3.66
PA14_39280	PA1950	rbsK	ribokinase	-2.74	-2.52
PA14_39300	PA1949	rbsR	ribose operon repressor RbsR	-2.28	-1.95
PA14_39320	PA1948	rbsC	membrane protein component of ABC ribose transporter	-2.38	-1.95
PA14_39330	PA1947	rbsA	ribose transport protein RbsA	-11.01	-11.11
PA14_39520	PA1933	PA1933	probable hydroxylase large subunit	2.28	5.60
PA14_39530	PA1932	PA1932	Prob. hydroxylase molybdopterin-containing	2.07	4.87
PA14_39660	PA1921	PA1921	hypothetical protein	3.90	7.38
PA14_39880	-	-	-	2.09	1.67
PA14_39945	PA1901	phzC2	phenazine biosynthesis protein PhzC	1.89	1.60
PA14_39945	PA4212	phzC1	phenazine biosynthesis protein PhzC	1.89	1.60
PA14_39960	PA1900	phzB2	probable phenazine biosynthesis protein	2.05	1.67
PA14_39970	PA1899	phzA2	probable phenazine biosynthesis protein	2.19	2.00
PA14_39980	PA1898	qscR	quorum-sensing control repressor	-3.43	-3.40
PA14_39990	PA1897	PA1897	hypothetical protein	-6.91	-7.42
PA14_40010	PA1896	PA1896	hypothetical protein	-7.13	-6.78
PA14_40020	PA1895	PA1895	hypothetical protein	-6.30	-5.31
PA14_40030	PA1894	PA1894	hypothetical protein	-4.49	-5.42
PA14_40040	PA1893	PA1893	hypothetical protein	-5.86	-5.78
PA14_40050	PA1892	PA1892	hypothetical protein	-5.56	-5.11
PA14_40060	PA1891	PA1891	hypothetical protein	-7.63	-6.31
PA14_40080	PA1889	PA1889	hypothetical protein	1.90	2.71
PA14_40110	PA1887	PA1887	hypothetical protein	-2.19	-2.33
PA14_40250	PA1875	PA1875	probable outer membrane protein precursor	-1.74	-1.88
PA14_40260	PA1874	PA1874	hypothetical protein	-1.75	-1.89
PA14_40290	PA1871	lasA	LasA protease precursor	2.22	2.45
PA14_40300	PA1870	PA1870	hypothetical protein	1.92	3.38
PA14_40770	PA1838	cysI	sulfite reductase	1.72	1.54
PA14_40820	-	-	-	-2.04	
PA14_40850	PA1831	PA1831	hypothetical protein	1.65	
PA14_41090	PA1812	mltD	membrane-bound lytic murein transglycosylase D precursor	2.00	1.90
PA14_41110	PA1811	nppA1	NppA1	1.70	

PA14_41480	PA1786	nasS	NasS	-91.2	-121
PA14_41490	PA1785	nasT	NasT	-83.4	-92.8
PA14_41500	PA1784	PA1784	hypothetical protein	-2.38	-3.35
PA14_41510	PA1783	nasA	nitrate transporter	-162	-651
PA14_41520	PA1782	PA1782	probable serine/threonine-protein kinase	-96.4	-151
PA14_41530	PA1781	nirB	assimilatory nitrite reductase large subunit	-50.4	-137
PA14_41540	PA1780	nirD	assimilatory nitrite reductase small subunit	-64.2	-340
PA14_41560	PA1779	PA1779	assimilatory nitrate reductase	-39.9	-90.0
PA14_41563	PA1778	cobA	uroporphyrin-III C-methyltransferase	-25.4	-36.8
PA14_41690	PA1768	PA1768	hypothetical protein	2.15	
PA14_41730	PA1766	PA1766	hypothetical protein	1.54	1.55
PA14_41780	PA1762	PA1762	hypothetical protein	-2.06	-2.14
PA14_41790	PA1761	PA1761	hypothetical protein	-1.93	-1.97
PA14_41800	PA1760	PA1760	probable transcriptional regulator	-2.07	-1.96
PA14_41840	PA1756	cysH	3'-phosphoadenosine-5'-phosphosulfate reductase	1.72	1.59
PA14_41920	PA1750	PA1750	phospho-2-dehydro-3-deoxyheptonate aldolase	1.59	
PA14_42100	PA1735	PA1735	hypothetical protein	-3.82	-2.85
PA14_42130	PA1733	PA1733	conserved hypothetical protein	-3.11	-2.30
PA14_42140	PA1732	PA1732	conserved hypothetical protein	-4.20	-2.38
PA14_42150	PA1731	PA1731	conserved hypothetical protein	-4.76	-2.83
PA14_42160	PA1730	PA1730	conserved hypothetical protein	-5.29	-3.25
PA14_42180	PA1729	PA1729	conserved hypothetical protein	-1.69	-1.87
PA14_42200	PA1728	PA1728	hypothetical protein	-1.92	-2.11
PA14_42270	PA1723	pscJ	type III export protein PscJ	2.51	4.39
PA14_42280	PA1722	pscI	type III export protein PscI	2.98	4.17
PA14_42290	PA1721	pscH	type III export protein PscH	3.24	4.79
PA14_42300	PA1720	pscG	type III export protein PscG	3.57	5.10
PA14_42310	PA1719	pscF	type III export protein PscF	5.39	5.91
PA14_42320	PA1718	pscE	type III export protein PscE	5.19	7.50
PA14_42350	PA1716	pscC	Type III secretion outer membrane protein PscC precursor	3.03	4.88
PA14_42380	PA1714	exsD	ExsD	2.54	4.04
PA14_42390	PA1713	exsA	transcriptional regulator ExsA	2.15	2.76
PA14_42400	PA1712	exsB	exoenzyme S synthesis protein B	2.10	2.37
PA14_42440	PA1709	popD	Translocator outer membrane protein PopD precursor	7.22	11.7
PA14_42450	PA1708	popB	translocator protein PopB	7.54	12.8
PA14_42460	PA1707	pcrH	regulatory protein PcrH	6.95	9.44
PA14_42470	PA1706	pcrV	type III secretion protein PcrV	4.48	7.72
PA14_42480	PA1705	pcrG	regulator in type III secretion	4.60	8.69
PA14_42500	PA1703	pcrD	type III secretory apparatus protein PcrD	2.70	3.75
PA14_42510	PA1702	pcr4	Pcr4	7.36	14.8
PA14_42520	PA1701	pcr3	Pcr3	6.22	11.7
PA14_42550	PA1698	popN	Type III secretion outer membrane protein PopN precursor	5.38	9.13
PA14_42570	PA1697	PA1697	ATP synthase in type III secretion system	4.50	7.93
PA14_42580	PA1696	pscO	translocation protein in type III secretion	7.97	16.0
PA14_42600	PA1695	pscP	translocation protein in type III secretion	6.67	10.7
PA14_42610	PA1694	pscQ	translocation protein in type III secretion	7.22	12.0
PA14_42620	PA1693	pscR	translocation protein in type III secretion	12.58	20.71
PA14_42640	PA1691	pscT	translocation protein in type III secretion	5.68	9.16

PA14_42660	PA1690	pscU	translocation protein in type III secretion	3.45	6.19
PA14_43110	PA1655	PA1655	probable glutathione S-transferase	1.69	
PA14_43130	PA1654	PA1654	probable aminotransferase	1.51	
PA14_43160	PA1651	PA1651	probable transporter	-1.89	-2.12
PA14_43220	PA1646	PA1646	probable chemotaxis transducer	-2.79	-2.19
PA14_43420	PA1631	PA1631	probable acyl-CoA dehydrogenase	-1.68	-1.54
PA14_43570	PA1620	PA1620	hypothetical protein	-2.42	-3.17
PA14_43580	PA1619	PA1619	probable transcriptional regulator	-2.18	-2.41
PA14_43900	-	-	-	3.14	4.47
PA14_44060	PA1581	sdhC	succinate dehydrogenase (C subunit)	2.71	1.91
PA14_44240	PA1566	pauA3	Glutamylpolyamine synthetase	-42.6	-42.0
PA14_44260	PA1565	pauB2	FAD-dependent oxidoreductase	-23.4	-24.3
PA14_44620	PA1533	PA1533	conserved hypothetical protein	1.91	2.19
PA14_44710	PA1524	xdhA	xanthine dehydrogenase	-1.94	-2.48
PA14_44740	PA1523	xdhB	xanthine dehydrogenase	-1.73	-2.01
PA14_44760	PA1522	PA1522	hypothetical protein	-1.76	-1.87
PA14_44850	PA1515	alc	allantoicase	-2.10	-1.70
PA14_44960	PA1506	PA1506	hypothetical protein	-1.86	
PA14_45120	PA1492	PA1492	hypothetical protein	-2.81	-2.11
PA14_45130	PA1491	PA1491	probable transporter	-2.52	-2.70
PA14_45400	PA1474	PA1474	hypothetical protein	-1.67	-1.65
PA14_45460	PA1467	PA1467	hypothetical protein	-2.27	-1.96
PA14_45480	PA1465	PA1465	hypothetical protein	-2.18	
PA14_45510	PA1463	PA1463	hypothetical protein	-1.58	
PA14_45560	PA1460	motC	MotC	-1.92	-1.69
PA14_45580	PA1459	PA1459	probable methyltransferase	-1.69	-1.56
PA14_45660	PA1453	flhF	flagellar biosynthesis protein FlhF	-2.00	-1.58
PA14_45780	PA1445	fliO	flagellar protein FliO	-1.70	-1.58
PA14_45830	PA1441	PA1441	putative flagellar hook-length control protein FliK	-2.69	-2.20
PA14_46100	PA1419	PA1419	probable transporter	-2.13	-2.95
PA14_46120	PA1417	PA1417	probable decarboxylase	-2.32	-2.44
PA14_46140	PA1416	PA1416	conserved hypothetical protein	-2.22	
PA14_46250	PA1407	PA1407	hypothetical protein	1.96	2.55
PA14_46280	PA1404	PA1404	hypothetical protein	2.99	3.52
PA14_46290	PA1403	PA1403	probable transcriptional regulator	-1.90	
PA14_46750	PA1356	PA1356	hypothetical protein	-1.76	-2.14
PA14_46810	PA1351	PA1351	probable sigma-70 factor, ECF subfamily	-1.73	-1.95
PA14_46910	PA1342	aatJ	AatJ	-2.00	-2.40
PA14_46920	PA1341	aatQ	AatQ	-2.42	-2.57
PA14_46930	PA1340	aatM	AatM	-2.43	-2.66
PA14_46950	PA1339	aatP	AatP	-2.49	-2.76
PA14_46960	PA1338	ggt	gamma-glutamyltranspeptidase precursor	-3.05	-3.18
PA14_46970	PA1337	ansB	glutaminase-asparaginase	-2.21	-2.95
PA14_46980	PA1336	aauS	AauS	-1.78	-1.82
PA14_46990	PA1335	aauR	AauR	-2.20	-1.97
PA14_47090	PA1327	PA1327	probable protease	-1.57	-1.95
PA14_47100	PA1326	ilvA2	threonine dehydratase, biosynthetic	-3.84	-3.45
PA14_47150	PA1321	cyoE	cytochrome o ubiquinol oxidase protein CyoE	2.92	3.96
PA14_47160	PA1320	cyoD	cytochrome o ubiquinol oxidase subunit IV	2.83	3.79
PA14_47180	PA1319	cyoC	cytochrome o ubiquinol oxidase subunit III	4.06	5.70
PA14_47190	PA1318	cyoB	cytochrome o ubiquinol oxidase subunit I	4.77	5.88

PA14_47210	PA1317	cyoA	cytochrome o ubiquinol oxidase subunit II	5.79	6.54
PA14_47920	PA1260	lhpP	ABC transporter periplasmic-binding protein, LhpP	-8.56	-9.82
PA14_47930	PA1259	lhpH	LhpH	-16.9	-9.67
PA14_47970	PA1255	lhpK	D-hydroxyproline epimerase, LhpK	-3.90	-2.74
PA14_48000	PA1254	lhpC	delta1-pyrroline-4-hydroxy-2-carboxylate deaminase, LphC	-4.63	-3.92
PA14_48020	PA1252	dpkA	DpkA	-2.79	-1.79
PA14_48530	PA1221	PA1221	hypothetical protein	2.06	1.96
PA14_48540	PA1220	PA1220	hypothetical protein	1.63	1.70
PA14_48550	PA1219	PA1219	hypothetical protein	2.13	1.81
PA14_48560	PA1218	PA1218	hypothetical protein	2.65	2.24
PA14_48570	PA1217	PA1217	probable 2-isopropylmalate synthase	2.72	2.61
PA14_48590	PA1216	PA1216	hypothetical protein	2.55	2.14
PA14_48600	PA1215	PA1215	hypothetical protein	2.00	1.75
PA14_48630	PA1212	PA1212	probable major facilitator superfamily (MFS) transporter	1.95	1.62
PA14_48840	PA1195	ddaH	dimethylarginine dimethylaminohydrolase DdaH	-3.62	-4.40
PA14_48860	PA1193	PA1193	hypothetical protein	1.53	2.03
PA14_48940	PA0723	coaB	coat protein B of bacteriophage Pf1	-1.74	
PA14_48950	PA0722	PA0722	hypothetical protein of bacteriophage Pf1	2.33	2.34
PA14_49220	PA1176	napF	ferredoxin protein NapF	-2.22	-2.29
PA14_49300	PA1169	PA1169	probable lipoxygenase	3.91	3.47
PA14_49310	PA1168	PA1168	hypothetical protein	4.39	2.98
PA14_50080	PA1105	fliJ	flagellar protein FliJ	-1.79	
PA14_50100	PA1104	fliI	flagellum-specific ATP synthase FliI	-1.74	-1.61
PA14_50130	PA1102	fliG	flagellar motor switch protein FliG	-1.57	
PA14_50140	PA1101	fliF	Flagella M-ring outer membrane protein precursor	-2.55	-1.97
PA14_50250	PA1095	PA1095	hypothetical protein	-1.70	
PA14_50300	PA1091	fgtA	flagellar glycosyl transferase, FgtA	-1.74	-1.67
PA14_50320	PA1089	PA1089	conserved hypothetical protein	-1.87	-1.77
PA14_50330	PA1088	PA1088	hypothetical protein	-2.11	-1.87
PA14_50340	PA1087	flgL	flagellar hook-associated protein type 3 FlgL	-1.84	-1.66
PA14_50360	PA1086	flgK	flagellar hook-associated protein 1 FlgK	-2.30	-2.05
PA14_50380	PA1085	flgJ	flagellar protein FlgJ	-2.45	-2.08
PA14_50410	PA1084	flgI	flagellar P-ring protein precursor FlgI	-2.99	-2.26
PA14_50420	PA1083	flgH	flagellar L-ring protein precursor FlgH	-2.35	-1.94
PA14_50430	PA1082	flgG	flagellar basal-body rod protein FlgG	-1.91	-1.90
PA14_50440	PA1081	flgF	flagellar basal-body rod protein FlgF	-2.71	-2.05
PA14_50520	PA1074	braC	branched-chain amino acid transport protein BraC	-2.17	-2.32
PA14_50530	PA1073	braD	branched-chain amino acid transport protein BraD	-2.92	-2.94
PA14_50540	PA1072	braE	branched-chain amino acid transport protein BraE	-3.02	-3.40
PA14_50550	PA1071	braF	branched-chain amino acid transport protein BraF	-3.34	-3.58
PA14_50560	PA1070	braG	branched-chain amino acid transport protein BraG	-3.73	-3.74
PA14_50640	PA1063	PA1063	hypothetical protein	-2.25	
PA14_50670	PA1060	PA1060	hypothetical protein	-2.14	-1.97
PA14_50860	PA1043	PA1043	hypothetical protein	-1.51	-1.64
PA14_50880	PA1041	PA1041	probable outer membrane protein precursor	-2.00	-2.56
PA14_50950	PA1034	PA1034	hypothetical protein	2.04	
PA14_51040	PA1028	amaA	L-Pipecolate oxidase	-2.57	-2.70
PA14_51170	PA1017	pauA	pimeloyl-CoA synthetase	-2.30	

PA14_51520	-	-	-	2.09	2.91
PA14_51530	-	-	-	4.15	6.06
PA14_51720	PA0972	tolB	TolB protein	2.35	2.11
PA14_51730	PA0971	tolA	TolA protein	1.61	2.58
PA14_51830	PA0962	dps	DNA-binding protein from starved cells, Dps	2.19	2.58
PA14_51840	PA0961	PA0961	probable cold-shock protein	1.85	1.78
PA14_51850	PA0960	PA0960	hypothetical protein	-1.65	-1.66
PA14_51860	PA0959	PA0959	hypothetical protein	-1.74	-1.97
PA14_51880	PA0958	oprD	Basic amino acid, basic peptide and imipenem outer membrane porin OprD precursor	-4.06	-5.67
PA14_52050	PA0944	purN	phosphoribosylaminoimidazole synthetase	1.72	
PA14_52120	-	-	-	2.11	2.25
PA14_52290	PA0925	PA0925	hypothetical protein	1.97	1.88
PA14_52350	PA0920	PA0920	alanyl-phosphatidylglycerol synthase	1.81	2.54
PA14_52580	PA0904	lysC	aspartate kinase alpha and beta chain	1.54	
PA14_52660	PA0899	aruB	N2-Succinylarginine dihydrolase	-1.54	-1.57
PA14_52840	PA0884	PA0884	probable C4-dicarboxylate-binding periplasmic protein	-3.25	-1.91
PA14_52850	PA0883	PA0883	probable acyl-CoA lyase beta chain	-14.9	-5.11
PA14_52870	PA0882	PA0882	hypothetical protein	-6.94	-4.42
PA14_52880	PA0881	PA0881	hypothetical protein	-8.73	-3.06
PA14_52900	PA0879	PA0879	probable acyl-CoA dehydrogenase	-4.33	-4.01
PA14_53140	PA0861	rbdA	RbDA	-1.60	-1.80
PA14_53160	PA0859	PA0859	hypothetical protein	-1.86	-1.51
PA14_53250	PA0852	cbpD	chitin-binding protein CbpD precursor	2.27	1.89
PA14_53250	PA0852	PA0852	Uncharacterized protein	2.27	1.89
PA14_53400	PA0840	PA0840	probable oxidoreductase	-1.98	
PA14_53770	PA0812	PA0812	hypothetical protein	-2.02	-2.04
PA14_53790	PA0810	PA0810	probable haloacid dehalogenase	-1.60	-1.67
PA14_54080	PA0788	PA0788	hypothetical protein	-1.76	-2.00
PA14_54400	PA0765	mucC	positive regulator for alginate biosynthesis MucC	1.76	2.47
PA14_54630	PA0746	PA0746	probable acyl-CoA dehydrogenase	-1.61	-1.62
PA14_54670	PA0743	PA0743	probable 3-hydroxyisobutyrate dehydrogenase	-1.51	-1.72
PA14_54820	PA0731	PA0731	hypothetical protein	1.58	
PA14_54830	PA0730	PA0730	probable transferase	-6.41	-7.66
PA14_55660	PA4283	recD	exodeoxyribonuclease V alpha chain	-1.70	
PA14_55760	PA4291	PA4291	hypothetical protein	1.72	
PA14_55790	PA4294	PA4294	hypothetical protein	-1.71	-1.98
PA14_55840	PA4298	PA4298	hypothetical protein	-2.59	-2.97
PA14_55850	PA4299	tadD	TadD	-2.22	-2.38
PA14_55880	PA4301	tadB	TadB	-2.66	-2.54
PA14_55890	PA4302	tadA	TadA ATPase	-2.35	-2.45
PA14_55900	PA4303	tadZ	TadZ	-2.48	-2.95
PA14_55920	PA4304	rcpA	RcpA	-2.36	-2.71
PA14_55930	PA4305	rcpC	RcpC	-2.58	-2.65
PA14_55960	PA4307	pctC	chemotactic transducer PctC	-1.63	-1.95
PA14_56000	PA4309	pctA	chemotactic transducer PctA	-1.61	
PA14_56300	PA4333	PA4333	probable fumarase	2.00	2.13
PA14_56430	PA4341	PA4341	probable transcriptional regulator	-10.8	-8.71
PA14_56450	PA4342	PA4342	probable amidase	-1.85	
PA14_56470	PA4343	PA4343	probable major facilitator superfamily (MFS)	-3.35	

			transporter		
PA14_56770	PA4365	lysE	Lysine efflux permease	-5.08	-3.99
PA14_57060	PA4390	PA4390	hypothetical protein	2.51	4.35
PA14_57110	PA4394	PA4394	conserved hypothetical protein	1.75	3.61
PA14_57720	PA4443	cysD	ATP sulfurylase small subunit	1.77	1.72
PA14_57730	PA4444	mltB1	soluble and membrane-bound lytic transglycosylases	1.55	
PA14_58030	PA4470	fumC1	fumarate hydratase	-2.84	-2.31
PA14_58150	PA4481	mreB	rod shape-determining protein MreB	1.58	1.51
PA14_58220	PA4486	PA4486	conserved hypothetical protein	1.86	1.81
PA14_58350	PA4496	dppA1	probable binding protein component of ABC transporter	-2.68	-3.35
PA14_58360	PA4497	dppA2	probable binding protein component of ABC transporter	-2.87	-3.65
PA14_58410	PA4501	opdD	Glycine-glutamate dipeptide porin OpdP	-12.66	-11.76
PA14_58420	PA4502	dppA4	Prob. binding protein component of ABC transporter	-6.69	-6.87
PA14_58440	PA4503	dppB	dipeptide ABC transporter permease DppB	-6.76	-6.82
PA14_58450	PA4504	dppC	dipeptide ABC transporter permease DppC	-6.22	-6.49
PA14_58470	PA4505	dppD	dipeptide ABC transporter ATP-binding protein	-7.04	-7.53
PA14_58490	PA4506	dppF	dipeptide ABC transporter ATP-binding protein	-7.64	-7.67
PA14_58500	PA4507	PA4507	hypothetical protein	-2.76	-2.17
PA14_58510	PA4508	PA4508	probable transcriptional regulator	-3.62	-3.37
PA14_58690	PA4523	PA4523	hypothetical protein	-1.52	
PA14_59470	-	-	-	1.93	1.90
PA14_60230	PA4545	comL	competence protein ComL	1.69	1.60
PA14_60400	PA4563	rpsT	30S ribosomal protein S20	1.67	
PA14_60500	PA4572	fklB	peptidyl-prolyl cis-trans isomerase FklB	-1.96	-2.11
PA14_60570	PA4578	PA4578	hypothetical protein	1.63	
PA14_60630	PA4582	PA4582	conserved hypothetical protein	-2.35	-2.04
PA14_60650	PA4583	PA4583	conserved hypothetical protein	-2.00	-1.82
PA14_60710	PA4588	gdhA	glutamate dehydrogenase	17.23	16.54
PA14_60730	PA4589	PA4589	probable outer membrane protein precursor	1.85	1.69
PA14_60750	PA4590	pra	protein activator	2.52	2.01
PA14_61290	PA4632	PA4632	hypothetical protein	1.56	
PA14_61300	PA4633	PA4633	probable chemotaxis transducer	-1.97	-1.84
PA14_61390	PA4639	PA4639	hypothetical protein	1.93	2.30
PA14_61880	PA4678	rimI	peptide n-acetyltransferase RimI	1.68	1.57
PA14_62240	PA4702	PA4702	hypothetical protein	-2.00	-2.04
PA14_62250	PA4703	PA4703	hypothetical protein	-1.55	-1.82
PA14_62300	PA4708	phuT	Heme-transport protein, PhuT	-1.77	
PA14_62350	PA4710	phuR	Heme/Hemoglobin uptake outer membrane receptor PhuR precursor	1.60	2.16
PA14_62600	PA4731	panD	aspartate 1-decarboxylase precursor	1.97	1.67
PA14_62930	PA4758	carA	carbamoyl-phosphate synthase small chain	1.77	-
PA14_63190	PA4779	PA4779	hypothetical protein	-2.58	-2.29
PA14_63200	PA4780	PA4780	conserved hypothetical protein	-2.81	-2.89
PA14_63210	PA4781	PA4781	cyclic di-GMP phosphodiesterase	-1.84	-1.57
PA14_64270	PA4858	PA4858	conserved hypothetical protein	-118	-211
PA14_64280	PA4859	PA4859	probable permease of ABC transporter	-80.2	-215
PA14_64290	PA4860	PA4860	probable permease of ABC transporter	-137	-327

PA14_64300	PA4861	PA4861	Prob. ATP-binding component of ABC transporter	-78.2	-248
PA14_64310	PA4862	PA4862	Prob. ATP-binding component of ABC transporter	-42.5	-83.3
PA14_64320	PA4863	PA4863	hypothetical protein	-8.11	-7.59
PA14_64335	PA4864	ureD	urease accessory protein	-4.13	-3.91
PA14_64350	PA4865	ureA	urease gamma subunit	-3.37	-3.72
PA14_64360	PA4866	PA4866	conserved hypothetical protein	-4.15	-4.48
PA14_64370	PA4867	ureB	urease beta subunit	-3.80	-4.46
PA14_64390	PA4868	ureC	urease alpha subunit	-3.60	-3.80
PA14_64480	PA4876	osmE	osmotically inducible lipoprotein OsmE	1.92	3.69
PA14_64520	PA4880	PA4880	probable bacterioferritin	2.96	6.44
PA14_64650	PA4891	ureE	urease accessory protein UreE	-5.75	-7.86
PA14_64660	PA4892	ureF	urease accessory protein UreF	-7.79	-6.70
PA14_64670	PA4893	ureG	urease accessory protein UreG	-5.97	-5.89
PA14_64680	PA4894	PA4894	hypothetical protein	-4.44	-5.38
PA14_64770	PA4901	mdlC	benzoylformate decarboxylase	-2.68	
PA14_64850	PA4908	PA4908	hypothetical protein	-24.3	-26.9
PA14_64860	PA4909	PA4909	Prob. ATP-binding component of ABC transporter	-20.3	-20.1
PA14_64870	PA4910	PA4910	branched chain amino acid ABC transporter ATP binding protein	-27.3	-28.5
PA14_64880	PA4911	PA4911	Prob. permease of ABC branched-chain amino acid transporter	-26.2	-30.2
PA14_64890	PA4912	PA4912	branched chain amino acid ABC transporter membrane protein	-23.3	-35.0
PA14_64900	PA4913	PA4913	Prob. binding protein component of ABC transporter	-9.74	-10.6
PA14_64910	PA4914	amaR	transcriptional regulator, AmaR	-1.85	-2.12
PA14_64920	PA4915	PA4915	probable chemotaxis transducer	-1.72	-2.04
PA14_64930	PA4916	nrtR	Nudix-related transcriptional regulator NrtR	-1.66	
PA14_64950	PA4918	pcnA	nicotinamidase, PcnA	-2.99	-2.74
PA14_64990	PA4921	choE	cholinesterase, ChoE	-2.61	-2.02
PA14_65000	PA4922	azu	azurin precursor	2.16	2.08
PA14_65050	PA4926	PA4926	conserved hypothetical protein	-3.12	-3.10
PA14_65060	PA4927	PA4927	conserved hypothetical protein	-6.52	-6.45
PA14_65090	PA4929	PA4929	hypothetical protein	-2.55	-2.77
PA14_65750	PA4974	PA4974	probable outer membrane protein precursor	1.53	
PA14_66340	PA5019	PA5019	conserved hypothetical protein	-1.82	-1.61
PA14_66400	PA5022	PA5022	conserved hypothetical protein	1.79	1.67
PA14_66510	PA5030	PA5030	probable major facilitator superfamily (MFS) transporter	5.88	5.91
PA14_66580	PA5037	PA5037	hypothetical protein	1.54	1.54
PA14_66690	PA5047	PA5047	hypothetical protein	-1.53	
PA14_66820	PA5056	phaC1	poly(3-hydroxyalkanoic acid) synthase 1	-1.74	-1.84
PA14_66830	PA5057	phaD	poly(3-hydroxyalkanoic acid) depolymerase	-1.75	-1.95
PA14_66840	PA5058	phaC2	poly(3-hydroxyalkanoic acid) synthase 2	-2.06	-2.61
PA14_66850	PA5059	PA5059	probable transcriptional regulator	-2.08	-2.61
PA14_67040	PA5075	PA5075	probable permease of ABC transporter	-2.21	-2.18
PA14_67050	PA5076	PA5076	probable binding protein component of ABC transporter	-1.94	-2.07
PA14_67065	PA5077	opgH	OpgH	1.64	2.37
PA14_67090	PA5078	opgG	OpgG	1.95	2.57
PA14_67240	PA5091	hutG	N-formylglutamate amidohydrolase	-2.33	-2.66

PA14_67250	PA5092	hutI	imidazolone-5-propionate hydrolase HutI	-2.90	-2.77
PA14_67260	PA5093	PA5093	probable histidine/phenylalanine ammonia-lyase	-3.25	-3.28
PA14_67270	PA5094	PA5094	probable ATP-binding component of ABC transporter	-2.69	-2.62
PA14_67280	PA5095	PA5095	probable permease of ABC transporter	-4.34	-4.63
PA14_67300	PA5096	PA5096	Prob. binding protein component of ABC transporter	-7.77	-7.27
PA14_67310	PA5097	PA5097	probable amino acid permease	-6.02	-6.21
PA14_67320	PA5098	hutH	histidine ammonia-lyase	-6.38	-7.01
PA14_67340	PA5099	PA5099	probable transporter	-5.05	-4.06
PA14_67350	PA5100	hutU	urocanase	-3.24	-2.83
PA14_67370	PA5101	PA5101	hypothetical protein	-1.96	-2.12
PA14_67380	PA5102	PA5102	hypothetical protein	-2.49	-2.13
PA14_67400	PA5103	puuR	PuuR	-1.72	-2.28
PA14_67510	PA5112	estA	esterase EstA	-1.70	-1.88
PA14_67670	PA5124	ntrB	two-component sensor NtrB	-254	
PA14_67720	PA5128	secB	secretion protein SecB	2.03	1.62
PA14_67770	PA5131	pgm	phosphoglycerate mutase	1.75	2.31
PA14_67840	PA5137	PA5137	hypothetical protein	-2.67	-2.82
PA14_67850	PA5138	PA5138	hypothetical protein	-2.96	-3.25
PA14_68060	PA5152	PA5152	probable ATP-binding component of ABC transporter	-2.61	-3.05
PA14_68070	PA5153	PA5153	amino acid (lysine/arginine/ornithine/histidine/ octopine) ABC transporter periplasmic binding protein	-5.82	-5.96
PA14_68080	PA5154	PA5154	probable permease of ABC transporter	-6.74	-7.18
PA14_68090	PA5155	PA5155	amino acid (lysine/arginine/ornithine/histidine/ octopine) ABC transporter membrane protein	-6.78	-4.87
PA14_68140	PA5160	PA5160	drug efflux transporter	1.83	1.91
PA14_68280	PA5168	dctQ	DctQ	-2.85	-2.05
PA14_68290	PA5169	dctM	DctM	-2.18	-2.54
PA14_68400	PA5178	PA5178	conserved hypothetical protein	2.03	1.92
PA14_68440	PA5181	PA5181	probable oxidoreductase	-1.76	-1.94
PA14_68510	PA5187	PA5187	probable acyl-CoA dehydrogenase	-2.08	-2.22
PA14_68530	PA5188	PA5188	probable 3-hydroxyacyl-CoA dehydrogenase	-2.61	
PA14_68750	PA5205	PA5205	conserved hypothetical protein	1.65	
PA14_69330	PA5251	PA5251	hypothetical protein	1.69	1.77
PA14_69660	PA5276	lppL	Lipopeptide LppL precursor	3.57	
PA14_69795	PA5287	amtB	ammonium transporter AmtB	-15.7	-19.2
PA14_69810	PA5288	glnK	nitrogen regulatory protein P-II 2	-2.68	-2.51
PA14_70100	PA5309	pauB4	FAD-dependent oxidoreductase	-1.67	-1.83
PA14_70120	PA5311	PA5311	probable major facilitator superfamily transporter	-2.39	-2.19
PA14_70160	PA5313	gabT2	Transaminase	-1.88	-1.75
PA14_70190	PA5316	rpmB	50S ribosomal protein L28	1.81	
PA14_70450	PA5337	rpoZ	RNA polymerase omega subunit	1.90	
PA14_70650	PA5352	PA5352	conserved hypothetical protein	-29.0	-14.1
PA14_70670	PA5353	glcF	glycolate oxidase subunit GlcF	-15.6	-20.0
PA14_70680	PA5354	glcE	glycolate oxidase subunit GlcE	-25.5	-16.5
PA14_70690	PA5355	glcD	glycolate oxidase subunit GlcD	-9.09	-8.42
PA14_71000	PA5376	cbcV	CbcV	-1.66	-1.66
PA14_71070	PA5380	gbdR	GbdR	-9.34	-9.10

PA14_71180	PA5390	PA5390	probable peptidic bond hydrolase	-1.94	
PA14_71240	PA5396	PA5396	hypothetical protein	-2.57	-2.70
PA14_71250	PA5397	PA5397	hypothetical protein	-6.10	-6.03
PA14_71260	PA5398	dgcA	DgcA, Dimethylglycine catabolism	-4.22	-4.21
PA14_71280	PA5399	dgcB	DgcB, Dimethylglycine catabolism	-2.66	-2.96
PA14_71300	PA5400	PA5400	probable electron transfer flavoprotein alpha subunit	-4.16	-2.66
PA14_71410	PA5410	gbcA	GbcA	-6.64	-6.33
PA14_71420	PA5411	gbcB	GbcB	-2.77	-2.74
PA14_71460	PA5415	glyA1	serine hydroxymethyltransferase	-4.76	-4.96
PA14_71470	PA5416	soxB	sarcosine oxidase beta subunit	-3.55	-3.57
PA14_71500	PA5418	soxA	sarcosine oxidase alpha subunit	-3.21	-2.52
PA14_71530	PA5420	purU2	formyltetrahydrofolate deformylase	-4.55	-4.11
PA14_71880	PA5444	PA5444	conserved hypothetical protein	-1.64	-1.53
PA14_71940	PA5450	wzt	ABC subunit of A-band LPS efflux transporter	-1.71	-1.66
PA14_71970	PA5452	wbpW	phosphomannose isomerase/GDP-mannose WbpW	-2.19	-1.73
PA14_71990	PA5453	gmd	GDP-mannose 4,6-dehydratase	-1.64	
PA14_72390	PA5484	kinB	KinB	1.69	3.56
PA14_72600	PA5502	PA5502	hypothetical protein	1.52	
PA14_72780	PA5516	pdxY	pyridoxamine kinase	1.51	
PA14_72870	PA5523	PA5523	probable aminotransferase	-2.81	-1.97
PA14_72890	PA5525	PA5525	probable transcriptional regulator	-1.96	-1.85
PA14_72960	PA5530	PA5530	C5-dicarboxylate transporter	13.3	12.4
PA14_73090	PA5542	PA5542	Pseudomonas imipenem beta-lactamase PIB-1	-2.22	-1.90
PA14_73100	PA5543	PA5543	hypothetical protein	-3.39	-2.21
PA14_73110	PA5544	PA5544	conserved hypothetical protein	-2.52	-2.63
PA14_73170	PA5549	glmS	glucosamine--fructose-6-phosphate aminotransferase	4.51	2.59
PA14_73190	PA5550	glmR	GlmR transcriptional regulator	3.79	2.25
PA14_00150	PA0014	PA0014	hypothetical protein		2.37
PA14_00430	PA0034	PA0034	probable two-component response regulator		1.86
PA14_00480	PA0039	PA0039	hypothetical protein		1.68
PA14_01300	PA0106	coxA	cytochrome c oxidase, subunit I		-2.12
PA14_01310	PA0107	PA0107	conserved hypothetical protein		-2.30
PA14_01320	PA0108	coIII	cytochrome c oxidase, subunit III		-2.11
PA14_01350	PA0111	PA0111	hypothetical protein		-2.58
PA14_01380	PA0113	PA0113	probable cytochrome c oxidase assembly factor		-2.56
PA14_01840	PA0149	PA0149	probable sigma-70 factor, ECF subfamily		-3.30
PA14_01900	PA0153	pcaH	protocatechuate 3,4-dioxygenase, beta subunit		1.85
PA14_01940	PA0156	triA	Resistance-Nodulation-Cell Division (RND) triclosan efflux membrane fusion protein, TriA		1.94
PA14_01960	PA0157	triB	Resistance-Nodulation-Cell Division (RND) triclosan efflux membrane fusion protein, TriB		1.85
PA14_01980	PA0159	PA0159	probable transcriptional regulator		1.77
PA14_01990	PA0160	PA0160	hypothetical protein		2.00
PA14_02460	PA0195.1	-	-		-2.81
PA14_02810	PA0229	pcaT	dicarboxylic acid transporter PcaT		2.53
PA14_02830	PA0230	pcaB	3-carboxy-cis,cis-muconate cycloisomerase		1.52
PA14_02840	PA0231	pcaD	beta-ketoadipate enol-lactone hydrolase		2.02
PA14_02850	PA0232	pcaC	gamma-carboxymuconolactone decarboxylase		2.20

PA14_03090	PA0250	PA0250	conserved hypothetical protein		-1.50
PA14_03160	PA0256	PA0256	hypothetical protein		-1.52
PA14_03210	PA0261	PA0261	hypothetical protein		-2.18
PA14_03240	PA0263	hcpC	secreted protein Hcp		-2.16
PA14_03240	PA1512	hcpA	secreted protein Hcp		-2.16
PA14_03240	PA5267	hcpB	secreted protein Hcp		-2.16
PA14_03670	PA0281	cysW	sulfate transport protein CysW		1.93
PA14_03700	PA0283	sbp	sulfate-binding protein precursor		1.57
PA14_03760	PA0287	gpuP	3-guanidinopropionate transport protein		-4.00
PA14_03855	PA0295	PA0295	probable periplasmic polyamine binding protein		-1.61
PA14_04040	PA0309	PA0309	hypothetical protein		2.07
PA14_04330	PA0332	PA0332	hypothetical protein		-1.59
PA14_04340	PA0333	PA0333	hypothetical protein		-1.83
PA14_04510	PA0344	PA0344	hypothetical protein		1.72
PA14_04640	PA0354	PA0354	conserved hypothetical protein		3.07
PA14_04650	PA0355	pfpI	protease PfpI		3.31
PA14_04930	PA0376	rpoH	sigma factor RpoH		1.61
PA14_05020	PA0384	PA0384	hypothetical protein		-1.50
PA14_05050	PA0387	PA0387	conserved hypothetical protein		-1.54
PA14_05190	PA0396	pilU	twitching motility protein PilU		-1.55
PA14_05600	PA0431	PA0431	hypothetical protein		1.55
PA14_05620	PA0432	sahH	S-adenosyl-L-homocysteine hydrolase		1.84
PA14_05650	PA0435	PA0435	hypothetical protein		2.83
PA14_05890	PA0452	PA0452	probable stomatin-like protein		-1.73
PA14_06010	PA0460	PA0460	hypothetical protein		1.74
PA14_06060	PA0463	creB	two-component response regulator CreB		1.55
PA14_06300	PA0483	PA0483	probable acetyltransferase		-1.55
PA14_06390	PA0490	PA0490	hypothetical protein		1.75
PA14_06460	PA0495	PA0495	hypothetical protein		-1.64
PA14_06530	PA0502	PA0502	probable biotin biosynthesis protein bioH		-1.54
PA14_06980	PA0536	PA0536	hypothetical protein		1.84
PA14_06990	PA0537	PA0537	conserved hypothetical protein		1.77
PA14_07110	PA0547	PA0547	probable transcriptional regulator		1.77
PA14_07210	PA0554	PA0554	hypothetical protein		1.92
PA14_07230	PA0555	fda	fructose-1,6-bisphosphate aldolase		2.43
PA14_07340	PA0564	PA0564	probable transcriptional regulator		1.74
PA14_07480	-	-	-		1.70
PA14_07500	PA0575	PA0575	conserved hypothetical protein		-1.65
PA14_07630	PA0585	PA0585	hypothetical protein		-1.84
PA14_07950	PA0610	prtN	transcriptional regulator PrtN		1.64
PA14_08380	PA0653	PA0653	conserved hypothetical protein		1.62
PA14_08420	PA0656	PA0656	probable HIT family protein		-1.52
PA14_08695	PA4276	secE	secretion protein SecE		1.66
PA14_09160	PA4235	ftnA	bacterial ferritin		1.62
PA14_09180	PA4234	uvrA	excinuclease ABC subunit A		1.51
PA14_09200	PA4232	ssb	single-stranded DNA-binding protein		1.52
PA14_09210	PA4231	pchA	salicylate biosynthesis isochorismate synthase		1.63
PA14_09230	PA4229	pchC	pyochelin biosynthetic protein PchC		1.68
PA14_09240	PA4228	pchD	pyochelin biosynthesis protein PchD		1.87
PA14_09660	PA4198	PA4198	probable AMP-binding enzyme		1.88
PA14_10490	PA4134	PA4134	hypothetical protein		-5.84

PA14_10500	PA4133	PA4133	cytochrome c oxidase subunit (cbb3-type)		-5.50
PA14_10560	PA4129	PA4129	hypothetical protein		-1.53
PA14_10770	PA4112	PA4112	probable sensor/response regulator hybrid		-1.82
PA14_11120	PA4080	PA4080	probable response regulator		-1.51
PA14_11900	PA4016	PA4016	hypothetical protein		1.86
PA14_12080	PA4001	sltB1	soluble lytic transglycosylase B		1.64
PA14_12160	PA3992	sltB3	SltB3		1.63
PA14_12610	PA3963	PA3963	probable transporter		2.86
PA14_12710	PA3954	PA3954	hypothetical protein		-1.66
PA14_12840	PA3945	PA3945	conserved hypothetical protein		-1.56
PA14_13200	-	-	-		-1.96
PA14_13210	-	-	-		-1.96
PA14_13410	PA3903	prfC	peptide chain release factor 3		1.50
PA14_13420	PA3902	PA3902	hypothetical protein		2.43
PA14_13580	PA3891	opuCA	OpuC ABC transporter, ATP-binding protein, OpuCA		3.81
PA14_13590	PA3890	opuCB	OpuC ABC transporter, permease protein, OpuCB		4.41
PA14_13600	PA3889	opuCC	OpuC ABC transporter, periplasmic substrate-binding protein, OpuCC		3.12
PA14_13610	PA3888	opuCD	OpuC ABC transporter, permease protein, OpuCD		2.84
PA14_13620	PA3887	nhaP	Na+/H+ antiporter NhaP		-1.83
PA14_13630	-	-	-		2.12
PA14_14100	PA3858	PA3858	probable amino acid-binding protein		-1.61
PA14_14230	PA3848	PA3848	hypothetical protein		-1.51
PA14_14270	PA3846	PA3846	hypothetical protein		-1.79
PA14_15050	PA3791	PA3791	hypothetical protein		3.44
PA14_15080	PA3789	PA3789	hypothetical protein		10.41
PA14_15350	-	-	-		1.52
PA14_15430	PA3867	PA3867	probable DNA invertase		1.59
PA14_15770	PA3762	PA3762	hypothetical protein		1.64
PA14_16020	PA3740	PA3740	hypothetical protein		-1.62
PA14_16350	PA3714	PA3714	probable two-component response regulator		-1.52
PA14_16630	PA3692	lptF	Lipotoxon F, LptF		3.83
PA14_16640	PA3691	PA3691	hypothetical protein		3.53
PA14_16680	PA3688	PA3688	hypothetical protein		-1.78
PA14_17030	PA3659	PA3659	probable aminotransferase		-1.61
PA14_17320	PA3635	eno	enolase		1.61
PA14_17590	PA3612	PA3612	conserved hypothetical protein		2.17
PA14_17600	PA3611	PA3611	hypothetical protein		2.93
PA14_17730	PA3598	PA3598	conserved hypothetical protein		2.98
PA14_18020	PA3578	PA3578	conserved hypothetical protein		-1.68
PA14_18510	PA3544	algE	Alginate production outer membrane protein AlgE precursor		-2.42
PA14_18800	PA3520	PA3520	hypothetical protein		-4.74
PA14_19100	PA3479	rhlA	rhamnosyltransferase chain A		-1.73
PA14_19205	PA3470	PA3470	hypothetical protein		1.51
PA14_19350	PA3461	PA3461	conserved hypothetical protein		5.68
PA14_19360	PA3460	PA3460	probable acetyltransferase		5.08
PA14_19370	PA3459	PA3459	probable glutamine amidotransferase		3.42
PA14_19740	PA3426	PA3426	probable enoyl CoA-hydratase/isomerase		-1.61
PA14_20020	PA3407	hasAp	heme acquisition protein HasAp		-3.30

PA14_20280	PA3386	PA3386	conserved hypothetical protein		-1.79
PA14_20320	PA3383	PA3383	binding protein component of ABC phosphonate transporter		2.78
PA14_20370	PA3379	PA3379	conserved hypothetical protein		3.77
PA14_20560	PA3366	amiE	aliphatic amidase		-1.59
PA14_21190	PA3311	nbdA	NbdA		-1.99
PA14_21510	PA3289	PA3289	hypothetical protein		-1.79
PA14_21670	PA3274	PA3274	hypothetical protein		3.62
PA14_21690	PA3272	PA3272	probable ATP-dependent DNA helicase		1.64
PA14_21830	-	-	-		3.44
PA14_21970	PA3249	PA3249	probable transcriptional regulator		-2.07
PA14_22020	PA3244	minD	cell division inhibitor MinD		1.57
PA14_22400	PA3231	PA3231	hypothetical protein		2.45
PA14_22410	PA3230	PA3230	conserved hypothetical protein		1.99
PA14_22450	PA3227	ppiA	peptidyl-prolyl cis-trans isomerase A		1.91
PA14_22880	-	-	-		2.29
PA14_23360	PA3160	wzz	O-antigen chain length regulator		2.13
PA14_23370	PA3148	wbpI	UDP-N-acetylglucosamine 2-epimerase WbpI		2.05
PA14_23400	-	-	-		1.72
PA14_23420	-	-	-		1.71
PA14_23430	-	-	-		2.00
PA14_23440	-	-	-		1.86
PA14_23450	PA3146	wbpK	probable NAD-dependent epimerase/dehydratase WbpK		1.95
PA14_24140	PA3094	PA3094	probable transcriptional regulator		1.51
PA14_24440	PA3069	PA3069	hypothetical protein		2.46
PA14_24640	PA3050	pyrD	dihydroorotate dehydrogenase		1.55
PA14_24730	PA3043	PA3043	conserved hypothetical protein		1.92
PA14_24740	PA3042	PA3042	hypothetical protein		2.44
PA14_24760	PA3041	PA3041	hypothetical protein		2.38
PA14_24770	PA3040	PA3040	conserved hypothetical protein		2.11
PA14_24970	PA3023	PA3023	conserved hypothetical protein		1.83
PA14_25080	PA3014	faoA	fatty-acid oxidation complex alpha-subunit		1.75
PA14_25250	PA3001	PA3001	probable glyceraldehyde-3-phosphate dehydrogenase		1.96
PA14_25390	PA2991	sth	soluble pyridine nucleotide transhydrogenase		1.54
PA14_25610	PA2972	PA2972	conserved hypothetical protein		1.75
PA14_25820	PA2955	PA2955	hypothetical protein		-1.60
PA14_25880	PA2951	etfA	electron transfer flavoprotein alpha-subunit		1.67
PA14_25920	PA2948	cobM	precorrin-3 methylase		1.74
PA14_25960	PA2945	PA2945	conserved hypothetical protein		1.54
PA14_26070	PA2936	PA2936	hypothetical protein		-3.10
PA14_26080	PA2935	PA2935	hypothetical protein		-3.04
PA14_26600	PA2896	sbrI	SbrI		2.14
PA14_26610	PA2895	sbrR	SbrR		1.76
PA14_26770	PA2884	PA2884	hypothetical protein		1.63
PA14_26780	PA2883	PA2883	hypothetical protein		1.51
PA14_27220	PA2850	ohr	organic hydroperoxide resistance protein		-1.78
PA14_27230	PA2849	ohrR	OhrR		-1.57
PA14_27720	PA2816	PA2816	hypothetical protein		1.93
PA14_27730	PA2815	PA2815	probable acyl-CoA dehydrogenase		3.61

PA14_27810	PA2809	copR	two-component response regulator, CopR		-1.79
PA14_27850	PA2806	PA2806	conserved hypothetical protein		-1.85
PA14_27930	PA2799	PA2799	hypothetical protein		-1.60
PA14_28030	PA2790	PA2790	hypothetical protein		-1.64
PA14_28060	PA2787	cpg2	carboxypeptidase G2 precursor		-1.60
PA14_28110	PA2782	bamI	biofilm-associated metzincin Inhibitor, BamI		-1.91
PA14_28170	PA2777	PA2777	conserved hypothetical protein		1.55
PA14_28240	-	-	-		3.28
PA14_28260	-	-	-		-1.79
PA14_28370	PA2763	PA2763	hypothetical protein		-1.87
PA14_28380	PA2762	PA2762	hypothetical protein		-1.69
PA14_28450	PA2755	eco	ecotin precursor		1.71
PA14_28520	-	-	-		3.00
PA14_28530	PA2751	PA2751	conserved hypothetical protein		2.57
PA14_28750	-	-	-		2.71
PA14_29120	PA2708	PA2708	hypothetical protein		2.42
PA14_29150	PA2706	PA2706	hypothetical protein		1.85
PA14_29160	PA2705	PA2705	hypothetical protein		1.62
PA14_29280	PA2694	trx2	Trx2		2.35
PA14_29330	-	-	-		-2.07
PA14_29820	PA2651	PA2651	conserved hypothetical protein		2.12
PA14_30050	PA2634	aceA	isocitrate lyase AceA		2.10
PA14_30820	PA2573	PA2573	probable chemotaxis transducer		-1.91
PA14_30830	PA2572	PA2572	probable two-component response regulator		-1.74
PA14_30840	PA2571	PA2571	probable two-component sensor		-1.95
PA14_30900	-	-	-		3.98
PA14_30910	-	-	-		3.29
PA14_31290	PA2570	lecA	LecA		-1.79
PA14_31400	PA2561	ctpH	CtpH		1.71
PA14_31530	PA2553	PA2553	probable acyl-CoA thiolase		-1.53
PA14_31610	PA2549	PA2549	conserved hypothetical protein		1.72
PA14_31760	PA2536	PA2536	probable phosphatidate cytidylyltransferase		-1.61
PA14_31870	PA2528	muxA	MuxA		2.19
PA14_31890	PA2527	muxB	MuxB		1.95
PA14_31900	PA2526	muxC	MuxC		1.78
PA14_31920	PA2525	opmB	OpmB		2.32
PA14_32480	PA2486	ptrC	Pseudomonas type III repressor gene C, PtrC		2.97
PA14_32630	PA2475	PA2475	probable cytochrome P450		-1.88
PA14_33480	PA2414	PA2414	L-sorbosone dehydrogenase		4.55
PA14_33500	PA2413	pvdH	L-2,4-diaminobutyrate:2-ketoglutarate 4-aminotransferase, PvdH		2.69
PA14_33580	PA2405	fpvJ	FpvJ		-9.38
PA14_33690	PA2397	pvdE	pyoverdine biosynthesis protein PvdE		-3.35
PA14_33720	PA2394	pvdN	PvdN		-3.97
PA14_33730	PA2393	PA2393	putative dipeptidase		-2.85
PA14_33740	PA2392	pvdP	PvdP		-2.38
PA14_33930	PA2375	PA2375	hypothetical protein		-1.53
PA14_33940	PA2374	tseF	TseF		-1.94
PA14_33960	PA2373	vgrG3	VgrG3		-2.19
PA14_33970	-	-	-		-2.41
PA14_33990	PA2371	clpV3	ClpV3		-2.73

PA14_34000	PA2370	hsiH3	HsiH3		-2.64
PA14_34010	PA2369	hsiG3	HsiG3		-2.80
PA14_34020	PA2368	hsiF3	HsiF3		-2.48
PA14_34030	PA2367	hcp3	Hcp3		-2.08
PA14_34050	PA2366	hsiC3	HsiC3		-2.71
PA14_34070	PA2365	hsiB3	HsiB3		-2.77
PA14_34080	PA2364	lip3	Lip3		-2.24
PA14_34100	PA2363	hsiJ3	HsiJ3		-1.95
PA14_34110	PA2362	dotU3	DotU3		-2.60
PA14_34130	PA2361	icmF3	IcmF3		-2.48
PA14_34140	PA2360	hsiA3	hypothetical protein		-2.22
PA14_34180	PA2357	msuE	NADH-dependent FMN reductase MsuE		-5.45
PA14_34200	PA2355	PA2355	probable FMNH2-dependent monooxygenase		-3.01
PA14_34610	-	-	-		1.66
PA14_34960	PA2291	PA2291	probable glucose-sensitive porin		-1.71
PA14_34970	PA2290	gcd	glucose dehydrogenase		-1.62
PA14_35070	PA2281	PA2281	probable transcriptional regulator		1.90
PA14_35190	PA2272	pbpC	penicillin-binding protein 3A		1.51
PA14_35550	PA2245	pslO	hypothetical protein		2.64
PA14_35570	PA2244	pslN	hypothetical protein		3.28
PA14_35640	PA2239	pslI	PslI		-1.94
PA14_35650	PA2238	pslH	PslH		-1.88
PA14_35670	PA2237	pslG	PslG		-1.72
PA14_35900	-	-	-		-1.65
PA14_36350	PA2189	PA2189	hypothetical protein		4.61
PA14_36370	PA2181	PA2181	hypothetical protein		3.09
PA14_36390	PA2179	PA2179	hypothetical protein		5.44
PA14_36400	-	-	-		2.10
PA14_36410	PA2178	PA2178	hypothetical protein		4.73
PA14_36420	PA2177	PA2177	probable sensor/response regulator hybrid		1.78
PA14_36450	PA2176	PA2176	hypothetical protein		3.66
PA14_36460	PA2175	PA2175	hypothetical protein		3.14
PA14_36500	PA2172	PA2172	hypothetical protein		8.48
PA14_36520	PA2171	PA2171	hypothetical protein		6.16
PA14_36540	PA2168	PA2168	hypothetical protein		3.08
PA14_36550	PA2167	PA2167	hypothetical protein		3.37
PA14_36580	PA2164	PA2164	probable glycosyl hydrolase		4.86
PA14_36590	PA2163	PA2163	hypothetical protein		4.69
PA14_36605	PA2162	PA2162	probable glycosyl hydrolase		4.84
PA14_36620	PA2161	PA2161	hypothetical protein		7.01
PA14_36630	PA2160	PA2160	probable glycosyl hydrolase		6.59
PA14_36650	PA2159	PA2159	conserved hypothetical protein		5.85
PA14_36660	PA2158	PA2158	probable alcohol dehydrogenase (Zn-dependent)		6.59
PA14_36680	PA2156	PA2156	conserved hypothetical protein		5.95
PA14_36700	PA2154	PA2154	conserved hypothetical protein		4.63
PA14_36760	PA2150	PA2150	conserved hypothetical protein		5.96
PA14_36770	PA2149	PA2149	hypothetical protein		5.91
PA14_36780	PA2148	PA2148	conserved hypothetical protein		5.22
PA14_36830	PA2145	PA2145	hypothetical protein		3.34
PA14_36840	PA2144	glgP	glycogen phosphorylase		5.05
PA14_36850	PA2143	PA2143	hypothetical protein		3.36

PA14_36860	-	-	-		-1.91
PA14_36870	PA2142	PA2142	probable short-chain dehydrogenase		6.53
PA14_36880	PA2141	PA2141	hypothetical protein		5.41
PA14_36890	PA2140	PA2140	probable metallothionein		4.06
PA14_36900	-	-	-		3.92
PA14_36930	PA2136	PA2136	hypothetical protein		3.65
PA14_36940	-	-	-		3.51
PA14_36960	PA2135	PA2135	probable transporter		4.90
PA14_37130	PA2122	PA2122	hypothetical protein		-2.62
PA14_37320	PA2109	PA2109	hypothetical protein		1.99
PA14_37340	PA2108	PA2108	probable decarboxylase		4.65
PA14_37380	PA2097	PA2097	probable flavin-binding monooxygenase		-1.79
PA14_37680	PA2075	PA2075	hypothetical protein		-1.84
PA14_37690	PA2072	PA2072	conserved hypothetical protein		-1.55
PA14_38080	PA2044	PA2044	hypothetical protein		1.64
PA14_38370	PA2021	PA2021	hypothetical protein		2.82
PA14_38770	PA1990	pqqH	PqqH		1.55
PA14_38780	PA1989	pqqE	pyrroloquinoline quinone biosynthesis protein E		2.04
PA14_38790	PA1988	pqqD	pyrroloquinoline quinone biosynthesis protein D		1.77
PA14_38800	PA1987	pqqC	pyrroloquinoline quinone biosynthesis protein C		1.97
PA14_38820	PA1986	pqqB	pyrroloquinoline quinone biosynthesis protein B		2.54
PA14_39190	PA1959	bacA	bacitracin resistance protein		1.53
PA14_39270	PA1951	fapF	FapF		-1.71
PA14_39350	PA1946	rbsB	binding protein component precursor of ABC ribose transporter		-1.70
PA14_39540	PA1931	PA1931	probable ferredoxin		1.59
PA14_39560	PA1930	PA1930	probable chemotaxis transducer		-1.65
PA14_39780	PA1914	PA1914	conserved hypothetical protein		-2.01
PA14_39790	PA1913	PA1913	hypothetical protein		-1.88
PA14_40100	PA1888	PA1888	hypothetical protein		-1.81
PA14_40200	PA1880	PA1880	probable oxidoreductase		-1.54
PA14_40240	PA1876	PA1876	probable ATP-binding/permease fusion ABC transporter		-1.85
PA14_40380	PA1864	PA1864	probable transcriptional regulator		-2.71
PA14_40430	PA1860	PA1860	hypothetical protein		-1.76
PA14_40490	PA1857	PA1857	conserved hypothetical protein		1.63
PA14_40570	PA1851	PA1851	hypothetical protein		-1.54
PA14_40750	-	-	-		-2.10
PA14_40840	PA1832	PA1832	probable protease		1.64
PA14_41300	-	-	-		2.17
PA14_41470	PA1787	acnB	aconitate hydratase 2		1.77
PA14_41575	PA1776	sigX	ECF sigma factor SigX		1.60
PA14_41650	PA1771	estX	EstX		1.61
PA14_41710	PA1767	PA1767	hypothetical protein		1.67
PA14_41760	PA1763	PA1763	hypothetical protein		-1.95
PA14_42010	PA1742	pauD2	Glutamine amidotransferase class I		-1.58
PA14_42250	PA1725	pscL	type III export protein PscL		3.52
PA14_42260	PA1724	pscK	type III export protein PscK		4.15
PA14_42340	PA1717	pscD	type III export protein PscD		3.46
PA14_42360	PA1715	pscB	type III export apparatus protein		5.54
PA14_42410	PA1711	exsE	ExsE		2.25

PA14_42430	PA1710	exsC	ExsC, exoenzyme S synthesis protein C precursor.		3.05
PA14_42530	PA1700	pcr2	Pcr2		4.30
PA14_42540	PA1699	pcr1	Pcr1		6.14
PA14_42630	PA1692	PA1692	probable translocation protein in type III secretion		4.10
PA14_43030	PA1658	hsiC2	HsiC2		-1.64
PA14_43040	PA1657	hsiB2	HsiB2		-1.66
PA14_43510	PA1625	PA1625	conserved hypothetical protein		1.80
PA14_43540	PA1622	PA1622	probable hydrolase		-1.69
PA14_43550	PA1621	PA1621	probable hydrolase		-1.69
PA14_43640	PA1614	gpsA	glycerol-3-phosphate dehydrogenase, biosynthetic		1.89
PA14_43670	PA1611	PA1611	hybrid sensor kinase		1.81
PA14_43730	PA1606	PA1606	hypothetical protein		3.98
PA14_43740	PA1605	PA1605	hypothetical protein		2.78
PA14_43840	PA1597	PA1597	hypothetical protein		2.46
PA14_44010	PA1585	sucA	2-oxoglutarate dehydrogenase (E1 subunit)		2.06
PA14_44020	PA1584	sdhB	succinate dehydrogenase (B subunit)		1.68
PA14_44030	PA1583	sdhA	succinate dehydrogenase (A subunit)		2.00
PA14_44050	PA1582	sdhD	succinate dehydrogenase (D subunit)		2.23
PA14_44210	PA1567	PA1567	conserved hypothetical protein		-2.21
PA14_44230	-	-	-		-5.73
PA14_44290	PA1562	acnA	aconitate hydratase 1		2.07
PA14_44640	PA1531	PA1531	hypothetical protein		-1.57
PA14_44770	PA1521	PA1521	probable guanine deaminase		-1.61
PA14_44800	PA1519	PA1519	probable transporter		-2.08
PA14_44890	PA0263	hcpC	secreted protein Hcp		-2.26
PA14_44890	PA1512	hcpA	secreted protein Hcp		-2.26
PA14_44890	PA5267	hcpB	secreted protein Hcp		-2.26
PA14_44950	PA1507	PA1507	probable transporter		2.01
PA14_44980	PA1504	PA1504	probable transcriptional regulator		1.57
PA14_45100	PA1494	muiA	mucoidy inhibitor gene A		3.99
PA14_45260	-	-	-		1.95
PA14_46070	PA1421	gbuA	guanidinobutyrase		-1.85
PA14_46110	PA1418	PA1418	probable sodium:solute symport protein		-2.58
PA14_46230	PA1409	aphA	acetylpolyamine aminohydrolase		1.86
PA14_46240	PA1408	PA1408	hypothetical protein		1.92
PA14_46260	PA1406	PA1406	hypothetical protein		-1.52
PA14_46510	-	-	-		-1.53
PA14_46520	-	-	-		-1.56
PA14_46530	-	-	-		-1.65
PA14_46860	PA1346	PA1346	hypothetical protein		1.84
PA14_47120	PA1324	PA1324	hypothetical protein		4.77
PA14_47130	PA1323	PA1323	hypothetical protein		3.64
PA14_47450	PA1295	PA1295	conserved hypothetical protein		1.96
PA14_47460	PA1294	rnd	ribonuclease D		2.19
PA14_47530	PA1289	PA1289	hypothetical protein		-1.71
PA14_47840	PA1268	lhpA	Hydroxyproline 2-epimerase, LhpA		-2.88
PA14_47850	PA1267	lhpB	D-hydroxyproline dehydrogenase beta-subunit, LphB		-3.88
PA14_47960	PA1256	lhpO	ABC transporter ATP-binding protein, LhpO		-6.15
PA14_48160	PA1243	PA1243	probable sensor/response regulator hybrid		3.59
PA14_48170	PA1242	sprP	SprP		3.46

PA14_49160	PA1181	PA1181	conserved hypothetical protein		-1.68
PA14_49200	PA1178	oprH	PhoP/Q and low Mg2+ inducible outer membrane protein H1 precursor		1.60
PA14_49210	PA1177	napE	periplasmic nitrate reductase protein NapE		-2.27
PA14_49230	PA1175	napD	NapD protein of periplasmic nitrate reductase		-1.64
PA14_49250	PA1174	napA	periplasmic nitrate reductase protein NapA		-1.60
PA14_49270	PA1172	napC	cytochrome c-type protein NapC		-1.59
PA14_49290	PA1170	PA1170	conserved hypothetical protein		1.85
PA14_49360	PA1163	ndvB	NdvB		-1.56
PA14_49940	PA1115	PA1115	hypothetical protein		2.12
PA14_49960	PA1114	PA1114	hypothetical protein		2.54
PA14_50010	PA1112	PA1112	conserved hypothetical protein		1.88
PA14_50020	PA1111	PA1111	hypothetical protein		2.21
PA14_50310	PA1090	PA1090	hypothetical protein		-1.56
PA14_50480	PA1077	flgB	flagellar basal-body rod protein FlgB		-1.53
PA14_50870	PA1042	PA1042	conserved hypothetical protein		-2.04
PA14_51050	PA1027	amaB	delta1-Piperideine-6-carboxylate dehydrogenase		-2.78
PA14_51490	PA0990	PA0990	conserved hypothetical protein		3.19
PA14_51510	PA0988	PA0988	hypothetical protein		1.64
PA14_51740	PA0970	tolR	TolR protein		1.52
PA14_51810	PA0964	pmpR	pqsR-mediated PQS regulator, PmpR		1.52
PA14_51820	PA0963	aspS	aspartyl-tRNA synthetase		1.53
PA14_52230	PA0931	pirA	ferric enterobactin receptor PirA		1.92
PA14_52910	PA0878	PA0878	hypothetical protein		-2.31
PA14_53220	PA0854	fumC2	fumarate hydratase		1.85
PA14_53260	PA0851	PA0851	hypothetical protein		-1.56
PA14_53370	PA0843	plcR	phospholipase accessory protein PlcR precursor		2.74
PA14_53410	PA0839	PA0839	probable transcriptional regulator		-2.14
PA14_53420	PA0838	PA0838	probable glutathione peroxidase		-1.76
PA14_53520	PA0831	oruR	transcriptional regulator OruR		1.53
PA14_53800	PA0809	PA0809	probable transporter		-2.33
PA14_53820	PA0807	ampDh3	AmpDh3		2.03
PA14_54240	PA0776	PA0776	hypothetical protein		-1.79
PA14_54390	PA0766	mucD	serine protease MucD precursor		2.40
PA14_54410	PA0764	mucB	negative regulator for alginate biosynthesis MucB		3.02
PA14_54420	PA0763	mucA	anti-sigma factor MucA		2.77
PA14_54430	PA0762	algU	sigma factor AlgU		2.78
PA14_54730	PA0738	PA0738	conserved hypothetical protein		2.84
PA14_54740	PA0737	PA0737	hypothetical protein		2.41
PA14_54750	-	-	-		1.86
PA14_55000	-	-	-		-3.04
PA14_55220	PA0703	PA0703	probable major facilitator superfamily (MFS) transporter		-1.65
PA14_55780	PA4293	pprA	two-component sensor PprA		-1.94
PA14_55820	PA4297	tadG	TadG		-2.05
PA14_55860	PA4300	tadC	TadC		-2.72
PA14_56030	PA4311	PA4311	conserved hypothetical protein		1.65
PA14_56050	PA4313	PA4313	hypothetical protein		1.58
PA14_56220	PA4328	PA4328	hypothetical protein		-1.52
PA14_56380	PA4337	PA4337	hypothetical protein		1.71
PA14_56390	PA4338	PA4338	hypothetical protein		2.26

PA14_56480	PA4344	PA4344	probable hydrolase		2.02
PA14_56510	PA4345	PA4345	hypothetical protein		2.85
PA14_56660	PA4356	xenB	xenobiotic reductase		2.20
PA14_56750	PA4364	PA4364	hypothetical protein		-3.22
PA14_56780	PA4366	sodB	superoxide dismutase		2.21
PA14_57650	PA4438	PA4438	conserved hypothetical protein		1.53
PA14_57820	PA4451	PA4451	conserved hypothetical protein		1.68
PA14_57990	PA4467	PA4467	hypothetical protein		-2.45
PA14_58050	PA4472	pmbA	PmbA protein		-1.63
PA14_58210	PA4485	PA4485	conserved hypothetical protein		1.91
PA14_58330	PA4495	PA4495	hypothetical protein		2.61
PA14_58375	PA4498	mdpA	metallo-dipeptidase aeruginosa, MdpA		-1.62
PA14_58580	PA4515	PA4515	conserved hypothetical protein		2.32
PA14_58600	PA4516	PA4516	hypothetical protein		1.74
PA14_58800	PA4531	PA4531	hypothetical protein		1.97
PA14_58820	PA4533	PA4533	hypothetical protein		2.13
PA14_58830	PA4534	PA4534	hypothetical protein		2.12
PA14_59180	-	-	-		1.82
PA14_59560	-	-	-		2.31
PA14_60520	PA4573	PA4573	hypothetical protein		-1.98
PA14_60970	PA4608	PA4608	hypothetical protein		-1.57
PA14_61270	PA4630	PA4630	hypothetical protein		-1.88
PA14_61400	PA4640	mqoB	malate:quinone oxidoreductase		1.87
PA14_61410	-	-	-		-1.55
PA14_61580	PA4655	hemH	ferrochelatase		1.65
PA14_61650	PA4661	pagL	Lipid A 3-O-deacylase		2.41
PA14_61770	PA4670	prs	ribose-phosphate pyrophosphokinase		1.57
PA14_61910	PA4680	PA4680	hypothetical protein		-1.94
PA14_61960	PA4684	PA4684	hypothetical protein		1.53
PA14_62260	PA4704	cbpA	cAMP-binding protein A		-1.76
PA14_62680	PA4738	PA4738	conserved hypothetical protein		2.79
PA14_62690	PA4739	PA4739	conserved hypothetical protein		2.98
PA14_62780	PA4746	PA4746	conserved hypothetical protein		1.62
PA14_63250	PA4785	PA4785	probable acyl-CoA thiolase		2.10
PA14_63270	PA4786	PA4786	probable short-chain dehydrogenase		2.32
PA14_63650	PA4815	PA4815	hypothetical protein		2.38
PA14_64050	PA4843	gcbA	GcbA		-1.61
PA14_64080	PA4845	dipZ	thiol:disulfide interchange protein DipZ		1.54
PA14_64430	-	-	-		1.99
PA14_64490	PA4877	PA4877	hypothetical protein		3.11
PA14_64500	PA4878	brlR	BrlR		-1.93
PA14_65720	PA4972	PA4972	hypothetical protein		1.72
PA14_66630	PA5041	pilP	type 4 fimbrial biogenesis protein PilP		-1.61
PA14_66640	PA5042	pilO	type 4 fimbrial biogenesis protein PilO		-1.65
PA14_66650	PA5043	pilN	type 4 fimbrial biogenesis protein PilN		-1.72
PA14_67440	PA5106	PA5106	conserved hypothetical protein		1.55
PA14_67450	PA5107	blc	outer membrane lipoprotein Blc		1.51
PA14_67490	PA5110	fbp	fructose-1,6-bisphosphatase		1.83
PA14_67500	PA5111	gloA3	lactoylglutathione lyase		3.40
PA14_67600	PA5119	glnA	glutamine synthetase		-1.98
PA14_67680	PA5125	ntrC	two-component response regulator NtrC		-241

PA14_68120	PA5158	PA5158	probable outer membrane protein precursor		1.52
PA14_68300	PA5170	arcD	arginine/ornithine antiporter		-1.59
PA14_68330	PA5171	arcA	arginine deiminase		-1.62
PA14_68350	PA5173	arcC	carbamate kinase		-1.58
PA14_68430	PA5180	PA5180	conserved hypothetical protein		-2.02
PA14_68450	-	-	-		1.78
PA14_68460	-	-	-		2.27
PA14_68660	PA5197	rimK	ribosomal protein S6 modification protein		1.57
PA14_68810	PA5209	PA5209	hypothetical protein		2.24
PA14_68840	PA5212	PA5212	hypothetical protein		3.03
PA14_68850	PA5213	gcvP1	glycine cleavage system protein P1		-1.61
PA14_69030	PA5227	PA5227	conserved hypothetical protein		1.71
PA14_69260	PA5245	PA5245	conserved hypothetical protein		1.78
PA14_69270	PA5246	PA5246	conserved hypothetical protein		2.37
PA14_69600	PA5271	PA5271	hypothetical protein		-1.59
PA14_69850	PA5291	betT2	BetT2		2.18
PA14_69925	PA5297	poxB	pyruvate dehydrogenase (cytochrome)		4.67
PA14_69950	PA5299	PA5299	hypothetical protein		1.74
PA14_70040	PA5304	dadA	D-amino acid dehydrogenase, small subunit		-1.56
PA14_70170	PA5314	PA5314	hypothetical protein		-1.69
PA14_70270	PA5322	algC	phosphomannomutase AlgC		1.90
PA14_70280	PA5323	argB	acetylglutamate kinase		1.59
PA14_70740	PA5359	PA5359	hypothetical protein		-1.74
PA14_71310	PA5401	PA5401	hypothetical protein		-3.54
PA14_71400	-	-	-		-2.38
PA14_71490	PA5417	soxD	sarcosine oxidase delta subunit		-4.76
PA14_71510	PA5419	soxG	sarcosine oxidase gamma subunit		-4.19
PA14_71560	PA5421	fdhA	glutathione-independent formaldehyde dehydrogenase		-1.79
PA14_71570	PA5422	PA5422	hypothetical protein		2.14
PA14_71890	PA5445	PA5445	probable coenzyme A transferase		3.38
PA14_71960	PA5451	wzm	membrane subunit of A-band LPS efflux transporter		-1.69
PA14_72060	PA5460	PA5460	hypothetical protein		-2.33
PA14_72090	PA5463	PA5463	hypothetical protein		1.89
PA14_72110	PA5464	PA5464	hypothetical protein		1.69
PA14_72300	PA5477	PA5477	hypothetical protein		1.83
PA14_72380	PA5483	algB	two-component response regulator AlgB		3.71
PA14_72450	PA5489	dsbA	thiol:disulfide interchange protein DsbA		1.85
PA14_72760	PA5514	PA5514	probable beta-lactamase		2.26
PA14_72840	PA5521	PA5521	probable short-chain dehydrogenase		2.10
PA14_72920	PA5527	PA5527	hypothetical protein		-1.82

Table A4. Genes involved in (A) synthesis of virulence factors were downregulated, whereas genes involved in (B) macrophage uptake were upregulated, in NtrBC mutants. Fastq and count files for all samples are available on the NCBI Gene Expression Omnibus (GEO) under accession number GSE145591. Analysis revealed differential expression of genes belonging to the ciprofloxacin resistome that were significantly downregulated in NtrB and/or NtrC mutants relative to PA14 WT. Data are expressed as mean fold-change (FC) values from three biological replicates. Blank cells indicate no change in expression.

PA14 ID	Name	Annotation	FC Δ*ntrB*	FC Δ*ntrC*
A. Synthesis of siderophores and phenazines				
PA14_18020	PA3578	PhzF family phenazine biosynthesis protein		-1.7
PA14_29650	*ppyR*	psl and pyoverdine operon regulator	-4.1	-4.8
PA14_33270	*pvdG*	PvdG	-4.0	-7.6
PA14_33280	*pvdL*	PvdL	-4.3	-6.1
PA14_33530	*fpvF*	FpvF	-2.5	-4.0
PA14_33540	*fpvE*	FpvE	-8.1	-6.5
PA14_33550	*fpvD*	FpvD	-4.6	-6.6
PA14_33560	*fpvC*	FpvC	-3.4	-5.8
PA14_33570	*fpvK*	FpvK	-6.4	-8.0
PA14_33590	*fpvH*	FpvH	-5.5	-5.9
PA14_33600	*fpvG*	FpvG	-2.7	-4.2
PA14_33630	*pvdJ*	PvdJ	-2.4	-2.4
PA14_33650	*pvdD*	pyoverdine synthetase D	-2.1	-2.0
PA14_33680	*fpvA*	ferripyoverdine receptor	-1.9	-2.8
PA14_33690	*pvdE*	pyoverdine biosynthesis protein PvdE		-3.3
PA14_33710	*pvdO*	PvdO	-5.1	-3.7
PA14_33810	*pvdA*	L-ornithine N5-oxygenase	-2.5	-3.5
PA14_33820	*pvdQ*	3-oxo-C12-homoserine lactone acylase PvdQ	-4.1	-5.9
PA14_39980	*qscR*	quorum-sensing control repressor	-3.4	-3.4
B. Macrophage uptake				
PA14_09260	*pchR*	transcriptional regulator PchR	1.7	1.7
PA14_09440	*phzE2*	phenazine biosynthesis protein PhzE	1.9	1.7
PA14_09440	*phzE1*	phenazine biosynthesis protein PhzE	1.9	1.7
PA14_14680	PA3818	extragenic suppressor protein SuhB	1.5	1.5
PA14_14820	*ndk*	nucleoside diphosphate kinase	1.6	
PA14_15970	*rpsP*	30S ribosomal protein S16	1.7	
PA14_20970	PA3331	cytochrome P450	1.7	1.5
PA14_21000	PA3329	hypothetical protein	1.7	
PA14_42250	*pscL*	type III export protein PscL		3.5
PA14_42260	*pscK*	type III export protein PscK		4.2
PA14_42270	*pscJ*	type III export protein PscJ	2.5	4.4
PA14_42280	*pscI*	type III export protein PscI	3.0	4.2
PA14_42290	*pscH*	type III export protein PscH	3.2	4.8
PA14_42340	*pscD*	type III export protein PscD		3.5
PA14_42350	*pscC*	Type III secretion outer membrane protein PscC	3.0	4.9

		precursor		
PA14_42360	*pscB*	type III export apparatus protein		5.5
PA14_42380	*exsD*	ExsD	2.5	4.0
PA14_42430	*exsC*	ExsC, exoenzyme S synthesis protein C precursor.		3.0
PA14_42440	*popD*	Translocator outer membrane protein PopD precursor	7.2	11.7
PA14_42450	*popB*	translocator protein PopB	7.5	12.7
PA14_42460	*pcrH*	regulatory protein PcrH	7.0	9.4
PA14_42470	*pcrV*	type III secretion protein PcrV	4.5	7.7
PA14_42480	*pcrG*	regulator in type III secretion	4.6	8.7
PA14_42500	*pcrD*	type III secretory apparatus protein PcrD	2.7	3.8
PA14_42520	*pcr3*	Pcr3	6.2	11.7
PA14_42550	*popN*	Type III secretion outer membrane protein PopN precursor	5.4	9.1
PA14_42570	PA1697	ATP synthase in type III secretion system	4.5	7.9
PA14_42660	*pscU*	translocation protein in type III secretion	3.4	6.2
PA14_52230	*pirA*	ferric enterobactin receptor PirA		1.9
PA14_53250	*cbpD*	chitin-binding protein CbpD precursor	2.3	1.9
PA14_53250	PA0852	Uncharacterized protein	2.3	1.9
PA14_58600	PA4516	hypothetical protein		1.7
PA14_60400	*rpsT*	30S ribosomal protein S20	1.7	
PA14_61770	*prs*	ribose-phosphate pyrophosphokinase		1.6
PA14_62350	*phuR*	Heme/Hemoglobin uptake outer membrane receptor PhuR precursor	1.6	2.2
PA14_62780	PA4746	conserved hypothetical protein		1.6
PA14_72960	PA5530	C5-dicarboxylate transporter	13.3	12.4

Table A5. Primers used for studies described in Chapter 5.

Primer name	Sequence (5' > 3')
Complementation primers	
lasI-fwd	TTTCGCCATCAACTCTGGACA
lasI-rev	CGTACAGTCGGAAAAGCCCA
rhlI-fwd	GTCCATGGCACCTATCCCAA
rhlI-rev	AGACCACCATTTCCGAGGAG
pqsH-fwd	GGGGGGCCCGGTTACCTCTTGCACGCGA
pqsH-rev	GATAAGCTTAGCGACCATCGCCGAAGTC
RT-qPCR primers	
phzA1-fwd	TAAAACGTAATCGCGAGTTCATG
phzA1-rev	TTTTATTTGCGGAACGGCTATT
pyS2-fwd	GCAGCACAAAGTCACCGAAGG
pyS2-rev	CCGTGGGAAACCACTTCAGC
algU-fwd	GATATCGACAATGCCGTTCC
algU-rev	CAGGACTTGCGCTTCTTCTT
pvdS-fwd	GGCAAGTGGGAGGTGAACTA
*pvdS*rev	AAGTACTTGCGCACCGTCTC
lasR-fwd	TCACATTGGCTTCCGAGCAG
lasR-rev	AAACCGGTGGTTCTGACCAG
plcH-fwd	CATGGAATGGGTCAACCTGT
plcH-rev	AGATCGAGGCGTTCTTCTTG

Table A6. FIMO software detected 259 NtrC binding targets in the promoter regions of *P. aeruginosa* coding sequences. Many targets had multiple (two or four) NtrC binding sites, shown as redundant Names with Start and Stop delineating how many bp upstream of the start codon NtrC bound. FIMO calculated the Score for each binding event, as well as *P* and *Q* value. The matched sequence corresponding to NtrC binding motif is shown.

Name	Start	Stop	Score	*P* value	*Q* value	Matched Sequence
PA14_08650	91	105	10.7	7.37E-05	0.626	AAGAGTTTTCTCTTA
PA14_08650	91	105	10.7	7.42E-05	0.626	TAAGAGAAAACTCTT
PA14_21800	87	101	11.9	2.33E-05	0.531	CGGCAGAAAATTTTT
PA14_21800	87	101	11.9	2.47E-05	0.541	AAAAATTTTCTGCCG
PA14_28740	35	49	12.7	1.11E-05	0.44	TAGTATATAGTGCGG
PA14_28740	35	49	12.6	1.13E-05	0.44	CCGCACTATATACTA
PA14_51660	39	53	11.2	4.60E-05	0.608	AGGCGTATAATACTG
PA14_51660	39	53	11.2	4.73E-05	0.608	CAGTATTATACGCCT
PA14_54840	266	280	11.7	2.98E-05	0.563	CAATTTTTCTTCTG
PA14_54840	266	280	11.7	3.01E-05	0.563	CAGAAGAAAAAATTG
PA14_65210	84	98	11.7	2.96E-05	0.563	CAGCAGAATAATTTT
PA14_65210	84	98	11.6	3.06E-05	0.563	AAAATTATTCTGCTG
PA14_00520	386	400	11.5	3.57E-05	0.592	AAATAGTATCTTTTA
PA14_00520	386	400	11.5	3.61E-05	0.592	TAAAAGATACTATTT
PA14_00970	151	165	10.9	6.03E-05	0.608	CAGCGGGTTGTTCTG
PA14_00970	151	165	10.9	6.13E-05	0.608	CAGAACAACCCGCTG
PA14_01840	76	90	10.8	6.53E-05	0.608	AAGCATTATCATTTG
PA14_01840	76	90	10.7	6.93E-05	0.616	CAAATGATAATGCTT
pcaG	152	166	12.1	2.00E-05	0.498	CAGCACATCCTCCTG
pcaG	152	166	12.1	2.03E-05	0.499	CAGGAGGATGTGCTG
cheA	186	200	10.3	9.62E-05	0.653	CAGCGGAATGTTCGG
cheA	186	200	10.3	9.83E-05	0.66	CCGAACATTCCGCTG
PA14_02390	237	251	10.8	6.42E-05	0.608	TCGCATATTTTTCTA
PA14_02390	237	251	10.8	6.53E-05	0.608	TAGAAAAATATGCGA
PA14_02410	100	114	10.8	6.42E-05	0.608	TCGCATATTTTTCTA
PA14_02410	100	114	10.8	6.53E-05	0.608	TAGAAAAATATGCGA
PA14_02450	226	240	10.5	8.48E-05	0.633	CAAAGTTTTGCTTTG
PA14_02450	226	240	10.5	8.62E-05	0.635	CAAAGCAAAACTTTG
PA14_02930	164	178	11.1	4.92E-05	0.608	AAGGAGATTATTTGA
PA14_02930	164	178	11.1	4.96E-05	0.608	TCAAATAATCTCCTT
PA14_03160	270	284	12.6	1.23E-05	0.44	AAGTATTTACTGTTA

PA14_03160	270	284	12.5	1.25E-05	0.44	TAACAGTAAATACTT
PA14_03163	291	305	12.6	1.23E-05	0.44	AAGTATTTACTGTTA
PA14_03163	291	305	12.5	1.25E-05	0.44	TAACAGTAAATACTT
PA14_03310	233	247	11.3	4.18E-05	0.599	CAGGATAACCTTCTC
PA14_03310	233	247	11.3	4.30E-05	0.599	GAGAAGGTTATCCTG
oprE	79	93	10.9	6.08E-05	0.608	CGGTACAATATTCCT
oprE	79	93	10.9	6.08E-05	0.608	AGGAATATTGTACCG
ptsP	164	178	10.5	8.81E-05	0.635	CAGCGTTTCGTCCTG
ptsP	164	178	10.4	8.97E-05	0.635	CAGGACGAAACGCTG
PA14_05500	111	125	14.6	1.06E-06	0.259	AAGCAGAAAATTCTG
PA14_05500	111	125	14.6	1.08E-06	0.259	CAGAATTTTCTGCTT
PA14_05500	108	122	11.0	5.40E-05	0.608	AAGCAGAATTTTCTG
PA14_05500	108	122	11.0	5.49E-05	0.608	CAGAAAATTCTGCTT
PA14_05660	124	138	11.9	2.38E-05	0.539	CAGGAGAATCTTCTC
PA14_05660	124	138	11.9	2.43E-05	0.541	GAGAAGATTCTCCTG
glcB	451	465	11.5	3.54E-05	0.592	AAGAATAAAGCCCTG
glcB	451	465	11.5	3.59E-05	0.592	CAGGGCTTTATTCTT
PA14_07430	528	542	10.7	7.08E-05	0.616	CGGCATATTGTTATG
PA14_07430	528	542	10.6	7.59E-05	0.626	CATAACAATATGCCG
rpoD	24	38	10.7	7.29E-05	0.625	AGGTATAATCCTCTG
rpoD	24	38	10.6	7.79E-05	0.626	CAGAGGATTATACCT
PA14_08330	59	73	11.9	2.40E-05	0.541	AAGAATATGATGCTG
PA14_08330	59	73	11.9	2.43E-05	0.541	CAGCATCATATTCTT
speD	114	128	11.0	5.69E-05	0.608	CGGAAGATTCTTCCG
speD	114	128	11.0	5.69E-05	0.608	CGGAAGAATCTTCCG
PA14_08470	276	290	10.6	8.07E-05	0.626	CAGGACATCCTCTTG
PA14_08470	276	290	10.5	8.11E-05	0.626	CAAGAGGATGTCCTG
argC	1	15	10.6	8.07E-05	0.626	CAGGACATCCTCTTG
argC	1	15	10.5	8.11E-05	0.626	CAAGAGGATGTCCTG
PA14_08640	126	140	14.8	9.22E-07	0.259	CAGAATGTTCTTCTG
PA14_08640	126	140	14.7	9.47E-07	0.259	CAGAAGAACATTCTG
PA14_08640	129	143	14.1	2.13E-06	0.259	CAGCAGAATGTTCTT
PA14_08640	129	143	14.1	2.23E-06	0.259	AAGAACATTCTGCTG
phzA1	551	565	11.4	3.70E-05	0.594	CGAAATTTCATCCTA
phzA1	551	565	11.4	3.75E-05	0.594	TAGGATGAAATTTCG
phzM	131	145	11.4	3.70E-05	0.594	CGAAATTTCATCCTA
phzM	131	145	11.4	3.75E-05	0.594	TAGGATGAAATTTCG

PA14_09570	63	77	14.4	1.45E-06	0.259	AAAAATATTCTTTTA
PA14_09570	63	77	14.4	1.47E-06	0.259	TAAAAGAATATTTTT
PA14_09580	31	45	14.4	1.45E-06	0.259	AAAAATATTCTTTTA
PA14_09580	31	45	14.4	1.47E-06	0.259	TAAAAGAATATTTTT
aph	199	213	10.9	5.98E-05	0.608	AAGCAGGAAGTGCTG
aph	199	213	10.9	5.98E-05	0.608	CAGCACTTCCTGCTT
PA14_10940	363	377	11.0	5.69E-05	0.608	CAGGACATTCCCCTG
PA14_10940	363	377	11.0	5.73E-05	0.608	CAGGGGAATGTCCTG
PA14_12570	289	303	11.1	5.05E-05	0.608	CGACGTATTCTTTTA
PA14_12570	289	303	11.0	5.31E-05	0.608	TAAAAGAATACGTCG
PA14_12890	106	120	10.5	8.55E-05	0.635	CAGGATGTCGTCCTG
PA14_12890	106	120	10.5	8.69E-05	0.635	CAGGACGACATCCTG
PA14_13140	70	84	11.4	3.95E-05	0.599	CAGAAGAATCTTCGT
PA14_13140	70	84	11.4	3.98E-05	0.599	ACGAAGATTCTTCTG
moaE	153	167	10.3	9.55E-05	0.65	CCGGATAATGTTCGA
moaE	153	167	10.3	9.76E-05	0.66	TCGAACATTATCCGG
PA14_13460	44	58	13.1	6.75E-06	0.369	CAGCATAAAATGATA
PA14_13460	44	58	13.1	6.83E-06	0.369	TATCATTTTATGCTG
PA14_13670	7	21	10.8	6.71E-05	0.611	TAGCGGTATCTCCTG
PA14_13670	7	21	10.8	6.76E-05	0.611	CAGGAGATACCGCTA
PA14_13940	293	307	12.4	1.49E-05	0.447	AAGAATAAAACCTTG
PA14_13940	293	307	12.4	1.50E-05	0.447	CAAGGTTTTATTCTT
PA14_13940	246	260	11.0	5.40E-05	0.608	TAAGAGATACTCTTG
PA14_13940	246	260	11.0	5.40E-05	0.608	CAAGAGTATCTCTTA
PA14_14280	235	249	11.2	4.76E-05	0.608	CAGCAGATCAAGCTG
PA14_14280	235	249	11.2	4.76E-05	0.608	CAGCTTGATCTGCTG
PA14_14430	150	164	10.5	8.81E-05	0.635	CAAAATATTTCTTTA
PA14_14430	150	164	10.4	8.92E-05	0.635	TAAAGAAATATTTTG
PA14_14430	277	291	10.4	9.41E-05	0.642	AGGAAAATTATTCTA
PA14_14430	277	291	10.3	9.62E-05	0.653	TAGAATAATTTTCCT
leuA	166	180	12.7	1.07E-05	0.44	CAGAATTTTCCATTG
leuA	166	180	12.7	1.09E-05	0.44	CAATGGAAAATTCTG
PA14_15050	193	207	12.7	1.07E-05	0.44	CAGAATTTTCCATTG
PA14_15050	193	207	12.7	1.09E-05	0.44	CAATGGAAAATTCTG
PA14_15830	68	82	10.7	6.88E-05	0.616	CGGCGTTTTCTTTTA
PA14_15830	68	82	10.7	7.29E-05	0.625	TAAAAGAAAACGCCG
PA14_15850	137	151	13.0	8.02E-06	0.427	TGGCATGAAATTCTG

PA14_15850	137	151	12.9	8.60E-06	0.44	CAGAATTTCATGCCA
PA14_16960	73	87	10.5	8.62E-05	0.635	CAGCAGGTTGTTCGG
PA14_16960	73	87	10.4	8.87E-05	0.635	CCGAACAACCTGCTG
PA14_17000	307	321	10.4	9.28E-05	0.636	CAGCAGAACGCACTG
PA14_17000	307	321	10.4	9.41E-05	0.642	CAGTGCGTTCTGCTG
pyrH	235	249	11.1	5.02E-05	0.608	AAACGCATTCTTCTA
pyrH	235	249	11.1	5.05E-05	0.608	TAGAAGAATGCGTTT
PA14_17250	64	78	10.9	5.94E-05	0.608	TAGCGGAAAGTCCTG
PA14_17250	64	78	10.9	5.98E-05	0.608	CAGGACTTTCCGCTA
pyrG	66	80	10.7	7.37E-05	0.626	CAGGAGTTTGCTTTG
pyrG	66	80	10.6	7.53E-05	0.626	CAAAGCAAACTCCTG
alg8	254	268	11.9	2.33E-05	0.531	AAGGATTTCATCCTG
alg8	254	268	11.9	2.33E-05	0.531	CAGGATGAAATCCTT
argF	20	34	10.9	6.18E-05	0.608	CAGCATAAAGCGTCG
argF	20	34	10.9	6.18E-05	0.608	CGACGCTTTATGCTG
PA14_18620	245	259	10.9	6.18E-05	0.608	CGACGCTTTATGCTG
PA14_18620	245	259	10.9	6.18E-05	0.608	CAGCATAAAGCGTCG
PA14_18960	230	244	10.6	7.66E-05	0.626	CAGTATGATTTTTTA
PA14_18960	230	244	10.6	7.90E-05	0.626	TAAAAAATCATACTG
PA14_19170	219	233	10.9	5.82E-05	0.608	CAGCGTATTCCCCTA
PA14_19170	219	233	10.9	5.98E-05	0.608	TAGGGGAATACGCTG
PA14_19190	225	239	10.9	5.82E-05	0.608	CAGCGTATTCCCCTA
PA14_19190	225	239	10.9	5.98E-05	0.608	TAGGGGAATACGCTG
PA14_19480	55	69	10.6	7.79E-05	0.626	TAATTTATTCTTTTT
PA14_19480	55	69	10.6	7.90E-05	0.626	AAAAAGAATAAATTA
PA14_19490	137	151	10.6	7.79E-05	0.626	TAATTTATTCTTTTT
PA14_19490	137	151	10.6	7.90E-05	0.626	AAAAAGAATAAATTA
PA14_19530	117	131	11.0	5.54E-05	0.608	AAACAGAATATTCGT
PA14_19530	117	131	11.0	5.58E-05	0.608	ACGAATATTCTGTTT
PA14_20510	688	702	11.0	5.31E-05	0.608	CAAGGTTTTCTATTG
PA14_20510	688	702	11.0	5.31E-05	0.608	CAATAGAAAACCTTG
PA14_21020	259	273	11.0	5.44E-05	0.608	CAGAATTAACAGTTA
PA14_21020	259	273	11.0	5.54E-05	0.608	TAACTGTTAATTCTG
PA14_21030	209	223	11.0	5.44E-05	0.608	CAGAATTAACAGTTA
PA14_21030	209	223	11.0	5.54E-05	0.608	TAACTGTTAATTCTG
oprP	166	180	10.5	8.29E-05	0.627	CGGCAGAAACTCTTG
oprP	166	180	10.5	8.75E-05	0.635	CAAGAGTTTCTGCCG

rdgC	64	78	11.9	2.33E-05	0.531	CGGCAGAAAATTTTT
rdgC	64	78	11.9	2.47E-05	0.541	AAAAATTTTCTGCCG
PA14_22075	23	37	10.3	9.95E-05	0.66	CAGCAGGATGTTTCA
PA14_22075	23	37	10.3	9.95E-05	0.66	TGAAACATCCTGCTG
PA14_22130	251	265	11.3	4.27E-05	0.599	TAGAATGAAATCTTC
PA14_22130	251	265	11.3	4.30E-05	0.599	GAAGATTTCATTCTA
PA14_22210	19	33	10.9	5.79E-05	0.608	CGGGATTTTGTGTTT
PA14_22210	19	33	10.9	5.98E-05	0.608	AAACACAAAATCCCG
edd	116	130	11.6	3.08E-05	0.563	TGGCAGATTCTCCTA
edd	116	130	11.6	3.22E-05	0.576	TAGGAGAATCTGCCA
rpsA	173	187	11.3	4.15E-05	0.599	CAGCAAATTGTCCTG
rpsA	173	187	11.3	4.24E-05	0.599	CAGGACAATTTGCTG
orfE	229	243	12.1	2.05E-05	0.5	AAACATAAAAAGCTA
orfE	229	243	12.0	2.07E-05	0.502	TAGCTTTTTATGTTT
PA14_23420	10	24	10.9	5.98E-05	0.608	TGGTTTTATATTTTG
PA14_23420	10	24	10.9	6.24E-05	0.608	CAAAATATAAAACCA
PA14_23430	63	77	12.3	1.57E-05	0.447	AAGCAGATAATATTT
PA14_23430	63	77	12.3	1.57E-05	0.447	AAATATTATCTGCTT
PA14_24770	326	340	10.8	6.49E-05	0.608	AAGGATGAACTGTTG
PA14_24770	326	340	10.8	6.53E-05	0.608	CAACAGTTCATCCTT
PA14_24960	30	44	13.2	6.08E-06	0.344	CAGCAGATAGTTCTT
PA14_24960	30	44	13.2	6.31E-06	0.351	AAGAACTATCTGCTG
PA14_26070	90	104	11.6	3.06E-05	0.563	AAATATATTCCGTTG
PA14_26070	90	104	11.6	3.11E-05	0.563	CAACGGAATATATTT
PA14_26080	286	300	11.6	3.06E-05	0.563	AAATATATTCCGTTG
PA14_26080	286	300	11.6	3.11E-05	0.563	CAACGGAATATATTT
PA14_26150	28	42	10.3	9.89E-05	0.66	TGGCACAATCTACCG
PA14_26150	28	42	10.3	9.95E-05	0.66	CGGTAGATTGTGCCA
PA14_26160	24	38	10.3	9.89E-05	0.66	TGGCACAATCTACCG
PA14_26160	24	38	10.3	9.95E-05	0.66	CGGTAGATTGTGCCA
PA14_26420	272	286	15.0	6.96E-07	0.259	TAGTATAACATTTTA
PA14_26420	272	286	15.0	7.16E-07	0.259	TAAAATGTTATACTA
PA14_26450	351	365	15.0	6.96E-07	0.259	TAGTATAACATTTTA
PA14_26450	351	365	15.0	7.16E-07	0.259	TAAAATGTTATACTA
PA14_26450	753	767	10.9	5.90E-05	0.608	CGGGATAATCTTCGG
PA14_26450	753	767	10.8	6.29E-05	0.608	CCGAAGATTATCCCG
PA14_26730	66	80	12.0	2.13E-05	0.513	TAGCTCATTGTTCTG

PA14_26730	66	80	12.0	2.15E-05	0.514	CAGAACAATGAGCTA
mttC	151	165	12.2	1.74E-05	0.447	TAACGGATTGTTCTA
mttC	151	165	12.2	1.75E-05	0.447	TAGAACAATCCGTTA
PA14_27050	82	96	12.2	1.74E-05	0.447	TAACGGATTGTTCTA
PA14_27050	82	96	12.2	1.75E-05	0.447	TAGAACAATCCGTTA
PA14_27980	82	96	10.8	6.29E-05	0.608	AACTATAAAATTCTT
PA14_27980	82	96	10.8	6.33E-05	0.608	AAGAATTTTATAGTT
PA14_27980	97	111	10.6	7.59E-05	0.626	CAATATTTATTTTTG
PA14_27980	97	111	10.6	7.79E-05	0.626	CAAAAATAAATATTG
PA14_27990	207	221	10.8	6.29E-05	0.608	AACTATAAAATTCTT
PA14_27990	207	221	10.8	6.33E-05	0.608	AAGAATTTTATAGTT
PA14_27990	192	206	10.6	7.59E-05	0.626	CAATATTTATTTTTG
PA14_27990	192	206	10.6	7.79E-05	0.626	CAAAAATAAATATTG
PA14_28280	222	236	10.4	8.97E-05	0.635	CGAAAGATTGTTCTC
PA14_28280	222	236	10.4	9.16E-05	0.636	GAGAACAATCTTTCG
PA14_28370	359	373	11.1	4.88E-05	0.608	TGGAATGAAGTTTTG
PA14_28370	359	373	11.1	5.12E-05	0.608	CAAAACTTCATTCCA
PA14_28400	209	223	12.8	1.01E-05	0.44	CAGAACATTGTTCGA
PA14_28400	209	223	12.7	1.02E-05	0.44	TCGAACAATGTTCTG
PA14_28410	142	156	12.8	1.01E-05	0.44	CAGAACATTGTTCGA
PA14_28410	142	156	12.7	1.02E-05	0.44	TCGAACAATGTTCTG
rplT	63	77	12.3	1.53E-05	0.447	CAGAATTTTCTTGTG
rplT	63	77	12.3	1.57E-05	0.447	CACAAGAAAATTCTG
PA14_28920	85	99	11.3	4.15E-05	0.599	CAGCATATTGCCCCG
PA14_28920	85	99	11.3	4.18E-05	0.599	CGGGGCAATATGCTG
PA14_28990	83	97	10.8	6.65E-05	0.611	AAACAGAAAAATCTG
PA14_28990	83	97	10.8	6.76E-05	0.611	CAGATTTTTCTGTTT
PA14_29410	3	17	12.3	1.54E-05	0.447	AAGCATTACCTGCTG
PA14_29410	3	17	12.3	1.57E-05	0.447	CAGCAGGTAATGCTT
PA14_29575	196	210	11.9	2.45E-05	0.541	TGAAGTAAAATTTTG
PA14_29575	196	210	11.9	2.50E-05	0.542	CAAAATTTTACTTCA
PA14_29575	191	205	11.4	3.81E-05	0.594	AAGTGCAAAATTTTA
PA14_29575	191	205	11.4	3.81E-05	0.594	TAAAATTTTGCACTT
PA14_29590	188	202	10.3	9.83E-05	0.66	AACTATATTGTTCTT
PA14_29750	31	45	11.1	5.05E-05	0.608	CAAGATTTCCTCCTG
PA14_29750	31	45	11.1	5.09E-05	0.608	CAGGAGGAAATCTTG
PA14_30440	293	307	11.5	3.49E-05	0.592	CAGCAGGTACTGTTG

PA14_30440	293	307	11.5	3.52E-05	0.592	CAACAGTACCTGCTG
PA14_30460	176	190	10.6	8.07E-05	0.626	TAGCATATTAAGATA
PA14_30460	176	190	10.5	8.24E-05	0.626	TATCTTAATATGCTA
PA14_30740	427	441	12.6	1.20E-05	0.44	CAGGAGAATGTTTTT
PA14_30740	427	441	12.6	1.22E-05	0.44	AAAAACATTCTCCTG
PA14_31100	341	355	11.0	5.40E-05	0.608	CAGCACGTCGTGCTG
PA14_31100	341	355	11.0	5.40E-05	0.608	CAGCACGACGTGCTG
gcvH2	207	221	11.4	3.66E-05	0.592	CGGGACTTTGTTCTG
gcvH2	207	221	11.4	3.78E-05	0.594	CAGAACAAAGTCCCG
pvdS	564	578	12.6	1.13E-05	0.44	CAACATAATTTGTTG
pvdS	564	578	12.6	1.14E-05	0.44	CAACAAATTATGTTG
pvdG	66	80	12.6	1.13E-05	0.44	CAACATAATTTGTTG
pvdG	66	80	12.6	1.14E-05	0.44	CAACAAATTATGTTG
sndH	127	141	11.0	5.28E-05	0.608	AAGCACTTCCTTCTG
sndH	127	141	11.0	5.40E-05	0.608	CAGAAGGAAGTGCTT
fpvA	27	41	11.4	3.88E-05	0.599	TAGTATGACGTTTTA
fpvA	27	41	11.3	4.04E-05	0.599	TAAAACGTCATACTA
PA14_34070	12	26	14.2	1.97E-06	0.259	CAAAATAAAATTTTC
PA14_34070	12	26	14.2	1.99E-06	0.259	GAAAATTTTATTTTG
PA14_34080	182	196	14.2	1.97E-06	0.259	CAAAATAAAATTTTC
PA14_34080	182	196	14.2	1.99E-06	0.259	GAAAATTTTATTTTG
PA14_34290	27	41	12.7	1.06E-05	0.44	AAGCAGATTCTCCTA
PA14_34290	27	41	12.7	1.08E-05	0.44	TAGGAGAATCTGCTT
PA14_34320	161	175	10.7	6.98E-05	0.616	CAGCAAAAACTGTTG
PA14_34320	161	175	10.7	7.08E-05	0.616	CAACAGTTTTTGCTG
PA14_34330	244	258	10.7	6.98E-05	0.616	CAGCAAAAACTGTTG
PA14_34330	244	258	10.7	7.08E-05	0.616	CAACAGTTTTTGCTG
PA14_34640	14	28	10.6	7.90E-05	0.626	TGGAATTTTGTTTGG
PA14_34640	14	28	10.5	8.24E-05	0.626	CCAAACAAAATTCCA
gntR	167	181	10.6	7.90E-05	0.626	TGGAATTTTGTTTGG
gntR	167	181	10.5	8.24E-05	0.626	CCAAACAAAATTCCA
PA14_34880	123	137	10.9	6.24E-05	0.608	CAGCATAACTTGTTA
PA14_34880	123	137	10.8	6.33E-05	0.608	TAACAAGTTATGCTG
PA14_36560	270	284	13.5	4.72E-06	0.294	AAGAATTTTATTTTC
PA14_36560	270	284	13.4	4.82E-06	0.294	GAAAATAAAATTCTT
glgA	84	98	13.5	4.72E-06	0.294	AAGAATTTTATTTTC
glgA	84	98	13.4	4.82E-06	0.294	GAAAATAAAATTCTT

glgA	369	383	11.4	3.92E-05	0.599	TGGGACATTCTGTTG
glgA	369	383	11.3	4.02E-05	0.599	CAACAGAATGTCCCA
pcoA	257	271	10.6	7.94E-05	0.626	CAGCAGAACCTGCTC
pcoA	257	271	10.6	7.99E-05	0.626	GAGCAGGTTCTGCTG
PA14_38180	111	125	14.1	2.26E-06	0.259	TAGTATTTTATTTTC
PA14_38180	111	125	14.0	2.36E-06	0.259	GAAAATAAAATACTA
PA14_38180	69	83	11.3	4.12E-05	0.599	GGAAATATTGTGTTG
PA14_38180	69	83	11.3	4.18E-05	0.599	CAACACAATATTTCC
PA14_39150	22	36	12.3	1.61E-05	0.447	AAACAGATTGTCCTA
PA14_39150	22	36	12.3	1.63E-05	0.447	TAGGACAATCTGTTT
PA14_39160	112	126	12.3	1.61E-05	0.447	AAACAGATTGTCCTA
PA14_39160	112	126	12.3	1.63E-05	0.447	TAGGACAATCTGTTT
rbsB	26	40	11.5	3.61E-05	0.592	AAGCAAAATATCCTG
rbsB	26	40	11.5	3.64E-05	0.592	CAGGATATTTTGCTT
PA14_39670	14	28	12.3	1.63E-05	0.447	CAACATGATGTGTTT
PA14_39670	14	28	12.3	1.66E-05	0.447	AAACACATCATGTTG
modA	28	42	11.2	4.41E-05	0.608	TGGAATATAGCGCTA
modA	28	42	11.2	4.54E-05	0.608	TAGCGCTATATTCCA
PA14_40790	74	88	13.7	3.62E-06	0.294	TAGAATATTTTTCTA
PA14_40790	74	88	13.7	3.65E-06	0.294	TAGAAAAATATTCTA
PA14_40790	61	75	12.8	9.81E-06	0.44	TAGAATAAATTTCTA
PA14_40790	61	75	12.8	9.90E-06	0.44	TAGAAATTTATTCTA
PA14_40800	35	49	13.7	3.62E-06	0.294	TAGAATATTTTTCTA
PA14_40800	35	49	13.7	3.65E-06	0.294	TAGAAAAATATTCTA
PA14_40800	48	62	12.8	9.81E-06	0.44	TAGAATAAATTTCTA
PA14_40800	48	62	12.8	9.90E-06	0.44	TAGAAATTTATTCTA
PA14_41420	32	46	11.3	4.12E-05	0.599	TCGCATAATGTTTCG
PA14_41420	32	46	11.3	4.15E-05	0.599	CGAAACATTATGCGA
PA14_41430	255	269	11.5	3.57E-05	0.592	CAGCATGACGTCCTG
PA14_41430	255	269	11.4	3.66E-05	0.592	CAGGACGTCATGCTG
pcrV	94	108	11.1	5.21E-05	0.608	CAGCAGTTCCTCCTG
pcrV	94	108	11.0	5.28E-05	0.608	CAGGAGGAACTGCTG
pcrD	43	57	10.8	6.49E-05	0.608	CAGCAGGATGTCCTT
pcrD	43	57	10.8	6.57E-05	0.608	AAGGACATCCTGCTG
pscR	139	153	10.6	7.79E-05	0.626	CGGCGGAATCTGCTG
pscR	139	153	10.6	7.94E-05	0.626	CAGCAGATTCCGCCG
alkA	221	235	10.5	8.75E-05	0.635	CAGCATTTCGCCCTG

alkA	221	235	10.4	9.01E-05	0.635	CAGGGCGAAATGCTG
PA14_43430	194	208	14.3	1.62E-06	0.259	CGAAATATAATTTTG
PA14_43430	194	208	14.3	1.69E-06	0.259	CAAAATTATATTTCG
PA14_43430	138	152	12.3	1.53E-05	0.447	AAGGATTTTATTTTC
PA14_43430	138	152	12.3	1.57E-05	0.447	GAAAATAAAATCCTT
PA14_43430	199	213	11.3	4.27E-05	0.599	TATAATTTTGTTTTA
PA14_43430	199	213	11.3	4.30E-05	0.599	TAAAACAAAATTATA
PA14_43430	32	46	10.6	8.07E-05	0.626	CGAAATATAGTTTCA
PA14_43430	32	46	10.5	8.15E-05	0.626	TGAAACTATATTTCG
PA14_43440	34	48	14.3	1.62E-06	0.259	CGAAATATAATTTTG
PA14_43440	34	48	14.3	1.69E-06	0.259	CAAAATTATATTTCG
PA14_43440	90	104	12.3	1.53E-05	0.447	AAGGATTTTATTTTC
PA14_43440	90	104	12.3	1.57E-05	0.447	GAAAATAAAATCCTT
PA14_43440	29	43	11.3	4.27E-05	0.599	TATAATTTTGTTTTA
PA14_43440	29	43	11.3	4.30E-05	0.599	TAAAACAAAATTATA
PA14_43440	196	210	10.6	8.07E-05	0.626	CGAAATATAGTTTCA
PA14_43440	196	210	10.5	8.15E-05	0.626	TGAAACTATATTTCG
aer	339	353	11.5	3.61E-05	0.592	AAGCATTTACCTCTG
aer	339	353	11.4	3.75E-05	0.594	CAGAGGTAAATGCTT
PA14_44950	502	516	10.6	7.84E-05	0.626	CAAAAAATTACTTTG
PA14_44950	502	516	10.6	7.84E-05	0.626	CAAAGTAATTTTTTG
PA14_45170	109	123	14.1	2.32E-06	0.259	TCACATAAAATTCTG
PA14_45170	109	123	14.0	2.34E-06	0.259	CAGAATTTTATGTGA
PA14_45250	284	298	10.9	6.13E-05	0.608	CAGCAGAATCAATTG
PA14_45250	284	298	10.8	6.33E-05	0.608	CAATTGATTCTGCTG
ccmE	94	108	10.4	8.87E-05	0.635	CAGGTTGATGTTCTG
ccmE	94	108	10.4	8.92E-05	0.635	CAGAACATCAACCTG
cheY	34	48	11.6	3.26E-05	0.577	CCACACATTCTTTTG
cheY	34	48	11.6	3.30E-05	0.581	CAAAAGAATGTGTGG
flhA	82	96	11.3	4.04E-05	0.599	CAAAAGTTTGTTCGG
flhA	82	96	11.3	4.04E-05	0.599	CCGAACAAACTTTTG
lasR	155	169	11.0	5.24E-05	0.608	TCGCATAAAATGTGA
lasR	155	169	11.0	5.28E-05	0.608	TCACATTTTATGCGA
PA14_47420	42	56	11.3	4.15E-05	0.599	CAGTATATTACCTGG
PA14_47420	42	56	11.3	4.27E-05	0.599	CCAGGTAATATACTG
PA14_47430	12	26	11.3	4.15E-05	0.599	CAGTATATTACCTGG
PA14_47430	12	26	11.3	4.27E-05	0.599	CCAGGTAATATACTG

PA14_47440	198	212	13.4	4.77E-06	0.294	GAGAATATTGTTCTT
PA14_47440	198	212	13.4	4.82E-06	0.294	AAGAACAATATTCTC
aprA	148	162	10.4	9.01E-05	0.635	CGGTAGTTTATCTTT
aprA	148	162	10.4	9.22E-05	0.636	AAAGATAAACTACCG
PA14_48140	397	411	10.9	5.76E-05	0.608	CAATATTTTGTGATG
PA14_48140	397	411	10.9	5.82E-05	0.608	CATCACAAAATATTG
PA14_48140	539	553	10.5	8.24E-05	0.626	AAGGATATAACCCTT
PA14_48140	539	553	10.5	8.29E-05	0.627	AAGGGTTATATCCTT
PA14_48140	694	708	10.4	9.28E-05	0.636	CAAAGTATTGAACTG
PA14_48140	694	708	10.4	9.28E-05	0.636	CAGTTCAATACTTTG
PA14_48150	575	589	10.9	5.76E-05	0.608	CAATATTTTGTGATG
PA14_48150	575	589	10.9	5.82E-05	0.608	CATCACAAAATATTG
PA14_48150	433	447	10.5	8.24E-05	0.626	AAGGATATAACCCTT
PA14_48150	433	447	10.5	8.29E-05	0.627	AAGGGTTATATCCTT
PA14_48150	278	292	10.4	9.28E-05	0.636	CAGTTCAATACTTTG
PA14_48150	278	292	10.4	9.28E-05	0.636	CAAAGTATTGAACTG
PA14_48460	64	78	10.5	8.48E-05	0.633	CAGCACTTTCTCTTC
PA14_48460	64	78	10.5	8.75E-05	0.635	GAAGAGAAAGTGCTG
PA14_48530	136	150	12.5	1.30E-05	0.44	CCGCAGAATCTTCTG
PA14_48530	136	150	12.5	1.31E-05	0.44	CAGAAGATTCTGCGG
PA14_48760	409	423	11.1	5.15E-05	0.608	CAGGACGTTGTTCTT
PA14_48760	409	423	11.1	5.18E-05	0.608	AAGAACAACGTCCTG
PA14_48790	4	18	11.6	3.16E-05	0.567	TAAAGTTTTACTTTA
PA14_48790	4	18	11.6	3.16E-05	0.567	TAAAGTAAAACTTTA
PA14_49030	344	358	10.9	5.94E-05	0.608	CGGTTTATAATGTTG
PA14_49030	344	358	10.9	6.03E-05	0.608	CAACATTATAAACCG
PA14_49040	314	328	11.2	4.73E-05	0.608	AAGCTTAAACTTCTA
PA14_49040	314	328	11.1	4.84E-05	0.608	TAGAAGTTTAAGCTT
PA14_49440	417	431	12.8	9.39E-06	0.44	CAAGATAATGCGCTA
PA14_49440	417	431	12.8	9.39E-06	0.44	TAGCGCATTATCTTG
PA14_49440	611	625	11.0	5.40E-05	0.608	CAATATGTAGTGTTT
PA14_49440	611	625	11.0	5.44E-05	0.608	AAACACTACATATTG
nrdA	302	316	12.8	9.39E-06	0.44	TAGCGCATTATCTTG
nrdA	302	316	12.8	9.39E-06	0.44	CAAGATAATGCGCTA
nrdA	108	122	11.0	5.40E-05	0.608	CAATATGTAGTGTTT
nrdA	108	122	11.0	5.44E-05	0.608	AAACACTACATATTG
PA14_49650	14	28	11.5	3.40E-05	0.592	CAACATTTAATTTGT

PA14_49650	14	28	11.5	3.52E-05	0.592	ACAAATTAAATGTTG
PA14_49860	35	49	11.2	4.41E-05	0.608	CAGCATAATGCGTGG
PA14_49860	35	49	11.2	4.57E-05	0.608	CCACGCATTATGCTG
fliC	212	226	13.6	4.03E-06	0.294	CAACATTTTCTTTTT
fliC	212	226	13.5	4.26E-06	0.294	AAAAAGAAAATGTTG
flgF	119	133	10.4	8.92E-05	0.635	TAATACATTGATTTA
flgF	119	133	10.4	9.10E-05	0.636	TAAATCAATGTATTA
PA14_51550	204	218	10.5	8.75E-05	0.635	TAGTAGAATCCGTTT
PA14_51550	204	218	10.5	8.81E-05	0.635	AAACGGATTCTACTA
PA14_51590	129	143	13.5	4.72E-06	0.294	AAGAATATAATTCGA
PA14_51590	129	143	13.4	4.77E-06	0.294	TCGAATTATATTCTT
PA14_52000	11	25	10.9	5.94E-05	0.608	CAGCGGTTTGTTCTT
PA14_52000	11	25	10.9	6.03E-05	0.608	AAGAACAAACCGCTG
PA14_52130	103	117	11.6	3.26E-05	0.577	TAGCATAATGCCTTT
PA14_52130	103	117	11.5	3.40E-05	0.592	AAAGGCATTATGCTA
PA14_52140	179	193	12.3	1.68E-05	0.447	CGGCATAATCTTCCA
PA14_52140	179	193	12.2	1.74E-05	0.447	TGGAAGATTATGCCG
lpxO2	40	54	12.3	1.68E-05	0.447	CGGCATAATCTTCCA
lpxO2	40	54	12.2	1.74E-05	0.447	TGGAAGATTATGCCG
PA14_52890	150	164	10.3	9.89E-05	0.66	CAGGTTGATCTTCTG
PA14_52890	150	164	10.3	9.95E-05	0.66	CAGAAGATCAACCTG
pbpG	234	248	12.6	1.13E-05	0.44	GAGCATAAAATGCTC
pbpG	234	248	12.6	1.13E-05	0.44	GAGCATTTTATGCTC
plcH	58	72	10.7	7.42E-05	0.626	TCACATTTTATTTGA
plcH	58	72	10.6	7.59E-05	0.626	TCAAATAAAATGTGA
oruR	63	77	12.1	2.00E-05	0.498	CAAGGTTATCTTCTG
oruR	63	77	12.1	2.01E-05	0.498	CAGAAGATAACCTTG
PA14_53530	48	62	12.1	2.00E-05	0.498	CAAGGTTATCTTCTG
PA14_53530	48	62	12.1	2.01E-05	0.498	CAGAAGATAACCTTG
PA14_53570	210	224	10.7	7.08E-05	0.616	CAGCACGATCTGCTC
PA14_53570	210	224	10.7	7.13E-05	0.618	GAGCAGATCGTGCTG
PA14_53580	135	149	10.7	7.08E-05	0.616	CAGCACGATCTGCTC
PA14_53580	135	149	10.7	7.13E-05	0.618	GAGCAGATCGTGCTG
PA14_53620	1052	1066	11.0	5.62E-05	0.608	CAGAACGTTCTTCTC
PA14_53620	1052	1066	11.0	5.66E-05	0.608	GAGAAGAACGTTCTG
PA14_53700	29	43	10.6	8.07E-05	0.626	CGAAATATTATGCGC
PA14_53700	29	43	10.5	8.15E-05	0.626	GCGCATAATATTTCG

PA14_53720	58	72	10.6	8.07E-05	0.626	CGAAATATTATGCGC
PA14_53720	58	72	10.5	8.15E-05	0.626	GCGCATAATATTTCG
putA	98	112	11.7	2.98E-05	0.563	TGGGATGTTATATTA
putA	98	112	11.6	3.08E-05	0.563	TAATATAACATCCCA
PA14_54180	352	366	11.7	2.98E-05	0.563	TGGGATGTTATATTA
PA14_54180	352	366	11.6	3.08E-05	0.563	TAATATAACATCCCA
algU	496	510	11.2	4.44E-05	0.608	CAGCACAAGATACTG
algU	496	510	11.2	4.54E-05	0.608	CAGTATCTTGTGCTG
nadB	424	438	12.3	1.65E-05	0.447	CAACACGATGTACTG
nadB	424	438	12.3	1.65E-05	0.447	CAGTACATCGTGTTG
PA14_54610	25	39	11.1	5.18E-05	0.608	CGGGATGTTGTTTTG
PA14_54610	25	39	11.0	5.49E-05	0.608	CAAAACAACATCCCG
PA14_54620	64	78	11.1	5.18E-05	0.608	CGGGATGTTGTTTTG
PA14_54620	64	78	11.0	5.49E-05	0.608	CAAAACAACATCCCG
PA14_54690	35	49	10.3	9.95E-05	0.66	CGGGATAAACCGCTG
PA14_54830	383	397	10.3	9.83E-05	0.66	GAGCATTTTGTATTC
PA14_54850	65	79	11.7	2.98E-05	0.563	CAATTTTTCTTCTG
PA14_54850	65	79	11.7	3.01E-05	0.563	CAGAAGAAAAAATTG
PA14_54850	353	367	11.5	3.46E-05	0.592	CAGCAGATAGCGTTG
PA14_54850	353	367	11.5	3.52E-05	0.592	CAACGCTATCTGCTG
PA14_54860	12	26	10.4	8.97E-05	0.635	TAGAACAACGTTCGA
PA14_54860	12	26	10.4	9.01E-05	0.635	TCGAACGTTGTTCTA
PA14_54890	16	30	11.8	2.59E-05	0.555	CAGCACAATAATTTT
PA14_54890	16	30	11.8	2.69E-05	0.561	AAAATTATTGTGCTG
PA14_55070	506	520	14.0	2.43E-06	0.259	CAGAATAATCTCTTT
PA14_55070	506	520	14.0	2.46E-06	0.259	AAAGAGATTATTCTG
PA14_55080	141	155	14.0	2.43E-06	0.259	CAGAATAATCTCTTT
PA14_55080	141	155	14.0	2.46E-06	0.259	AAAGAGATTATTCTG
PA14_56910	184	198	10.8	6.49E-05	0.608	CAGCAGGATGTCCTT
PA14_56910	184	198	10.8	6.57E-05	0.608	AAGGACATCCTGCTG
murG	4	18	10.7	7.08E-05	0.616	AAAGGTAATGTCCTG
murG	4	18	10.7	7.08E-05	0.616	CAGGACATTACCTTT
rpsI	6	20	10.6	7.72E-05	0.626	CGACATAATGAGCTA
rpsI	6	20	10.6	8.07E-05	0.626	TAGCTCATTATGTCG
PA14_57680	93	107	12.0	2.19E-05	0.518	TGGAGTAATCTGCTA
PA14_57680	93	107	12.0	2.22E-05	0.518	TAGCAGATTACTCCA
PA14_57690	38	52	12.0	2.19E-05	0.518	TGGAGTAATCTGCTA

PA14_57690	38	52	12.0	2.22E-05	0.518	TAGCAGATTACTCCA
PA14_58500	34	48	12.5	1.26E-05	0.44	TGGCAGTAAATTCTA
PA14_58500	34	48	12.5	1.31E-05	0.44	TAGAATTTACTGCCA
PA14_58510	94	108	12.5	1.26E-05	0.44	TGGCAGTAAATTCTA
PA14_58510	94	108	12.5	1.31E-05	0.44	TAGAATTTACTGCCA
PA14_58540	28	42	11.7	2.94E-05	0.563	GAGAATTTACTCCTG
PA14_58540	28	42	11.7	2.94E-05	0.563	CAGGAGTAAATTCTC
lpxO1	88	102	11.7	2.94E-05	0.563	CAGGAGTAAATTCTC
lpxO1	88	102	11.7	2.94E-05	0.563	GAGAATTTACTCCTG
PA14_59220	21	35	10.9	6.13E-05	0.608	GAGTATTTCCTGCTG
PA14_59220	21	35	10.9	6.13E-05	0.608	CAGCAGGAAATACTC
PA14_59230	53	67	10.9	6.13E-05	0.608	CAGCAGGAAATACTC
PA14_59230	53	67	10.9	6.13E-05	0.608	GAGTATTTCCTGCTG
pilL2	205	219	10.9	6.13E-05	0.608	GAGTATTTCCTGCTG
pilL2	205	219	10.9	6.13E-05	0.608	CAGCAGGAAATACTC
PA14_59550	325	339	11.8	2.66E-05	0.559	TGGCATTATCTCTTA
PA14_59550	325	339	11.7	2.87E-05	0.563	TAAGAGATAATGCCA
PA14_59630	53	67	10.5	8.41E-05	0.633	GAGTATTTCCTACTG
PA14_59630	53	67	10.5	8.48E-05	0.633	CAGTAGGAAATACTC
PA14_59640	544	558	10.5	8.41E-05	0.633	GAGTATTTCCTACTG
PA14_59640	544	558	10.5	8.48E-05	0.633	CAGTAGGAAATACTC
PA14_59950	124	138	11.4	3.78E-05	0.594	CAGCAGATTCAACTG
PA14_59950	124	138	11.4	3.88E-05	0.599	CAGTTGAATCTGCTG
PA14_60030	266	280	14.2	1.91E-06	0.259	CCACATAAAATTCTG
PA14_60030	266	280	14.2	1.93E-06	0.259	CAGAATTTTATGTGG
PA14_60030	28	42	13.5	4.32E-06	0.294	TGGCATAATATGCCA
PA14_60030	28	42	13.5	4.32E-06	0.294	TGGCATATTATGCCA
PA14_60040	77	91	13.5	4.32E-06	0.294	TGGCATATTATGCCA
PA14_60040	77	91	13.5	4.32E-06	0.294	TGGCATAATATGCCA
dtd	57	71	11.0	5.73E-05	0.608	TCAAATAAAGTTTTT
dtd	57	71	10.9	5.76E-05	0.608	AAAAACTTTATTTGA
mexC	77	91	10.8	6.53E-05	0.608	TCAAATGATCTTTTG
mexC	77	91	10.8	6.57E-05	0.608	CAAAAGATCATTTGA
nfxB	70	84	10.8	6.53E-05	0.608	TCAAATGATCTTTTG
nfxB	70	84	10.8	6.57E-05	0.608	CAAAAGATCATTTGA
PA14_61150	193	207	13.3	5.32E-06	0.305	TAAAATTAACTCCTG
PA14_61150	193	207	13.3	5.32E-06	0.305	CAGGAGTTAATTTTA

PA14_61170	104	118	13.3	5.32E-06	0.305	CAGGAGTTAATTTTA
PA14_61170	104	118	13.3	5.32E-06	0.305	TAAAATTAACTCCTG
PA14_61200	117	131	10.4	9.01E-05	0.635	CGGTATTACATATTT
PA14_61200	117	131	10.4	9.28E-05	0.636	AAATATGTAATACCG
hprA	190	204	10.4	9.01E-05	0.635	CGGTATTACATATTT
hprA	190	204	10.4	9.28E-05	0.636	AAATATGTAATACCG
PA14_61320	200	214	10.8	6.76E-05	0.611	CAGCAGAACCCTCTG
PA14_61320	200	214	10.7	6.98E-05	0.616	CAGAGGGTTCTGCTG
PA14_61330	212	226	10.8	6.76E-05	0.611	CAGCAGAACCCTCTG
PA14_61330	212	226	10.7	6.98E-05	0.616	CAGAGGGTTCTGCTG
ilvI	248	262	10.5	8.69E-05	0.635	CAGAATAAAGCTTGA
ilvI	248	262	10.4	8.97E-05	0.635	TCAAGCTTTATTCTG
PA14_62170	289	303	10.5	8.69E-05	0.635	CAGAATAAAGCTTGA
PA14_62170	289	303	10.4	8.97E-05	0.635	TCAAGCTTTATTCTG
pcnB	252	266	10.7	7.25E-05	0.625	TAACTGATTCTTTTG
pcnB	252	266	10.7	7.29E-05	0.625	CAAAAGAATCAGTTA
PA14_62690	168	182	14.5	1.25E-06	0.259	AAGGATTTTATTTTA
PA14_62690	168	182	14.5	1.27E-06	0.259	TAAAATAAAATCCTT
PA14_62690	152	166	11.1	4.96E-05	0.608	TAACTTATTGTTTTT
PA14_62690	152	166	11.1	5.05E-05	0.608	AAAAACAATAAGTTA
glmM	19	33	11.8	2.66E-05	0.559	AAGTATTTTCTGCTC
glmM	19	33	11.8	2.71E-05	0.561	GAGCAGAAAATACTT
PA14_63120	252	266	10.7	7.04E-05	0.616	TGGCAGAACGTGCTG
PA14_63120	252	266	10.7	7.22E-05	0.624	CAGCACGTTCTGCCA
PA14_63230	112	126	10.4	9.22E-05	0.636	TAAAATGAAGTCTTT
PA14_63230	112	126	10.4	9.28E-05	0.636	AAAGACTTCATTTTA
PA14_63240	29	43	10.4	9.22E-05	0.636	TAAAATGAAGTCTTT
PA14_63240	29	43	10.4	9.28E-05	0.636	AAAGACTTCATTTTA
PA14_63960	109	123	11.7	3.03E-05	0.563	AGAAATGATATACTA
PA14_63960	109	123	11.6	3.06E-05	0.563	TAGTATATCATTTCT
PA14_63970	19	33	11.7	3.03E-05	0.563	AGAAATGATATACTA
PA14_63970	19	33	11.6	3.06E-05	0.563	TAGTATATCATTTCT
osmE	227	241	11.2	4.63E-05	0.608	CAGCAGGAAGTCCTG
osmE	227	241	11.2	4.70E-05	0.608	CAGGACTTCCTGCTG
PA14_64530	124	138	10.6	7.79E-05	0.626	AAAAATAATCAATTA
PA14_64530	124	138	10.6	7.90E-05	0.626	TAATTGATTATTTTT
rnr	107	121	11.7	2.96E-05	0.563	CAGCAGAATAATTTT

rnr	107	121	11.6	3.06E-05	0.563	AAAATTATTCTGCTG
PA14_65840	331	345	10.4	9.28E-05	0.636	CAGCGCAATGCACTG
PA14_65840	331	345	10.4	9.34E-05	0.64	CAGTGCATTGCGCTG
glnE	171	185	10.6	7.84E-05	0.626	CGAAATGTAGTTTTA
glnE	171	185	10.5	8.11E-05	0.626	TAAAACTACATTTCG
aceE	97	111	10.6	7.84E-05	0.626	CGAAATGTAGTTTTA
aceE	97	111	10.5	8.11E-05	0.626	TAAAACTACATTTCG
PA14_66410	33	47	10.5	8.55E-05	0.635	CAGCACAATGCTCGG
PA14_66410	33	47	10.4	8.87E-05	0.635	CCGAGCATTGTGCTG
PA14_67120	236	250	12.4	1.46E-05	0.447	CAGCAGAATGCGTTG
PA14_67120	236	250	12.4	1.48E-05	0.447	CAACGCATTCTGCTG
thiI	282	296	10.9	6.03E-05	0.608	CGGAATTATATCTGA
thiI	282	296	10.8	6.29E-05	0.608	TCAGATATAATTCCG
glnA	41	55	10.9	6.03E-05	0.608	CGGAATTATATCTGA
glnA	41	55	10.8	6.29E-05	0.608	TCAGATATAATTCCG
PA14_68070	27	41	11.8	2.64E-05	0.559	CAGCAGGATCTTCTT
PA14_68070	27	41	11.8	2.71E-05	0.561	AAGAAGATCCTGCTG
PA14_68110	138	152	14.7	9.56E-07	0.259	CAAGATATTGTTTTA
PA14_68110	138	152	14.7	9.83E-07	0.259	TAAAACAATATCTTG
PA14_68470	134	148	11.0	5.58E-05	0.608	TGGAGCAATGTTCTG
PA14_68470	134	148	11.0	5.69E-05	0.608	CAGAACATTGCTCCA
PA14_68480	76	90	11.0	5.58E-05	0.608	TGGAGCAATGTTCTG
PA14_68480	76	90	11.0	5.69E-05	0.608	CAGAACATTGCTCCA
PA14_68530	21	35	10.8	6.76E-05	0.611	TGAAATTTAGTCTTG
PA14_68530	21	35	10.7	7.04E-05	0.616	CAAGACTAAATTTCA
PA14_68550	108	122	10.8	6.76E-05	0.611	TGAAATTTAGTCTTG
PA14_68550	108	122	10.7	7.04E-05	0.616	CAAGACTAAATTTCA
betT1	450	464	11.0	5.44E-05	0.608	TGGTACTACATGCTG
betT1	450	464	11.0	5.49E-05	0.608	CAGCATGTAGTACCA
PA14_71190	140	154	11.5	3.59E-05	0.592	CAGGGTGATGTTCTG
PA14_71190	140	154	11.5	3.64E-05	0.592	CAGAACATCACCCTG
PA14_71320	53	67	11.9	2.50E-05	0.542	TAATACAATAATTTA
PA14_71320	53	67	11.8	2.53E-05	0.545	TAAATTATTGTATTA
PA14_71430	51	65	10.9	5.94E-05	0.608	GAGAATTTTGTCTTT
PA14_71430	51	65	10.9	5.98E-05	0.608	AAAGACAAAATTCTC
rmd	316	330	12.3	1.58E-05	0.447	TAGCGTGTTGTTCTG
rmd	316	330	12.3	1.65E-05	0.447	CAGAACAACACGCTA

PA14_72010	78	92	12.3	1.58E-05	0.447	TAGCGTGTTGTTCTG
PA14_72010	78	92	12.3	1.65E-05	0.447	CAGAACAACACGCTA
PA14_72370	459	473	10.6	7.59E-05	0.626	AAGCATGATGTTTTC
PA14_72370	459	473	10.6	7.99E-05	0.626	GAAAACATCATGCTT
PA14_72470	65	79	13.5	4.39E-06	0.294	CGGCATTATATACTT
PA14_72470	65	79	13.5	4.62E-06	0.294	AAGTATATAATGCCG
engB	105	119	13.5	4.39E-06	0.294	CGGCATTATATACTT
engB	105	119	13.5	4.62E-06	0.294	AAGTATATAATGCCG
metN	112	126	11.2	4.70E-05	0.608	GAGCATTTTACCTTG
metN	112	126	11.2	4.80E-05	0.608	CAAGGTAAAATGCTC
metN	21	35	10.8	6.71E-05	0.611	CAGCAGAAAGCGCTT
metN	21	35	10.8	6.76E-05	0.611	AAGCGCTTTCTGCTG
PA14_73020	79	93	13.6	4.18E-06	0.294	TAGTATAACGTTTTA
PA14_73020	79	93	13.5	4.36E-06	0.294	TAAAACGTTATACTA
PA14_73030	20	34	13.6	4.18E-06	0.294	TAGTATAACGTTTTA
PA14_73030	20	34	13.5	4.36E-06	0.294	TAAAACGTTATACTA
amiA	50	64	12.5	1.31E-05	0.44	TAATATAACGTATTA
amiA	50	64	12.5	1.32E-05	0.44	TAATACGTTATATTA
PA14_73050	36	50	12.5	1.31E-05	0.44	TAATATAACGTATTA
PA14_73050	36	50	12.5	1.32E-05	0.44	TAATACGTTATATTA
atpB	21	35	10.6	7.53E-05	0.626	CAGCAGAAACCGCTT
atpB	21	35	10.6	7.59E-05	0.626	AAGCGGTTTCTGCTG

Table A7. Primers used for studies described in Chapter 6.

Primer name	Sequence (5' > 3')
Knockout primers	
rpoN-fwd	TTTCGCCATCAACTCTGGACA
rpoN-rev	CGTACAGTCGGAAAAGCCCA

Table A8. All genes differentially expressed in PA14 Δ*ntrBC*, but not Δ*rpoN*, mutant strains. Gene expression for *ntrBC* mutants is expressed as fold-change (FC) relative to PA14 wild-type (WT). Briefly, swarm plates were inoculated with 5 µl of planktonic cells suspended at OD_{600} = 0.4-0.6 in basal medium (BM2) supplemented with 0.1% casamino acids and 0.4% glucose, then incubated for 18-24 h at 37°C. Swarming cells were harvested from the surface grown colony and RNA was isolated using Qiagen RNEasy MiniPrep kit.

PAO1 Locus	Name	Annotation	FC Δ*ntrBC*
PA0021	PA0021	conserved hypothetical protein	5.24
PA0044	*exoT*	exoenzyme T	5.83
PA0070	*tagQ1*	TagQ1	2.55
PA0074	*ppkA*	serine/threonine protein kinase PpkA	2.32
PA0076	*tagF1*	TagF1	2.67
PA0080	*tssJ1*	TssJ1	3.46
PA0087	*tssE1*	TssE1	3.84
PA0125	PA0125	hypothetical protein	-7.82
PA0128	PA0128	conserved hypothetical protein	-2.28
PA0131	*bauB*	BauB	-2.71
PA0132	*bauA*	Beta-alanine:pyruvate transaminase	-3.13
PA0166	PA0166	probable transporter	-2.85
PA0192	PA0192	probable TonB-dependent receptor	-2.23
PA0198	*exbB1*	transport protein ExbB	-2.74
PA0221	PA0221	probable aminotransferase	-2.82
PA0222	PA0222	hypothetical protein	-3.68
PA0231	*pcaD*	beta-ketoadipate enol-lactone hydrolase	2.15
PA0234	PA0234	hypothetical protein	-2.44
PA0239	PA0239	hypothetical protein	-3.24
PA0240	PA0240	probable porin	-2.38
PA0247	*pobA*	p-hydroxybenzoate hydroxylase	-2.56
NA	NA	NA	-2.13
NA	NA	NA	-3.3
PA0267	PA0267	hypothetical protein	2.08
PA0298	*spuB*	Glutamylpolyamine synthetase	-2.73
PA0339	PA0339	hypothetical protein	2.29
PA0349	PA0349	hypothetical protein	-2.18
PA0354	PA0354	conserved hypothetical protein	-2.03
PA0362	*fdx1*	ferredoxin [4Fe-4S]	-2.47
PA0369	PA0369	Uncharacterized protein	2.86
PA0384	PA0384	hypothetical protein	2.85
PA0466	PA0466	hypothetical protein	7.85
PA0467	PA0467	conserved hypothetical protein	2.11
PA0482	*glcB*	malate synthase G	3.64
PA0523	*norC*	nitric-oxide reductase subunit C	-4.15
PA0540	PA0540	hypothetical protein	3.46
PA0546	*metK*	methionine adenosyltransferase	2.17
PA0554	PA0554	hypothetical protein	-2.02
PA0569	PA0569	hypothetical protein	3.29
PA0571	PA0571	hypothetical protein	12.44

NA	NA	NA	-6.48
PA0579	*rpsU*	30S ribosomal protein S21	-2.63
PA0668	*tyrZ*	tyrosyl-tRNA synthetase 2	-2.64
PA4277	*tufB*	elongation factor Tu	-3.99
PA4275	*nusG*	transcription antitermination protein NusG	-3.39
PA4268	*rpsL*	30S ribosomal protein S12	-2.89
PA4267	*rpsG*	30S ribosomal protein S7	-3.76
PA4265	*tufA*	elongation factor Tuf	-2.38
PA4263	*rplC*	50S ribosomal protein L3	-4.71
PA4259	*rpsS*	30S ribosomal protein S19	-7.59
PA4258	*rplV*	50S ribosomal protein L22	-5.57
PA4255	*rpmC*	50S ribosomal protein L29	-3.75
PA4252	*rplX*	50S ribosomal protein L24	-4.82
PA4251	*rplE*	50S ribosomal protein L5	-3.14
PA4237	*rplQ*	50S ribosomal protein L17	-3.39
PA4180	PA4180	probable acetolactate synthase large subunit	3.08
PA4176	*ppiC2*	peptidyl-prolyl cis-trans isomerase C2	2.28
PA4167	PA4167	probable oxidoreductase	-2.91
NA	NA	NA	2.8
PA4156	*fvbA*	FvbA	-2.66
PA4116	*bphO*	heme oxygenase, BphO	2.15
PA4094	PA4094	probable transcriptional regulator	-3.8
PA4092	*hpaC*	4-hydroxyphenylacetate 3-monooxygenase small chain	-3.16
PA4070	PA4070	probable transcriptional regulator	-2.38
PA4022	*hdhA*	hydrazone dehydrogenase, HdhA	-113.34
PA4021	PA4021	probable transcriptional regulator	-3
PA3995	PA3995	probable transcriptional regulator	2.48
PA3979	PA3979	hypothetical protein	-2.17
PA3965	PA3965	probable transcriptional regulator	-2.29
PA3935	*tauD*	taurine dioxygenase	-2.28
PA3877	*narK1*	nitrite extrusion protein 1	-7.08
PA3876	*narK2*	nitrite extrusion protein 2	-2.55
PA3862	*dauB*	NAD(P)H-dependent anabolic L-arginine dehydrogenase, DauB	-2.18
PA3852	PA3852	hypothetical protein	2.93
PA3848	PA3848	hypothetical protein	2.58
PA3829	PA3829	hypothetical protein	2.22
NA	NA	NA	-2.12
PA3807	*ndk*	nucleoside diphosphate kinase	-2.04
NA	NA	NA	-2.39
NA	NA	NA	-2.12
PA3752	PA3752	hypothetical protein	2.67
PA3744	*rimM*	16S rRNA processing protein	-2.3
PA3743	*trmD*	tRNA (guanine-N1)-methyltransferase	-3.63
PA3721	*nalC*	NalC	2.09
PA3719	*armR*	antirepressor for MexR, ArmR	3.73
PA3717	PA3717	probable peptidyl-prolyl cis-trans isomerase, FkbP-type	-2.25
PA3707	*wspB*	hypothetical protein	2.25
PA3706	*wspC*	probable protein methyltransferase	2.1
PA3705	*wspD*	hypothetical protein	2.23
PA3704	*wspE*	probable chemotaxis sensor/effector fusion protein	2.73
PA3702	*wspR*	WspR	2.12

PA3697	PA3697	hypothetical protein	2.26
PA3687	*ppc*	phosphoenolpyruvate carboxylase	2.12
PA3682	PA3682	hypothetical protein	2.08
PA3676	*mexK*	MexK	-2.04
PA3671	PA3671	probable permease of ABC transporter	-2.81
PA3628	PA3628	putative esterase	2.14
PA3621	*fdxA*	ferredoxin I	-4.81
PA3614	PA3614	hypothetical protein	3.2
PA3609	*potC*	polyamine transport protein PotC	-3.36
PA3607	*potA*	polyamine transport protein PotA	-3.82
PA3602	PA3602	conserved hypothetical protein	3.4
PA3562	*fruI*	phosphotransferase system transporter enzyme I, FruI	-2.08
PA3553	*arnC*	ArnC	2.08
PA3526	*motY*	MotY	-7.1
PA3485	*tsi3*	Tsi3	3.07
PA3454	PA3454	probable acyl-CoA thiolase	3.45
PA3406	*hasD*	transport protein HasD	-2.45
PA3397	*fprA*	FprA	-2.26
PA3389	PA3389	probable ring-cleaving dioxygenase	-2.4
PA3365	PA3365	probable chaperone	-2.92
PA3364	*amiC*	aliphatic amidase expression-regulating protein	-2.53
PA3352	PA3352	hypothetical protein	-2.18
PA3338	PA3338	hypothetical protein	2.07
PA3304	PA3304	conserved hypothetical protein	2.18
PA3284	PA3284	hypothetical protein	-3.52
PA3271	PA3271	probable two-component sensor	5.71
PA3221	*csaA*	CsaA protein	3.97
PA3214	PA3214	hypothetical protein	2.79
PA3213	PA3213	hypothetical protein	2.06
PA3207	PA3207	hypothetical protein	2.5
PA3186	*oprB*	Glucose/carbohydrate outer membrane porin OprB precursor	-11.65
PA3176	*gltS*	glutamate/sodium ion symporter, GltS	-2.16
PA3162	*rpsA*	30S ribosomal protein S1	-2.05
PA3100	*xcpU*	General secretion pathway outer membrane protein H precursor	6.31
PA3098	*xcpW*	general secretion pathway protein J	4.1
NA	NA	NA	3.12
PA3079	PA3079	hypothetical protein	-2.55
PA2991	*sth*	soluble pyridine nucleotide transhydrogenase	2.67
PA2990	PA2990	probable phosphodiesterase	2.36
PA2971	PA2971	conserved hypothetical protein	-3.5
PA2949	PA2949	esterase	3.16
PA2946	PA2946	hypothetical protein	-2.41
PA2945	PA2945	conserved hypothetical protein	-3.76
PA2916	PA2916	hypothetical protein	10.24
PA2911	PA2911	probable TonB-dependent receptor	-4.09
PA2885	*atuR*	putative repressor of atu genes	-2.81
PA2851	*efp*	translation elongation factor P	-3.17
PA2841	PA2841	probable enoyl-CoA hydratase/isomerase	2.74
NA	NA	NA	3.42
NA	NA	NA	3.75
PA2809	*copR*	two-component response regulator, CopR	2.4

PA2808	*ptrA*	Pseudomonas type III repressor A	4.64
PA2807	PA2807	hypothetical protein	36.26
PA2806	PA2806	conserved hypothetical protein	4.15
PA2796	*tal*	transaldolase	2.54
PA2776	*pauB3*	FAD-dependent oxidoreductase	-2.83
PA2768	PA2768	hypothetical protein	-3.92
PA2749	*endA*	DNA-specific endonuclease I	-2.54
PA2745	PA2745	probable hydrolase	2.76
NA	NA	NA	-2.56
PA2725	PA2725	probable chaperone	2.25
PA2703	*tsi2*	Tsi2	4.16
PA2698	PA2698	probable hydrolase	2.54
PA2683	PA2683	probable serine/threonine dehydratase, degradative	2.31
PA2683	*tsi5*	Tsi5	2.31
PA2682	PA2682	conserved hypothetical protein	2.38
PA2679	PA2679	hypothetical protein	11.02
PA2623	*icd*	isocitrate dehydrogenase	2.51
PA2619	*infA*	initiation factor	-4.41
PA2605	PA2605	conserved hypothetical protein	3.07
PA2585	*uvrC*	excinuclease ABC subunit C	2.55
NA	NA	NA	-3.41
PA2561	*ctpH*	CtpH	-3.01
PA2530	PA2530	hypothetical protein	2.37
PA2489	PA2489	probable transcriptional regulator	2.11
PA2462	PA2462	hypothetical protein	-2.91
PA2453	PA2453	hypothetical protein	-2.28
PA2390	*pvdT*	PvdT	-2.08
PA2384	PA2384	hypothetical protein	4.67
PA2341	PA2341	probable ATP-binding component of ABC maltose/mannitol transporter	-2.04
PA2288	PA2288	hypothetical protein	2.84
PA2285	PA2285	hypothetical protein	-2.5
PA2277	*arsR*	ArsR protein	4.41
PA2268	PA2268	hypothetical protein	3.25
NA	NA	NA	-2.26
PA2212	PA2212	conserved hypothetical protein	-2.56
PA2211	PA2211	conserved hypothetical protein	-3.83
PA2208	PA2208	hypothetical protein	-3.27
PA2207	PA2207	hypothetical protein	-2.9
PA2127	*cgrA*	cupA gene regulator A, CgrA	-2.03
PA2121	PA2121	probable transcriptional regulator	2.48
PA2116	PA2116	conserved hypothetical protein	2.3
PA2109	PA2109	hypothetical protein	-2.72
PA2084	PA2084	probable asparagine synthetase	-3.78
PA2083	PA2083	probable ring-hydroxylating dioxygenase subunit	-2.83
PA2080	*kynU*	kynureninase KynU	2.28
PA2064	*pcoB*	copper resistance protein B precursor	32.81
PA2048	PA2048	hypothetical protein	3.45
PA2047	*cmrA*	chloramphenicol resistance activator CmrA	2.65
PA1973	*pqqF*	pyrroloquinoline quinone biosynthesis protein F	2.4
PA1959	*bacA*	bacitracin resistance protein	-2.39

PA1943	PA1943	hypothetical protein	2.11
PA1923	PA1923	hypothetical protein	-3.14
NA	NA	NA	-7.33
PA1920	*nrdD*	class III (anaerobic) ribonucleoside-triphosphate reductase subunit, NrdD	-2.69
PA1884	PA1884	probable transcriptional regulator	2.26
PA1865	PA1865	hypothetical protein	2.04
PA1864	PA1864	probable transcriptional regulator	-5.12
PA1853	PA1853	probable transcriptional regulator	8.05
PA1839	PA1839	hypothetical protein	-2.11
PA1800	*tig*	trigger factor	-2.22
NA	NA	NA	-2.36
PA1764	PA1764	hypothetical protein	-2.86
PA1751	PA1751	hypothetical protein	2.04
PA1723	*pscJ*	type III export protein PscJ	2.15
PA1718	*pscE*	type III export protein PscE	4.41
PA1717	*pscD*	type III export protein PscD	3.02
PA1710	*exsC*	ExsC, exoenzyme S synthesis protein C precursor.	5.3
PA1706	*pcrV*	type III secretion protein PcrV	7.1
PA1694	*pscQ*	translocation protein in type III secretion	3.37
PA1693	*pscR*	translocation protein in type III secretion	2.56
PA1692	PA1692	probable translocation protein in type III secretion	7.13
PA1690	*pscU*	translocation protein in type III secretion	2
PA1679	PA1679	hypothetical protein	-7.06
PA1677	PA1677	conserved hypothetical protein	2.91
PA1651	PA1651	probable transporter	-2.25
PA1645	PA1645	hypothetical protein	2.26
PA1636	kdpD	two-component sensor KdpD	2.25
PA1624	PA1624	hypothetical protein	2.21
PA1612	PA1612	hypothetical protein	2.17
PA1603	PA1603	probable transcriptional regulator	2.03
PA1590	*braB*	branched chain amino acid transporter	2.61
PA1576	PA1576	probable 3-hydroxyisobutyrate dehydrogenase	2.75
PA1573	PA1573	conserved hypothetical protein	2.25
PA1568	PA1568	conserved hypothetical protein	-3.29
PA1555	*ccoP2*	Cytochrome c oxidase, cbb3-type, CcoP subunit	-4.21
PA1555	*ccoQ2*	Cytochrome c oxidase, cbb3-type, CcoQ subunit	-4.21
PA1544	*anr*	transcriptional regulator Anr	2.34
PA1542	PA1542	hypothetical protein	-2
PA1538	PA1538	probable flavin-containing monooxygenase	-2.79
PA1537	PA1537	probable short-chain dehydrogenase	-2.37
PA1517	PA1517	conserved hypothetical protein	-2.1
PA1456	*cheY*	two-component response regulator CheY	-2.34
PA1453	*flhF*	flagellar biosynthesis protein FlhF	-3.24
PA1452	*flhA*	flagellar biosynthesis protein FlhA	-4.2
PA1434	PA1434	hypothetical protein	2.01
PA1423	*bdlA*	BdlA	-5.82
PA1418	PA1418	probable sodium:solute symport protein	-4.64
PA1410	PA1410	probable periplasmic spermidine/putrescine-binding protein	-3.5
NA	NA	NA	-2.01
PA1363	PA1363	ECF sigma factor	-2.17

PA1342	*aatJ*	AatJ	-2.16
PA1326	*ilvA2*	threonine dehydratase, biosynthetic	-2.09
PA1325	PA1325	conserved hypothetical protein	-2.5
PA1321	*cyoE*	cytochrome o ubiquinol oxidase protein CyoE	2.24
PA1316	PA1316	probable major facilitator superfamily (MFS) transporter	-2.13
PA1314	PA1314	hypothetical protein	3.09
PA1260	*lhpP*	ABC transporter periplasmic-binding protein, LhpP	-3.38
PA1259	*lhpH*	LhpH	-2.79
PA1240	PA1240	probable enoyl-CoA hydratase/isomerase	4.35
PA1239	PA1239	hypothetical protein	2.75
PA1234	PA1234	hypothetical protein	2.69
PA1199	PA1199	probable lipoprotein	2.42
NA	NA	NA	-3.05
PA1149	PA1149	hypothetical protein	2.93
PA1120	*tpbB*	diguanylate cyclase TpbB	2.44
PA1103	PA1103	probable flagellar assembly protein	-2.16
PA1102	*fliG*	flagellar motor switch protein FliG	-4.12
PA1101	*fliF*	Flagella M-ring outer membrane protein precursor	-14.41
PA1095	PA1095	hypothetical protein	-34.21
PA1093	PA1093	hypothetical protein	-66.12
PA1092	*fliC*	flagellin type B	-157.39
PA1088	PA1088	hypothetical protein	-2.49
PA1087	*flgL*	flagellar hook-associated protein type 3 FlgL	-4.7
PA1086	*flgK*	flagellar hook-associated protein 1 FlgK	-5.69
PA1084	*flgI*	flagellar P-ring protein precursor FlgI	-10.21
PA1083	*flgH*	flagellar L-ring protein precursor FlgH	-14.33
PA1082	*flgG*	flagellar basal-body rod protein FlgG	-14.01
PA1081	*flgF*	flagellar basal-body rod protein FlgF	-22.84
PA1079	*flgD*	flagellar basal-body rod modification protein FlgD	-16.92
PA1078	*flgC*	flagellar basal-body rod protein FlgC	-20
NA	NA	NA	-2.22
PA1047	PA1047	probable esterase	2.38
PA1038	PA1038	hypothetical protein	2.3
PA1035	PA1035	hypothetical protein	-3.14
PA1034	PA1034	hypothetical protein	-2.3
PA1014	*wapB*	1,2-glucosyltransferase WapB	-2.15
NA	NA	NA	-2.25
PA0978	PA0978	conserved hypothetical protein	-2.66
PA0957	PA0957	hypothetical protein	-2.03
PA0931	*pirA*	ferric enterobactin receptor PirA	-2.44
PA0927	*ldhA*	D-lactate dehydrogenase (fermentative)	2.99
PA0921	PA0921	hypothetical protein	-2.43
PA0911	*alpE*	AlpE	-2.31
PA0895	*aruC*	N2-Succinylornithine 5-aminotransferase (SOAT) = N2-acetylornithine 5-aminotransferase (ACOAT)	-2.11
PA0858	PA0858	conserved hypothetical protein	-2.26
PA0857	*bolA*	morphogene protein BolA	2.94
PA0855	PA0855	hypothetical protein	6.32
PA0845	*cerN*	CerN	-2
PA0835	*pta*	phosphate acetyltransferase	2.03
NA	NA	NA	-2.4

PA0811	PA0811	probable major facilitator superfamily (MFS) transporter	-2.15
PA0792	*prpD*	propionate catabolic protein PrpD	2.63
PA0759	PA0759	conserved hypothetical protein	2.12
PA0731	PA0731	hypothetical protein	2.33
NA	NA	NA	2.04
NA	NA	NA	-2.36
PA0703	PA0703	probable major facilitator superfamily (MFS) transporter	3.38
PA0687	*hxcS*	HxcS	-3.13
PA4289	PA4289	probable transporter	2.43
PA4291	PA4291	hypothetical protein	2.39
PA4309	*pctA*	chemotactic transducer PctA	-4.28
PA4399	PA4399	conserved hypothetical protein	2.17
PA4464	*ptsN*	nitrogen regulatory IIA protein	-2.8
PA4468	*sodM*	superoxide dismutase	-2.09
PA4471	PA4471	hypothetical protein	-2.51
PA4498	*mdpA*	metallo-dipeptidase aeruginosa, MdpA	2.11
PA4500	*dppA3*	probable binding protein component of ABC transporter	-2.27
PA4508	PA4508	probable transcriptional regulator	-2.12
PA4514	PA4514	probable outer membrane receptor for iron transport	-2.86
PA4515	PA4515	conserved hypothetical protein	-3.04
PA4520	PA4520	probable chemotaxis transducer	-2.09
NA	NA	NA	-4.03
PA4525	*pilA*	type 4 fimbrial precursor PilA	-8.55
PA4537	PA4537	hypothetical protein	2.23
NA	NA	NA	-2.31
NA	NA	NA	-2.17
NA	NA	NA	-2.16
NA	NA	NA	-2.95
NA	NA	NA	-2.07
NA	NA	NA	-4.62
NA	NA	NA	-7.32
NA	NA	NA	-6.03
NA	NA	NA	-4.34
NA	NA	NA	-3.77
NA	NA	NA	-2.52
NA	NA	NA	-3.04
NA	NA	NA	-3.29
NA	NA	NA	-2.4
NA	NA	NA	-2
NA	NA	NA	-2.95
NA	NA	NA	-2.32
NA	NA	NA	-3.76
PA4547	*pilR*	two-component response regulator PilR	2.38
PA4553	*pilX*	type 4 fimbrial biogenesis protein PilX	2.35
PA4563	*rpsT*	30S ribosomal protein S20	-3.48
PA4568	*rplU*	50S ribosomal protein L21	-4.22
PA4584	PA4584	conserved hypothetical protein	-2.32
PA4599	*mexC*	Resistance-Nodulation-Cell Division (RND) multidrug efflux membrane fusion protein MexC precursor	-3.39
PA4630	PA4630	hypothetical protein	-4.35
PA4633	PA4633	probable chemotaxis transducer	-6.82

PA4659	PA4659	probable transcriptional regulator	4.09
PA4660	*phr*	deoxyribodipyrimidine photolyase	2.56
PA4672	PA4672	peptidyl-tRNA hydrolase	-2.91
PA4714	PA4714	conserved hypothetical protein	-2.04
PA4736	PA4736	hypothetical protein	2.25
PA4741	*rpsO*	30S ribosomal protein S15	-3.19
PA4746	PA4746	conserved hypothetical protein	-2.94
PA4765	*omlA*	Outer membrane lipoprotein OmlA precursor	-2.07
PA4773	*speD2*	SpeD2	2.15
PA4776	*pmrA*	PmrA: two-component regulator system response regulator PmrA	2.12
PA4777	*pmrB*	PmrB: two-component regulator system signal sensor kinase PmrB	2.02
NA	NA	NA	-3.18
PA4821	PA4821	probable transporter	-2.12
PA4838	PA4838	hypothetical protein	-2.14
PA4852	PA4852	conserved hypothetical protein	-2.69
PA4853	*fis*	DNA-binding protein Fis	-4.87
PA4873	PA4873	probable heat-shock protein	2.41
PA4881	PA4881	hypothetical protein	-6.64
PA4927	PA4927	conserved hypothetical protein	2.19
PA4928	PA4928	conserved hypothetical protein	-2.83
PA4958	PA4958	hypothetical protein	2.32
PA4980	PA4980	probable enoyl-CoA hydratase/isomerase	-4.03
NA	NA	NA	-4
PA4986	PA4986	probable oxidoreductase	-4.21
PA5024	PA5024	conserved hypothetical protein	-4.39
PA5030	PA5030	probable major facilitator superfamily (MFS) transporter	2.28
PA5049	*rpmE*	50S ribosomal protein L31	-2.91
PA5097	PA5097	probable amino acid permease	-4.23
PA5113	PA5113	hypothetical protein	2.02
PA5137	PA5137	hypothetical protein	-2.27
PA5152	PA5152	probable ATP-binding component of ABC transporter	-5.06
PA5153	PA5153	amino acid (lysine/arginine/ornithine/histidine/octopine) ABC transporter periplasmic binding protein	-5.06
PA5155	PA5155	amino acid (lysine/arginine/ornithine/histidine/octopine) ABC transporter membrane protein	-3.93
PA5157	PA5157	probable transcriptional regulator	2.62
PA5158	PA5158	probable outer membrane protein precursor	2.26
PA5159	PA5159	multidrug resistance protein	5.41
PA5169	*dctM*	DctM	-3.34
PA5192	*pckA*	phosphoenolpyruvate carboxykinase	-2.09
PA5206	*argE*	acetylornithine deacetylase	2.11
PA5244	PA5244	conserved hypothetical protein	-2.05
PA5271	PA5271	hypothetical protein	2.28
PA5286	PA5286	conserved hypothetical protein	-3.88
PA5294	PA5294	putative multidrug efflux pump	2.04
PA5303	PA5303	conserved hypothetical protein	-2.39
PA5315	*rpmG*	50S ribosomal protein L33	-4.84
PA5316	*rpmB*	50S ribosomal protein L28	-4.1
PA5324	*sphR*	Sphingosine-responsive Regulator, SphR	-2.24
PA5366	*pstB*	ATP-binding component of ABC phosphate transporter	-2.07

PA5376	*cbcV*	CbcV	2.23
PA5381	PA5381	hypothetical protein	-2.78
PA5388	*caiX*	CaiX	-3.65
PA5394	*cls*	cardiolipin synthase	2.23
PA5395	PA5395	conserved hypothetical protein	2.99
PA5409	PA5409	hypothetical protein	2.54
PA5415	*glyA1*	serine hydroxymethyltransferase	-2.31
PA5476	*citA*	citrate transporter	2.01
PA5479	*gltP*	proton-glutamate symporter	-3.89
PA5480	PA5480	hypothetical protein	-5.09
PA5483	*algB*	two-component response regulator AlgB	-2.32
PA5486	PA5486	conserved hypothetical protein	-2.11
PA5522	*pauA6*	Glutamylpolyamine synthetase	-2.03
PA5523	PA5523	probable aminotransferase	-3.37
PA5524	PA5524	probable short-chain dehydrogenase	-2.37
PA5542	PA5542	Pseudomonas imipenem beta-lactamase PIB-1	-4.11
PA5543	PA5543	hypothetical protein	-2.33
PA5544	PA5544	conserved hypothetical protein	-6.89
PA5550	*glmR*	GlmR transcriptional regulator	-2.87
PA5559	*atpE*	ATP synthase C chain	-2.62
PA5560	*atpB*	ATP synthase A chain	-3.04
PA5565	*gidA*	glucose-inhibited division protein A	-2.49

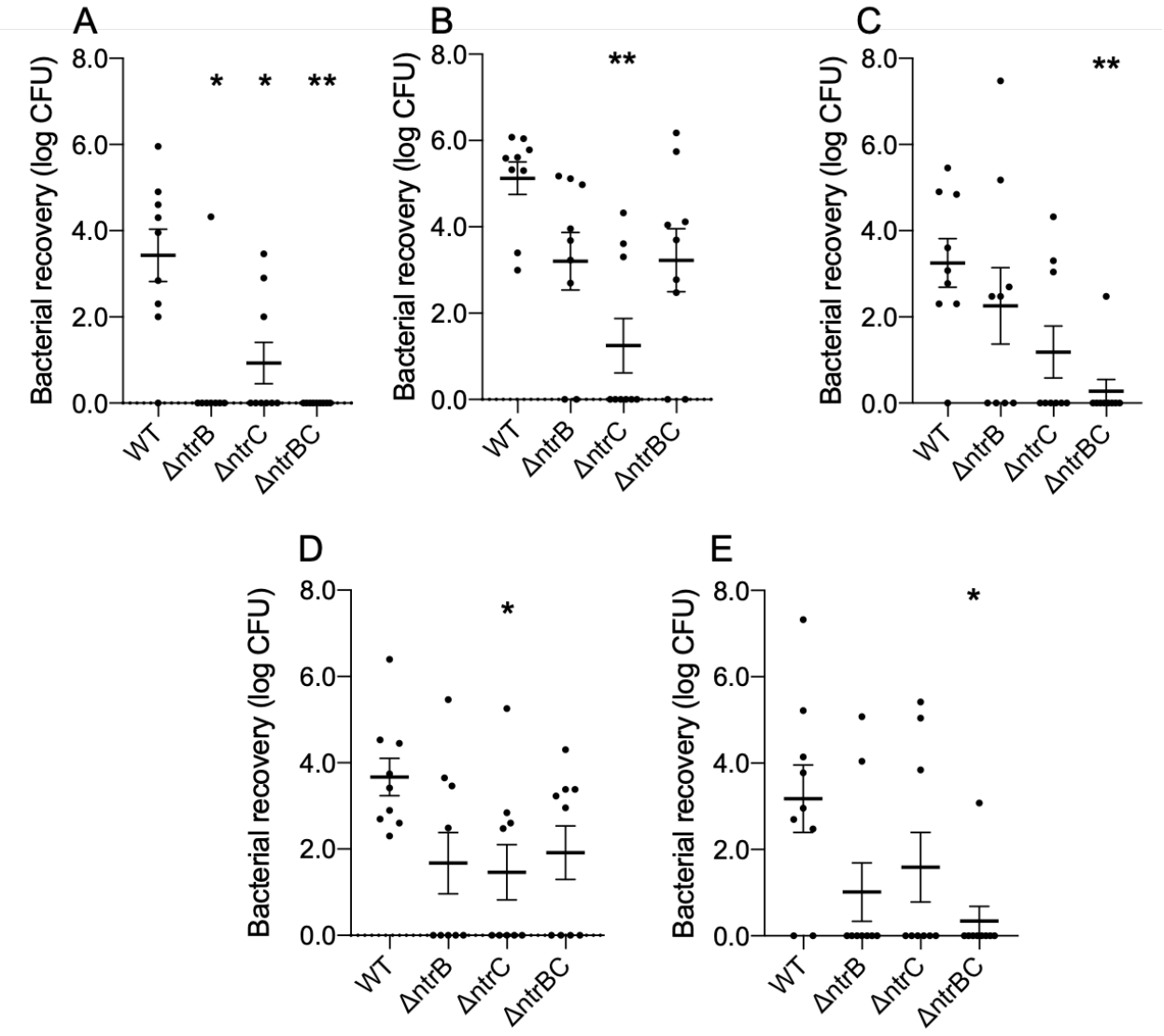

Figure A1. Dissemination of mutants from abscesses to organs was reduced in mutants compared to PA14 wild-type (WT) in an acute model of CD-1 infection. Briefly, mice were subcutaneously injected 5±3 x 10^7 CFU planktonic cells and abscesses were formed for 24 h. At the experimental endpoint, organs were harvested in phosphate buffered saline (PBS), homogenized and plated on LB for bacterial enumeration. Organs included the heart (A), lungs (B), liver (C), spleen (D) and kidney (E). Data are presented as mean ± standard error of the mean (SEM) from four independent experiments each including 1-3 individual mice per bacterial strain *(n = 9)*. * $P < 0.05$, ** $P < 0.01$ according to Kruskal-Wallis nonparametric test followed by Dunn's post-hoc analysis.

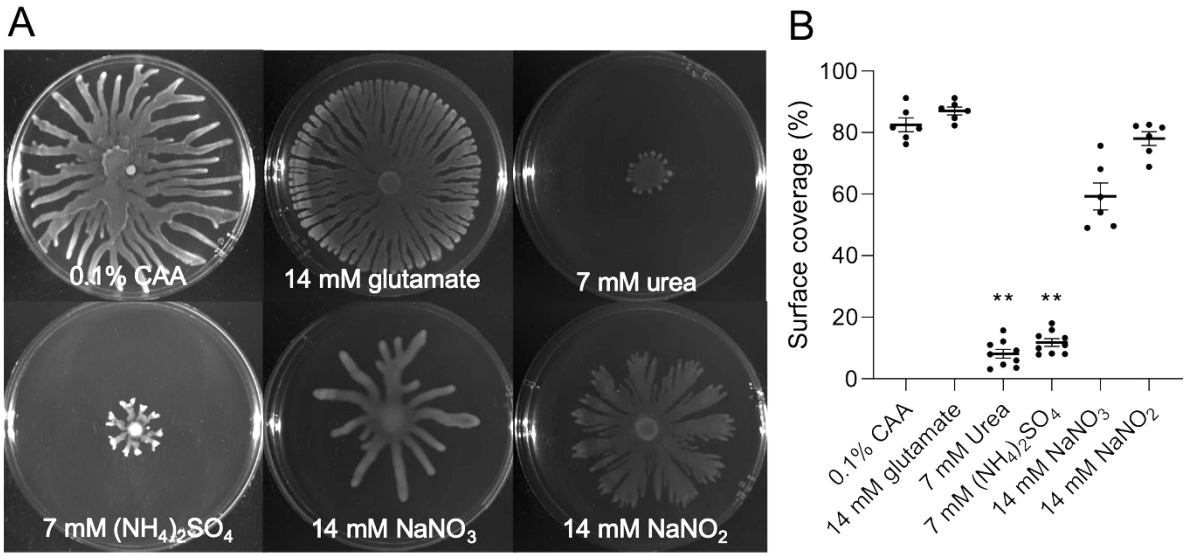

Figure A2. Swarming motility of wild-type (WT) PA14 was influenced by nitrogen source. (A) Representative images depict swarming motility of WT PA14 in the presence of different nitrogenous compounds. (B) Swarming motility was reduced by substituting casamino acids (CAA) for urea or ammonium sulfate ($(NH_4)_2SO_4$) in swarm plates. Modified swarm plates were inoculated with 5 µl of planktonic cells suspended at an OD_{600} = 0.4-0.6 in basal medium (BM2) supplemented with nitrogen source as indicated and 0.4% glucose, then incubated for 18-24 h at 37ºC. Images captured using a BioRad ChemiDoc. Raw surface area coverage (%) of swarming colonies was assessed using ImageJ software. Data reported as mean ± standard error of the mean (SEM) from three independent experiments containing 2-3 biological replicates each (n = 6-9). ** $P < 0.01$ according to Kruskal-Wallis nonparametric test followed by Dunn's post-hoc analysis.

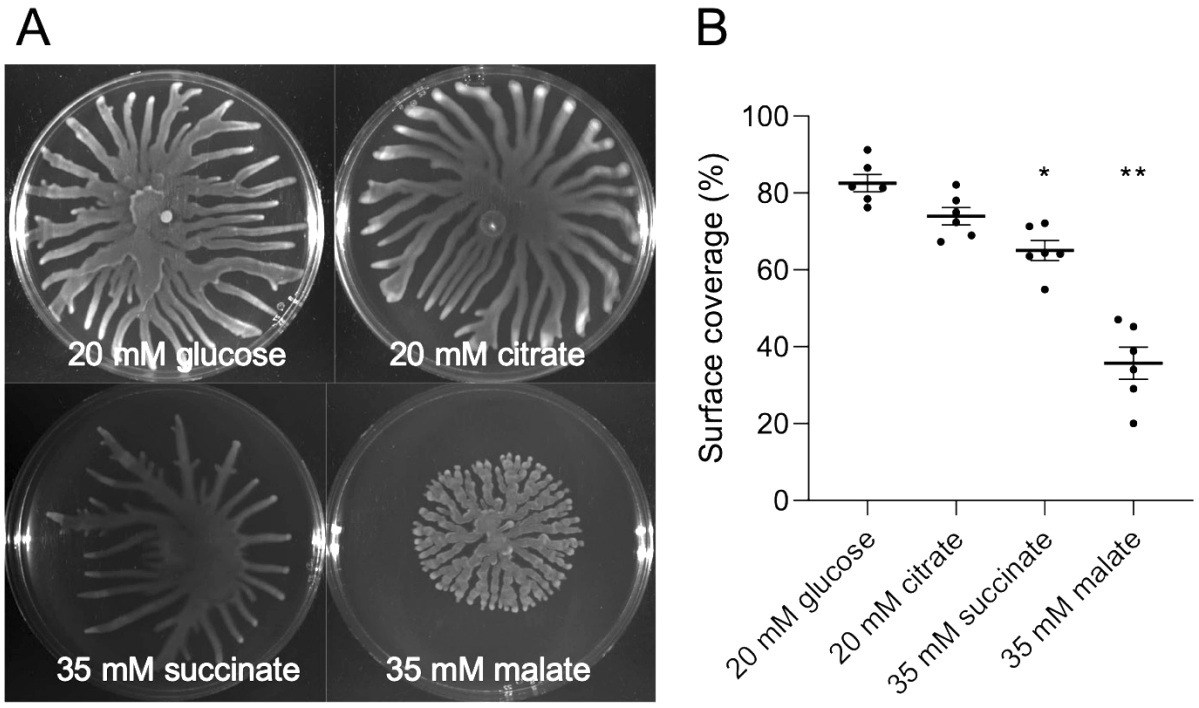

Figure A3. Swarming motility of wild-type (WT) PA14 was influenced by carbon source. (A) Representative images depict swarming motility of WT PA14 in the presence of different carbon-containing compounds. (B) Swarming motility was reduced by substituting glucose for succinate or malate in swarm plates. Modified swarm plates were inoculated with 5 µl of planktonic cells suspended at an OD_{600} = 0.4-0.6 in basal medium (BM2) supplemented with carbon source as indicated and 0.1% casamino acids (CAA), then incubated for 18-24 h at 37ºC. Images captured using a BioRad ChemiDoc. Raw surface area coverage (%) of swarming colonies was assessed using ImageJ software. Data reported as mean ± standard error of the mean (SEM) from three independent experiments containing 2 biological replicates each (n = 6). * $P < 0.05$, ** $P < 0.01$ according to Kruskal-Wallis nonparametric test followed by Dunn's post-hoc analysis.

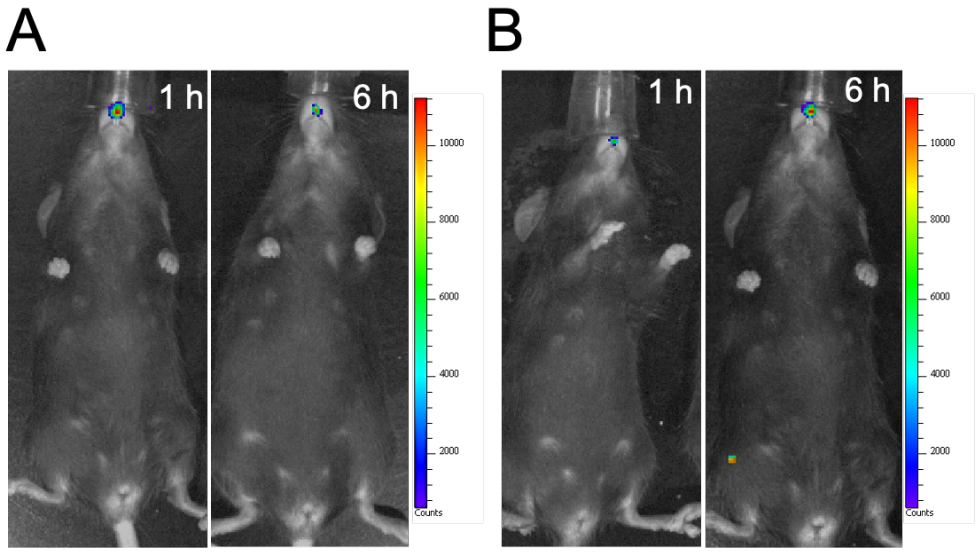

Figure A4. Clinically important species of bacteria elicited reactive oxygen species production in the nasal cavity. (A) *S. aureus* USA300 or (B) *P. aeruginosa* LESB58 were inoculated dropwise in the left naris of C57Bl/6 mice (10^7 or 10^6 CFU, respectively). Localization of oxidative species to the site of infection was tracked using the chemiluminescent L-012 sodium salt probe (25 mg/kg). One representative image is shown.

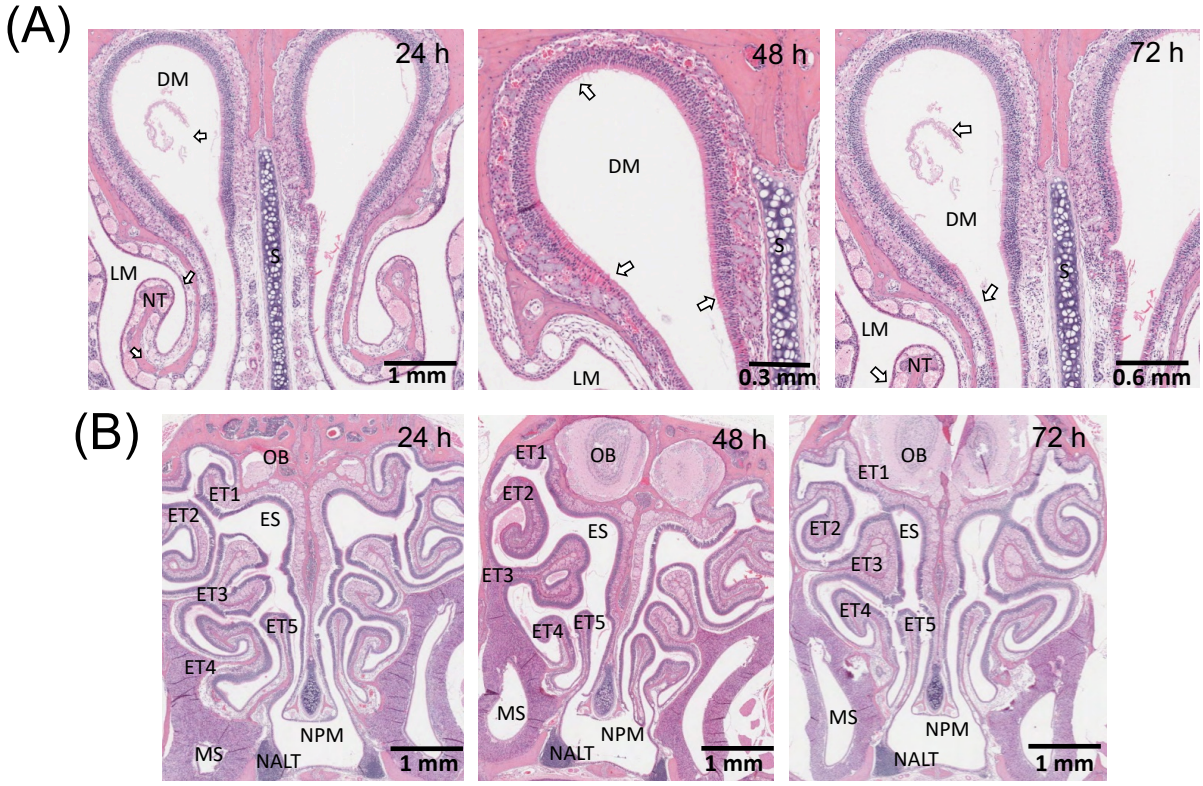

Figure A5. Bacterial induction of inflammation in the murine nasal cavity was partly mediated by neutrophils. Histological sections treated with hematoxylin and eosin stain revealed reactive mucosa that was most pronounced at 24 h post-infection, but sustained up to 72 h. *S. aureus* USA300 was inoculated dropwise in the left naris of C57Bl/6 mice (~10^7 CFU) providing a within-subject control in the right naris. Focal neutrophil infiltration (30-40x more neutrophils per high power field) was observed at (A) 2 mm and (B) 6 mm deep cross-sections of the nasal cavity. Sinus secretions (mucus) with admixed cells were most abundant at 24 h post-infection. Arrowheads indicate mucus producing cells and regions of inflammation. Abbreviations used: DM = dorsal meatus, ES = ethmoid sinus, ET = ethmoturbinate, LM = lateral meatus, MS = maxillary sinus, NT = nasoturbinate, NPM = nasopharyngeal meatus, NALT = nasal associated lymphoid tissue, OB = olfactory bulb, S = septum.

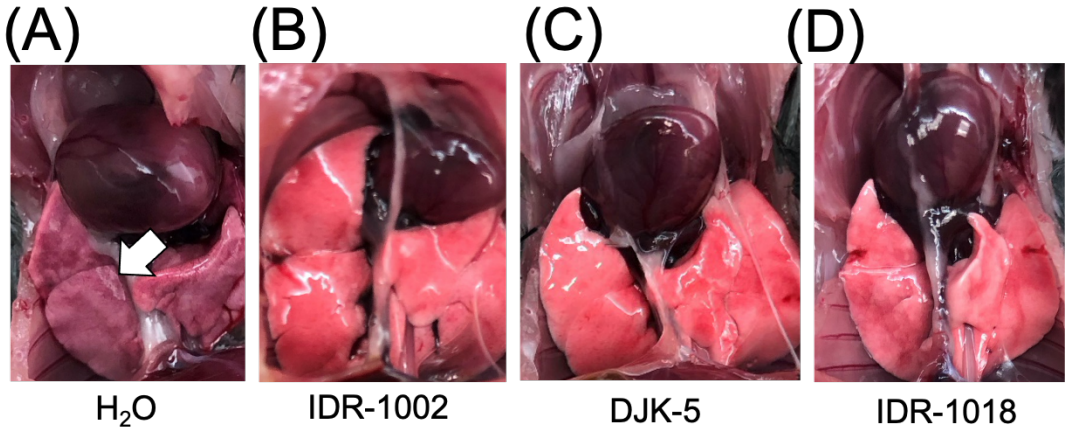

Figure A6. Host defense peptides prevented lung lesions caused by bacterial dissemination or aspiration from sinus infection in situ. *P. aeruginosa* LESB58 was inoculated dropwise in the left naris of C57Bl/6 mice (~10^6 CFU). 24 h post-infection, mice were intranasally treated with endotoxin-free H_2O (vehicle) or peptide (2.5–7.5 mg/kg). 48 h later, mice were euthanized, and lung tissue was evaluated for lesions. Bacterial aggregation was observed in lungs treated with H_2O only, as denoted by the arrowhead. One representative image is shown.

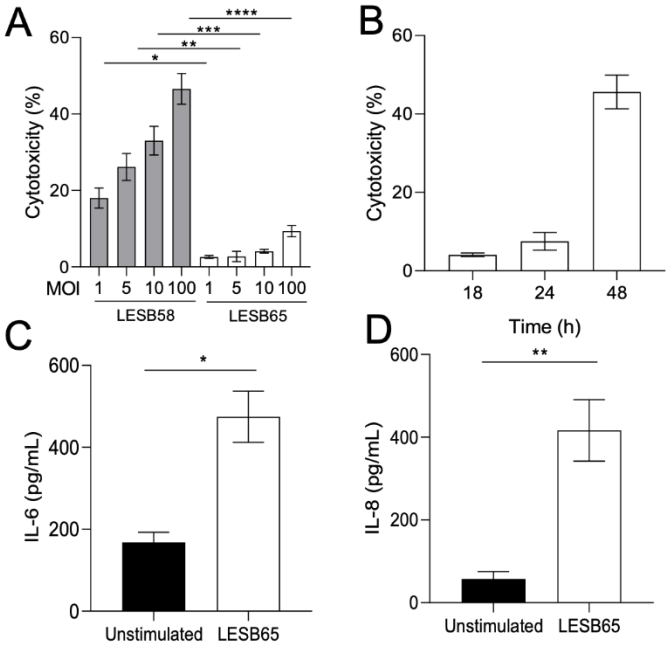

Figure A7. Host response to *P. aeruginosa* LESB strains *in vitro*. (A) Human bronchial epithelial cells (HBE) were infected with *P. aeruginosa* LESB58 or LESB65 at a multiplicity of infection (MOI) of 1, 5, 10 or 100 for 18 h. Amount of LDH in host-cell supernatants was quantified for determination of cytotoxicity. (B) At MOI = 10, *P. aeruginosa* LESB65 took 48 h to elicit cytotoxicity like that caused by LESB58 in 18 h. *P. aeruginosa* LESB65 caused significant production of (C) pro-inflammatory cytokine (IL-6) and (D) chemokine (IL-8) by HBE cells 18 h post-infection. Data are shown as mean ± SEM. ** $P < 0.01$, *** $P < 0.001$, **** $P < 0.0001$ according to Student's t-test. Experiments were performed by Dr. Grace Ka-Yee Choi and Pavneet Kalsi.

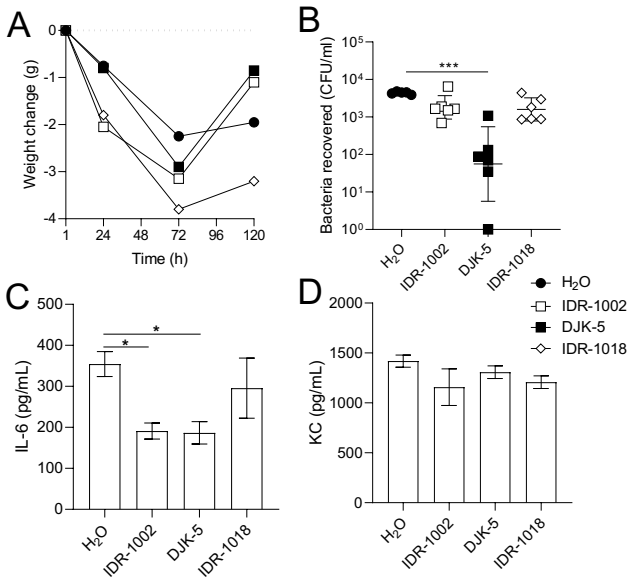

Figure A8. Host-defense peptides exhibited immunomodulatory and/or antimicrobial activities during LESB65 infected mice. *P. aeruginosa* LESB65-Lux encapsulated in alginate were inoculated dropwise in the left nare of C57Bl/6 mice (~10^6 CFU). Mice were treated with endotoxin-free H_2O (vehicle) or peptide (1.25 mg/kg) using a Respimat® device 24 h post-infection. (A) Weight was recorded at 0-, 24-, 72- and 120-h post-infection, and mean weight change from day 0 are reported. Lung homogenates were used to (B) enumerate bacterial burden and determine the production of (C) pro-inflammatory cytokine (IL-6) and (D) chemokine (KC/CXCL1). (A, B) Data are shown as geometric mean ± SD or (C, D) mean ± SEM. $n \geq 6$. * $P < 0.05$, *** $P < 0.001$ according to Kruskal-Wallis test followed by Dunn's correction. Dr. Grace Ka-Yee Choi performed these experiments.

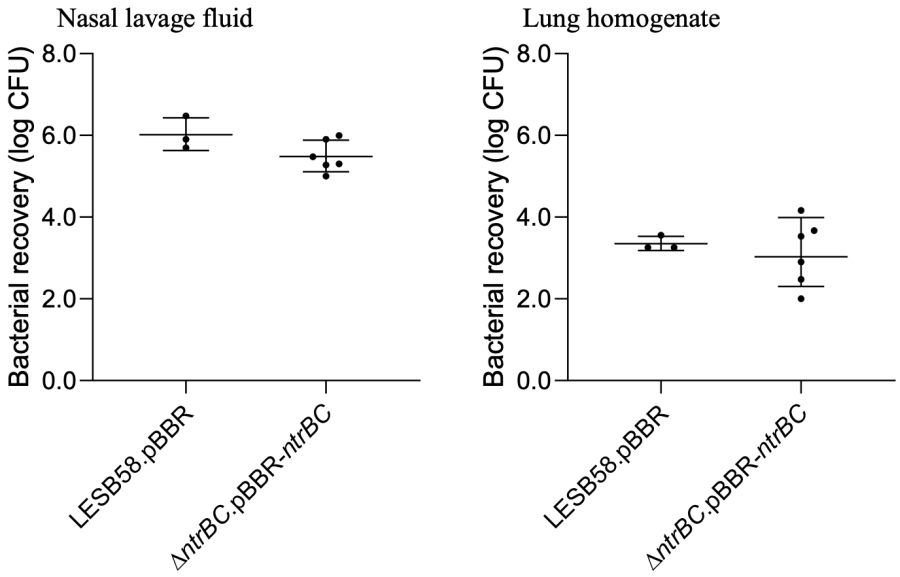

Figure A9. Complementation of the nitrogen regulatory two-component system, NtrBC, restored infectivity of *P. aeruginosa* in a murine model of sinusitis. Stationary-phase bacteria were inoculated dropwise in the left nare of C57Bl/6 mice (10^6 CFU). 72 h later mice were euthanized, and lung tissue or nasal lavage fluid was collected for bacterial enumeration. Similar levels of bacteria were recovered from the lungs and nasal cavities of mice infected with *P. aeruginosa* with empty vector (pBBR1MCS-5) and vector containing *ntrBC*. Data are presented as geometric mean ± standard deviation for two independent experiments containing 1-3 biological replicates each (n = 3-6).

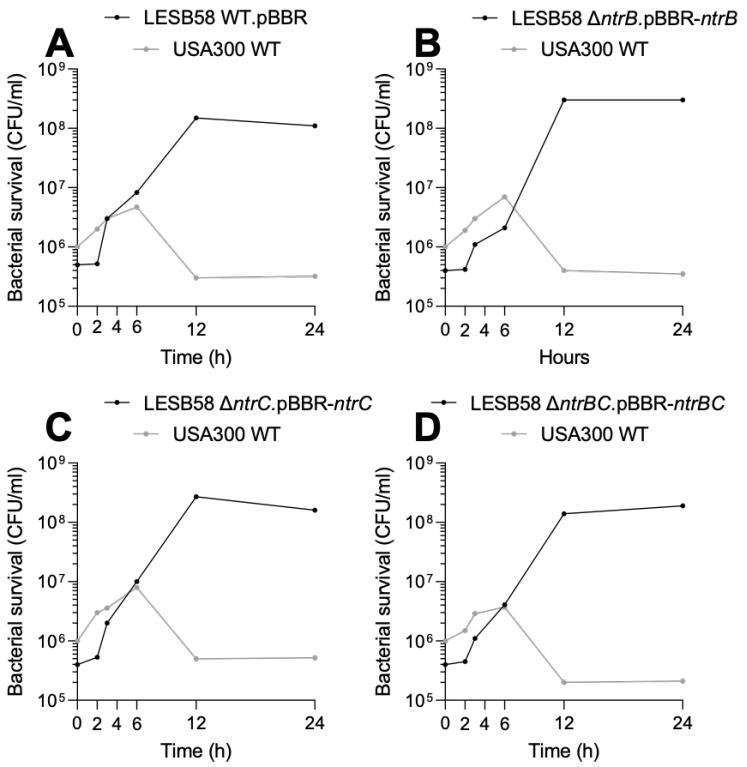

Figure A10. Complementation of *P. aeruginosa* LESB58 Δ*ntrB*, Δ*ntrC* and Δ*ntrBC* strains restored interspecies competition with *S. aureus* USA300. *P. aeruginosa* LESB58 (A) WT, (B) Δ*ntrB.ntrB*, (C) Δ*ntrC.ntrC* or (D) Δ*ntrBC.ntrBC* complemented strains were seeded at a starting OD_{600} = 0.1 in batch cultures that were sampled in 2-, 6- or 12-h intervals and plated on selective media for bacterial enumeration. Data are presented as mean ± standard error of the mean (SEM) for three independent experiments (n = 3).

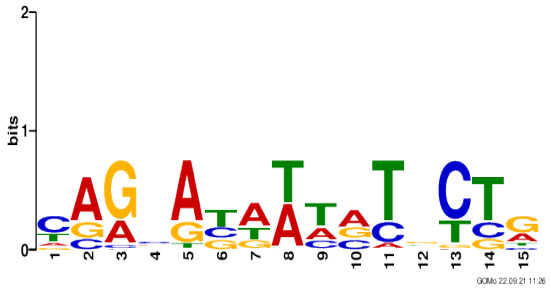

Figure A11. NtrC binding motif calculated using Autoseed software followed by manual refinement with available HT-SELEX and ChIP-Seq data.

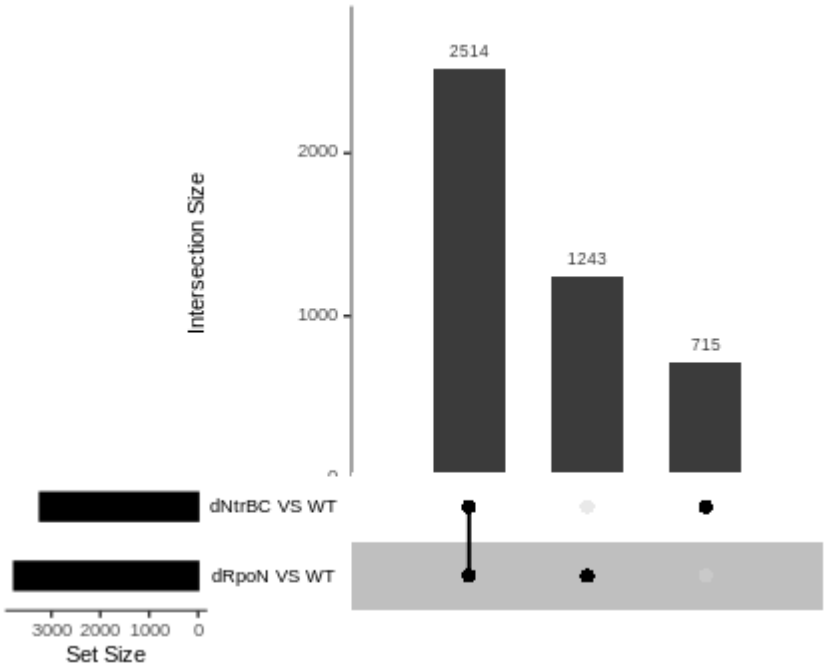

Figure A12. NtrBC and RpoN influence the transcriptome of PA14 significantly and have overlapping regulons. PA14 Δ*ntrBC* and Δ*rpoN* exhibited dysregulated expression of 3,229 and 3,757 genes, respectively, 2,514 of which were common between the mutants.